Technologies and control strategies for active railway suspension actuators

By

Hazlina Md Yusof

A doctoral thesis submitted in partial fulfilment of the requirements for the award of

Doctor of Philosophy

Loughborough University

October 2012

Abstract

Future railway trends require travelling at high speeds without deterioration in the ride quality, but further improvement of the ride quality by optimisation of the passive suspension components has reached its limits. This suggests that active suspensions should be used. Rigorous studies over the past four decades have shown that this technique is able to overcome the passive suspension limitation in terms of improving the overall ride performance of the railway vehicle with the incorporation of additional active elements i.e. actuators, sensors and processors.

The work in this thesis investigates a novel method for controlling the actuators within the suspension system, something which has been neglected in previous studies. It is a particular problem because at higher frequencies, when the suspension is providing isolation of the car body from the track irregularities, the actuator must accommodate the suspension movements whilst producing very small forces, otherwise the ride quality substantially deteriorates. Instead of considering more complex active suspension control strategies, which tend to be complex and may be impractical, the performance of the actuator across the secondary suspension is investigated. This research looks into improving actuator technologies for railway secondary suspensions in order to achieve the full benefits of active control. This thesis explores novel methods to improve the ride quality of the railway vehicle through secondary suspension actuator and controller design, with the ultimate aim of integrating this technology into a fully active railway vehicle.

The focus of this active suspension research is therefore upon incorporating real actuator technology, instead of the usual assumption of ideal actuators. For meaningful and reliable research a simple, well established active control strategy is used for assessment to highlight the degradation in the suspension performance compared with the ideal actuators. Preliminary investigation demonstrates significant degradation of the ride quality caused by real actuators in the secondary suspension, and this research looks at methods to reduce this effect. Including actuators within a secondary suspension system is a difficult actuator

problem compared to the normal application of actuators such as position control. This is because the actuator controller design process requires the consideration of the interaction of the vehicle suspension.

The actuators that have been identified as suitable for the application are the electromechanical and servo-hydraulic types, and these are incorporated across the secondary suspension. The effects of the actuator dynamics have been analysed. Practical classical controllers are used to provide force-feedback control of both types of actuator in the secondary suspension. A variety of actuator control techniques are considered including: optimisation of the actuator controller parameters to solve the multi-objective and multivariable problem, the introduction of feed forward techniques and the use of optimal control approaches.

Keywords: Railway vehicle; Active suspension; Actuators;

Acknowledgement

In the name of Allah, the Most Gracious and the Most Merciful.

Alhamdulillah, all praises to Allah for the strengths and His blessing in completing this thesis.

First and foremost, I wish to express my sincere gratitude to my supervisors, Prof. Roger Goodall and Dr. Roger Dixon for their invaluable knowledge, encouragement, guidance, direction, and perseverance throughout the course of my research. Both of my supervisors are my source of motivation, encouragement and also inspiration. One simply could not wish for better or friendlier supervisors.

I would also like to extend my appreciation to my sponsor, the Ministry of Higher Education of Malaysia and my employer, International Islamic University Malaysia, for the funding given to fulfil my PhD studies.

For my colleagues in the Control Systems Group, past and present, for their useful discussions and also advice, thank you very much.

My deepest gratitude goes to my beloved parents, Prof. Md Yusof Abu Bakar and Ms. Amrah Haron, and also to my brother, Hazrul, thank you for the unconditional prayers, love, understanding and also the financial support over the many years I have been in the university.

To my dearest husband, Ahmad Zawawi Hashim, words could not express how much I appreciate and thank you for the unconditional love, kindness, support, sacrifices and understanding during the most difficult times of the completion of this thesis.

And at the same time to my precious four, Nurul Ain, Muhammad Afiq, Nurul Izzah, and Nurul Iman, please forgive me for being unable to be around with all of you as much as I would really love to. Without your sacrifices, this thesis would not have been possible. And to those who have come across my life throughout the duration of my life, thank you for all the wonderful moments.

Hazlina Md Yusof, July 2012

Table of Contents

Abstract……i

Acknowledgement……..iii

Table of Contents……..……..iv

List of Figure…….…..ix

List of Tables……..…….xvi

List of Symbols…….……..xviii

Abbreviation..……...……...…..xxii

Chapter 1 Introduction 1

1.1 Background and Overview 1

1.2 Active suspension technology 3

1.2.1 Active secondary suspension and control 6

1.2.2 Actuator technology in active secondary suspension 8

1.3 Problem statement and research objectives 9

1.4 Thesis structure 11

1.5 Thesis contribution 12

1.6 Summary 14

Chapter 2 Literature Review 16

2.1 Introduction 16

2.2 Overview of active secondary suspension research 17

2.3 Actuators for active secondary suspension 21
2.3.1 Electromechanical 23
2.3.2 Electrohydraulic servo 24
2.3.3 Pneumatic 24
2.3.4 Other kinds of actuator and their benefits 25
2.4 Genetic Algorithm optimisation 26
2.5 Actuator control 27
2.6 Summary 28
Chapter 3 Assessment Methods, Model Derivation and Analysis of Passive and Active Railway Vehicles 29
3.1 Track Profile 30
3.1.1 Random Input 30
3.2 Vehicle assessment to stochastic inputs 33
3.2.1 Frequency domain analysis 33
3.2.2 Covariance analysis 34
3.2.3 Time domain analysis 36
3.3 Modelling of a single railway vehicle 36
3.4 Railway vehicle model verification and simulations 41
3.4.1 Eigenvalue analysis 41
3.4.2 Step responses 42
3.4.3 Ride acceleration analysis 44
3.5 Ideal active secondary suspension 44
3.5.1 Local skyhook control 47
3.5.2 Modal control 49
3.6 Results and analysis 51
3.6.1 Ride quality analysis 51

3.6.2 Frequency Analysis 52

3.7 Summary 55

Chapter 4 Optimisation of Actuator Control 56

4.1 Introduction 57

4.2 Selection of actuators for active suspension 58

4.3 Actuator modelling 61

4.3.1 Electromechanical actuator 61

4.3.2 Electrohydraulic actuator 66

4.4 Actuator outline design 69

4.4.1 Outline design of the electromechanical actuator 70

4.4.2 Outline design of the electrohydraulic actuator 72

4.5 Initial force loop design of the actuator 74

4.5.1 Electromechanical actuator 75

4.5.2 Electrohydraulic actuator 78

4.6 Actuator performance in quarter car railway vehicle suspension 80

4.7 Actuator performance in the active secondary vehicle suspension (quarter car) 85

4.8 Improvement of actuated active suspension using the Genetic Algorithm 89

4.8.1 Active suspension actuator controller parameter optimisation using NSGA-II (OPT I) 89

4.8.2 Actuator in the secondary suspension controller parameter and additional stiffness optimisation using NSGA-II (OPT II) 92

4.9 Simulation results 93

4.10 Actuators in suspension analysis at 3Hz 100

4.10.1 Electromechanical actuator analysis 100

4.10.2 Electrohydraulic actuator analysis 104

4.11 Summary 106

Chapter 5 Optimised Actuator Control with Feed Forward 108

5.1 1BFeed forward control strategy 109

5.1.1 Reference feed forward 109

5.1.2 Disturbance feed forward 110

5.2 Feed forward control strategy for the electromechanical actuator 112

5.2.1 Reference feed forward *(Force → Voltage)* 112

5.2.2 Disturbance feed forward 114

5.3 Feed forward control of the electrohydraulic actuator 121

5.3.1 Velocity based disturbance feed forward 121

5.4 Improvement of feed forward control strategy using NSGA- II 123

5.4.1 Electromechanical actuator controller optimisation 123

5.4.2 Electrohydraulic actuator controller optimisation 127

5.4.3 NSGA-II optimisation simulation results 128

5.5 Controller performance assessment in the Side-view vehicle 131

5.6 Robustness of the active suspension actuator controller 137

5.6.1 Robustness of the active suspension actuator controller on the quarter car railway vehicle 137

5.6.2 Robustness of the active suspension actuator controller on the side-view railway vehicle 140

5.7 Summary 147

Chapter 6 Validation with more complex active suspension strategy 149

6.1 Validation model 150

6.2 Validation results 152

6.2.1 Electromechanical actuator analysis 155

6.2.2 Electrohydraulic actuator 165

6.3 Conclusion 172

Chapter 7 Optimal Control 173

7.1 Linear Quadratic Gaussian (LQG) control design 174

7.1.1 Linear Quadratic (LQR) optimal control 175

7.1.2 Estimator 178

7.2 Performance analysis 181

7.2.1 LQR 181

7.2.2 LQG 185

7.3 Robustness test 186

7.4 Summary 188

Chapter 8 Conclusions and Future Works 190

8.1 Conclusions from the research 190

8.2 Future Works 194

References 196

Appendices 205

A:Railway Vehicle Parameters……...……207

B: State Space Matrices for Active Vertical Secondary Suspension……...…210

List of Figures

Figure 1.1: Dynamic elements in high speed vehicle scheme 4

Figure 1.2 : Components of a railway vehicle suspension (Goodall, (2011)) 4

Figure 1.3: Suspension configurations (a) passive (b) active 5

Figure 1.4: General view of active suspension 5

Figure 1.5: Design requirements for suspension system 7

Figure 1.6: "Skyhook damping" concept 7

Figure 1.7: Overall model structure of actuated active suspension 8

Figure 1.8: Actuator placement in the suspension 9

Figure 1.9 : Thesis flow chart 15

Figure 3.1: Side-view model of a single railway vehicle 38

Figure 3.2: Air spring model 39

Figure 3.3: Step track inputs 43

Figure 3.4: Vehicle body accelerations response to step track input 43

Figure 3.5 : Active suspension configuration 45

Figure 3.6: Skyhook damping 45

Figure 3.7: Practical skyhook implementation 46

Figure 3.8 : Basic translated skyhook control 46

Figure 3.9: Local skyhook control strategy 48

Figure 3.10 : Modal control strategy for the vertical side-view model 49

Figure 3.11 : Side-view model p.s.d.s – Front acceleration 53

Figure 3.12: Side-view model p.s.d.s - Centre acceleration 54

Figure 3.13: Side-view model p.s.d.s – Rear acceleration 54

Figure 4.1 : Actuator modelling and assessment process 58

Figure 4.2 : Force controlled actuator scheme 59

Figure 4.3 : Electromechanical actuator 62
Figure 4.4 : Equivalent electromechanical actuator 62
Figure 4.5 : DC motor equivalent circuit 62
Figure 4.6: Linear model of the DC motor 64
Figure 4.7: Linearised model of an electromechanical actuator model 65
Figure 4.8 : Electrohydraulic actuator model 67
Figure 4.9 : Linearised model of an electrohydraulic actuator 69
Figure 4.10: Actuator force control 75
Figure 4.11 : Open loop uncompensated electromechanical actuator 76
Figure 4.12: Open loop of controlled electromechanical actuator 76
Figure 4.13: Force following of the closed-loop electromechanical actuator 77
Figure 4.14: Open loop uncompensated electrohydraulic actuator 78
Figure 4.15: Open loop of controlled electrohydraulic actuator 79
Figure 4.16: Force following of the closed-loop electrohydraulic actuator 79
Figure 4.17 : Force controlled actuator 81
Figure 4.18: Open loop of controlled electromechanical actuator in the secondary suspension 83
Figure 4.19: Open loop of controlled electrohydraulic actuator in the secondary suspension 83
Figure 4.20: Force following of the closed-loop electromechanical actuator in the secondary suspension 84
Figure 4.21: Force following of the closed-loop electrohydraulic actuator in the secondary suspension 84
Figure 4.22 : Vehicle dynamic model 85
Figure 4.23: Effect of real actuators on ride quality 88
Figure 4.24: Force analysis 88

Figure 4.25: Trade off plot for EMA and EHA for controller parameter optimisation 91
Figure 4.26: Trade off plot for EMA and EHA for controller parameter optimisation and actuator stiffness 92
Figure 4.27: P.s.ds for the electromechanical actuator effect in the quartercar vehicle..... 94
Figure 4.28: P.s.d.s for the electrohydraulic actuator effect in the quartercar vehicle..... 94
Figure 4.29 : Front p.s.d.s for the electromechanical actuator effect in the sideview vehicle 95
Figure 4.30: Rear p.s.d.s for the electromechanical actuator effect in the sideview vehicle . 95
Figure 4.31: Front p.s.d.s for the electrohydraulic actuator effect in the sideview vehicle ... 96
Figure 4.32: Rear p.s.d.s for the electrohydraulic actuator effect in the sideview vehicle 96
Figure 4.33 : Bar chart of the quarter car vehicle r.m.s. results 98
Figure 4.34 : Bar chart of the front side-view vehicle r.m.s. results 99
Figure 4.35 : Bar chart of the rear side-view vehicle r.m.s. results..... 99
Figure 4.36: Electromechanical actuator analysis..... 102
Figure 4.37: Magnitude plot of electromechanical actuator at 1-10 Hz..... 103
Figure 4.38: Motor torque (T_M) vs load torque (T_L) p.s.d.s 104
Figure 4.39: Electrohydraulic actuator analysis..... 105
Figure 4.40: Magnitude Plot of the electrohydraulic actuator at 1-10Hz..... 106
Figure 5.1 : Reference feed forward 110
Figure 5.2: Disturbance feed forward 111
Figure 5.3 : Reference feed forward scheme for the electromechanical actuator 112
Figure 5.4: Reference feed forward for the electromechanical actuator 113
Figure 5.5 : Comparison between the reference feed forward control strategy p.s.d.s with the ideal and force feedback control strategy for the electromechanical actuator . 114
Figure 5.6: Disturbance feed forward 115
Figure 5.7 : Disturbance feed forward configuration for the electromechanical actuator ... 116
Figure 5.8 : Vertical body acceleration p.s.d.s for the electromechanical actuator 117

Figure 5.9: Current Control of the actuator..... 119
Figure 5.10: Acceleration feed forward control..... 119
Figure 5.11: Vertical body acceleration p.s.d.s for the electromechanical actuator with acceleration feed forward control..... 120
Figure 5.12 : Feed forward configuration for the electrohydraulic actuator..... 122
Figure 5.13: Vertical body acceleration p.s.d.s for the electrohydraulic actuator with velocity feed forward..... 122
Figure 5.14: Trade-off plot for the NSGA-II optimisation of the velocity feed forward controller optimisation and for the varied actuator stiffness..... 124
Figure 5.15: Trade-off plot for the NSGA-II optimisation of the acceleration based feed forward controller optimisation and for the varied actuator stiffness..... 126
Figure 5.16 : Trade-off plot for the NSGAII optimisation of the controller optimisation and for the varied actuator stiffness..... 127
Figure 5.17: P.s.ds for the effect of the electromechanical actuator with the optimised velocity based disturbance feed forward control in the quartercar vehicle actuator..... 130
Figure 5.18: P.s.ds for the effect of the electromechanical actuator with the optimised acceleration based disturbance feed forward control in the quartercar vehicle actuator..... 130
Figure 5.19: P.s.ds for the effect of the electrohydraulic actuator with the optimised feed. 131
Figure 5.20: Front p.s.d.s for the electromechanical actuator with optimised velocity based disturbance feed forward control effect in the sideview vehicle..... 132
Figure 5.21: Rear p.s.d.s for the electromechanical actuator with optimised velocity based disturbance feed forward control effect in the sideview vehicle..... 133
Figure 5.22: Front p.s.d.s for the electromechanical actuator with optimised acceleration based disturbance feed forward control effect in the sideview vehicle..... 133

Figure 5.23: Rear p.s.d.s for the electromechanical actuator with optimised acceleration based disturbance feed forward control effect in the sideview vehicle..... 134
Figure 5.24: Front p.s.d.s for the electrohydraulic actuator with optimised feed 134
Figure 5.25: Rear p.s.d.s for the electrohydraulic actuator with optimised feed 135
Figure 6.1 : Complementary filter structure..... 151
Figure 6.2 : Complementary filter incorporated with modal control structure 151
Figure 6.3: Bar chart of percentage of the ride performance degradation/improvement of actuator and controller scheme effects with the different active suspension controller strategies (with respect to the ideal) for the electromechanical actuator in the side-view vehicle..... 155
Figure 6.4: Bar chart of percentage of ride performance degradation/improvement of actuator and controller scheme effects with the different active suspension controller strategies (with respect to the ideal) for the electromechanical actuator in the side-view vehicle. 156
Figure 6.5: Effect of electromechanical actuator with feedback controller 157
Figure 6.6: Effect of electromechanical actuator with feedback controller 157
Figure 6.7 : Front and rear accelerations linear p.s.d.s for electromechanical actuator 158
Figure 6.8: Effect of electromechanical actuator with the velocity based disturbance feed forward controller- Front acceleration p.s.d.s 158
Figure 6.9: Effect of electromechanical actuator with the velocity based disturbance feed forward controller- Rear acceleration p.s.d. 159
Figure 6.10: Effect of electromechanical actuator with the acceleration based disturbance feed forward controller- Front acceleration p.s.d.s 159
Figure 6.11: Effect of electromechanical actuator with the acceleration based disturbance feed forward controller- Rear acceleration p.s.d. 160
Figure 6.12: Bar chart of percentage of the actuator force degradation/improvement of

actuator and controller scheme effects within the different active suspension controller strategies (with respect to the ideal) for the electromechanical actuator in the side-view vehicle..... 161
Figure 6.13: Bar chart of percentage of the actuator force degradation/improvement of actuator and controller scheme effects within the different active suspension controller strategies (with respect to the ideal) for the electromechanical actuator in the side-view vehicle..... 161
Figure 6.14: Effect of electromechanical actuator with feedback controller 162
Figure 6.15: Effect of electromechanical actuator with feedback controller 162
Figure 6.16: Effect of electromechanical actuator with the velocity based disturbance feed forward controller- Front force p.s.d.s 163
Figure 6.17 : Effect of electromechanical actuator with the velocity based disturbance feed forward controller - Rear force p.s.d.s 163
Figure 6.18: Effect of electromechanical actuator with the acceleration based disturbance feed forward controller- Front force p.s.d.s 164
Figure 6.19 : Effect of electromechanical actuator with the acceleration based disturbance feed forward controller - Rear force p.s.d.s 164
Figure 6.20: Bar chart of percentage of ride performance degradation/improvement of actuator and controller scheme effects with the different active suspension controller strategies (with respect to the ideal) for the electrohydraulic actuator in the side-view vehicle..... 165
Figure 6.21: Bar chart of percentage of ride performance degradation/improvement of actuator and controller scheme effects with the different active suspension controller strategies (with respect to the ideal) for the electrohydraulic actuator in the side-view vehicle..... 166
Figure 6.22 : Effect of electrohydraulic actuator with feedback controller 166

Figure 6.23: Effect of electrohydraulic actuator with feedback controller 167
Figure 6.24: Effect of electrohydraulic actuator with feed forward controller 167
Figure 6.25: Effect of electrohydraulic actuator with feed forward controller 168
Figure 6.26: Bar chart of percentage of the actuator force degradation/improvement of actuator and controller scheme effects within the different active suspension controller strategies (with respect to the ideal) for the electrohydraulic actuator in the side-view vehicle..... 169
Figure 6.27: Bar chart of percentage of the actuator force degradation/improvement of actuator and controller scheme effects within the different active suspension controller strategies (with respect to the ideal) for the electrohydraulic actuator in the side-view vehicle..... 169
Figure 6.28: Effect of electrohydraulic actuator with feedback controller 170
Figure 6.29: Effect of electrohydraulic actuator - Rear force p.s.d.s 170
Figure 6.30: Effect of electrohydraulic actuator - Front force p.s.d.s 171
Figure 6.31 : Effect of electrohydraulic actuator – Rear force p.s.d.s 171
Figure 7.1 : Linear Quadratic Regulator (LQG) scheme 175
Figure 7.2: Actuator controller configuration for a combined system 176
Figure 7.3: LQG..... 180
Figure 7.4 : Force following output for EMA..... 181
Figure 7.5: Force following output for EHA 182
Figure 7.6 Acceleration p.s.d. of the LQR control designed electromechanical actuator in the active secondary suspension 183
Figure 7.7 : Acceleration p.s.d. of the LQR control designed electrohydraulic actuator in the active secondary suspension 184
Figure 7.8: Force p.s.d. of the LQR control designed electromechanical actuator in the active secondary suspension..... 184

Figure 7.9: Force p.s.d. of the LQR control designed electrohydraulic actuator in the active secondary suspension..... 185

List of Tables

Table 3.1: Eigenvalues of the railway vehicle model 42

Table 3.2: R.m.s. results for the passive vehicle 44

Table 3.3 : R.m.s results 51

Table 4.1: R.m.s. and maximum values for ideal actuators based on stochastic input 70

Table 4.2: Parameters for the electromechanical actuator 72

Table 4.3: Electrohydraulic actuator parameters 74

Table 4.4: R.M.S. results for the quarter car model 87

Table 4.5: Final parameters for the controller optimisation (black) in comparison with the manually tuned (red) 91

Table 4.6: Final parameters for the controller optimisation 93

Table 4.7: R.M.S results for the quarter car model 97

Table 4.8: R.M.S. results for the side-view model 98

Table 4.9: Electromechanical analyses at 3Hz 101

Table 4.10:Electrohydraulic analyses at 3Hz 105

Table 5.1: R.M.S. results 113

Table 5.2: R.M.S. results 116

Table 5.3: RMS results 120

Table 5.4: RMS results 123

Table 5.5: Final parameters for the controller optimisation 124

Table 5.6: Final parameters for the controller optimisation 126

Table 5.7 : Final parameters for the controller optimisation 127

Table 5.8: Comparison of ride results for the disturbance feed forward controller strategies for the electromechanical actuator compared to the ideal 135

Table 5.9: Comparison of ride results of the disturbance feed forward controller strategies for the electrohydraulic actuator compared to the ideal 136
Table 5.10: Effect on the ride quality for the variation of motor inertia, Jm , for the quarter rail vehicle with the velocity based disturbance feed forward control strategy 138
Table 5.11: Effect on the ride quality for the variation of motor back e.m.f., Ke , for the quarter rail vehicle with the velocity based disturbance feed forward control strategy 139
Table 5.12: Effect on the ride quality for the variation of motor inertia, Jm , for the quarter rail vehicle with the acceleration based disturbance feed forward control strategy 139
Table 5.13: Effect on the ride quality for the variation of motor back e.m.f., Ke , for the quarter rail vehicle with the acceleration based disturbance feed forward control strategy 140
Table 5.14: Effect on the ride quality for the variation of flow gain rate, Kq 140
Table 5.15: Effect of ride quality to varying motor inertia ,Jm (%g) with the velocity based disturbance feed forward control strategy 142
Table 5.16: Effect of force to varying motor inertia ,Jm (kN) with the velocity based disturbance feed forward control strategy 142
Table 5.17: Effect of ride quality to varying motor back emf , Ke (%g) with the velocity based disturbance feed forward control strategy 143
Table 5.18: Effect of force to varying motor back emf , Ke (kN) with the velocity based disturbance feed forward control strategy 143
Table 5.19: Effect of ride quality to varying motor inertia ,Jm (%g) with the acceleration based disturbance feed forward control strategy 144
Table 5.20: Effect of force to varying motor inertia ,Jm (kN) with the acceleration based disturbance feed forward control strategy 144

Table 5.21: Effect of ride quality to varying motor back emf , Ke (%g) with the acceleration based disturbance feed forward control strategy 145

Table 5.22: Effect of force to varying motor back emf , Ke (kN) with the acceleration based disturbance feed forward control strategy..... 145

Table 5.23: Effect of ride quality to varying valve flow gain,Kq (%g)..... 146

Table 5.24: Effect of force to varying valve flow gain,Kq (kN) 146

Table 6.1: Comparison of ride results for the electromechanical actuator controller strategies with the modal control and with modal complementary filter control (highlighted in yellow) 153

Table 7.1: R.m.s results of LQR control actuator design..... 183

Table 7.2: R.m.s. results of LQG control actuator design..... 186

Table 7.3: R.m.s. results for electromechanical actuator parameter variation 187

Table 7.4: R.m.s. results for electrohydraulic actuator parameter variation 187

Table 7.5: R.m.s results for vehicle mass variation 188

List of Symbols

Symbol	Meaning	*SI Units*
A		
A	System state space model matrix	
A_r	track roughness factor	m
B		
B	State space model input matrix	
B_u	State space model input matrix (actuator forces)	
B_w	State space model input matrix (track input)	
C		
C	State space model matrix, system output	
c_{sky}	Skyhook damping coefficient	N/ms^{-1}
c_{sf}	Skyhook damping coefficient, front	N/ms^{-1}
c_{sr}	Skyhook damping coefficient, rear	N/ms^{-1}
c_p	Primary suspension damping coefficient	N/ms^{-1}
c_r	secondary suspension damping coefficient	N/ms^{-1}
D		
D	State space model matrix disturbance	
D_u	State space model matrix disturbance, actuator inputs	
D_w	Direct transmission matrix (track inputs)	
F		
f_s	Spatial frequency	*cycles/m*
f_t	Temporal frequency	*Hz*
F_f	Force applied at the front secondary suspension	*N*
F_r	Force applied at the rear secondary suspension	*N*
f_f	Front actuator force	*N*
f_r	Rear actuator force	*N*

List of Symbols

Symbol	Meaning	*SI Units*
f_{act}	Actuator force	N
H		
$H(s)$	Transfer function	
$HPF(s)$	High Pass Filter	
J		
J_{bf}	Front bogie pitch inertia	kgm^2
J_{br}	Rear bogie pitch inertia	kgm^2
J_v	Vehicle body pitch inertia	kgm^2
K		
k	Spring constant	N/m
k_a	Change in area stiffness per bogie	N/m
k_p	Primary suspension spring stiffness per bogie	N/m
k_r	Air spring reservoir stiffness per bogie	N/m
k_s	Air spring stiffness per bogie	N/m
L		
l_b	Semi wheel to wheel spacing	M
l_v	Semi bogie to bogie spacing	M
l_t	Vehicle plus gangway length	M
M		
m_{bf}	Front bogie mass	Kg
m_{br}	Rear bogie mass	kg
m_{mpf}	Front airspring midpoint mass	kg
m_{mpr}	Rear airspring midpoint mass	kg
m_v	Vehicle body mass	kg

List of Symbols

Symbol	Meaning	*SI Units*
S		
S_s	Track spatial spectrum	$m^2(cycle/m)^{-1}$
S_T	Track temporal spectrum	$m^2(Hz)^{-1}$
U		
u	Input to state space matrix	
u_{act}	Actuator input	
V		
v	Velocity	ms^{-1}
X		
x_{act}	Actuator extension velocity	ms^{-1}
Z		
z_b	Vertical bogie displacement	m
z_{bf}	Front bogie vertical displacement	m
z_{br}	Rear/ Trailing bogie vertical displacement	m
z_f	Front vehicle body displacement	m
z_{mpf}	Front air spring displacement	m
z_{mpr}	Rear air spring displacement	m
z_r	Rear vehicle body displacement	m
z_t	Wheelset vertical displacement	m
$z_{t_{11}}$	Leading wheelset vertical displacement for the first bogie	m
$z_{t_{12}}$	Trailing wheelset vertical displacement for the first bogie	m
$z_{t_{21}}$	Leading wheelset vertical displacement for the second bogie	m
$z_{t_{22}}$	Trailing wheelset vertical displacement for the second bogie	m

List of Symbols

Symbol	Meaning	*SI Units*
z_v	Vehicle body vertical displacement	m
ω_t	temporal frequency	rad/s
ζ	track input	
θ_v	Vehicle body pitch motion	rad/s
θ_{bf}	Front bogie pitch motion	rad/s
θ_{br}	Rear bogie pitch motion	rad/s

Other symbols are defined as they appear

Abbreviations

DOF	Degree of Freedom
EHA	Electrohydraulic actuator
EMA	Electromechanical actuator
GA	Genetic algorithm
HPF	High pass filter
r.m.s.	Root mean square
p.s.d.	Power spectral density

Chapter 1

Introduction

This chapter introduces the topic by giving a brief background to railway vehicle suspension systems, active suspensions and the role of actuators in those systems. Then the research problem statement, thesis structure and the main contributions of this study are presented.

1.1 Background and Overview

In the very early years of railway transportation, the vehicles were constructed as purely mechanical systems. The overall system was simple yet sufficient in terms of the transportation of people and goods from one point to another. Over the past five decades a great number of research projects have been carried out, targeting how to improve vehicle suspension system performance for both automotive (Hrovat (1997)) and railway vehicles (Goodall and Kortum (2002)). Studies and implementation of active suspension for railway vehicle ride improvement began much later than its rivals in the transportation industry. For a purely mechanical suspension system, adding electrical and electronic devices to the suspension system promises significant benefits, and has provided improved ride experience to passengers for both industries; this was a necessity for the present rail industry to remain

competitive in the stiff transportation environment. An intense demand was set for the railway industry to provide better, high speed, lightweight railway vehicles in order to keep in pace. This means that improvements should lead towards a more efficient and effective operation (Goodall and Kortum (2002)), providing faster arrival time and increasing passengers intake per travel without compromising passenger comfort. The trend for railway vehicles towards being much faster and lighter can enable these objectives. Therefore future trains should be designed to be lighter and to operate at higher speed.

Among the notable high speed trains in service are Japan's Tokaido Shinkansen built by Kawasaki, and the French TGV launched in 1964 and 1990, with highest travelling speeds above 300 km/h and 515km/h respectively for conventional wheeled trains. China Railway High Speed Trains has also launched its high speed trains known as the CRH3 series – CRH3, CRH380AL and CRH380BL – offering speeds reaching up to 487km/h in 2008, 2010 and 2011. The development of the high speed train to date has proved that this method is a very efficient and economical way of transportation. The highest recorded speed of the Japanese Maglev train is 581km/h - developed by Central Japan Railway Company (JR Central) – which is faster than the conventional wheel rail speed record set by the French TGV.

The improvement of vehicle suspension systems has been the subject of intense research and development, both theoretically and practically. The development of components, i.e. actuators, sensors and low cost electronics, has motivated the industry and also researchers in the vehicle suspension area for future railway vehicle development.

Actuator technologies are the basis of active suspension among other components. Inclusion of actuators in the suspension is essential for the practicalities of active suspensions. While the active suspension brings improvement in the ride performance compared to the passive at a frequency of 1Hz, including actuators causes degradation of the ride quality at frequencies above 3Hz which is due to the actuator dynamics (Pratt (1996) ; Foo, et al. (1998) ; Md Yusof, et al. (2010) ; Md Yusof, et al. (2011)).

The focus of this thesis is to investigate the key issues of actuator technologies in the active secondary suspension, with particular attention being paid to improving the actuator performance in the suspension. In this thesis the actuators that will be considered are the electromechanical and electrohydraulic actuators. The actuator technologies developed are incorporated with the vehicle dynamics in order to achieve effective operation of the railway

vehicle, and provide performances comparable to the ideal. The following subsections will briefly introduce the basis of the research to give a better overview of actuator issues within active railway suspension technology, with the aim of improving ride performance.

1.2 Active suspension technology

To understand active suspension, it is essential to look at the arrangement of a high speed rail vehicle; a typical conventional four axled passenger train consists of the vehicle body, two bogies and four wheel sets (two per bogie) which are connected by springs, dampers and airsprings to form a wheel set as shown in Figure 1.1. Each body has six degrees of freedom; roll, yaw, pitch, longitudinal, lateral and vertical motion. These motions are highly coupled and also have some degree of non-linear behaviour which makes the railway vehicle system a dynamically complex system. A common approach for analysing the system is to break down the system into parts, i.e. segregating the lateral and vertical motions, as these modes do not significantly affect the physical dynamics of one another. For vertical suspension control, the side-view model of the railway vehicle is normally used, which will be discussed in Chapter 3.

The railway suspension is sub-categorised into two sections, which are the primary and secondary suspensions. To understand active suspensions, it is essential to look at the mechanical arrangement of a modern, high-speed rail vehicle. Figure 1.2 shows a railway vehicle suspension which supports the vehicle body. This two-stage suspension configuration provides a good ride quality for the passengers with the aid of the soft secondary suspension (airsprings) for the vertical and lateral. The connection between the wheel sets and the bogies forms the primary suspension, which deals mainly with the guidance and stability of the vehicle along the track. This connection is much stiffer compared to the secondary suspension.

The secondary suspension, on the other hand, usually consists of a very soft set of air springs that transmits intended low frequency movements to guide the vehicle to follow the track, at the same time isolating the vehicle body from high frequency irregularities. This ensures that passengers will not experience the vibration caused while the vehicle travels on an irregular track.

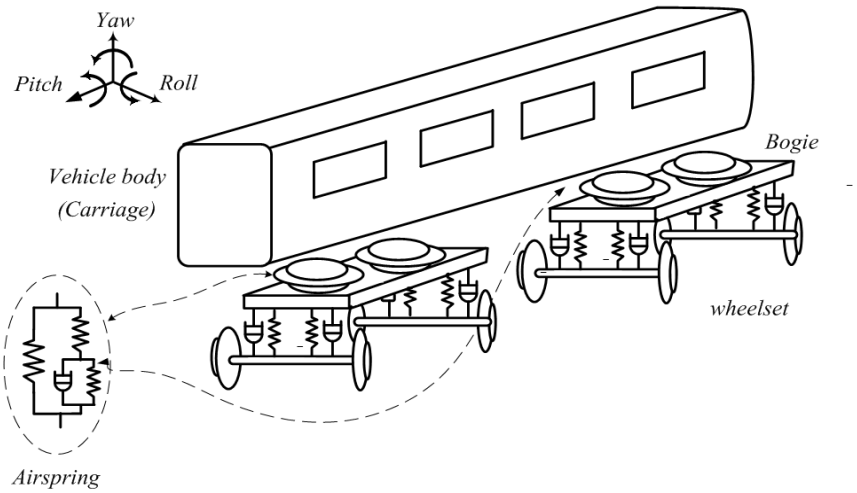

Figure 1.1: Dynamic elements in high speed vehicle scheme

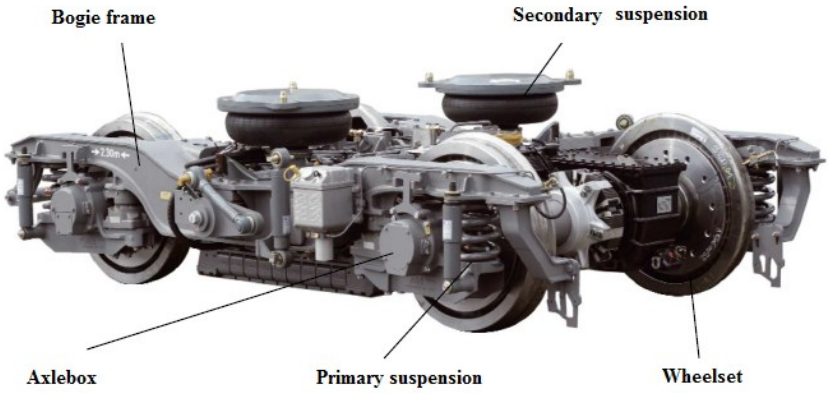

Figure 1.2 : Components of a railway vehicle suspension (Goodall, (2011))

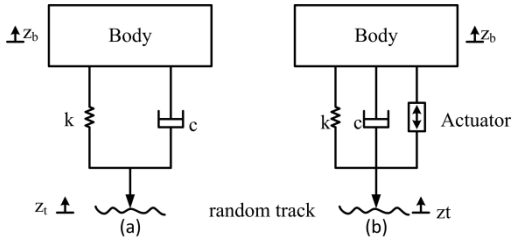

Figure 1.3: Suspension configurations (a) passive (b) active

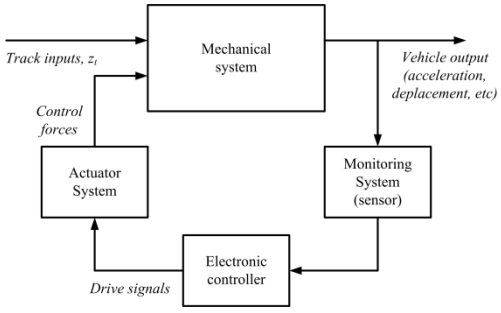

Figure 1.4: General view of active suspension

Figure 1.3 illustrates the basic configuration of the passive and active suspensions. The active suspensions, naturally, have advantages over the passive; the active suspension utilises sensors, electronic controllers and actuators with the existing mechanical system and the passive suspension on the other hand simply consists of coil or leaf springs, viscous dampers and torsion bar. The response of the active suspension system is controlled by the embedded control law in the controller (Goodall (1997)), which differs from the passive performance defined by fixed system parameters i.e. masses, spring rate, damping constants and others. The geometric arrangement creates a design trade-off to be met between the low frequency attenuation and reduction in the high frequency transmissibility in responding to the track profile (Pratt (1996)). To operate at high speed, the conventional suspension needs to be able to provide high frequency isolation which is an important feature in terms of the human anatomical response and general suspension requirement where the natural frequency must be maintained at around 1Hz. If the frequency is set too high the passengers will experience harshness, and if it is set too low undulations of the tracks will cause a "sea-sickness" feeling for the passengers during the ride. Therefore during the design of the suspension, the designer needs to reach a median choice of suspension stiffness, *k*, to accommodate the variation between the vehicle mass between the unladen and laden conditions. This leaves the designer with the variation of the damper constant to achieve an acceptable ride performance.

Active suspension, on the other hand can provide lower natural frequencies which give greater passenger comfort whilst at the same time maintaining a small static deflection. The active suspension is also able to provide a high speed response regardless of the track input,

and gives higher flexibility in the choice of dynamic response especially between the different modes of the vehicle.

The basic active suspension system scheme is as shown in Figure 1.4. Inputs to the system (track irregularities and load changes) are applied to the purely mechanical vehicle system and the outputs are used to indicate performance, i.e. normally the ride quality which is the quantified acceleration levels of the vehicle body, and also the allowable displacement of the suspension.

Active suspension incorporates sensors as measuring devices, an external power source to inject, store and dissipate energy, and actuators. The actuators with controllers provide control commands to improve the suspension performance. Although capable of being used as a stand-alone system, the active suspension always includes passive elements in parallel. This configuration is useful, in particular, for the vertical active suspension as the springs are able to support the steady state load due to the weight of the vehicle, which reduces the actuator size, power consumption and also the force required from the actuator. An active system adapts well to various levels of track irregularities and also external forces, providing a better compromised suspension than the passive, the properties of which are fixed. Although it is noted that active suspension requires high power consumption and sophisticated control implementation, the additional elements i.e. actuators and sensors enable the system to be receptive to any changes in speed, load or track features and at the same time maintain a good ride performance. When control is applied to the secondary suspension for ride quality enhancements it is normally known as an active secondary suspension.

1.2.1 Active secondary suspension and control

Active control for active secondary suspension improves the vehicle dynamic response and at the same time provides better isolation of the vehicle body from track irregularities compared to a purely passive system. The active control is applicable to all suspension degrees of freedom, and includes the yaw mode for a lateral active suspension and the pitching mode for the vertical direction.

Figure 1.5 illustrates the design requirements that need to be achieved when designing an active suspension controller. The inputs are shown on the left, which are the deterministic track, the stochastic track and the load changes. On the right hand side are the outputs to be controlled or monitored, which are the body acceleration levels (which is the main factor in the ride quality), the suspension deflection, the margin of stability and the curving performance (Goodall (1997)). The ride quality or body acceleration should be minimised as it is the main factor that determines the ride comfort. The suspension deflection has to be constrained to avoid reaching the limits of suspension movement. Stability and curving performance must be optimised if the lateral direction is to be controlled (Goodall and Mei (2006)).

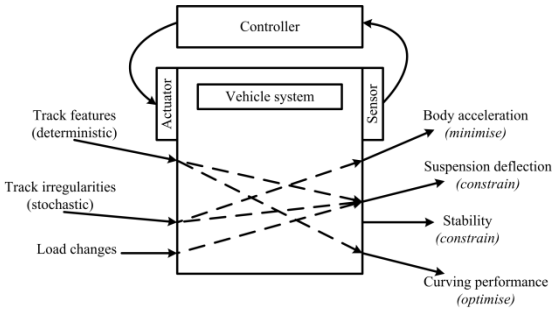

Figure 1.5: Design requirements for suspension system

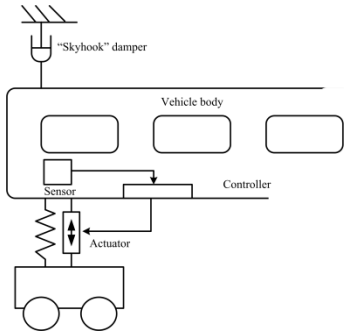

Figure 1.6: "Skyhook damping" concept

For the passive vertical secondary suspension, springs from the bogies to the body are in place to transmit low frequency movements so that the vehicle follows the tracks, and at the same time they isolate higher frequency irregularities to provide a good ride quality. The mass-spring in the suspension creates resonance and, to minimise the body resonance, a damping close to the critical damping is needed. The damper placed across the secondary suspension to provide this damping also causes the ride quality to degrade due to the increasing force acting on the body at high frequencies. Hence, there is a trade-off between the need for high damping to minimise resonance and low damping to minimise high frequency ride issues. This trade-off can be optimised by a well-known control law for active secondary suspension which is called 'skyhook damping', as illustrated in Figure 1.6. With a damper virtually connected to an absolute reference or 'hooked to the sky', the virtual

dampers can now be increased as much as required, because the damper is no longer transmitting the harsh vibration of the bogie (Goodall (1999)).

In practice the vehicle body acceleration is measured and processed by a controller to determine the actuator force. This concept has shown a tremendous improvement in the ride quality, which is important, however it causes a large deflection when encountering gradients. Therefore some care is needed in the controller design (Goodall (1999) ; Li and Goodall (1999)). It also relies on actuators to provide the damper force.

This thesis is focussed upon actuator control strategies and so needs to take a well-founded suspension control strategy as a starting point; the strategy that will be mostly used in this thesis is the "modal skyhook" strategy that will be explained in more detail in the vehicle modelling subsection.

1.2.2 Actuator technology in active secondary suspension

Actuators are force generating elements which are important components for active suspensions. An actuator is a mechanism whereby force and energy injection can complement the existing suspension function. Figure 1.7 shows the overall model structure of the actuated active secondary suspension. The input of the actuator is the voltage or power supply to the actuator and the output is a force which is applied to the railway vehicle model. The actuator movement (actuator displacement velocity) is a "physical feedback" which is determined by the effects of the actuator force (including any external disturbance) upon the load.

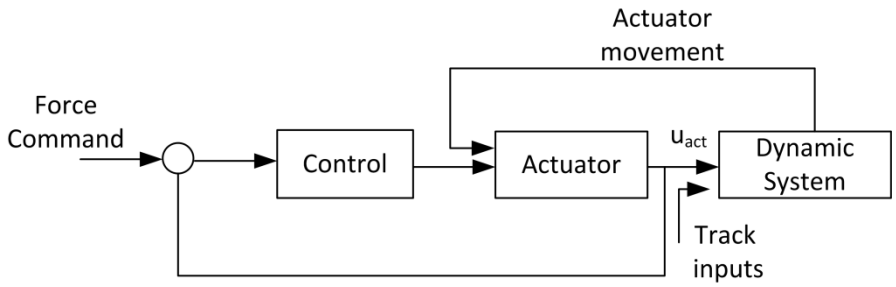

Figure 1.7: Overall model structure of actuated active suspension

Various kinds of actuators for active railway suspensions have been designed and tested (Pratt (1996) ; Goodall (1997)). Common actuators that are noted to be suitable for active railway suspensions are the electromechanical, electro hydraulic, electromagnetic actuators. These actuators have been discussed in the area of railway vehicle research and also in the automotive industry over the past decades. More details on the actuators and the developments will be elaborated in Chapter 4.

The placement of the actuator in the suspension determines the size required for the actuator and also the performance of the suspension. As illustrated in Figure 1.8(b), the actuator size can be reduced as the passive component supports the body mass in the vertical direction. Configurations in Figure 1.8(a) and (c) would be suitable and interesting to explore, but it is beneficial that the actuator should be placed in conjunction with passive components. The spring in Figure 1.8(b) will be similar to that used in a conventional passive suspension.

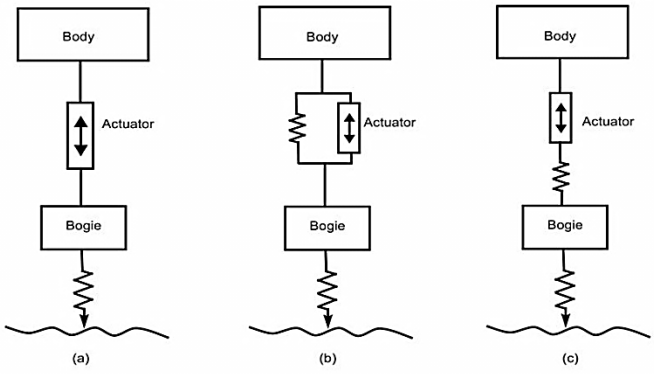

Figure 1.8: Actuator placement in the suspension

1.3 Problem statement and research objectives

Although the principles of active secondary suspension are now well established; there are still a few interesting areas that require attention, in particular relating to the selection of the most appropriate actuator technology. Identifying the sensors and controllers has been widely researched, but identifying a reliable, effective and efficient actuator still remains the biggest issue in active suspension technology, although a variety of other technologies have been considered along the way (Goodall, et al. (1993)) and much research has been carried

out in the past four decades looking at the possibilities of including actuator technologies in railway suspensions. Although these findings are interesting there has not yet been a breakthrough in the implementation as there are still reliability issues concerning the actuator technologies that have been used.

The actuators in the suspension are restricted by their own physical limitations (i.e. bandwidth, current, and force ratings) which makes the ability of the system to approach ideal difficult. Research studies that have included actuators in the secondary suspension have only compared the improvement achieved compared to the passive suspension; they have also had the actuator assessed outside the suspension system (Foo and Goodall (2000) ; Pacchioni (2010) ; Zheng (2011)), whereas most other research studies have only considered ideal actuators.

The focus of this thesis is to investigate the key issues concerning actuator technologies in the active secondary suspension, and examine possible solutions to improve the performance of an actuated active suspension. By encountering the degradation caused by the dynamic interaction of the actuator and the suspension, the ride quality of the vehicle while travelling on a straight track can be handled. Only then the feasibility of having a full active suspension for the railway vehicle can be fulfilled.

In this thesis, the actuators developed are incorporated with the vehicle dynamics in order to achieve effective operation of the railway vehicle. Investigation into suitable active secondary suspension actuator control technologies is carried out. The findings will be represented in terms of comparisons between the actuator technologies used and the ideal case.

The final stage of the research is to validate the actuator with the new control strategies alongside other active suspension controller strategies to ensure that these strategies produce similar results as in the previous configuration using the modified ‘skyhook’ damping active suspension control strategy.

1.4 Thesis structure

The thesis is structured in the following manner to ensure that a smooth flow of understanding is achieved. Figure 1.9 shows an illustration of the steps taken in this research to investigate suitable control strategies for an active secondary suspension actuator.

Chapter 2 is a detailed background survey on works involving actuator technologies in vehicle suspension, in particular in the automotive and railway industries.

In **Chapter 3,** the method of assessing the suspension performance is laid out. The types of track profile and assessment methods that will be used are explained. The side view vehicle model with two degree of freedom is developed. This chapter also includes the analysis and validation of the models and also the application of the active suspension control strategy. The results obtained from this chapter will be used as a reference or ideal case for the subsequent chapters in terms of actuator modelling and also performance comparisons.

Chapter 4 covers the extensive study of the electromechanical actuator (EMA) and electrohydraulic actuator (EHA) which will be used for the vertical active secondary suspension control. These actuators' parameters are derived from the ideal quarter car. The control design of the actuators is achieved taking into consideration the vehicle dynamics interaction, and the actuators are tuned to the best performance to produce a good force tracking output and also stable phase and gain margins. An extension of the assessment is carried out using a genetic algorithm to optimise the actuator controller parameters for a better performance. Another optimisation scheme is introduced to optimise the stiffness in the actuator which mimics the ideal of having a spring in series with the actuator. Both actuators are assessed in the quarter car suspension and progressed on to the vertical side view model. The suspension response with each actuator in situ is observed and discussed using a 3Hz analysis.

Chapter 5 considers another effort of improvement of the existing actuator with another classical approach. The feed forward control strategy is applied to the actuators, where the reference and disturbance feed forward is investigated and analysed for both actuators. Optimisation applied again to the force control loop in the feed forward control strategy is included. The system in the suspension is observed and analysed and the strategy is transferred to the actuators in the side view vehicle. A robustness check is done on the suspension system to confirm the validity of the strategy.

Chapter 6 demonstrates the adaptability of the developed actuator controller strategies using the complementary filter technique with a modal structure, which is another active suspension control strategy. This is to ensure that the developed control strategies for both actuator technologies will be able to provide a performance similar to the existing if not providing an improvement.

Chapter 7 investigates the optimal controller strategy with full-state feedback and Kalman filter estimators for the actuators in the suspension. Another robustness check is done on the suspension system to confirm the validity of the strategy.

Chapter 8 concludes the work done in this thesis. Major contributions and novel applications of the work are also highlighted with recommendations and suggestions for future work.

1.5 Thesis contribution

This thesis introduces a new approach to the design of the active vertical secondary suspension for a high-speed railway vehicle. Rather than focus on complex designs for the active damping control law, the approach here focuses on the actuator and its associated control to achieve a performance approaching the ideal.

The initial contribution is to carry out investigations to show that active railway vehicle suspension systems demonstrate a reduction in ride performance when the ideal actuator in the suspension is replaced with 'real' actuators. The 'real' actuators that are considered in this thesis are the electromechanical and electrohydraulic actuators.

Previous attempts to improve the active suspension performance via the control of the active suspension by other researchers have been carried out with an assumption of an ideal actuator. Most have concentrated on the investigation of complex outer-loop controllers (i.e. active suspension controllers); however high frequency (5-10Hz) degradation still occurs when a 'real' actuator is included. An initial investigation indicates that this is due to the complexity of the system when actuator dynamics are included. Including 'real' actuator in the suspension increases the system complexity, which makes the ideal impossible to achieve without a redesign of the control laws.

The main contribution of this thesis is to propose a different approach to improve the ride performance by engaging a more practical method to overcome the high frequency isolation issues of the active suspension actuators. The effort to improve the ride performance of the active secondary suspension is done via controlling the actuator within the suspension system, which is a method that has yet to be examined in any active suspension research. In this thesis several controllers have been tested for the active suspension actuators. The controllers that have been investigated are:

- The Proportional Integral and Phase Advanced controller with optimisation using the Genetic Algorithm (GA)
- GA optimisation of the Proportional Integral and Phase Advanced controller with additional actuator stiffness.
- The Feed forward controller and also the optimisation technique.
- Model based control using the Linear Quadratic Regulator (LQR) and the Linear Quadratic Gaussian (LQG) technique.

All the controllers were developed taking into consideration the actuators attached to the suspension (i.e. the interaction of both systems are considered). The simulation studies discussed in this thesis show that implementing practical classical and also optimal based controllers on the actuators across the secondary suspension with the consideration of the vehicle dynamics has not only improved the straight track ride performance, but has also reduced the force produced by the actuators in the suspension and hence reduces the actuator losses through inefficiencies. This has made the effort to approach the ideal performance possible.

Three conference papers and a journal paper have arisen from the work described. Herein:

H. Md. Yusof, R.M.Goodall, R. Dixon, (2010). "Active railway suspension controllers using electro-mechanical actuation technology", UKACC International Conference on Control

H. Md. Yusof, R.M.Goodall, R. Dixon, (2010). "Assessment of Actuator Requirements for Active Railway Suspensions", 5th IFAC Symposium on Mechatronic Systems, Cambridge, MA, USA, pp.369-376.

H. Md. Yusof, R.M.Goodall, R. Dixon, (2011). "Controller Strategies for Active Secondary Suspension Actuators", Proc 22nd Symposium on Dynamics of Vehicles on Roads and Tracks, Manchester, UK, pp.1-7, ISBN: 978 1 905476 59 6.

H. Md. Yusof, R.M.Goodall, R. Dixon, (2012). "Controller strategies for active secondary suspension actuators" to Control Engineering Practice (CEP). Submitted.

1.6 Summary

This chapter briefly introduced the on-going trends in railway transportation and the tendency of development for future practical applications of fully active secondary railway vehicles. The research problem is defined; the new concept for solving the active suspension actuator technologies problem is proposed and the aim of the research is identified with the contribution of the thesis highlighted. Finally, the objectives for achieving the aim are presented. The thesis structure is also laid out in this chapter.

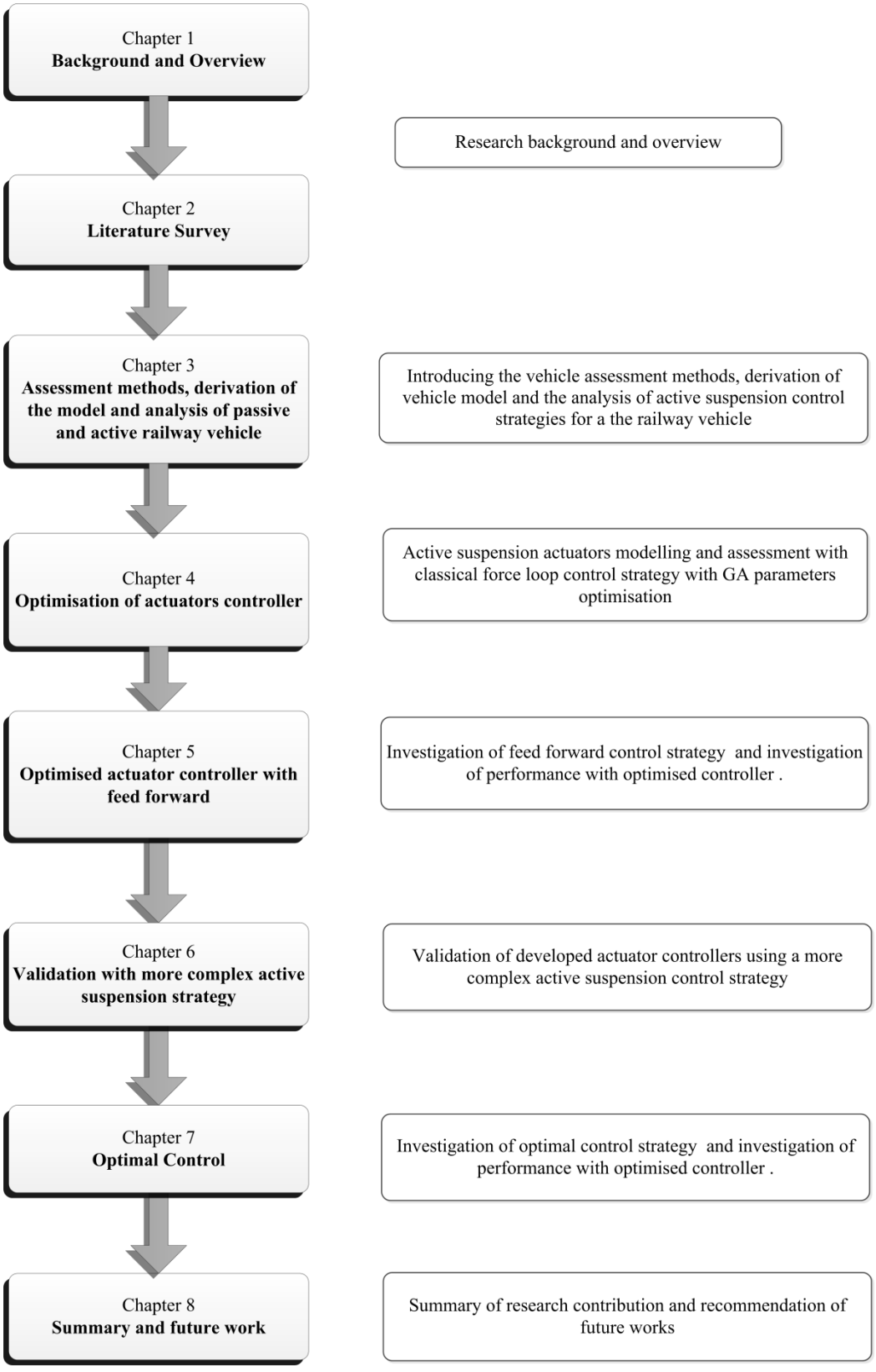

Figure 1.9 : Thesis flow chart

Chapter 2

Literature Review

This chapter discusses the related research into active suspension for railway vehicles. Background research has been done for vehicle active suspension, especially for railway and automotive vehicles. While there is significant research in both industries, this survey is limited to papers that include active suspensions for secondary suspension, concentrating on the improvement of ride quality. Literature on actuator technologies for active suspensions is then examined, and their issues within the suspension described. This chapter will investigate current and previous research on improving active secondary suspension actuator performance to achieve a 'real' active suspension rather than assuming an ideal actuator.

2.1 Introduction

Modern railway vehicles have improved tremendously from being purely mechanically engineered to being increasingly electronically dependent. Over the past five decades, railway industries have been actively researched and tested for active suspension

implementation. Although the suspensions remain as an aspect of vehicle design, the introduction of electronic control remains quite limited. Active suspension research is formed by active devices such as actuators, sensors, and computer modelling which represents the vehicle. Active suspension equipped vehicles should have the ability to isolate the passengers from track irregularities and provide an improved ride comfort, which is one of the issues in the railway industry. Passive configurations have reached their performance limit which makes the active suspension more promising for light weight high-speed railway vehicles.

Numerous studies on ground vehicles, especially automotive and railway vehicles, have been carried out in the past fifty years, highlighting the benefits of active suspension and also different kinds of power suspension. The focus in this research is on understanding the key issues for different kinds of actuators for active railway suspension, and then developing control strategies to ensure effective operation.

2.2 Overview of active secondary suspension research

Although the passive system currently in use has a considerably good reputation, it has however reached its performance limit due to the inherent trade-offs to be met in the design process (Pratt (1996) ; Goodall and Kortum (2002) ; Goodall (2009)). As early as the 1930s, the active suspension system was developed, but has only been seriously researched and developed 30 years later (Hedrick (1981) ; Goodall and Kortum (2002)). Active suspension has been reported in numerous publications for its excellent performance and adaptability to various types of track characteristic (Li and Goodall (1999) ; Orvnas (2008)).

Active control provides improved suspension performance, which gives a better ride quality for the passengers. Much more important is the ability to operate at high speeds whilst achieving the same ride quality, which is much the same philosophy as with tilting trains (Goodall (1997)), and in some cases it is possible that both tilt and an active secondary suspension (lateral and/or vertical) are needed. An alternative approach is to provide the same ride quality on a poorer track, in which case the objective is to reduce the track maintenance cost, and hence the operating cost of the railway (Goodall (1999)).

In the area of railway transportation, active control is meant to improve the ride comfort for the passengers. This is important as the competition from other means of transportation increases with the advancement of technologies. Other modes of transportation can easily incorporate the latest technologies and research findings, since modification does not cost as much compared to the railway industry.

Although the research for railway vehicles aimed at improving ride performance has been carried out extensively both theoretically and in laboratories, implementation requires much careful thought and validation as the cost is extremely high if not done properly. The design of the suspension plays an important role in achieving a good ride performance and also the safety of the vehicle. Apart from the tilting trains, active suspension has yet to make a breakthrough to the railway vehicle industry, even though the benefits are significant (Goodall (1999) ; Zhou (2010)).

The growing interest in active suspension is sparked by the possibility of introducing active elements such as sensors, actuators, and processors into the system (Pratt (1996) ; Goodall and Kortum (2002)). The motivation is also provided by the great efforts of the United States and European countries to improve ride quality for railway vehicles travelling at speeds higher than 200km/hr. Some general literature reviews and the background of active suspension are discussed, and serve as a good introduction to active suspensions, such as Karnopp and Heess (1991), Appleyard and Wellstead (1995) and Williams and Haddad (1997).

A number of state-of-the-art reviews on active suspension benefits to railway vehicles, emphasising ride quality and performance, have been published. In 1981, Hedrick published a review of state-of-the-art activities on railway active suspensions emphasising ride quality and performance. A similar review from the IAVSD activities was published in 1983 by Goodall, with another up-to-date version published in 1997. This was followed by the collaboration between Goodall and Kortum (2002) updating the mechatronics development of railway vehicles. This recently published paper was a more up to date review, covering the basics and classification of active suspension, current implementation and future ideas. The review also gives a speculative review of an actively guided railway vehicle without bogies, and future steer by wire railway vehicles. Active applications for suspensions are also given focus, with a promising future for active control and active element implementation for an electronically controlled

suspension. Another more recent survey by Bruni, et al. (2007), considers the application of various technologies to suspensions and running gears, with the focus on the complementary issues of control and monitoring. A comprehensive literature survey on concepts and previous works on active secondary suspension has also been provided by Orvnas (2008).

The performance of the active suspension has always focused on the improvement it offers with respect to its passive counterpart, and has often concluded with further discussion about possible advanced technologies to enhance the performance (Kortum, et al. (1998)). Reduction of the ride discomfort experienced by passengers mainly deals with the vertical vibration of the railway vehicle. The control of the vertical active secondary suspension can be categorised into classical and modern control methods.

The classical control of the secondary suspension is frequently used and adapted as it is less complicated (Williams (1986)) compared to modern based strategies, which makes a good starting point for the development of active railway suspension controller vehicles (Foo and Goodall (2000)). The 'skyhook' damping strategy was introduced by Karnopp (1983) and has usually been used as a starting point for the development of control strategies because this provides a better overall ride quality. This simple and informative strategy however has its trade-off, while encountering gradients that need to be accommodated, for example by carefully filtering out the low frequency components from the measurement such that the deflection outcome is reduced to an acceptable level (Williams and Best (1994)).

Modern control methods have been researched as a companion to classical control, both in terms of their robustness properties and also the provision of multi-objective solutions to eliminate the conflicting issues for the suspension performance requirements. Although better results are obtained, the controller normally results in being very complex and difficult to implement (Goodall and Kortum (2002)).

Active control technology for secondary suspension has been widely researched for lateral and tilting views, and the technology has improved to a level where the introduction would be straightforward. However, not much research has been done for the vertical direction as there are several issues that appear in this direction. Therefore it is important to identify possible solutions to improve the ride comfort for passengers. The

research in this area is very broad and covers many aspects of the rail vehicle from various directions. Therefore in this study, only the aspects of active secondary suspension which concentrate on the vertical view will be examined.

Several skyhook damping based controllers for the vertical view of the railway vehicle have been examined by Li and Goodall (1999) for a single stage suspension. Classical and modern based controller comparison has been carried out by Williams (1986), where modified skyhook damping, complimentary filters control and the optimal control method have been introduced into the secondary suspension control for the Maglev vehicle.

A comparative study by Pratt (1996) for active secondary suspension has been applied to British trains, in particular the MK III coach, comparing the classical control and modern control of the active secondary suspension. Foo and Goodall (2000) have applied skyhook control methods to compare with Linear Quadratic Gaussian (LQG) control as the active suspension controller of a flexible bodied railway vehicle. The benefits of optimal control for the stability and robustness of the whole system was tested in his thesis (Foo (2000)). These methods have also been explored by Paddison (1995), Pratt (1996), and Foo and Goodall (2000).

Another comparative study by Zheng (2011) has been performed to control the vehicle flexible body for reducing rigid and flexible modes using smart materials in addition to active suspension control. The classical method of modal control with skyhook damping, optimal control and the H- infinity control method were applied to the system.

Although there are many other active suspension control strategies that have been researched for other vehicle suspension directions, as well as other stages of the suspension, these will not be elaborated in detail as the concentration in this thesis is on the secondary suspension for the vertical direction. An example of other active suspension research in other directions would be the Japanese research conducted for eliminating the effect of lateral forces and the yawing movement on a seven degrees of freedom vehicle model (Sasaki, et al. (1994)). There is also the fully active lateral suspension system on the JR East E2 and E3 for the Shinkansen train that uses a sophisticated H-infinity controller and has exhibited improved performance for the yaw and roll modes of the vehicle body . Extensive reports on the active suspension control for tilting trains have also been provided by Persson, et al. (2009).

While many research attempts have been made to improve the suspension performance, very few have considered actuator dynamics in the system especially for reducing vehicle body vibration. Examples which have considered the importance of including actuators in the suspension to improve the ride performance are by Pratt and Goodall (1994), Foo and Goodall (2000), Pacchioni (2010), and the latest by Zheng (2011). Reports on other actuator placements for different modes have also been reported by other authors (Shimamune and Tanifuji (1995) ; Goodall (1997) ; Goodall (2009)). The next section will elaborate on the actuators that have been used for active secondary suspension especially for the vertical mode.

2.3 Actuators for active secondary suspension

While many research attempts have been made to improve the suspension performance, these have mostly assumed an ideal actuator. This assumption is that the actuator is able to provide any amount of force, irrespective of its stroke and velocity. However real actuators in active suspensions are subjected to operational constraints which makes achieving the ideal difficult. The ability of actuator technology in the suspension providing high frequency isolation has been questioned over the years of active suspension actuator research (Goodall, et al. (1993)).

Including the actuator in the suspension increases the system complexity compared to other actuator applications (Goodall and Speedie (2009) ; Md Yusof, et al. (2011)). An actuator implementing an active suspension function is not only required to provide negligible force at high frequency but should also be receptive to the fluctuation in the displacement across the actuator caused by track irregularities. This is a very important aspect which most actuator technology is unable to accommodate. Actuator technologies and their ability to respond to track irregularities, and their capability of providing effective control of the vehicle's dynamic modes, are the key issues in active suspension design.

A comprehensive analysis of the main actuator technologies (electro-mechanical, electro-hydraulic and electro-magnetic) has been carried out by Pratt (1996). The effects of including the practicalities of a variety of actuator technologies for railway active

suspensions indicated the degradation in performance which is introduced compared with the assumption of ideal actuators (Goodall, et al. (1993)). The degradation in the ride performance caused by actuator dynamics is noticeable and it is agreed that further action is required (Foo and Goodall (2000) ; Md Yusof, et al. (2010)).

The key issues in selection of an actuator are the bandwidth of operation, energy consumption, size, weight and cost. Several types of actuators have been studied and the advantages and disadvantages compared. General studies on common actuator technologies have been performed by various authors (Pratt (1996) ; Foo, et al. (1998) ; Kjellqvist (2002)) and compared to determine the best performance. In Europe, the major current applications are from Italy, Sweden, Spain and Austria. The majority of the actuators used here are for active tilting technologies and very few are for other directions of control.

There is also a limitation on the type or design of actuator to be used due to the compactness of the railway vehicle. Not only would this have an impact on the selection of actuators, but the selection of the actuator also depends on the trade-off of the actuator performance, complexity, the costs and energy demand of the systems, and the cost incurred, which means that only a few systems are released to the market.

The acknowledged possible actuator technologies for active railway suspension are servo hydraulic, servo pneumatic, electromechanical and electromagnetic. The possibilities of other actuators are also studied, though these types of actuators have yet to be tested and evaluated physically.

Actuators are an important component in an active suspension design to suppress the railway vehicle's vibration. A traditional approach is to locate the actuator across the secondary suspension. There have been suggestions to locate actuators at the inter connection between the coaches (Pratt and Goodall (1994) ; Goodall (2009)). Investigation on a third actuator in the centre has also been done by Foo (Foo, et al. (1998) ; Foo and Goodall (2000)).

2.3.1 Electromechanical

The electromechanical actuator has been developed over the last forty years to a state of high efficiency and reliability. An electromechanical actuator is powered by an electrical motor (AC or DC) which is able to rotate a screw mechanism (e.g. a roller or a ball screw). The rotary effect exerted upon the screw is transferred to a translational motion, or the force that acts on the body in which the actuator is mounted. In general electromechanical actuators are less compact than other actuator types (Pratt (1996)).

Pollard and Simons' (1983) studies on the electromechanical actuator led to an experimental research by Gautier et. al. during the late 1990s (Gautier, et al. (1999)). The studies justified that this actuator was chosen due to its low noise levels and compactness, which is contrary to the earlier statements by other authors. The early implementations of the electromechanical actuator were produced in the late 1970s by British Rail, where a prototype of a tilting train, APT (Advanced Passenger Train), was built and electromechanical actuators were adopted (Goodall and Pennington (1980)). The design of the APTs were far ahead of time, and the new technologies caused problems in the system (Pennington and Pollard (1983)). Another real life adaptation of this actuator was produced by Siemens SGP in the form of lateral suspension (Stribersky, et al. (1998)). Recently, electromechanical suspension based on a permanent magnet machine and a roller screw has been analysed by Kjellqvist and co-authors (Kjellqvist, et al. (2001)) for the lateral suspension, with suggestions on overcoming the design conflict between the size, temperature and dynamic properties. Pacchioni (2010) has looked at improving suspension performance by adding a stiffness in series with the electromechanical actuator for a two-axle railway vehicle with a single stage suspension, and evaluating the suspension with skyhook and LQG control strategies. Meanwhile Goodall and Speedie (2009) have made comparisons between actuator placements in the vehicle, in particular looking at inter-vehicle actuators rather than those across the secondary suspension.

2.3.2 Electrohydraulic servo

An electro hydraulic servo-drive consists of a control servo valve, linear hydraulic cylinder, flow or pressure control devices and transducers. This actuator is a specialist product and is used when reliability and proven performance are dominant (Goodall, et al. (1993) ; Cottell (1996)). This actuator has been compared and tested for the vertical secondary suspension with other actuators (Pratt (1996) ; Foo and Goodall (2000)). Experimental analysis on the performance of the hydraulic actuator compared to a pneumatic actuator has been carried out where it is noted that the controllable frequency of the hydraulic actuator is 10Hz compared to 2-3 Hz for the pneumatic actuator (Shimamune and Tanifuji (1995)). In terms of active suspension applications, there are many established research studies on hydraulics in the automotive industry, where the general concepts and methods of control can be applicable to the rail vehicle suspension (Satoh, et al. (1990) ; Williams (1997) ; Sam and Hudha (2006)). Investigation on electrohydraulic actuator placement in the suspension has also been demonstrated by Zheng (2011) for suppressing the vibration of flexible structures.

In general it has been suggested that this actuator would be particularly useful in a rail vehicle which has an existing hydraulic power pack installed, with the excess power being used to drive the active suspension (Goodall, et al. (1993)) . The hydraulic actuator is well studied and applied to railway applications. The main reason for this is due to its compactness, which makes it easy to fit in the narrow spaces between car body and bogies, although the hydraulic power pack is often quite a bulky piece of equipment.

2.3.3 Pneumatic

Principally pneumatic actuators are based on compressed air, where the air pressure is controlled, giving rise to the desired suspension characteristics. As described by Pollard and Simons (1983), in the vertical direction the air pressure in an already existing fixed reservoir volume can be actively controlled by a reservoir with variable volume.

The advantage with pneumatic actuators is that they can be linked to the existing pneumatic system of the vehicle, namely the air spring. This is a cheap solution and has

no leakage problems. However the large air compressibility means that the controllable bandwidth frequency is restricted to 2-3 Hz (Shimamune and Tanifuji (1995)), and the actuator efficiency is limited (Pratt (1996)).

In an investigation in a Japanese railway vehicle, a pneumatic actuator is examined and found to give a reduction in the lateral vibration of up to 50% at speeds up to 120 km/h. However, due to practicality and cost reasons, and also concerns over system reliability, the application of the pneumatic actuator has not been taken into further consideration (Tanifuji, et al. (2002)).

2.3.4 Other kinds of actuator and their benefits

The Electromagnetic actuator is an interesting active suspension actuator technology which has been studied for the Maglev (Magnetic levitation vehicle) system for use as low speed urban transport (Paddison (1995)). The record of the fastest train is a test train in Japan, which registered a top speed of 581km/hr, as reported by Givoni (2006). Research on this actuator for railway secondary suspension has been assessed by Williams (1986) for investigation purposes, although in reality the height and size of this actuator would be too large to operate across the railway secondary suspension spring. Another investigation by Foo (2000) examines the case of an electromagnetic actuator added in the centre of the car-body with an auxiliary mass of one tonne in order to suppress the symmetrical flexible mode. Although this is preferred because of its good frequency response (up to 50Hz), and also its robustness, it has its own drawbacks. The electromagnetic actuator suffers from a relatively high unit size and weight, which makes it unsuitable for use in the narrow place between the primary and secondary suspension. This actuator also has air gap variations between the magnets which causes it to be unstable, although this could be overcome with proper force feedback (Foo (2000)).

2.4 Genetic Algorithm optimisation

The Genetic algorithm (GA) technique has been investigated by many authors (Deb, et al. (2002) ; Coello Coello, et al. (2007)). GA is a search and optimisation tool, based on the genetic process of a biological organism in nature, which optimises as it evolves. This method, based on Darwinian principles, is a global, parallel, search and optimisation search which models the biological processes of natural selection and population genetics (Chipperfield, et al. (1994)). The method that was first proposed by Holland in 1975 has been successfully applied to fields of optimisation, machine learning, neural network, fuzzy logic controllers and others (Hong, et al. (2002)) and has been used by researchers in solving difficult problems such as parameters optimisation. While GA is not guaranteed to obtain the optimal solution, it does however provide appropriate solutions for a wider range of optimisation problems which other deterministic methods find difficult (Ayala and Coelho (2008)). The advantage of GA is that no gradient information and inherent parallelism in searching the design space is required, which makes GA a robust adaptive optimisation technique.

The use of simple GA in control applications has limitations, since the parameter optimisation technique normally has several objectives to be fulfilled. Therefore a multi-objective GA is required. A multi-objective GA is a modified version of the simple GA with the means to solve the selection of parameters to satisfy more than one objective. An example of a multi-objective toolbox is the one developed by the Department of Automatic Control and Systems Engineering at the University of Sheffield (Chipperfield, et al. (1994)), which caters for both single and multi-objective GA applications. Another example of a multi-objective GA toolbox is the Non-Dominated Sorting Genetic Algorithm (NGSA) developed by Srinivas and Deb (1994), which was later upgraded to NGSA-II, which addresses all the problems experienced by the previous computational complexity of non-dominated sorting, lack of elitism, and the need for specifying a tuneable parameter called the sharing parameter. The NGSA-II search method is convenient for users, since they are left to the task of setting the search spaces, the number of generation and population, the design of the objective functions and the constraints based on the requirements of the given problem, hence this GA application has been adapted. There are other multi-objective GA solution methods besides the one

mentioned, such as the Multi Objective Genetic algorithm (MOGA), the Vector Evaluated Genetic Algorithm (VEGA) and the Niched Pareto Genetic Algorithm (NPGA); each has its own speciality which will not be covered here as the main objective is optimise certain parameters of the actuator controller and not comparing the performances of the GAs.

As in railway engineering research, a number of published works have reported on the benefits and usefulness of GA. Among the recent applications for railway engineering in the Loughborough University Control System Group was one by Zhou (2010), where GA were used to optimise the controller parameters (PID and H-infinity) to reduce the trade-off for tilting control between curving performance and straight track ride quality. Michail (2009) has demonstrated a systematic approach, proposed to minimise the number of sensors used for the electromagnetic suspension system in order to satisfy the optimised deterministic and stochastic performance. The performance was also optimised by tuning the LQG and H-infinity controller parameters. Optimisation of the controller parameters and the fuzzy membership functions was obtained in the research on the Fuzzy-PID tilting control (Zamzuri, et al. (2007)). Other known GA optimisation research has been carried out to achieve the best compromise between ride-quality and suspension deflection for active suspensions of the inter-vehicle vertical active suspension controller (Mei and Goodall (2002)), and for optimising wheel profiles using GA (Persson and Iwnicki (2004)) (Persson and Iwnicki (2004)).

2.5 Actuator control

Including the actuator dynamics in the suspension has shown a degradation of the ride quality at higher frequencies (Goodall, et al. (1993) ; Md Yusof, et al. (2011)). The possibilities of intelligent actuators have been highlighted by Karnopp (Karnopp and Heess (1991)) and Williams (Williams (1994)) for the case of automotive vehicles. Several established control methods for the electrohydraulic actuator that had been used in the academic, industrial research and testing industry (mostly from the automotive and civil engineering field) had been reviewed by Plummer (2007). It has been highlighted that the improvement of the controller design had been done based on the knowledge of

the physical test system where in general, the test specimen dynamics are more complex. Therefore the techniques introduced are not universal, as each system has its own uniqueness and its potential must be explored individually.

While the research on the active suspension control law for railway vehicles is well established, there has not been any research on the control or regulation of the actuator for providing a better ride quality. This implementation of such local or inner loop control may have the capability of reducing the degradation at the primary suspension frequency. To date, this has only been a suggestion in the automotive industry, but it has not been researched yet in this industry or in the railway industry.

2.6 Summary

This chapter has covered previous works in active suspension control for improving the ride quality, and has discussed actuators that have been considered for active secondary suspension. The active secondary suspension actuator controller strategies have yet to be explored, therefore there are no direct references available. This gap in the literature provides the motivation for this research, and the justification for the original contribution arising from this thesis:-

1. The rigorous assessment of ride quality degradation due to real actuator technology.
2. The optimisation of actuator force control strategies in active railway suspension.
3. A consideration of applying advanced control concepts for actuator force control, i.e. Model based control approaches.

Chapter 3
Assessment Methods, Model Derivation and Analysis of Passive and Active Railway Vehicles

This chapter presents the development of the railway vehicle and also its performance assessment methods. The vehicle model developed is a linear and time invariant one which provides a satisfactory performance as its non-linear counterpart. The active suspension method of control is introduced to the vehicle to appreciate its benefits for the vehicle performance. The active suspension variables are also known as the idealised performance which, in this thesis, is the ultimate objective; these will be used to derive the actuator parameters in the following chapter. The measurements of the variables throughout this chapter and beyond are such that the ride quality is a quantified percentage of gravitational acceleration (%g), suspension deflection in millimetres (mm) and suspension controls in

Newtons (N). The vehicle model is evaluated with time history and power spectral density analysis to calculate the acceleration r.m.s as a measure of ride performance.

3.1 Track Profile

Railway vehicle suspensions are subjected to various inputs. The most common input terms for the vertical suspension are the stochastic and deterministic inputs. The stochastic inputs represent the irregular track surfaces which are also the misalignment of the track, and the deterministic input is an intended feature of the track such as a gradient for the vertical suspension or curve for the lateral suspension. An additional input that will not be discussed in this thesis would be the force input, which is normally applicable for lightweight vehicles that have a higher load variation compared to the high-speed vehicles.

3.1.1 Random Input

The track irregularity that is used in this thesis is representative of the measured and recorded track accepted by the UK Railway and also by other railway administrations. The recording is done based on a number of routes using high speed recording coaches. The data are frequently approximated as the fourth order relationship and represented by a spatial power spectrum as in equation (3.1):

$$S_s(f_s) = \frac{A_r}{f_s^2 + 5.86 f_s^3 + 17.29 f_s^4} m^2\ (cycle/m)^{-1} \tag{3.1}$$

where A_r is the vertical track roughness and f_s is the spatial frequency of the track in $cycle/m$. In assessing the secondary suspension, it is widely accepted to approximate equation (3.1) with a simpler expression by neglecting the higher terms as in equation (3.2).

Equation (3.2) is a simplified equation of the track spectrum that can be used as an approximation of equation (3.1):

$$S_s(f_s) = \frac{A_r}{f_s^2}\ m^2(cycle/m)^{-1} \tag{3.2}$$

The track information in equation (3.2) needs to be converted into a temporal form in order to be suitable for use in dynamic analysis. The principal dynamic modes of a railway vehicle lie within 0.1Hz and 20Hz. At these frequencies the dynamic modes of the railway vehicle will be excited by track inputs. The relationship between the spatial and temporal frequencies, f_t , is given by equation (3.3):

$$f_s(cycle/m) = \frac{f_t}{v}\ \frac{(cycle/s)}{(m/s)^{-1}} \tag{3.3}$$

The conversion of the spatial expression in equation (3.2) to a temporal frequency is given by the series of equations (3.4) to (3.8). Substituting (3.3) into (3.2), the track wavelengths in terms of the temporal frequency, f_t is given by:

$$S_T(f_t) = \frac{A_r \mathrm{v}}{f_t^2}\ m^2(Hz)^{-1} \tag{3.4}$$

Vehicle models are developed upon velocity input rather than a displacement. This is because the wheel sets are connected directly to the dampers, which necessitate track velocities as an input when the models are expressed in state-space formation. Converting the vertical track displacement spectrum (3.4) into a velocity input requires several

operations. Equation (3.4) has to be expressed in 'radian' terms instead of 'cycles' as shown in (3.5):

$$S_T(f_t) = \frac{A_r v}{2\,\pi\, f_t^2}\, m^2 \left(\frac{rad}{s}\right)^{-1} \tag{3.5}$$

Then the derivative of the above spectrum is obtained by simply multiplying the spectrum with $(2\pi f_t)^2$:

$$\dot{S}_T(f_t)\ (m/s)^2(rad/s)^{-1} = S_T(f_t)\, m^2(rad/s)^{-1} \times (2\pi f_t)^2 \tag{3.6}$$

This produces:

$$\dot{S}_T(\omega_t) = 2\pi A_r v(m/s)^2(rad/s)^{-1} \tag{3.7}$$

The final adjustment to equation (3.7) is required to convert the expression back to a 'cycles' term, which is shown in equation (3.8):

$$\dot{S}_T(f_t) = (2\pi)^2 A_r v(m/s)^2(Hz)^{-1} \tag{3.8}$$

The vertical track spectrum is 'flat' over all frequencies and it is essentially 'white noise' with a Gaussian distribution. The approximations made earlier ignore the fourth order expression in terms of a simpler inverse-square relationship, giving rise to the infinite bandwidth of this white noise, otherwise a high frequency roll-off of the expression given by (3.1) would occur, giving rise to a finite bandwidth velocity spectrum. In this thesis the random track input is generated from equation (3.8) with a track roughness, A_r, of 2.5×10^{-7} m, which represents a good track quality, and a velocity of 55m/s is used throughout this thesis.

3.2 Vehicle assessment to stochastic inputs

The analysis of the performance of a railway suspension relies on the accuracy of the ride quality and the track following capabilities in responding to the stochastic track features as detailed in Section 3.1. The ride quality is generated in response to a straight track and generally represented by the root mean square (r.m.s) acceleration experienced by the passenger when the vehicle is excited by the track roughness. The reason for this representation is because the deterioration in the ride quality perceived by the passengers is not a definite measurement. There are other factors that could affect the passenger's judgement and view such as the vehicle interior and also the passengers' personal opinion of the ride which is not a measurable item. Also a frequency weighted r.m.s calculation to allow for human susceptibility to different frequencies is commonly used for ride quality assessment, but this can lead to significant issues, so for a research study, the unweighted r.m.s is a sensible measure. Calculation of the r.m.s acceleration is frequently analysed using these three analysis methods: frequency response analysis, covariance analysis and also time history analysis.

3.2.1 Frequency domain analysis

The frequency domain technique can be used to evaluate vehicle ride accelerations and also the suspension deflections in response to track irregularities, and also the p.s.d. plots of the signals of interest.

Frequency response is a classical analysis of a control system where the transfer function provides a concise description of the system behaviour. In a linearised analysis, the use of the frequency response function has been the basis of frequency response analysis. Here the r.m.s acceleration level is determined from the acceleration spectrum resulting from the combination of the vehicle suspension transfer function and the track input spectrum.

The output power spectrum, $S_y(\omega)$, is equal to the square of the magnitude of the system transfer function of the frequency response, $H(j\omega)$ multiplied by the input power spectrum, $S_x(\omega)$:

$$S_y(\omega) = |H(j\omega)|^2 S_x(\omega) \tag{3.9}$$

The equation $H(j\omega)$ needs to be modified to take into account the delays between the front and rear vehicle which involves the delays between the bogies and also the wheel-sets. The transfer function of the front and rear velocity inputs to the output with the delays should be included to calculate the r.m.s. values from the equation below:

$$\sigma(\omega) = \sqrt{\int_0^\infty |H \quad (j\omega)|^2 S_x(\omega)} \tag{3.10}$$

Equation (3.10) requires numerical integration to infinity which is not practically possible. Therefore, in practice, the calculation uses a finite limit instead of the required numerical integration to infinity. This is not a problem for railway vehicle analysis as the higher frequency components are always attenuated by the suspension dynamics and the effect is negligible. Details of the use of the frequency domain to evaluate the rail vehicle with time delay p.s.d. plots are given in Section 3.6.2.

3.2.2 Covariance analysis

The covariance analysis is a Lyapunov equation approach, based upon the differential equation for the covariance matrix which is related to the state equation of the vehicle. The vehicle model can be represented in its linear state space formulation:

$$\dot{x} = Ax + B_w\dot{\zeta} \tag{3.11}$$

$$y = Cx + D_w\dot{\zeta} \tag{3.12}$$

where A is the system matrix and C is the output matrix. B_w and D_w are the disturbance inputs, while ζ is the track input being represented by a random white noise process described in Section 3.1.1.

The r.m.s. value of the outputs is calculated from the solution of the Lyapunov equation. The model does not contain direct feed through (i.e. it is strictly proper), therefore the matrix D_w is zero.

The auto correlation function of the track input is derived from the track p.s.d. function which is given by (3.13):

$$E\{\zeta(t)\zeta^T(t+\tau)\} = \int_{-\infty}^{\infty} S_T\left(\frac{\omega}{2\pi}\right) e^{\omega\tau j} d\omega \tag{3.13}$$

Integrating the auto correlation equation (3.13), means the equation could be stated simply as:

$$E\{\zeta(t)\zeta^T(t+\tau)\} = (2\pi)^2 A_r v\, \delta(\tau) = q_\omega(\tau) \tag{3.14}$$

The variance, $q_\omega(0)$, is the value of the correlation function at zero. The system given by equation (3.12) is excited by the random track input, which is a Gaussian white noise process. Equation (3.11) is subjected to a single random track input which is applicable for a two mass model. For a vertical side-view vehicle, the theory needs to be extended to include a time delayed wheel input. This will be used in the Lyapunov equation to provide the stationary state covariance matrix P_{xx} of the system:

$$AP_{xx} + P_{xx}A^T + B_w q_w B_w^T = 0 \tag{3.15}$$

where P_{xx} is a positive definite square matrix, and is symmetric if $B_w q_w B_w^T$ is symmetric. The covariance of the output vector is given by:

$$P_{yy} = CP_{xx}C^T \tag{3.16}$$

For the railway vehicle length and the travelling speed at $v\ (m/s)$, there will be a time delay due to the distance between the bogies and also between the front and rear suspension. The detailed auto correlation function of the track inputs can be found in Pratt (1996).

3.2.3 Time domain analysis

In time domain analysis, the r.m.s. of the vehicle model output signal responses is investigated with respect to the track data recordings. The r.m.s. value for a given output can be found using equation (3.17).

$$y_{r.m.s} = \sqrt{E[\,y^2(t)]} \tag{3.17}$$

or approximately

$$y_{r.m.s} \approx \sqrt{\frac{1}{n}\sum_{i=1}^{n} y_i^2} \tag{3.18}$$

where n is the number of elements in the data sample.

To analyse the frequency information of the signal, the Fast Fourier Transform (FFT) can be performed on the output response of the railway vehicle model by simulating it with the track data.

Clearly, the accuracy of the r.m.s. value depends upon the available duration of track data and the number of sample points n. The same applies if an FFT is performed; a sufficient number of points should be used to reveal accurate information concerning the signal frequency content.

The time analysis is the best solution when the model contains non-linearities. The frequency domain and covariance analysis described in the previous two sections could only be used to evaluate a vehicle with a linear state space format.

3.3 Modelling of a single railway vehicle

The dynamics of a real railway vehicle have significant nonlinearities which include the air spring behaviour, damper blow offs, and bump stop contact. Many modes of the vehicle are highly coupled which makes the vehicle dynamics very complex. The mathematical model

developed in this thesis is however linear and time-invariant. The real vehicle system operates about a static equilibrium position and for small perturbations around this point. This linear model can be used as a representation of the actual system.

Figure 3.1 shows the simplified mathematical model of the side-view railway vehicle, where the development includes the vehicle body, two bogies and four sets of wheels connected by relatively stiff primary vertical suspensions. The vehicle body and the two bogies each have two degrees of freedom, i.e. bounce and pitch mode. The secondary suspension from the bogies to the vehicle body is an air spring which consists of an air bag connected to a surge reservoir through a restricting orifice (Williams (1986)).

In order to study the vehicle vibration characteristic, the equations of motion based on Newton's second law for each mass are formulated. The vehicle body is influenced by passive secondary suspension components (springs and dampers) and by the active forces, f_f and f_r , if active suspension is implemented, these forces being produced by the actuators. The primary suspensions are influenced by both passive and active forces along with the track inputs. Therefore to model this system, the forces acting on each mass can be used to create the motion equation of each mass.

The passive side-view model has 18 states which includes four integrators to generate track positions $\left(\dot{z}_{t_{11}}\ \dot{z}_{t_{12}}\ \dot{z}_{t_{21}}\ \dot{z}_{t_{22}}\right)^T$ from track velocity inputs. The body and the two bogies each have four states for the bouncing and pitching motions, and the air spring models have an extra two states in order to describe the motions of the series spring-damper combinations.

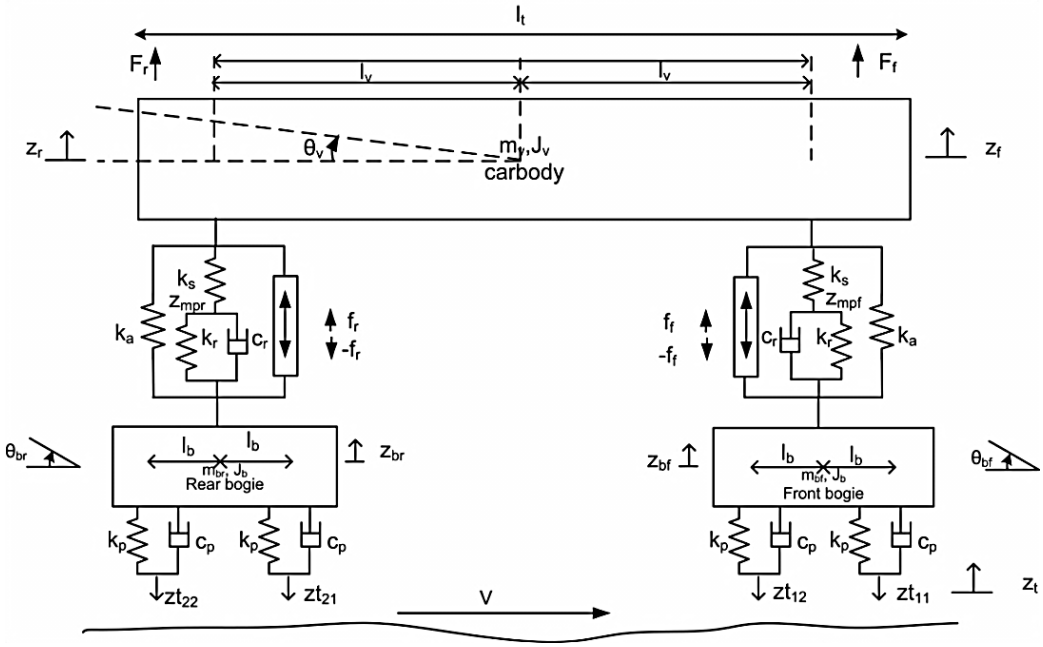

Figure 3.1: Side-view model of a single railway vehicle

From Figure 3.1, the displacements of the body at the front and rear secondary suspensions are given by equations (3.19) and (3.20):

$$z_f = z_v - l_v \cdot \theta_v \tag{3.19}$$

and

$$z_r = z_v + l_v \cdot \theta_v \tag{3.20}$$

where z_f and z_r are the vertical movement of the front and rear suspension, with θ_v as the pitch angle.

Figure 3.2 shows the air spring representation used in the model. The air springs consist of an air bag connected to a surge reservoir through a restricting orifice. This air spring model is drawn from the work of Williams (1986), which was adapted from Oda and Nishimura (1970), and is an acceptable representation of a conventional air spring dynamics with an auxiliary reservoir.

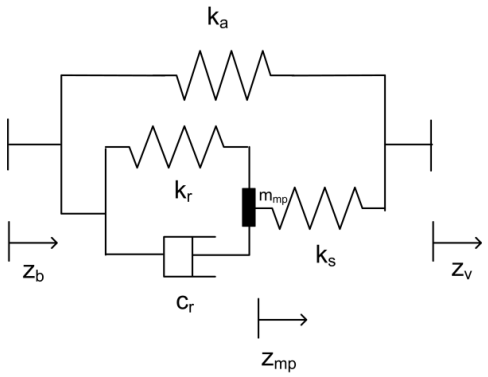

Figure 3.2: Air spring model

Equations (3.21) and (3.22) are the expressions of the internal dynamics of the front air spring and the rear air spring which adapts to fit into the framework of the side-view model. The change of area stiffness (k_a), which is usually small, has been assumed to be almost zero. The air spring mid-point mass, m_{mp} , is very small with respect to the rest of the vehicle system. Setting this mass to zero will lead to modelling procedure breakdown. But, the introduction of such a small mass can lead to simulation problems due to an imbalance in mixture modes present in the system. Therefore the air spring equation can be re-written to be placed in a state space model.

$$\ddot{z}_{mpf} = \frac{1}{m_{mpf}}\left[c_r\dot{z}_{bf} + k_r z_{bf} - c_r\dot{z}_{mpf} - (k_s + k_r)z_{mpf} + k_s z_{bf} + k_s l_t \theta_v\right] \tag{3.21}$$

$$\ddot{z}_{mpr} = \frac{1}{m_{mpr}}\left[c_r\dot{z}_{br} + k_r z_{br} - c_r\dot{z}_{mpr} - (k_s + k_r)z_{mpr} + k_s z_{bf} - k_s l_t \theta_v\right] \tag{3.22}$$

The passive air spring suspensions are restrained because they carry the weight of the vehicle, and their characteristics have been left unchanged because of the emphasis on the actuation control rather than on overall optimisation of the ride quality.

Applying Newton's second law and using the static equilibrium position as the origin for both the linear displacement of the centre of gravity, z_v, and the angular displacement of the vehicle body, θ_v, the equations of motion for the system are formulated. The equation of

motion for the bounce (balancing force in z direction) is given by equation (3.23), and the motion for the pitch moment is shown in equation(3.24).

$$\ddot{z}_v = \frac{1}{m_v}\big(-2(k_s + k_a)z_v + k_a z_{bf} + k_a z_{mpf} + k_a z_{br} + k_s z_{mpr} + f_f + f_r\big) \tag{3.23}$$

$$\ddot{\theta}_v = \frac{1}{J_v}\big(k_a l_v z_{bf} + k_s l_v z_{mpf} - k_a l_v z_{br} - k_s l_v z_{mpr} - 2(k_a{+}k_s)l_v^2\theta_v + l_v f_f - l_v f_r\big) \tag{3.24}$$

The equations of the bounce and the pitch motion for the front and rear bogies are derived in a similar manner as shown in equations (3.25)-(3.28).

The front bogie is given as:

$$\ddot{z}_{bf} = \frac{1}{m_b}[(k_s + k_a)z_v - \big(k_a + 2k_p\big)z_{bf} - 2c_p\dot{z}_{bf} - k_s z_{mpf} + (k_s{+}k_a)l_v\theta_v + k_p z_{t11} + c_p\dot{z}_{t11} + k_p z_{t12} + c_p\dot{z}_{t12} - f_f] \tag{3.25}$$

$$\ddot{\theta}_{bf} = \frac{1}{J_b}\big[-2k_p l_v^2\theta_{bf} - 2c_p l_v^2\dot{\theta}_{bf} - c_p l_v\dot{z}_{t11} - k_p l_v z_{t11} + c_p l_v\dot{z}_{t12} + k_p l_v z_{t12}\big] \tag{3.26}$$

and the rear bogie is given as:

$$\ddot{z}_{br} = \frac{1}{m_b}[(k_s + k_a)z_v - \big(k_a + 2k_p\big)z_{br} - 2c_p\,(k_s{+}k_a)l_v\theta_v + k_p z_{t22} + c_p\dot{z}_{t22} - f_r] \tag{3.27}$$

$$\ddot{\theta}_{br} = \frac{1}{J_b}\big[-2k_p l_v^2\theta_{br} - 2c_p l_v^2\dot{\theta}_{br} + c_p l_v\dot{z}_{t21} + k_p l_v z_{t21} - c_p l_v\dot{z}_{t22} + k_p l_v z_{t22}\big] \tag{3.28}$$

Equations (3.19)-(3.28) describe the system shown in Figure 3.1, and can be arranged in a state-space form for system analysis and further controller design:

$$\dot{x} = Ax + Bu + G\zeta \tag{3.29}$$

$$y = Cx + D_B u + G\zeta \tag{3.30}$$

where the state vector, *x,* is:

$$x = \left[z_v \;\; \dot{z}_v \;\; z_{bf} \;\; \dot{z}_{bf} \;\; z_{br} \;\; \dot{z}_{br} \;\; z_{mpf} \;\; z_{mpf} \;\; \theta_v \;\; \dot{\theta}_v \;\; \theta_{bf} \;\; \dot{\theta}_{bf} \;\; \theta_{br} \;\; \dot{\theta}_{br} \;\; z_{t_{11}} \;\; z_{t_{12}} \;\; z_{t_{21}} \;\; z_{t_{22}}\right] \tag{3.31}$$

$$\zeta = \left[\dot{z}_{t_{11}} \; \dot{z}_{t_{12}} \; \dot{z}_{t_{21}} \; \dot{z}_{t_{22}}\right]^T \tag{3.32}$$

The active force inputs are $u = \left[f_f \; f_r\right]^T$ for the front and rear suspensions, and ζ contains the four track inputs from the wheels in the front and rear bogies. The outputs of interest are the car body accelerations to determine the ride quality and the secondary suspension deflections, given by:

$$y = \left[\ddot{z}_v \quad \ddot{\theta}_v \quad \ddot{z}_f \quad \ddot{z}_r \quad \dot{z}_f - \dot{z}_{bf} \quad \dot{z}_r - \dot{z}_{br} \quad z_f - z_{bf} \quad z_r - z_{br}\right]^T \tag{3.33}$$

The nominal values of the vehicle parameters and the state-space model for this vehicle are extracted from a typical railway vehicle British Rail MK III coach (Williams (1986) ; Pratt (1996)) and are as given in Appendix A and B.

3.4 Railway vehicle model verification and simulations

3.4.1 Eigenvalue analysis

The eigenvalue analysis of the modelled side-view passive railway vehicle is carried out based upon the parameter values given in Appendix A. Table 3.1 tabulates the principal

eigenvalues of the side-view railway vehicle. Inspection of the damping and frequencies of the model shows similarity to the railway industry norms and also as compared to Williams (1986).

Table 3.1: Eigenvalues of the railway vehicle model

Model	Eigenvalue	Damping	Freq(Hz)
Body Bounce	-0.61 ± 4.28i	0.14	0.68
Body Pitch	-0.91 ± 5.24i	0.17	0.84
Front bogie Bounce	-21.60 ± 63.10i	0.32	10.6
Front Bogie Pitch	-39.60 ± 78.40i	0.45	13.97
Rear Bogie Bounce	-21.60 ± 63.10i	0.32	10.6
Rear Bogie Pitch	-39.60 ± 78.40i	0.45	13.97

3.4.2 Step responses

The vehicle model was verified by using sample step responses. The track velocity inputs, are given a pulse height of 0.01 m/s for 0.3s, corresponding to a 3mm increase in the track position. The delays between the wheelsets and bogies are given as 0.35s and 1 sec respectively as a test of the suspension performance response towards a given input. The actual time delays between the wheels in the same bogies are $2.l_b/v$, and the delays between bogies are $2.l_v/v$ where v is the speed of the vehicle. Figure 3.4 gives the acceleration and displacement of the suspension, where it is shown that the steady state of the acceleration falls to zero and the steady state displacement of the car body and the two bogies increases to 3mm, i.e. the bogies and body follow the track position.

The verification of the vehicle model using the eigenvalue and step response analysis on the passive model provides a confidence level on the accuracy of the system. In the next section this model will be extended to implement active control for the secondary suspension.

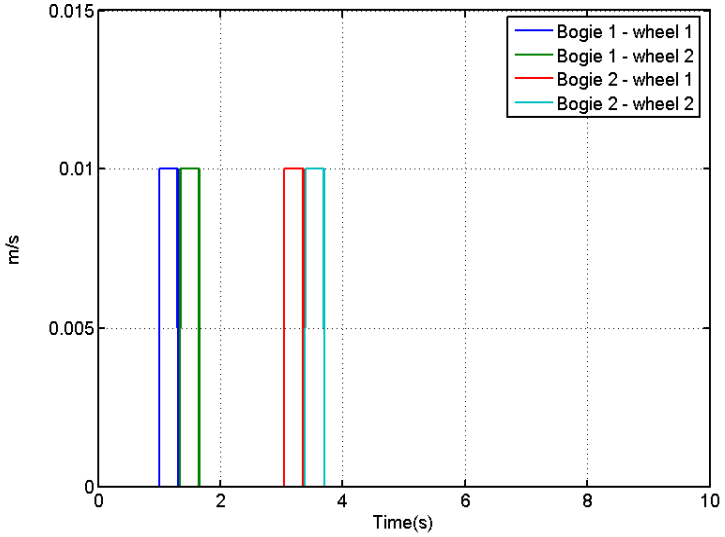

Figure 3.3: Step track inputs

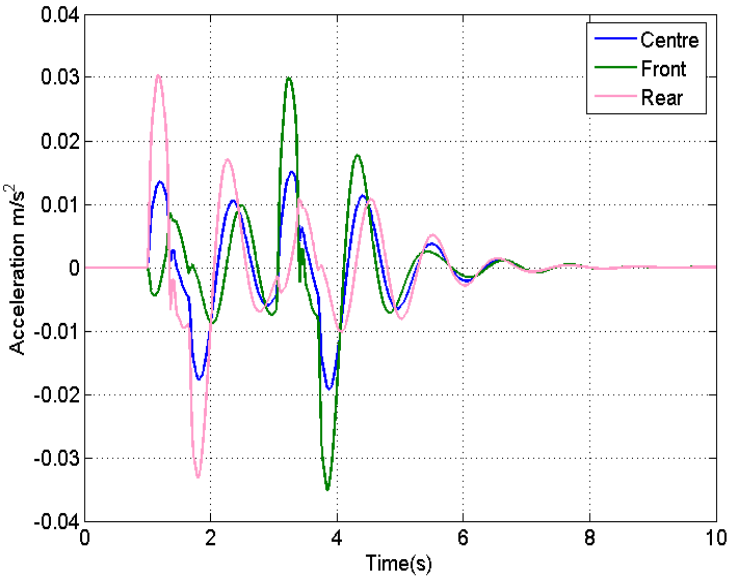

Figure 3.4: Vehicle body accelerations response to step track input

3.4.3 Ride acceleration analysis

The vertical acceleration of the vehicle body is analysed using the root means square (r.m.s.) values to evaluate the ride quality. The random track as described in Section 3.2.3 is used to quantify the ride quality by measuring the r.m.s. acceleration levels experienced by the vehicle body. The passive suspension r.m.s values are listed in Table 3.2.

Table 3.2: R.m.s. results for the passive vehicle

	Front	Centre	Rear
Acceleration (%g)	3.648	1.614	4.195
Deflection (mm)	12.3	/	9.1

3.5 Ideal active secondary suspension

Active control for the railway secondary suspension is used to isolate the vehicle body from the harshness of the track irregularities. Superior performance is achievable with active suspension compared to the passive which is highly dependable on the variation of the passive spring and dampers. Active suspension provides a much improved performance in terms of ride quality, or a satisfactory ride quality on a less well aligned track. In the second case the improvement makes the system much more cost beneficial to the rolling stock industry as the track maintenance cost can be reduced (Goodall and Mei (2006)).

Isolating the vehicle body from the vibration caused by the track irregularities method falls into three categories: adaptive passive, semi-active and fully active. Among the three methods, the fully active provides superior performance. A fully active suspension includes selecting suitable actuators and sensors, power requirements, closed loop performance, robustness and potential failure. This additional element in the suspension makes the system more complex but provides a better performance, which is either impossible or extremely difficult for a passive suspension to achieve.

A general scheme of active suspension is illustrated in Figure 3.5. From here it can be seen that the input and output relationship is provided by the suspension, and is dependent upon the configurations of the sensors and actuators and also upon the control strategy applied. This is in contrast to the passive suspension, for which the input and output relationship is determined solely on the passive components and also the geometrical arrangement of the vehicle.

Active control for secondary suspension can be used for the various directions in a number of possible configurations. This of course will affect the corresponding mode of the direction (i.e. vertical –pitch, lateral-yaw, roll-tilt).

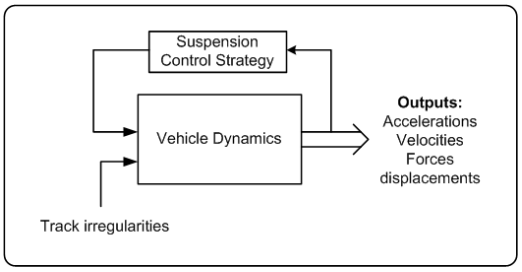

Figure 3.5 : Active suspension configuration

Active control with “skyhook damping” is known to provide an excellent capability for active secondary suspension. The principle, which comes from the work of Karnopp in the 1970s, introduces a suspension force proportional to the absolute vertical velocity of the vehicle body as in Figure 3.6, as a replacement for, or together with, a passive damper.

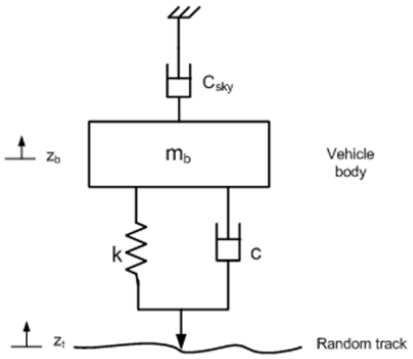

Figure 3.6: Skyhook damping

This strategy introduces a force proportional to the relative velocity across the suspension. The control action of the skyhook damper is dependent on the absolute velocity of the vehicle body, $\dot{z}_b$:

$$f_{act} = -c_{sky}\dot{z}_b \tag{3.34}$$

where f_{act} is the control force or the actuator force and c_{sky} is the skyhook damping gain. The damper connected to the absolute reference is a purely fictional configuration. This is because the absolute velocity is not practically measurable. Therefore it should be translated by integrating the accelerometer signal. The integrator is normally combined with a high-pass filter to form a "self-zeroing integrator", where the self-zeroing effect helps to minimise the problem of suspension deflection on gradients (Goodall and Speedie (2009)).

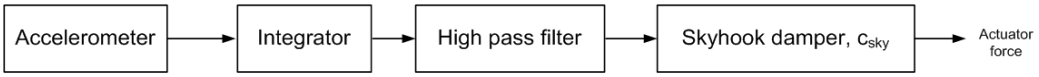

Figure 3.7: Practical skyhook implementation

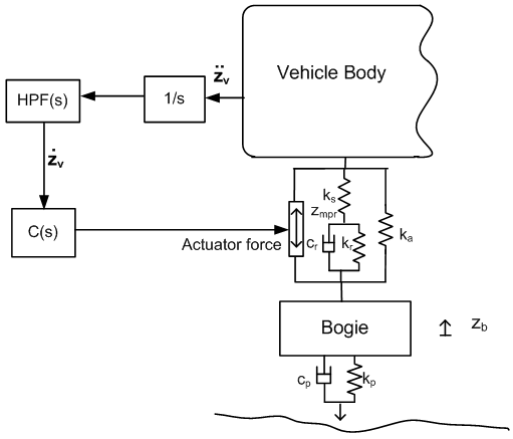

Figure 3.8 : Basic translated skyhook control

Figure 3.8 illustrates the active concept for a conventional actuator in the secondary suspension. In practice, the acceleration ($\ddot{z}_v$) of the vehicle body is measured above each bogie and integrated to derive the absolute velocity, ($\dot{z}_v$). A second order Butterworth high-pass filter (HPF) is chosen as in equation (3.35).

$$\frac{1}{s} \times HPF = \frac{s/\omega^2}{s^2/\omega^2 + 2\zeta\omega s + 1} \tag{3.35}$$

A cut off frequency, ω, of 0.1Hz, and a damping ratio of 0.7 is applied to the control strategy. Then the velocity is amplified with the skyhook damping, c_{sky} of 65kN/ms^{-1} , which then provides the "idealised" active force demand for the idealised or real actuator. Ideal values for the acceleration, velocity and force can be obtained with this active suspension configuration to derive the actuator parameters.

For the vertical side-view vehicle, the "*local"* or practical active secondary suspension control is included in this study. Another skyhook damping principle, the "*modal control*", is also adapted to manage different modes of the system which also enables different damping rates to be provided for the bounce and pitch modes.

3.5.1 Local skyhook control

The local control strategy with the skyhook damping for the side-view vehicle is a matter of appending the active control strategy to each end of the vehicle as illustrated in Figure 3.9.

The structure has the accelerometers above the secondary suspension at the front and rear of the vehicle to measure the accelerations, ($\ddot{z}_f$) and ($\ddot{z}_r$). The control demand, f_f and f_r , produced by the front and rear local control is fed into the corresponding actuator (ideal or real) which is physically placed in-between the vehicle body and the bogie.

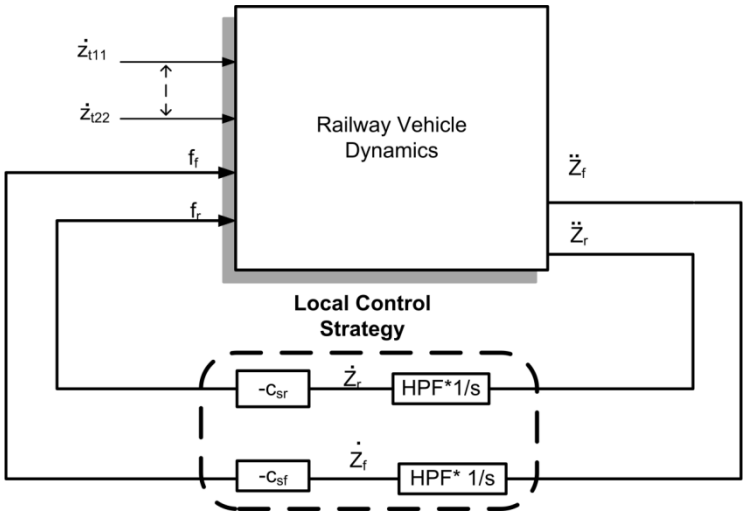

Figure 3.9: Local skyhook control strategy

The actuator forces for both sides are:

$$f_f = -c_{sf}\dot{z}_f \tag{3.36}$$

and

$$f_r = -c_{sr}\dot{z}_r \tag{3.37}$$

where z_f and z_r can be inferred from equations (3.19) and (3.20). Including equations (3.36) and (3.37) into (3.25) and (3.26) produces the following equations:

$$\ddot{z}_v = \frac{1}{m_v}\big(-2(k_s - k_a)z_v + k_a z_{bf} + k_a z_{mpf} + k_a z_{br} + k_s z_{mpr} - \big(c_{sf} + c_{sr}\big)\dot{z}_v - \big(c_{sf} + c_{sr}\big)l_v\dot{\theta}_v\big) \tag{3.38}$$

$$\ddot{\theta}_v = \frac{1}{J_v}\big(-2k_s l_v z_v - k_a l_v z_{bf} - k_s l_v z_{mpf} + k_a l_v z_{br} + k_s l_v z_{mpr} - 2(k_a l_v^2\theta_v + k_s l_v^2\theta_v) + \big(c_{sf} + c_{sr}\big){l_v}^2\,\dot{\theta}_v - \big(c_{sf} + c_{sr}\big)\dot{z}_v l_v\big) \tag{3.39}$$

From (3.38) and (3.39), it shown that the simplest choice about the system is to select $c_{sf} = c_{sr}$ to leave the modes uncoupled. The leaves the system configured in a manner similar to the passive, only with the advantage of the skyhook configuration which will be shown in Section 3.6.2.

3.5.2 Modal control

Modal control strategy is an extension strategy of the skyhook control strategy. This strategy works on the basis of the system modes being managed individually. The system measurements are decomposed individually and recombined to drive the actuators. The structure of the whole control system is shown in Figure 3.10.

Again there are accelerometers above the secondary suspension at the front and rear of the vehicle to measure the accelerations, ($\ddot{z}_f$) and ($\ddot{z}_r$), whereas the control demands, f_f and f_r , have been generated via the decomposition into modal components.

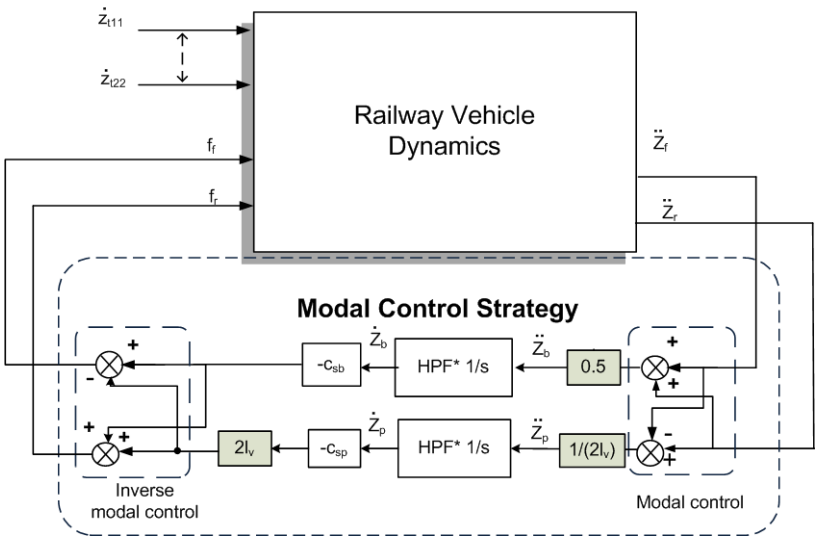

Figure 3.10 : Modal control strategy for the vertical side-view model

Building up the relationship between the bounce and pitch accelerations with equations (3.19) and (3.20), the bounce and pitch modes are derived by:

$$\ddot{z}_v = \frac{\ddot{z}_f + \ddot{z}_r}{2} \tag{3.40}$$

$$\ddot{\theta}_v = \frac{\ddot{z}_f - \ddot{z}_r}{2l_v} \tag{3.41}$$

and between the body velocities and actuator forces are:

$$f_f = -c_{sb}\dot{z}_v + l_v c_{sp}\dot{\theta}_v \tag{3.42}$$

$$f_r = -c_{sb}\dot{z}_v - l_v c_{sp}\dot{\theta}_v \tag{3.43}$$

where c_{sb} is the skyhook damper constant for the bounce mode, and c_{sp} is for the pitch. Implementing equations (3.42) and (3.43) into (3.23) and (3.24) results in:

$$\ddot{z}_v = \frac{1}{m_v}\left(-2(k_s - k_a)z_v + k_a z_{bf} + k_a z_{mpf} + k_a z_{br} + k_s z_{mpr} - 2c_{sb}\dot{z}_v\right) \tag{3.44}$$

$$\ddot{\theta}_v = \frac{1}{J_v}\left(-2k_s l_v z_v - k_a l_v z_{bf} - k_s l_v z_{mpf} + k_a l_v z_{br} + k_s l_v z_{mpr} - 2(k_a l_v^2\theta_v + k_s l_v^2\theta_v) - 2l_v c_{sp}\dot{\theta}_v\right) \tag{3.45}$$

From the derived equations (3.44) and (3.45), it clearly shows that the system has become completely uncoupled, and it is possible to apply different levels of control in particular to provide additional design possibilities for the active system. The choice of the cut off

frequency is carried out in a similar way to the local skyhook configuration, and the following damper rates of $c_{sb} = 80\ kN/ms^{-1}$ and $c_{sp} = 100\ kN/ms^{-1}$ satisfy the damping ratio of 0.7.

3.6 Results and analysis

3.6.1 Ride quality analysis

The performance of the vehicle model has been assessed for random track inputs as described in Section 3.1.1 for a travel speed of 55m/s. The root mean square (r.m.s.) values of the vertical acceleration of the vehicle body are used to evaluate the ride quality. All the accelerations are expressed in % g, the forces in kN and the suspension deflections in mm responding to the stochastic inputs. The ride quality of the passive vehicle model and the active suspensions are tabulated in Table 3.3. These results provide a benchmark for both the performance of the passive system and the performance with idealised actuators, against which the real actuator controller strategies can be assessed.

Table 3.3 : R.m.s results

	Accelerations (%g)			**Suspension Deflections (mm)**		**Force (kN)**	
	Front	**Centre**	**Rear**	**Front**	**Rear**	**Front**	**Rear**
Passive	3.648	1.614	4.195	12.3	9.1	/	/
Ideal (Local)	1.683	1.048	1.831	10.3	11.0	2.183	2.500
Ideal (Modal)	1.371	0.869	1.540	8.4	11.1	1.948	2.879

3.6.2 Frequency Analysis

The frequency analysis in Section 3.2.1 is implemented to the side-view vehicle taking account of the time delays. The body accelerations and suspension deflections in general are evaluated using equations (3.46) and (3.47):

$$\ddot{z}_{RIDE} = \sqrt{\int_0^\infty |H_{RIDE}(2\pi f j)|^2 S_T(f) df} \tag{3.46}$$

$$\dot{z}_{DEFL} = \sqrt{\int_0^\infty |H_{DEFL}(2\pi f j)|^2 S_T(f) df} \tag{3.47}$$

These equations will be used throughout the thesis for the vehicle model being developed, and onwards when the "ideal" and "real" actuators for active suspension will be discussed. Extension of equations (3.46) and (3.47) for the railway vehicle should include delays of the wheelset inputs. Although the wheelset inputs have the same input profile, it is however time delayed accordingly based upon the vehicle speed and also the vehicle geometry. The delays for a single rail vehicle with two bogies and four wheelsets are described in equation (3.48).

$$\dot{\zeta}(s) = \begin{bmatrix} \zeta(s) \\ e^{-s2l_b/v}\zeta(s) \\ e^{-s2l_v/v}\zeta(s) \\ e^{-s(2l_b+2l_v)/v}\zeta(s) \end{bmatrix} \tag{3.48}$$

The time delayed inputs in (3.48) and the state space model of the railway vehicle need to be combined to evaluate the ride quality and the suspension deflection for the side-view vertical train mode.

The p.s.d.s for the front, centre and rear accelerations of the vehicle with respect to the stochastic inputs are shown in Figures 3.11, 3.12, 3.13, respectively. The frequency responses between the wheelset vertical velocity input $(\dot{z}_{t11} - \dot{z}_{t22})$ and the body accelerations $(\ddot{z}_f, \ddot{z}_c, \ddot{z}_r)$ and also the suspension deflections (z_f, z_r) can be derived together with the track p.s.d. given by equation (3.8).

The p.s.d.s of the front and rear accelerations show the effectiveness of the active suspension strategies, which have reduced the peak at around 1Hz and have also improved the ride quality. The modal control strategy has resulted in better control for the overall system in terms of keeping the ride quality within 1%g and also keeping the ideal actuator force lower compared to the local strategy.

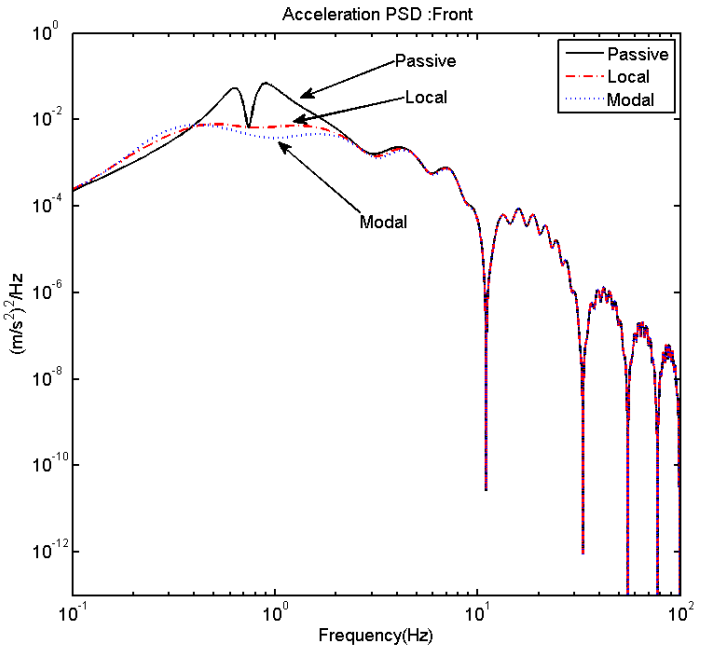

Figure 3.11 : Side-view model p.s.d.s – Front acceleration

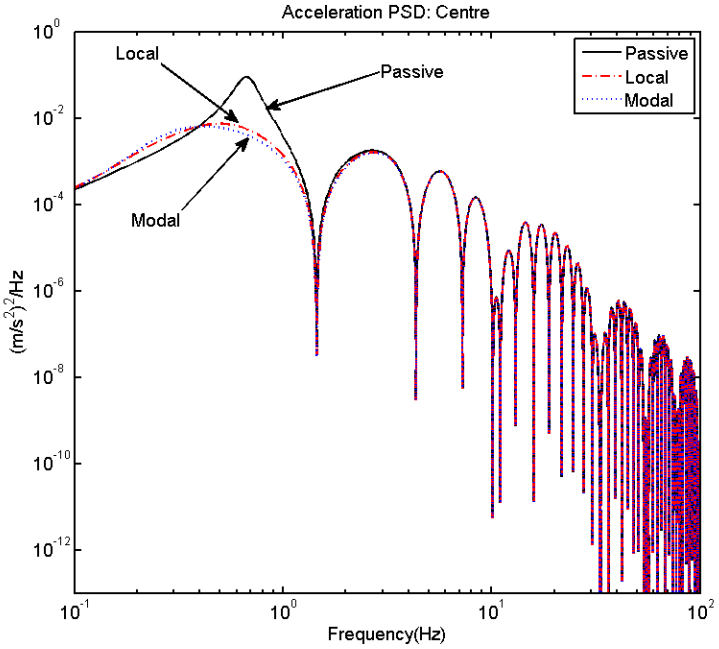

Figure 3.12: Side-view model p.s.d.s - Centre acceleration

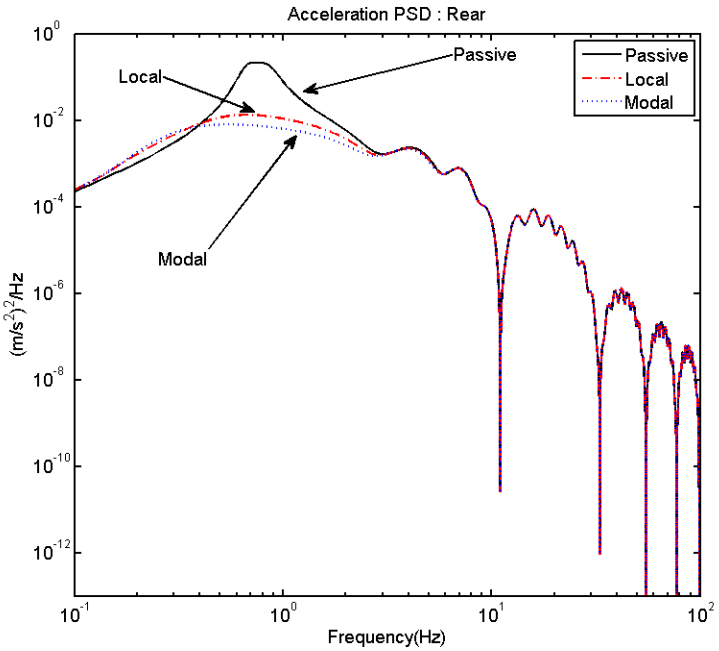

Figure 3.13: Side-view model p.s.d.s – Rear acceleration

3.7 Summary

This chapter introduced the representation of the random track input that is used in this thesis for assessing the vertical ride performance of the railway vehicle on a straight track. These techniques will be used in the following chapters to calculate the signals of interest in terms of frequency response analysis and also the calculation of the r.m.s. values. A side-view model vehicle has also been developed. Although there are significant non-linearities, a linear model has been considered because the system operates around a static equilibrium point which is used to develop a linear model. The model has been verified by checking the eigenvalues of the system and also for its step input response. This chapter has also introduced active control strategies based upon skyhook control strategies to eliminate the trade-off between resonance control and high frequency. The skyhook damping configuration, or absolute damping, involves a virtual damper connected to an inertial reference in the sky. This strategy has been translated to suit the application since pure skyhook damping is not possible. An accelerometer plus integrator is needed to derive the absolute velocity, although to overcome a long-term drift in the integrator, a high-pass filter has been introduced, which also reduces the size of deterministic deflection (which is not discussed in this thesis).

From this basic strategy, two different control strategies have been considered (local and modal) and applied. The introductions of these strategies and the results obtained have shown improvement in the suspension analysis which is not possible with the passive. The modal skyhook damping with the high-pass filter is the best configuration for the active system, giving a ride quality around 1% g and keeping the deflection upon stochastic input lower compare to the passive and local skyhook strategy.

Chapter 4

Optimisation of Actuator Control

This chapter contributes to the early stage of the thesis objectives which are to improve an actuated active suspension performance in the effort to achieve an almost ideal performance. Focus in this chapter will be on improving and applying corrective actions to the actuators in the suspension. This involves modelling, parameter selection and controlling the actuator according to the ideal suspension requirement. The actuator dynamics in the suspension are taken into consideration as part of the suspension performance analysis, where the actuators are placed within the secondary suspension, in parallel to the passive elements. Linearised representations of the selected actuators are used to match the real actuator behaviour. Although there are actuator non-linearities, it is usual to design with linear models in order to reflect the dynamic effects. The attention will be focused on the performance in comparison with the ideal performance at frequencies above 5Hz with the assumption that the low frequency response will remain satisfactory. Two methods to enhance the actuators' performance using the Genetic Algorithm are performed and this is followed by a 3Hz analysis of both actuators for a better understanding of the actuators' behaviour in the suspension.

4.1 Introduction

The actuator is an essential component of any active suspension and its performance has a significant impact on the overall success of an active suspension implementation. The ideal actuation which has been described in the previous chapter produces any amount of force required from it instantly, regardless of its movement in the suspension. An active suspension application is impossible to achieve without the use of real actuators. Practically, an actuator has to be fitted as a force generating device for the active suspension system. Designing the actuator is particularly difficult for an active suspension system and is not as straightforward as an actuator design in general. Therefore it is crucial to design the actuator from the active suspension perspective to approach the ideal performance.

It has been highlighted earlier that the actuators in the suspension suffer losses through their inefficiencies, which will limit the dynamic performance and in turn this places significant impact on the overall success of the active suspension implementation.

As a starting point, a classical force control loop is designed for the actuators and tested independently to check the actuator validity before being placed in the suspension. The performance of the active suspension considering the actuators with the interaction of the vehicle internal dynamics is highlighted. A corrective action is applied to the system and an optimisation technique is introduced. A consideration of the controller optimisation, including the actuator stiffness, is also presented. Finally an analysis at 3Hz for the actuators in the suspension is presented to determine the common issues for the actuators in the suspension, which will be given further attention in the coming chapters. The outline design and a dynamic model of the actuator developed for railway active suspension is illustrated in the simple flow chart as in Figure 4.1. The actuators parameter selection, basic control and the impact of the internal dynamic behaviour on the active suspension as a whole are all discussed in the following subsections.

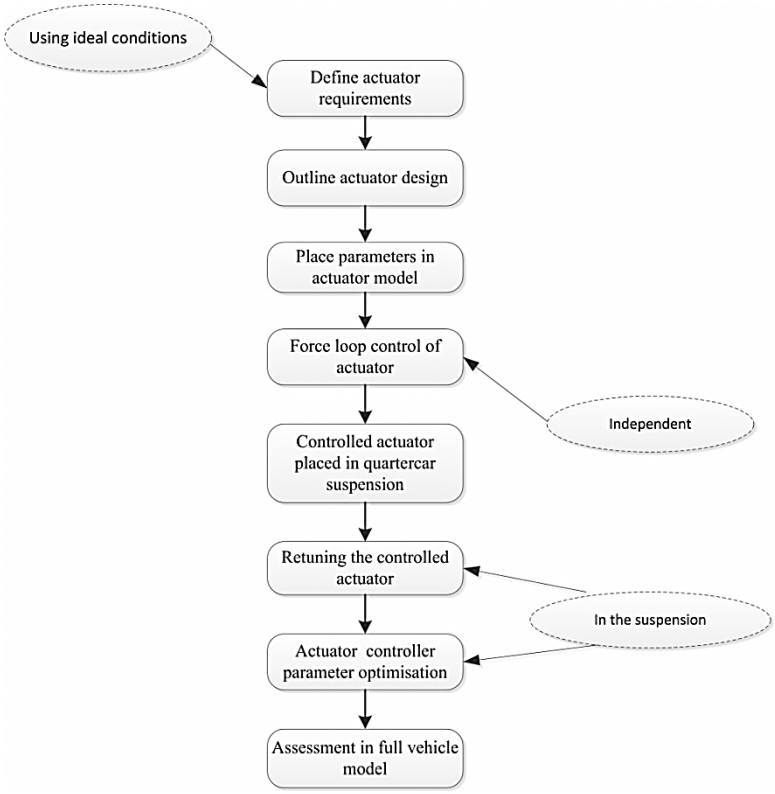

Figure 4.1 : Actuator modelling and assessment process

4.2 Selection of actuators for active suspension

Actuator implementation in an active suspension system has a significant impact on the overall success of the active suspension. As a force generating device, the actuator serves as an essential component of any active suspension. Studies by (Goodall, et al. (1993)) showed the overall success of the actuator in an active suspension compared with the passive suspension performance.

An actuator implementing an active suspension function would need to provide negligible force at these higher frequencies, while at the same time being susceptible to fluctuation in the displacement across the actuator, a role which many actuator technologies cannot readily accommodate (Pratt (1996)). As highlighted in Chapter 1, actuators placed in the secondary suspension as a replacement to the passive suspension makes the suspension behaviour completely controlled via active means. Although desirable, in practice it would be beneficial if the actuator is placed in parallel with the passive components. This arrangement

reduces the actuator size, while the passive component provides the constant force supporting the vehicle body mass in the vertical direction.

Figure 4.2 illustrates the basic model structure in which the input is the actuator input (here a voltage for the actuator) and the output is a force which is applied to the load (in this case a railway vehicle model). The actuator movement or the actuator velocity is essentially a "physical feedback"; it is determined by the effects of the actuator force (plus any external disturbances) upon the load and therefore cannot be deduced internally to the actuator itself. This brief illustration describes the complexity of the system which cannot be simply represented as an application-independent transfer function between the inputs and outputs of the actuator; this is the approach that is commonly used but is particularly inappropriate for an active suspension.

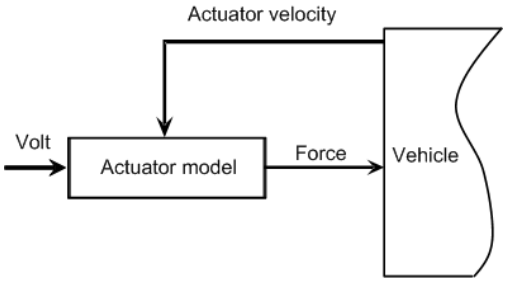

Figure 4.2 : Force controlled actuator scheme

There are three types of actuator technology that have been noted to be suitable for railway active suspension applications, some of which are readily available on active suspension test vehicles, and others which have been considered as possibilities. These actuators are the electrohydraulic, the electromechanical and the electromagnetic actuator. There are other actuation methods that have been taken into consideration; however most of them have their own drawbacks such as short stroke. These are still under development, which may lead to suitable active suspensions devices (Pratt (1996) ; Foo and Goodall (1998) ; Orvnas (2008)).

The selection of the actuator should be made by taking into consideration the possible benefits it would provide, which normally includes several main points. The logistics of selecting an actuator involve the maintainability and reliability of the selected technology, where the maintainability of an actuator is an important property. A complicated, difficult to

maintain actuator is likely to create problems, and will not be easy to manage, which would incur more cost. It is also important that active suspensions have a very good reliability and that the possibility of any failure lies within the capabilities of an appropriate maintenance programme.

The force to size ratio is also an important selection criteria for the actuator. The achievable force control bandwidth of an actuator is an understated issue in active suspensions and is frequently the reason behind the overly optimistic theoretical predictions of performance when compared with experimental assessments. An actuator is required to control the dynamic modes of the vehicle, which depends on the achievable force control bandwidth of the actuator. The force to size ratio for each of the actuators needs to be addressed to ensure that an actuator which is sized to provide the active suspension force and power level can fit within the confined space available between the body and the bogie. .While the performance of the actuator is important, the cost of each of the actuators must be considered due to the number of actuators required on a train to avoid significant cost increase over the existing rolling stock.

These properties are important in the context of an active railway suspension; other properties such as their cleanliness, noise production and hazardous nature have been omitted since it is assumed that these problems may be eliminated through the design of self-contained actuator units.

As the railway vehicles are designed to be compact, the selection of actuators is also limited. Electromechanical and electrohydraulic actuators are among the most suitable actuators used for active suspensions. For active suspension actuator control research, these two actuators are chosen due to the limited space available across the secondary suspension and the vehicle body. These actuators have also been used actively in the research of active suspensions.

4.3 Actuator modelling

4.3.1 Electromechanical actuator

The structure of the electromechanical actuator that is being used in this thesis is relatively simple, and it is easy to control. The electro-mechanical actuator used in this study has an electric motor driving a screw, where the rotary motion is converted to linear force through a highly efficient nut connected to the component to be driven. This arrangement normally has good reliability and efficiency excitation due to the armature of the motors. The input to the actuator is the armature voltage with a force output applied to the railway vehicle model as the load. For the active suspension application, there is however a physical feedback from the system into the actuator, i.e. the actuator movement across the suspension which will be discussed much later in this chapter.

Figure 4.3 illustrates the simpler version of the actuator. In practice, more complex arrangements such as the 'roller-nut' or 'recirculating ball screw' are generally used. 'Roller-nut' type actuators are similar to this construction only without an outer screw, but rather involve a planetary system which contains a series of rollers running along the main thread. Meanwhile, the 'recirculating-ball screw' mechanisms are different as they consist of a central pre-stressed screw thread which will cause the threads to form a race on which the ball bearing runs. However, the model used in this thesis is dynamically similar to these devices; the representation of the 'gearing' during rotary to linear motion conversion is described by this arrangement.

The equivalent schematic representation of the actuator is shown in Figure 4.4. While the motor turns, the compression of the screw generates force. A rigid conversion from the rotary to linear motion is produced through the ‘gearing’ motion. The stiffness and screw damping is represented by the springs and the damper on the right side of the figure. Although the screw thread will be stiff, it still possesses a finite stiffness and damping.

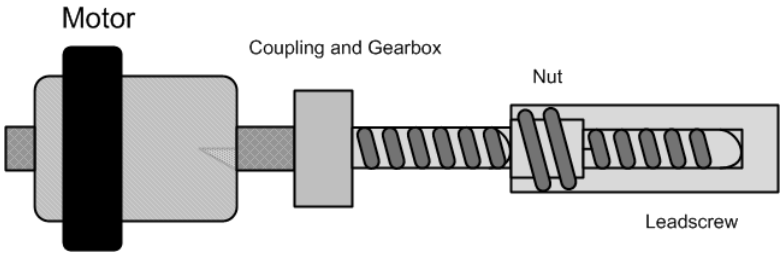

Figure 4.3 : Electromechanical actuator

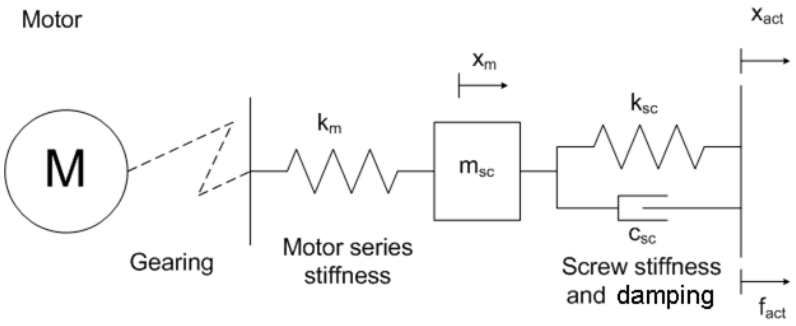

Figure 4.4 : Equivalent electromechanical actuator

The actuator is a combination of an electrical sub-system which is the motor, and a mechanical sub-system. A common actuator in control systems is the DC motor which directly provides rotary motion. The electric circuit of the armature and the rotor, where *e* is the back e.m.f. produced by the rotation of the motor, is shown in Figure 4.5.

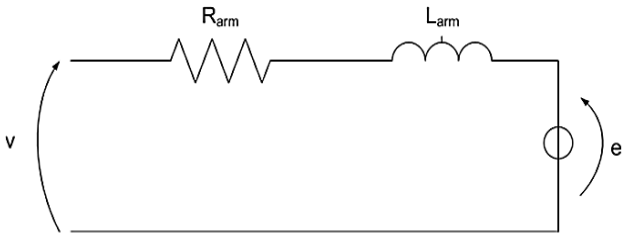

Figure 4.5 : DC motor equivalent circuit

From the dc motor equivalent circuit, the motor model is derived as in equations (4.1)-(4.3).

$$v_m = R_{arm}.i_a + L_{arm}\frac{di_a}{dt} + e \tag{4.1}$$

$$t_m = K_t i_a \tag{4.2}$$

$$e = K_e \dot{\theta}_m \tag{4.3}$$

The linear model of the DC motor is illustrated in Figure 4.6. The electrical time constant is taken into account in this equation; R_{arm} and L_{arm} being the winding resistance and inductance respectively. θ_m is the angular rotation of the motor and v_m is the applied motor voltage. The torque t_m is generated by the motor. Meanwhile K_t and K_e are the motor torque constant and the back-e.m.f. gain respectively. The combination of these equations produces the torque generated by the electric motor which is shown in equation (4.4):

$$\dot{t}_m = -\frac{R_{arm}}{L_{arm}}t_m + \frac{K_t}{L_{arm}}v_m - \frac{K_t K_e}{L_{arm}}\dot{\theta}_m \tag{4.4}$$

The mechanical inertia, J_m, and the inherent damping, C_m , with l being the screw pitch obtained from the dc motor rotary to linear "gearing", n are accounted by the dynamic equation (4.5):

$$\ddot{\theta}_m = \frac{t_m}{J_m} - \frac{C_m}{J_m}\dot{\theta}_m - \frac{k_m.l}{J_m}x_m - \frac{k_m.l^2}{J_m}\theta_m \tag{4.5}$$

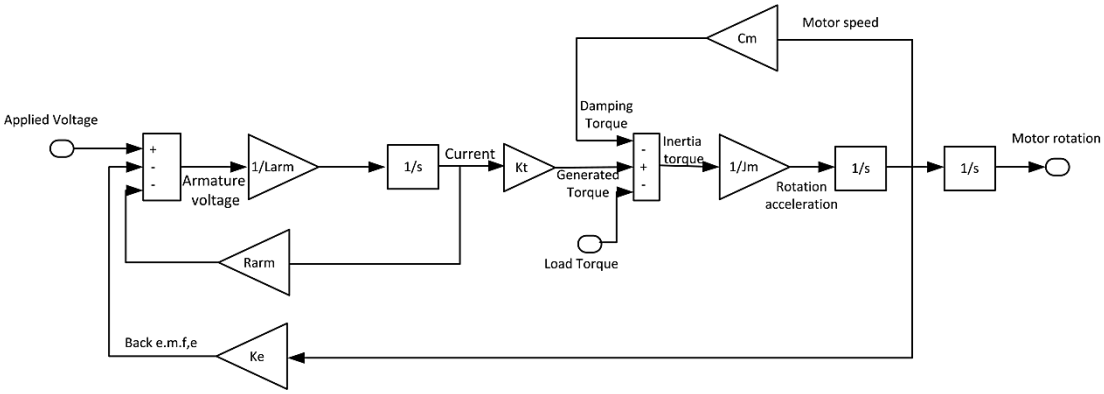

Figure 4.6: Linear model of the DC motor

A full schematic of the actuator is shown in Figure 4.7. The interconnected system of masses, dampers, and springs is represented by the equation (4.6), and m_s being the mass of the screw thread:

$$\ddot{x}_m = \frac{-(k_s + k_m)}{m_s} x_m - \frac{c_s}{m_s}\dot{x}_m + \frac{c_s}{m_s}\dot{x}_{act} - \frac{k_s}{m_s}x_{act} - \frac{k_m.l}{m_s}\theta_m \tag{4.6}$$

The force developed by this system is due to the compression of the lead screw and is given by the equation (4.7):

$$f_{act} = k_s x_m + c_s \dot{x}_m - k_s x_{act} - c_s \dot{x}_{act} \tag{4.7}$$

The state equation (4.8) and the output equation (4.9) are the combination of equations (4.1)-(4.7) and are the representation of an electromechanical actuator. The motor voltage, v, and the actuator extension, x_{act}, are the system inputs, and the output is the actuator force, f_{act}.

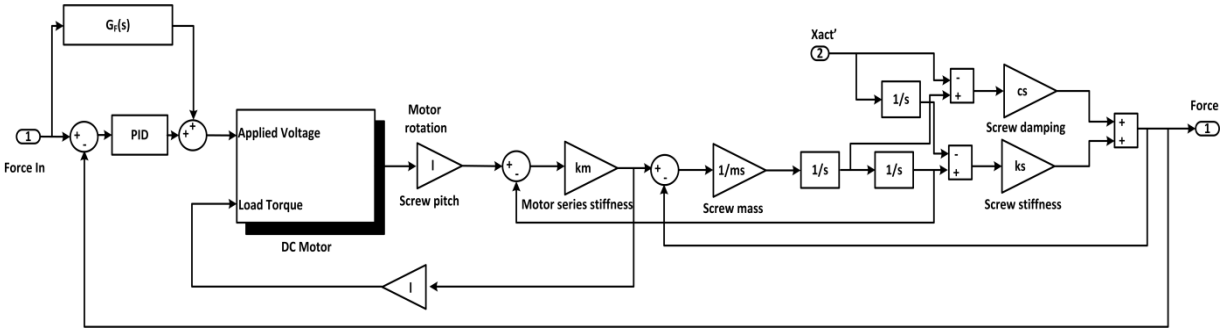

Figure 4.7: Linearised model of an electromechanical actuator model

$$\begin{bmatrix} \dot{t}_m \\ \dot{\theta}_m \\ \ddot{\theta}_m \\ \dot{x}_m \\ \ddot{x}_m \\ \dot{x}_{act} \end{bmatrix} = \begin{bmatrix} -\frac{R_{arm}}{L_{arm}} & 0 & -\frac{K_t K_e}{L_{arm}} & 0 & 0 & 0 \\ 0 & 0 & 1 & 0 & 0 & 0 \\ \frac{1}{J_m} & \frac{k_m l^2}{J_m} & -\frac{C_m}{J_m} & -\frac{k_m l}{J_m} & 0 & 0 \\ 0 & 0 & 0 & 0 & 1 & 0 \\ 0 & \frac{k_{mo} l}{m_s} & 0 & -\frac{(k_s + k_{mo})}{m_s} & -\frac{c_s}{m_s} & \frac{k_s}{m_s} \\ 0 & 0 & 0 & 0 & 0 & 0 \end{bmatrix} \begin{bmatrix} t_m \\ \theta_m \\ \dot{\theta}_m \\ x_m \\ \dot{x}_m \\ x_{act} \end{bmatrix} + \begin{bmatrix} \frac{K_t}{L_{arm}} & 0 \\ 0 & 0 \\ 0 & 0 \\ 0 & 0 \\ \frac{c_s}{m_s} & 0 \\ 0 & 1 \end{bmatrix} \begin{bmatrix} v_m \\ \dot{x}_{act} \end{bmatrix} \tag{4.8}$$

$$f_{act} = [0 \quad 0 \quad 0 \quad k_s \quad c_s \quad -k_s] \begin{bmatrix} t_m \\ \theta_m \\ \dot{\theta}_m \\ x_m \\ \dot{x}_m \\ x_{act} \end{bmatrix} + [0 \quad -c_s] \begin{bmatrix} v_m \\ \dot{x}_{act} \end{bmatrix} \tag{4.9}$$

4.3.2 Electrohydraulic actuator

The hydraulic actuator in this research would be regarded as an electrohydraulic actuator, although there is only a small distinction between this and the servohydraulic actuator. An electrohydraulic actuation is a combination of the electrical and the hydraulic which will then generate force. The electrical component delivers the primary stage of actuation, which is provided by a torque motor. The motor provides a torque proportional to the current delivered to it, and has a limited angle of movement.

The secondary hydraulic stage consists of a hydraulic cylinder connected to a hydraulic pressure via a throttling spool valve. The spool valve is spring loaded and actuated by the torque motor. Controlled oil flows into the cylinder to generate pressure and hence the output force because of the relative in-compressibility of the hydraulic oil.

For modelling purposes, segregation between the electrical and hydraulic parts of the actuator is made. The link between both is made though the positioning of the servo valve. The hydraulic aspects of the modelling procedure are shown as below, followed by the electrical subsystem. This model is a linearised model which incorporates the valve dynamics, oil bulk modulus and damping effects.

The actuator generates force by compression of the hydraulic fluid on either side of the cylinder. Compression or de-compression of the cylinder chamber is achieved via a throttled connection to either a hydraulic power supply or to tank pressure. Figure 4.8 shows the structure of an electrohydraulic actuator.

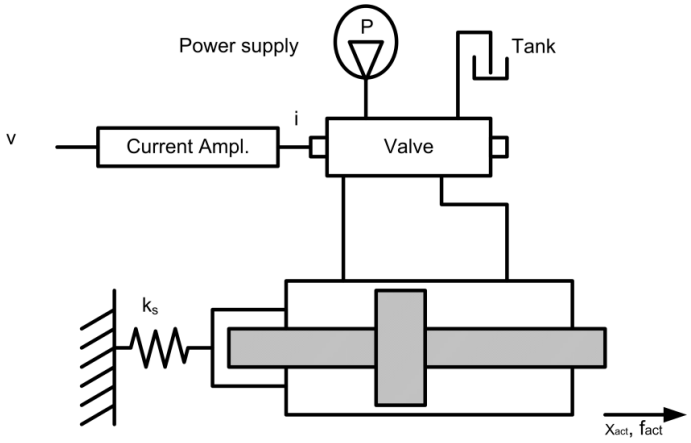

Figure 4.8 : Electrohydraulic actuator model

Assuming the torque motor, having a current of i, drives the spool, then the simplified form of this equation is given as in (4.10), where k_a is the gain of the servo-valve drive amplifier:

$$i = k_a \times v \tag{4.10}$$

The valve flow equation is given as:

$$Q_v = k_q \times i \tag{4.11}$$

where k_q is the valve gain. The cross-port leakage flow, Q_l is defined as below:

$$Q_l = k_l \left(\frac{k_{oil}(x_a - x_{act})}{A_c} \right) \tag{4.12}$$

Where x_a is the original position of the actuator and x_{act} is the actuator extension. k_{oil} and k_l are the oil column stiffness and the leakage gain respectively. The flow that moves the actuator is given by equation (4.13) :

$$\dot{x}_a = \frac{Q}{A_c} \tag{4.13}$$

Where Q, is the total oil flow through the actuator which is define by the equation below:

$$Q_v - Q_l = Q \tag{4.14}$$

In most physical systems the servo valve is not the main component, therefore it is best to represent it in the simplified form of the relatively low frequency spectrum (Foo (2000)). The transfer function of the servo valve and torque motor are described as in equation (4.15):

$$x_v = \frac{k_q . i}{s^2 + 2\zeta\omega s + \omega^2} \tag{4.15}$$

where ω is the servo valve frequency in rad/s and ζ is the damping ratio. Figure 4.9 is the linearised model of a servo-hydraulic element, incorporating valve dynamics, oil bulk modulus and damping effects (Neal (1974)) . The linearised model of this actuator is made with the assumption that the flow of fluid is proportional to the supplied current.

The state equation (4.16) and the output equation (4.17) are the combination of equations (4.10) to (4.15), which together represent an electrohydraulic actuator. The servo valve voltage, v and the actuator extension velocity, $\dot{x}_{act}$ are the system inputs, and the output is the actuator force f_{act}.

$$\begin{bmatrix} \dot{x}_v \\ \ddot{x}_v \\ \dot{x}_a \\ \dot{x}_{act} \end{bmatrix} = \begin{bmatrix} 0 & 1 & 0 & 0 \\ -2\zeta\omega_n & -\omega_n^2 & 0 & 0 \\ \frac{\omega_n^2}{A_c} & 0 & -\frac{k_{oil}k_l}{A_c^2} & \frac{k_{oil}k_l}{A_c^2} \\ 0 & 0 & 0 & 0 \end{bmatrix} \begin{bmatrix} x_v \\ \dot{x}_v \\ x_a \\ x_{act} \end{bmatrix} + \begin{bmatrix} 0 & 0 \\ k_a k_q & 0 \\ 0 & 0 \\ 0 & 1 \end{bmatrix} \begin{bmatrix} v \\ \dot{x}_{act} \end{bmatrix} \tag{4.16}$$

$$f_{act} = [0 \quad 0 \quad k_{oil} \quad -k_{oil}] \begin{bmatrix} x_v \\ \dot{x}_v \\ x_a \\ x_{act} \end{bmatrix} \tag{4.17}$$

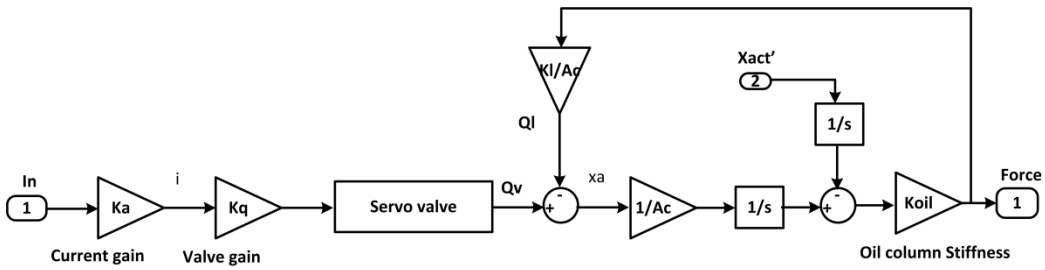

Figure 4.9 : Linearised model of an electrohydraulic actuator

4.4 Actuator outline design

From the idealised actuator in Chapter 3 the appropriate parameters (i.e. sizes, ratings) for the desired actuator can be obtained. The idealised actuator provides the information concerning the speed, acceleration and force level of the suspension. The outline design for the actuator was made based on the quarter vehicle active suspension, in order to reduce the complication of including the pitch mode.

Table 4.1 shows the r.m.s. values obtained from an idealised actuator from the quarter rail vehicle active suspension as shown previously in Figure 3.8. The maximum values used are

three times the r.m.s. value, which is a common design criterion when dealing with random track inputs. During the operation of an active suspension on a railway vehicle, an actuator may need to provide a stroke capability of at least ±80mm, which is within the capabilities of both the electromechanical can electrohydraulic actuators (Pratt (1993)).

Table 4.1: R.m.s. and maximum values for ideal actuators based on stochastic input

	R.m.s	Max	Unit
Actuator acceleration	0.167	0.502	ms^{-2}
Actuator velocity	0.027	0.083	ms^{-1}
Actuator force	1.72	5.15	kN

4.4.1 Outline design of the electromechanical actuator

Calculation of the actuator parameters begins with an assumption of a typical maximum linear motor speed of 3000 RPM. Then it is possible to determine the screw pitch and the gear ratio. The motor torque may be evaluated from the maximum force and the recently derived screw pitch. From the speed and torque evaluation, the rated motor power and peak torque are obtained. An appropriate motor may then be selected fulfilling the torque and power requirements. The motor's characteristics, which are the armature resistance and armature inductance, may be found in the manufacturer's data. Detailed calculations are as follows:

$$\omega_{max} = \frac{2\pi}{60} \times 3000 \quad {}^{rad}/_{s} \tag{4.18}$$

Derivations of the screw parameters are given by the following equations.

The screw gear ratio is given by:

$$n = \frac{\omega_{max}}{v_{max}} \quad {}^{rad}/_{m} \tag{4.19}$$

$$= 3340 \, {}^{rad}/_{m}$$

The screw pitch is given by:

$$l = \frac{1}{n} \ {}^{m}/_{rad} \\ = 0.91 \times 10^{-3} \ {}^{m}/_{rad} \tag{4.20}$$

The derivation of the motor rating is given below.

The rated torque is given by:

$$T_{rms} = \frac{F_{rms}}{n} = 0.515 \ Nm \tag{4.21}$$

The maximum force requirement produces a corresponding maximum motor torque, assuming a lossless screw:

$$T_{max} = \frac{F_{max}}{n} = 1.542 Nm \tag{4.22}$$

Using this information, a suitable motor is chosen since the maximum speed and torque are all known and give the motor inertia, torque constant, etc. The TC70650 series motor is chosen to give the appropriate motor specifications such as the motor inertia, motor damping, terminal resistance and the winding inductance. The parameters' values are listed in Table 4.2, where the motor parameters are provided by Motor Technology Ltd, and other typical mechanical parameters are derived from Pratt's thesis (1996).

Table 4.2: Parameters for the electromechanical actuator

Parameter	Symbol	Value
Motor torque constant	k_t	0.76 Nm/A
Motor back-emf gain	k_e	0.4393 V/rads^{-1}
Winding inductance	L_{arm}	4.2 mH
Winding resistance	R_{arm}	0.46 Ω
Motor inertia	J_m	2.9 ×10^{-3} kgm^2
Motor friction	C_m	795.8×10^{-6} Nmrads^{-1}
Motor series stiffness	k_{mo}	1 × 10^7 Nm^{-1}
Screw pitch	l	0.91 × 10^{-3} mrad^{-1}
Screw mass	m_s	2 kg
Screw stiffness	k_s	2 × 10^6 Nm^{-1}
Screw damping	c_s	4 ×10^3 Nsm^{-1}

4.4.2 Outline design of the electrohydraulic actuator

The hydraulic power pack is assumed to be a typical value of 3000 psi, and it is normal for the actuator to supply a maximum force at 2/3 of the maximum pressure, which gives a good operating band allowing for a suitable pressure drop across the valve at maximum flow, and from there the actuator cross-sectional area may be derived. The flow rating for the servo valve is obtained from the velocity requirement and the derived actuator area.

Assuming a ±25mA control input, where the flow or current constant, k_a , can be obtained from equation (4.10) and the servo valve flow gain equation (4.11). k_q would be obtained from the linearised flow characteristic of the valve.

Values for the oil stiffness (B_m) are obtained from the compressibility of the hydraulic oil. An assumption of the supply pressure and the spool mass are made, and given in the following equations.

The area of the actuator force is:

$$A_c = \frac{F_{max}}{0.67P_s} = 3.372 \times 10^{-4} m^2 \tag{4.23}$$

where P_s is the supply pressure and F_{max} is the maximum force.

Obtaining the area of the actuator force A_c, and knowing the maximum ideal actuator velocity, the maximum flow rate is calculated:

$$Q_R = A_c . v_{max} = 2.792 \times 10^{-5}\, m^3/s \tag{4.24}$$

The valve gain, k_q, is then calculated from the valve flow rate and also the rated current:

$$k_q = \frac{Q_R}{i} = 1.24 \times 10^{-3} m^3/s/A \tag{4.25}$$

Given that the typical maximum frequency is 100Hz for the servo valve, with a 40% damping Foo (2000), this gives a transfer function as follows:

$$H = \frac{(628.32)^2}{s^2 + 502.66s + (628.32)^2} \tag{4.26}$$

The actuator parameters' values for this actuator are listed in Table 4.3.

Table 4.3: Electrohydraulic actuator parameters

Parameter	Symbol	Value
Amplifier gain	k_a	2.5×10^{-3} A/V
Valve gain	k_q	1.24×10^{-3} $m^3/s/A$
Leakage gain	k_l	$1.48\times10^{-14} m^5 s^{-1}/Nm$
Cross sectional area of cylinder	A_c	$3.372\times10^{-4} m^2$
Bulk modulus	B_m	1.7×10^{9} N/m^2
Length	L	0.140m
Oil column stiffness	k_{oil}	8.19×10^{6} N/m
Damping of the servo valve	ζ	0.4
Servo valve frequency	ω_n	628.32 rad/s

4.5 Initial force loop design of the actuator

The structure of the force tracking control of the actuator is shown in Figure 4.11. A standard force loop control is used for both actuators with a consideration of Proportional plus Phase Advance control, and then tuned to obtain high closed loop bandwidth and a good low frequency tracking.

Here the inner loop controller is designed without connecting to the railway vehicle suspension, and the actuator velocity 'feedback', x_{act} is set to zero, i.e. the actuator is effectively locked. Thus, a very high bandwidth is expected. The controller parameters were tuned to achieve a reasonable phase and gain margin in the force loop. A fair comparison is made between the two actuators because the aim is to achieve the best performance while maintaining stability using similar controllers. The stability has been assessed on the basis of the open loop frequency response of the actuators using a Nichols chart.

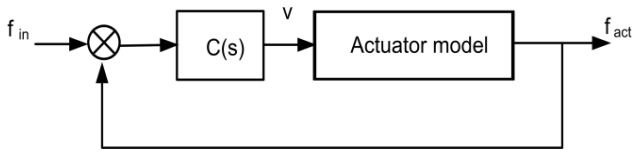

Figure 4.10: Actuator force control

A square wave force demand of 1kN at 10Hz is used to validate the actuator controller functionality as a replacement of the force signal from the active suspension controller. This is done purposely to validate the actuator before being placed in the suspension. Once the actuator is placed in the suspension, in a real application, the force command is produced by an active suspension controller in response to the excitation from the track.

4.5.1 Electromechanical actuator

After the electromechanical actuator has been modelled, a compensator is designed based on the open-loop force response. The controllers are tuned to give a stable gain and phase margin. The Nichols chart of the uncompensated electromechanical actuator from voltage input to force output is plotted in Figure 4.11, which shows that the system is unstable.

A force control loop using the classical *Proportional Integral plus Phase Advance* is designed to tune the actuator to achieve a gain margin of 14.8 dB, and a phase margin of 44.6 degree in the force loop as shown by the Nichols chart of Figure 4.12 with a bandwidth of 31 Hz. The controller equation for this actuator is formulated in equation (4.27):

$$G_c = \frac{0.0398(1 + 0.3s)(1 + \ 0.0086s)}{0.3s(1 + 0.0011s)} \tag{4.27}$$

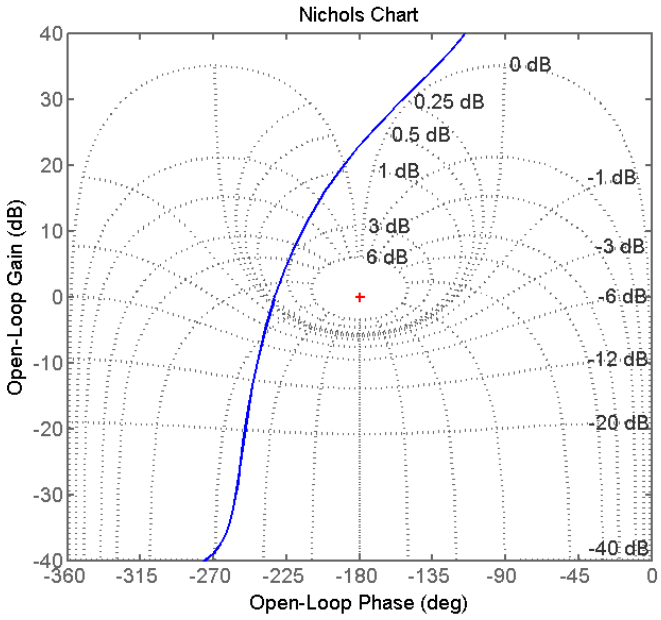

Figure 4.11 : Open loop uncompensated electromechanical actuator

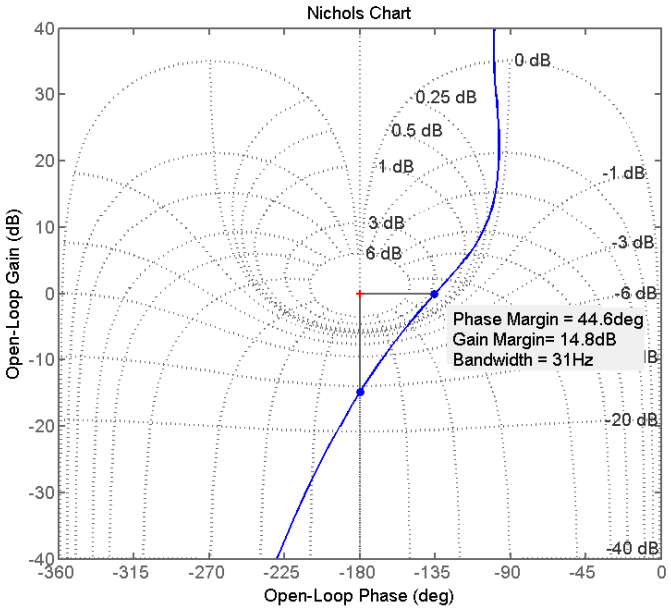

Figure 4.12: Open loop of controlled electromechanical actuator

The above controller was designed assuming the velocity input to be zero. However, the actuator in practice is connected to the secondary suspension, and the velocity input at the extension of the actuator affects the overall performance of the system which will change the actuator bandwidth and also restrict the actuator movement. This will be shown in Section 4.6 where the difficulty in controlling the actuator is demonstrated. It will also be seen that even though the vehicle modes are below 20Hz, the controlled actuator in the suspension does not perform very well in the active suspension environment above 5Hz. For this classical control strategy, the performance becomes worse when the actuator is applied in the side-view model.

Figure 4.13 shows the time response of the closed-loop electromechanical actuator to a square-wave force demand of 1kN at 10Hz.

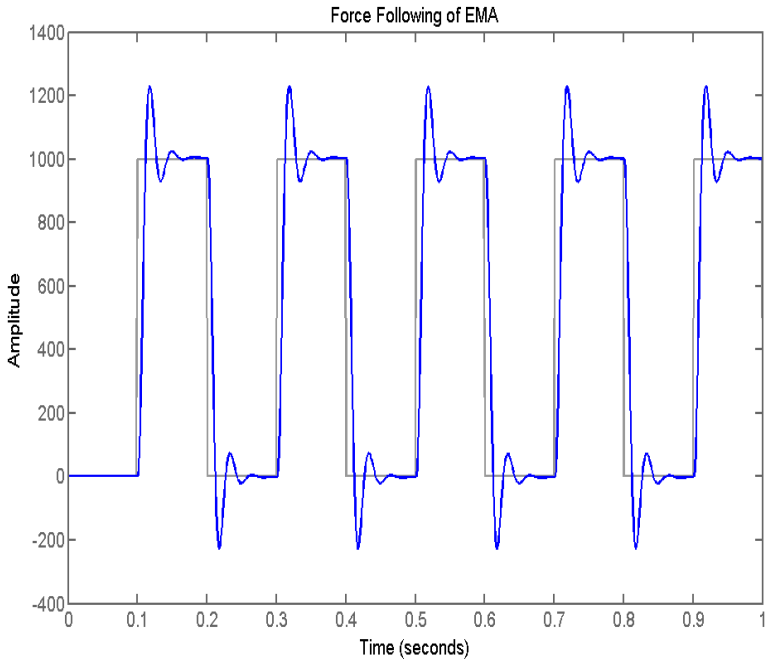

Figure 4.13: Force following of the closed-loop electromechanical actuator

4.5.2 Electrohydraulic actuator

The Nichols chart given in Figure 4.14 shows the uncompensated actuator. The electrohydraulic actuator voltage input to force output plot shows that the system is unstable.

The same type of controller is used to fulfil the task of giving an acceptable phase and gain margin of 58 degree and 13.2 dB respectively, with a bandwidth of 38.7 Hz (Figure 4.15). The controller for this actuator is as given in equation (4.28):

$$G_c = \frac{0.0003(1 + 0.0014s)(1 + 0.0113s)}{0.0014s(1 + 0.0022s)} \tag{4.28}$$

The bandwidth achieved is slightly lower than the electromechanical actuator, however it would still be high for the active suspension application. Again it is found important to be able to find the controller parameters which will satisfy the actuator validation test, and as before, in the time domain it is necessary to look at the response of the actuator towards a 'square wave' demand input of 1kN at 10Hz as shown in Figure 4.16.

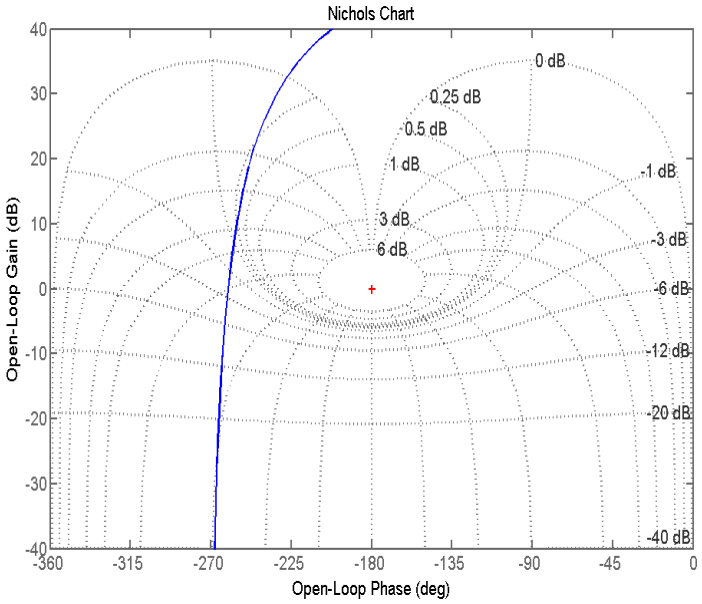

Figure 4.14: Open loop uncompensated electrohydraulic actuator

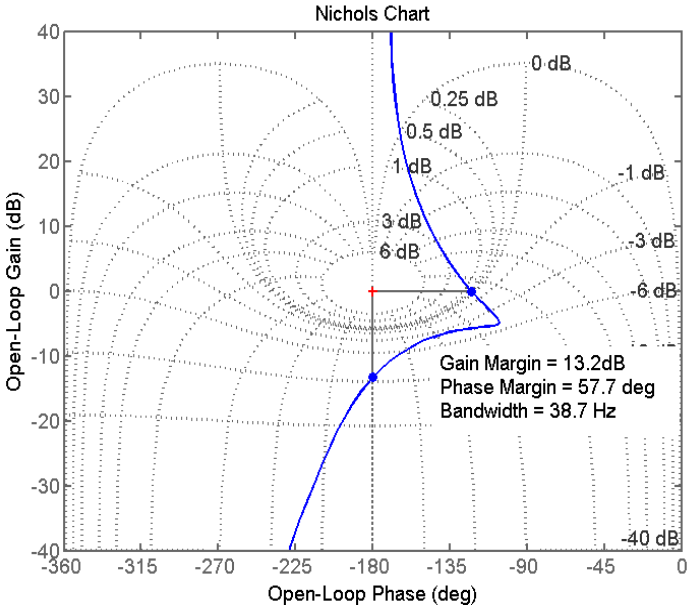

Figure 4.15: Open loop of controlled electrohydraulic actuator

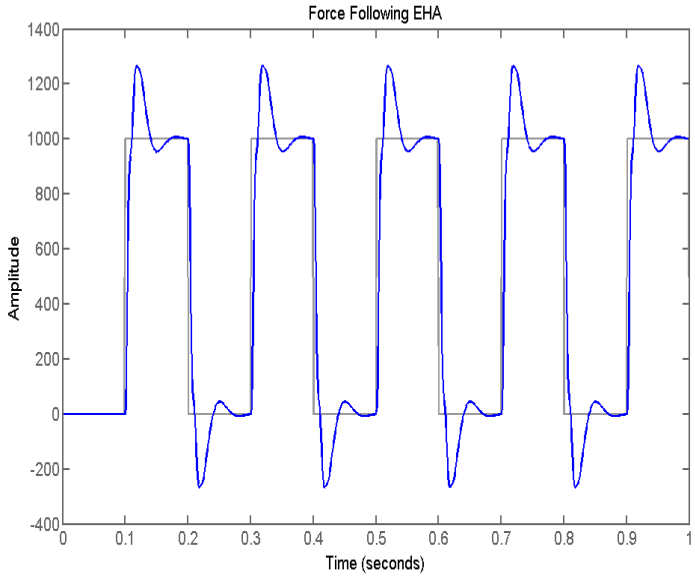

Figure 4.16: Force following of the closed-loop electrohydraulic actuator

4.6 Actuator performance in quarter car railway vehicle suspension

The validation carried out in Section 4.5 is solely to assess the actuator validity where the actuator velocity is set to zero. It has been noticed that if it is placed directly into the suspension system, instant degradation will be visible as the overall actuator bandwidth will decrease and the stability margin of the actuator will reduce; this has been highlighted earlier by (Goodall, et al. (1993) ; Md Yusof, et al. (2010)). Therefore it is important to revisit the actuator controller parameter tuning, taking into consideration the interaction between both model dynamics.

The difficulty of including a real actuator can be illustrated using the scheme of a force controlled actuator as shown in Figure 4.17, where the actuators are placed in parallel to the passive components across the secondary suspension (the most suitable choice of actuator placement to reduce the force placed on the actuator - refer to Chapter 1). The actuator extension velocity input or the actuator movement, $\dot{x}_{act}$, is obtained from the differential velocity movement of the attachment points of the vehicle where the actuator is placed; this will place impact upon the dynamic system and cause the actuator movement (no longer assumed to be zero). This is the most appropriate and practical of applications for the actuators in the secondary suspension (Goodall, et al. (1993)). The impact of the interaction between the actuator dynamics and the suspension performance needs to be analysed, considering the case of the individual actuators. Both actuators' force control loops must counteract in order to keep the actuator force error as close as possible to zero. Therefore it is obvious that the actuator needs to be re-tuned to adapt to the dynamic changes in the whole system (the actuator across the secondary suspension), in order to determine the capability of the actuator to achieve the force. The active control law and also the track inputs are not included yet as it would be beneficial to view how this arrangement affects the actuator despite the actuator controller having been re-tuned to the best performance. This is done to view the outcome based on the force command input, without the track excitation. This step is also important to ensure that the actuator controller in the suspension will provide sufficient performance.

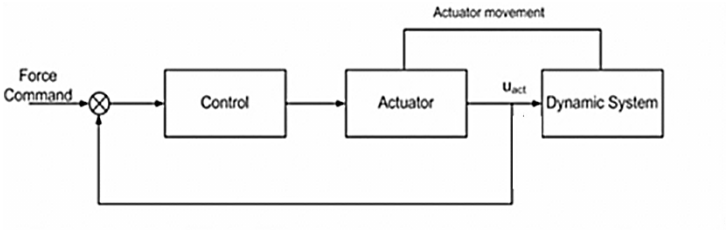

Figure 4.17 : Force controlled actuator

The two-mass vehicle model as described in Chapter 3, without the active suspension control law, is used to demonstrate this effect. This model is shown in Figure 3.8 and is represented by the state space model given in equations (4.29) and (4.30).

$$\begin{bmatrix} \dot{z}_v \\ \ddot{z}_v \\ \dot{z}_{mp} \\ \dot{z}_b \\ \ddot{z}_b \\ \dot{z}_t \end{bmatrix} = \begin{bmatrix} 0 & 1 & 0 & 0 & 0 & 0 \\ -\frac{(k_{az}+k_{sz})}{m_b} & 0 & \frac{k_{sz}}{m_b} & \frac{k_{az}}{m_b} & 0 & 0 \\ \frac{k_{sz}}{c_{rz}} & 0 & -\frac{(k_{sz}-k_{rz})}{c_{rz}} & \frac{k_{rz}}{c_{rz}} & 1 & 0 \\ 0 & 0 & 0 & 0 & 1 & 0 \\ \frac{(k_{az}+k_{sz})}{m_t} & 0 & -\frac{k_{sz}}{m_t} & \frac{-(k_{az}+k_{pz})}{m_t} & -\frac{c_{pz}k_{pz}}{m_t\, m_t} & \\ 0 & 0 & 0 & 0 & 0 & 0 \end{bmatrix} \begin{bmatrix} z_v \\ \dot{z}_v \\ z_{mp} \\ z_b \\ \dot{z}_b \\ z_t \end{bmatrix} + \begin{bmatrix} 0 & 0 \\ \frac{1}{m_b} & 0 \\ 0 & 0 \\ 0 & 0 \\ \frac{1}{m_b} & \frac{c_{pz}}{m_t} \\ 0 & 1 \end{bmatrix} \begin{bmatrix} u_{act} \\ \dot{z}_t \end{bmatrix} \quad (4.29)$$

$$\begin{bmatrix} z_v \\ \dot{z}_v \\ \ddot{z}_v \\ z_b \\ \dot{z}_b \\ d \\ \dot{d} \\ f_{act} \end{bmatrix} = \begin{bmatrix} 1 & 0 & 0 & 0 & 0 & 0 \\ 0 & 1 & 0 & 0 & 0 & 0 \\ -\frac{(k_{az}+k_{sz})}{m_b} & 0 & \frac{k_{sz}}{m_b} & \frac{k_{az}}{m_b} & 0 & 0 \\ 1 & 0 & 0 & 0 & 0 & 0 \\ 0 & 1 & 0 & 0 & 0 & 0 \\ 1 & 0 & 0 & -1 & 0 & 0 \\ 0 & 1 & 0 & 0 & -1 & 0 \\ 0 & 0 & 0 & 0 & 0 & 0 \end{bmatrix} \begin{bmatrix} z_v \\ \dot{z}_v \\ z_{mp} \\ z_b \\ \dot{z}_b \\ z_t \end{bmatrix} + \begin{bmatrix} 0 & 0 \\ 0 & 0 \\ \frac{1}{m_b} & 0 \\ 0 & 0 \\ 0 & 0 \\ 0 & 0 \\ 0 & 0 \\ 1 & 0 \end{bmatrix} \begin{bmatrix} u_{act} \\ \dot{z}_t \end{bmatrix} \quad (4.30)$$

Again, Nichols' chart is used to illustrate the complexity of the actuator dynamics when introduced within a vehicle suspension. The redesigned actuator controllers were not as easy as the independent actuators, which can be seen in Figures 4.18 – 4.19. The influence of the vehicle suspension dynamics on the actuator performance is clearly shown by looking at the loops frequencies below 10Hz for both actuators, which was highlighted earlier in the problem statement of the research. This is also visible for the force tracking performance illustrated in Figures 4.20 – 4.21. It has been observed where the force tracking output has shown difficulty in producing a steady force following output. This shows that even though the controller has been modified to produce the best force tracking output, and a good phase and gain margin, there are still issues at higher frequencies. This has changed the actuator characteristic in the suspension which will also change the overall performance of the suspension.

Since the actuator extension velocity also has effects on the overall dynamics of the actuator, the controller needs to be modified to obtain a good frequency tracking. The modified controllers for actuators are as in equations (4.31) and (4.32).

For the electromechanical actuator:

$$G_c = \frac{0.028(1 + 0.02s)(1 + 0.16s)}{0.02s(1 + 0.002s)} \tag{4.31}$$

and for the electrohydraulic actuator:

$$G_c = \frac{0.001(1 + 0.006s)(1 + \ 0.004s)}{0.006s(1 + 0.00044s)} \tag{4.32}$$

For the electromechanical actuator in the suspension, the performance is restricted by the screw stiffness and also the armature inertia. Increasing the gain and phase margin for bandwidth improvement will only excite the frequency oscillation at the region of 10Hz of the armature through the screw stiffness. As for the electrohydraulic actuator, the limitations arise from the valve spool dynamics and also the oil compressibility, and phase lag has to be increased to improve the bandwidth but then it also reduces the gain margin. For both actuators in the suspension system, achieving good force loop stability is an essential task

that needs to be fulfilled for a better vehicle performance. The actuator performance of the actuator is judged by its ability to isolate the vehicle from the acceleration environment on the vehicle body. This will be shown in the next section.

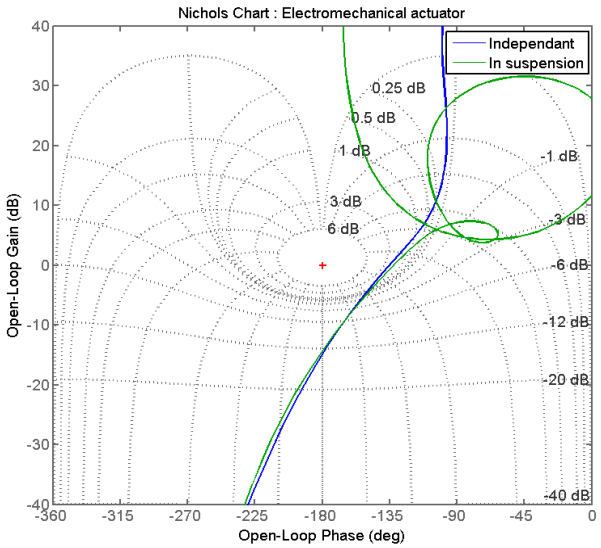

Figure 4.18: Open loop of controlled electromechanical actuator in the secondary suspension

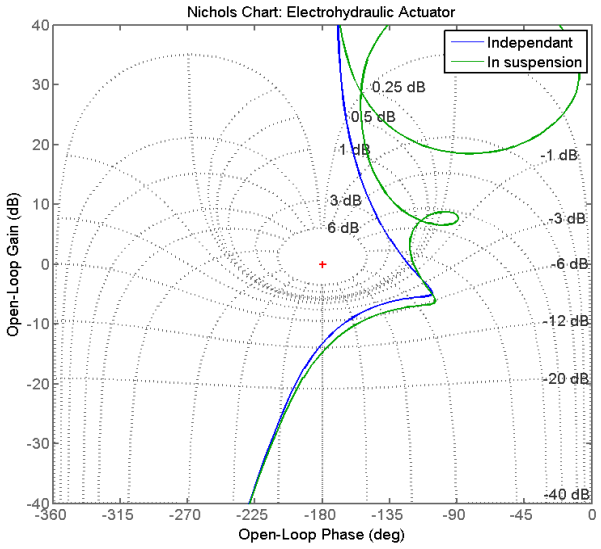

Figure 4.19: Open loop of controlled electrohydraulic actuator in the secondary suspension

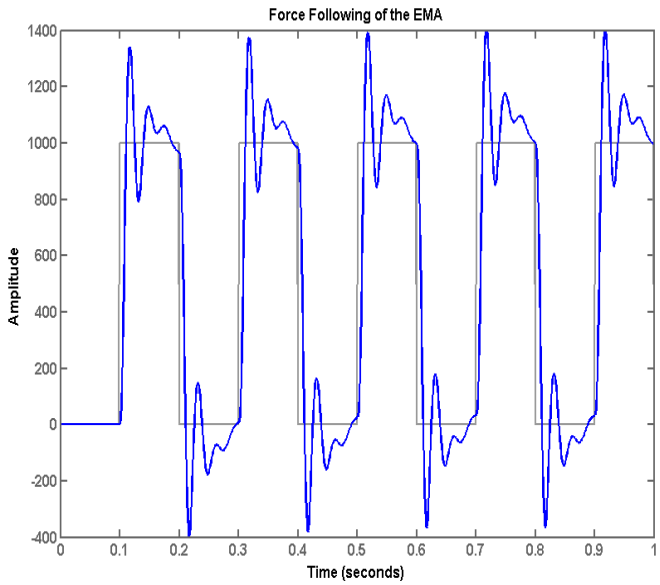

Figure 4.20: Force following of the closed-loop electromechanical actuator in the secondary suspension

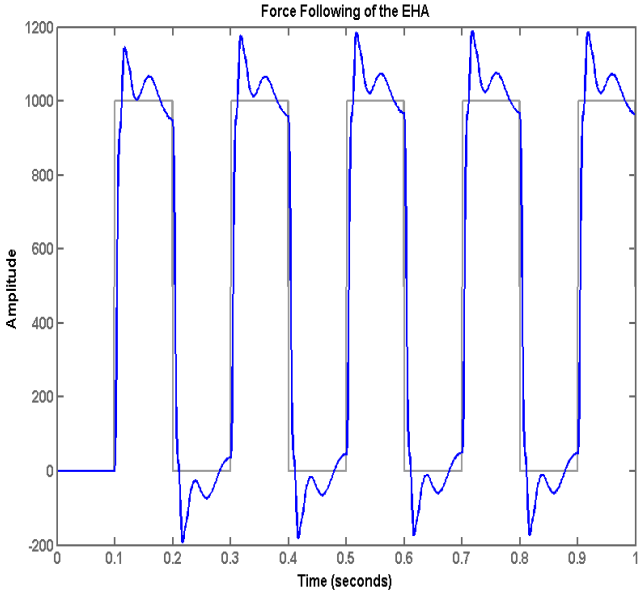

Figure 4.21: Force following of the closed-loop electrohydraulic actuator in the secondary suspension

4.7 Actuator performance in the active secondary vehicle suspension (quarter car)

The effects of "real" actuator dynamics on the overall performance of an active suspension will be demonstrated through the simple two mass model used in the previous section. The actuator models developed in Section 4.3 with the retuned controllers in Section 4.7 are linked to the vehicle model (as in equations (4.29) and (4.30)) and the active suspension control law (equations (3.34) and (3.35)), where the overall system performance is evaluated. The vehicle dynamic model, the active suspension controller and the actuator dynamics may be viewed as linked with the structure shown in Figure 4.22 with the structure given in equations (4.33) and (4.34).

$$\dot{x} = Ax + Bu_{act} + W\dot{\zeta} \tag{4.33}$$

$$y = Cx + Du_{act} + D_W\dot{\zeta} \tag{4.34}$$

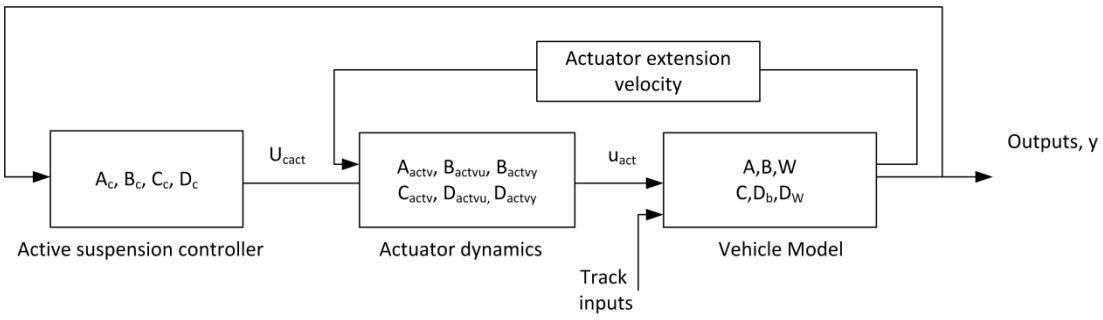

Figure 4.22 : Vehicle dynamic model

The actuator model has the general structure given by equations (4.35) and (4.36). Two inputs are required: the force command and the differential velocity movements between the attachment points to the vehicle, 'y_{act}', which are the differential velocity movements of the attachment points to the vehicle to which it is connected (also referred earlier as actuator extension velocity , x_{act}). A single output force is generated by the model.

$$\dot{x}_{actv} = Ax_{actv} + B_{actvu}u_{act} + B_{actvy}\dot{y}_{act} \tag{4.35}$$

$$u_{actv} = C_{act}x_{act} + D_{actvu}u_{act} + D_{acty}\dot{y}_{act} \tag{4.36}$$

The active suspension control law provides the force command to the actuator, which will in turn influence vehicle motions through the output force; the motion of the attachment points at the same time is being sent back to the actuator dynamic block. The actuator force control loop is included in the actuator dynamic model.

The control law, which includes the high pass filter introduced in Chapter 3, is used to improve low frequency performance; it has a general state space model which is given by the equations (4.37) and (4.38).

$$\dot{x}_c = A_c x_c + B_c y \tag{4.37}$$

$$u_{cact} = C_c x_c + D_c y \tag{4.38}$$

The vehicle contains information that is required by the actuator dynamic block and also the active suspension control law, which is given from the vehicle as seen in Figure 4.22.

This methodology applies to more complex models as the progress of the whole vehicle suspension is modelled in the next phase of this research. The electrohydraulic and electromechanical actuators were tested with identical skyhook damping on the two mass model.

The comparison of the power spectral densities of the body acceleration for both actuator technologies together with the ideal actuator, which is not influenced by internal dynamics, is shown in Figure 4.23.

The areas under the p.s.d. plots are representative of the vehicle ride quality for each of the actuators discussed in this research. The ride quality shows notable deterioration when 'real' actuator dynamics are included, even though the actuator controller is tuned to the best performance. Clearly it shows that when the actuator is linked with the vehicle there will be degradation in the ride quality. This is due to the technology used, as different actuators have different bandwidth limitations.

Time responses for the vehicle accelerations on the track irregularities are shown in Table 4.4, with a comparison between the passive and ideal suspension. From these results, the increases in body acceleration and the actuator force are obvious. In the case of real actuators, there is a high percentage of degradation compared to an ideal actuator.

The degradation in ride quality shown is due to the inability of the relevant actuator to supply appropriate control effort at frequencies above 3Hz onwards. At these frequencies, the active suspension control law does not perform, resulting in higher body velocities and hence higher actuator force demands. It is apparent that above 4Hz and 4.75Hz for the electromechanical and electrohydraulic actuators respectively, the response of the vehicle acceleration deviates from the ideal. The difficulty of this situation is shown in Figure 4.24 where the actuators' force is compared to the ideal. This degradation will also be visible when the actuators are placed in the front and rear suspension of the side-view model; the p.s.d.s and time responses will be illustrated towards the end of the chapter for comparison with the following effort to improve the actuator performance in the suspension to avoid repetition.

Table 4.4: R.M.S. results for the quarter car model

		Passive	**Ideal**	**EMA**	**EHA**
Acceleration	(%g)	2.431	1.700	4.331	2.809
Deflection (track input)	(mm)	10	8.0	8.5	8.3
Actuator Force	(kN)	-	1.718	6.884	5.558

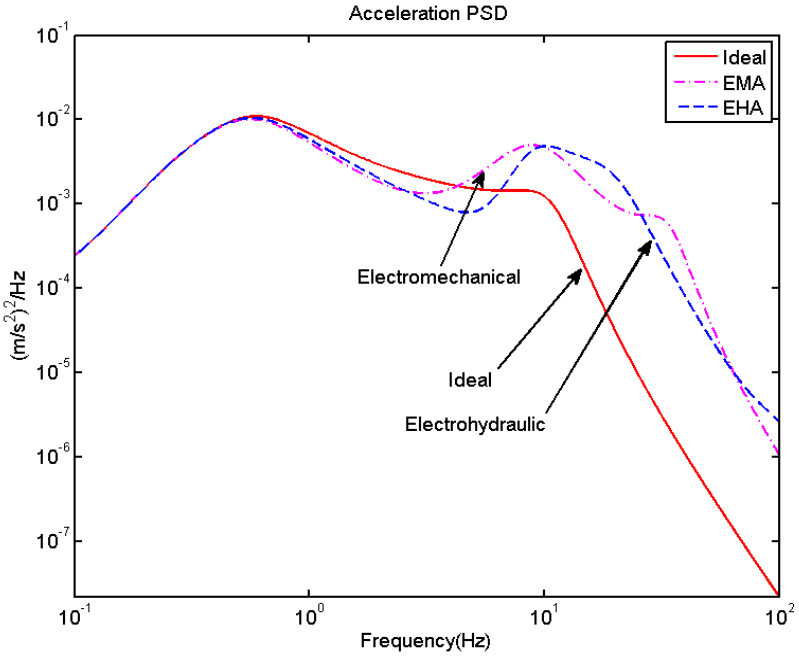

Figure 4.23: Effect of real actuators on ride quality

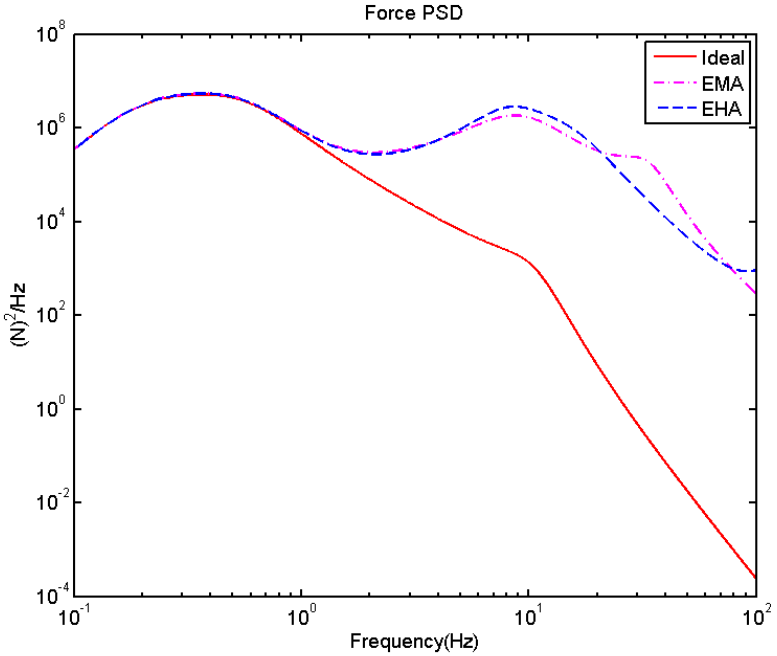

Figure 4.24: Force analysis

The next section extends the possibility of improving the active suspension actuator performance in the suspension by introducing the parameter optimisation technique to the actuator controllers. Here the multi-objective problem uses a genetic algorithm (GA) approach.

4.8 Improvement of actuated active suspension using the Genetic Algorithm

From the previous sub section observations, the actuated quartercar suspension performance has shown a noticeable deterioration compared to the ideal. Although the actuator controller was tuned to the best performance, using classical methods, as per the knowledge of the author, there could still be a better combination of parameters that could yield a better suspension performance.

The classical control consists of several parameters, which have been tuned empirically using the trial and error process. This process was iterated until the best solution was found which yields the force tracking output (Section 4.6) that achieves the best ride performance without violating the actuator and suspension requirements. This was a daunting process as tuning of the actuator had to be done while the actuator was in the suspension. No doubt this method will have left out the best combination possibility of the controller parameters. Furthermore, the task is even more laborious while the actuator is in the suspension. A more efficient method is to use a genetic algorithm method which helps to eliminate the manual selection process by formulating the problem into different objective functions. By using GA, the best combination of parameters that will satisfy the defined objectives could be obtained with much more ease.

4.8.1 Active suspension actuator controller parameter optimisation using NSGA-II (OPT I)

The objective optimisations were carried out to obtain the *Proportional Integral plus Phase Advanced* design parameters. Simulation results of the NGSA-II algorithm can evolve a ride

quality profile approaching the ideal without violating the actuator boundaries while traversing on an irregular railway track. The simulation also restricts the deflection of the secondary suspension to a limit of 35mm for the deterministic input.

Then the next element was checked, which was the rated voltage for the actuator so as not to violate the actuator requirement.

Tuning the actuator within the suspension controller using the NSGA-II optimisation method is aimed to achieve the ideal ride acceleration without causing large degradation in the other variables such as the suspension deflection, the actuator force requirement and also the command signals into the actuator. The objective here is not to tune the active suspension controller (skyhook), which therefore means that this outer controller has been left as it is without any modifications.

The penalty function approach is used to keep constraints within limits, e.g. the suspension deflection constraint. The genetic algorithms procedure was simulated for 300 generations with 50 populations. Optimisation of the actuator controller parameters is carried out within the quarter car suspension to reduce the simulations complication. The phase advance ratio, k was left out in the tuning process as to concentrate on the main controller parameters tuning.

Selection of the final controller parameters for both actuators was based on the 'Pareto curve' obtained from the trade-off plot for the vertical acceleration against the suspension deflection on a straight track as illustrated in Figure 4.25. The red '*' curve shows the optimisation of the electromechanical controller parameters, and the blue '*' curves are for the controller parameters and the electrohydraulic actuator.

In actuality, it was found very difficult to satisfy the ideal criteria for both actuators which could be visualised on the scattered plots of the individual actuator in the suspension trade-off. Very few solutions are able to be provided by the genetic algorithm for the electromechanical actuator in the suspension actuator, compared to the electrohydraulic actuator. However, this method has provided few solutions approaching the ideal.

Table 4.5 tabulates the actuator controller parameters obtained using the genetic algorithm process in comparison with the manually tuned actuator controller parameter (in red).

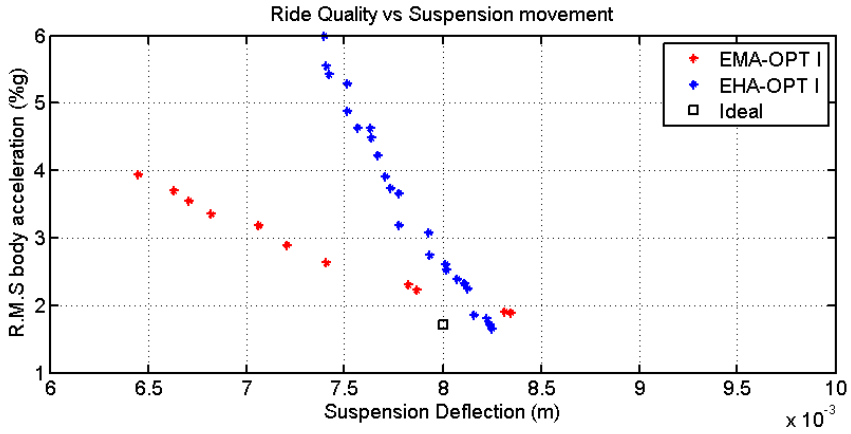

Figure 4.25: Trade off plot for EMA and EHA for controller parameter optimisation

Table 4.5: Final parameters for the controller optimisation (black) in comparison with the manually tuned (red)

Actuator	**k_p [V/N]**	**k_i [Vs/N]**	**w_c [rad/s]**
EMA	0.0867(0.0282)	0.0445(0.020)	254(200)
EHA	0.0033(0.0013)	0.0127(0.0062)	628(855)

The controller equation for this optimisation is as shown in equation (4.39) for the electromechanical actuator and in (4.40) for the electrohydraulic actuator.

$$G_c = \frac{0.0867(1 + 0.0445s)(1 + 0.141s)}{0.0445s(1 + 0.0018s)} \tag{4.39}$$

$$G_c = \frac{0.0033(1 + 0.0127s)(1 + \ 0.0033s)}{0.006s(1 + 0.0004135s)} \tag{4.40}$$

4.8.2 Actuator in the secondary suspension controller parameter and additional stiffness optimisation using NSGA-II (OPT II)

Another possible way to improve the performance of the active suspension is to 'soften' the actuator, by introducing additional stiffness in series for the actuators. NSGA-II was used with the same optimisation objective, but with an additional actuator stiffness parameter that needs to be re-optimised.

Final controller parameters for both actuators were selected based on the 'Pareto curve', presented in Table 4.6, and the trade-off plot for the vertical acceleration against the suspension deflection on a straight track is illustrated in Figure 4.26. Again, the phase advance ratio, k was left out in the tuning process.

By re-optimising the actuator stiffness, the genetic algorithm has been able to produce more controller solutions for both actuators, especially the electromechanical actuator. However for both actuators, the trade-off requires a slightly higher suspension deflection for better ride quality.

These final controller parameters are then used for r.m.s. and p.s.d.s analysis for both the quartercar and the side-view model.

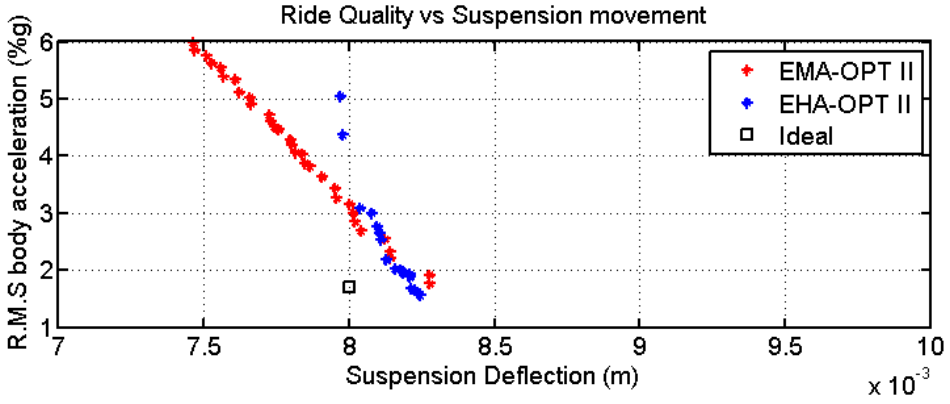

Figure 4.26: Trade off plot for EMA and EHA for controller parameter optimisation and actuator stiffness

Table 4.6: Final parameters for the controller optimisation

Actuator	k_p [V/N]	k_i [Vs/N]	w_c [rad/s]	Actuator Stiffness
EMA	0.0751	0.031	199.34	$k_s = 1.33\ MNm^{-1}$
EHA	0.00148	0.00334	379	$B_m = 1040\ MNm^{-2}$

The controller equation for this optimisation is as shown in equation (4.41) for the electromechanical actuator and in (4.42) for the electrohydraulic actuator.

$$G_c = \frac{0.0751(1 + 0.031s)(1 + 0.0142s)}{0.031s(1 + 0.0018s)} \tag{4.41}$$

$$G_c = \frac{0.00148(1 + 0.00334s)(1 + 0.0075s)}{0.00334s(1 + 0.0009328s)} \tag{4.42}$$

4.9 Simulation results

This section uses the previous section's findings to assess the effect of real actuators for the quarter and side-view vehicle model. The p.s.d. results for the quarter rail vehicle actuated suspension are shown in the following figures. Note that 'OPT I' refers to the optimisation without the inclusion of a series spring to soften the actuator, whereas 'OPT II' includes the spring. For both actuators all three methods show behaviour slightly better than the ideal at lower frequencies. The ride acceleration p.s.d.s with the electromechanical actuator in Figure 4.27, however, begin to deviate above 4Hz, and at 7Hz for the electrohydraulic actuator respectively (with the exception of OPT II, which deviates at a much higher frequency) as shown in Figure 4.28.

The p.s.d.s of the side-view vehicle using the same actuators is illustrated in Figures 4.29 - 4.30 for the electromechanical actuators and Figures 4.31 - 4.32 for the electrohydraulic

actuators. The equivalent p.s.d. results for the front and rear body accelerations, for both actuators in the suspension, again show the deterioration at higher frequencies.

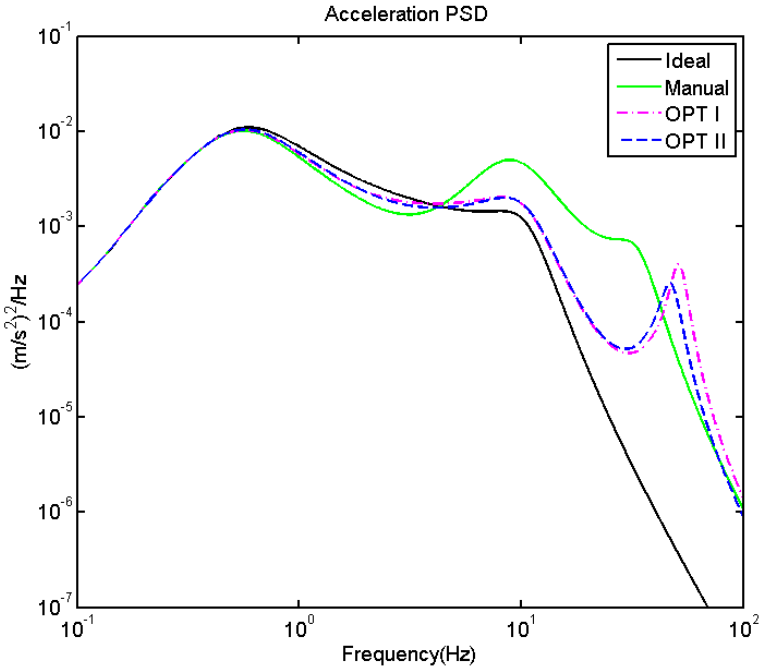

Figure 4.27: P.s.ds for the electromechanical actuator effect in the quartercar vehicle

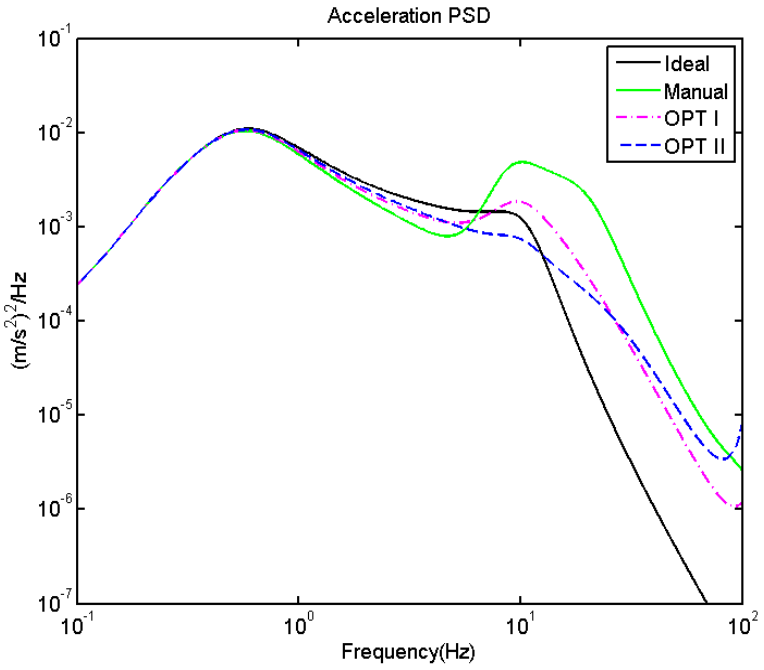

Figure 4.28: P.s.d.s for the electrohydraulic actuator effect in the quartercar vehicle

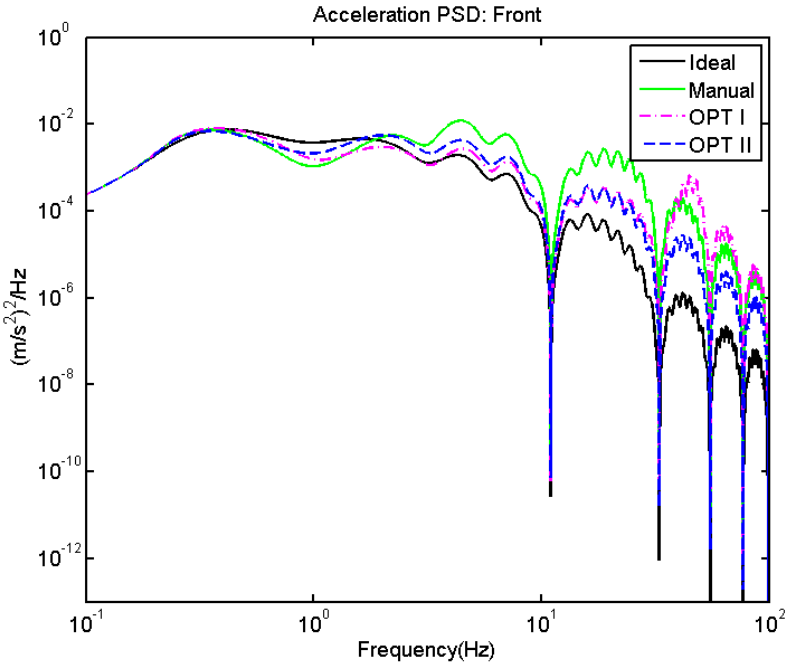

Figure 4.29 : Front p.s.d.s for the electromechanical actuator effect in the sideview vehicle

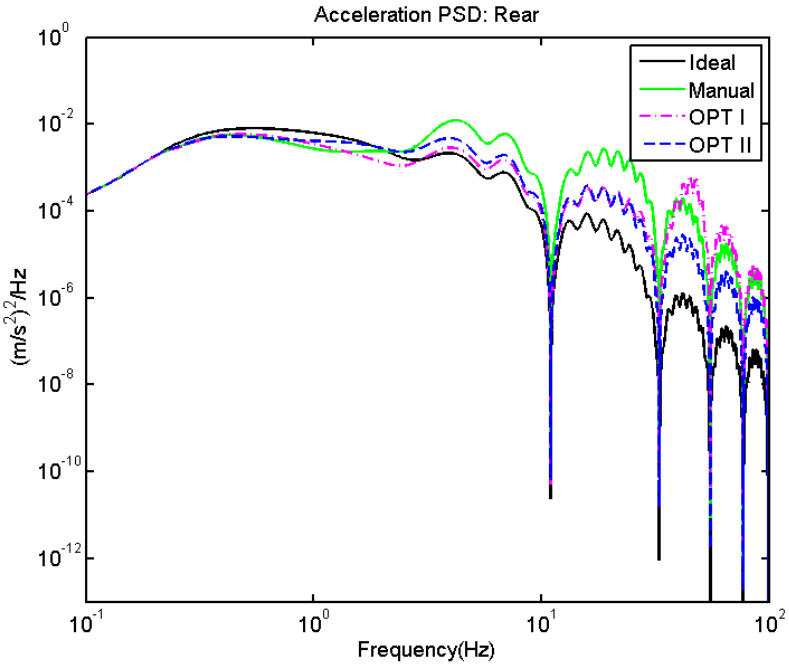

Figure 4.30: Rear p.s.d.s for the electromechanical actuator effect in the sideview vehicle

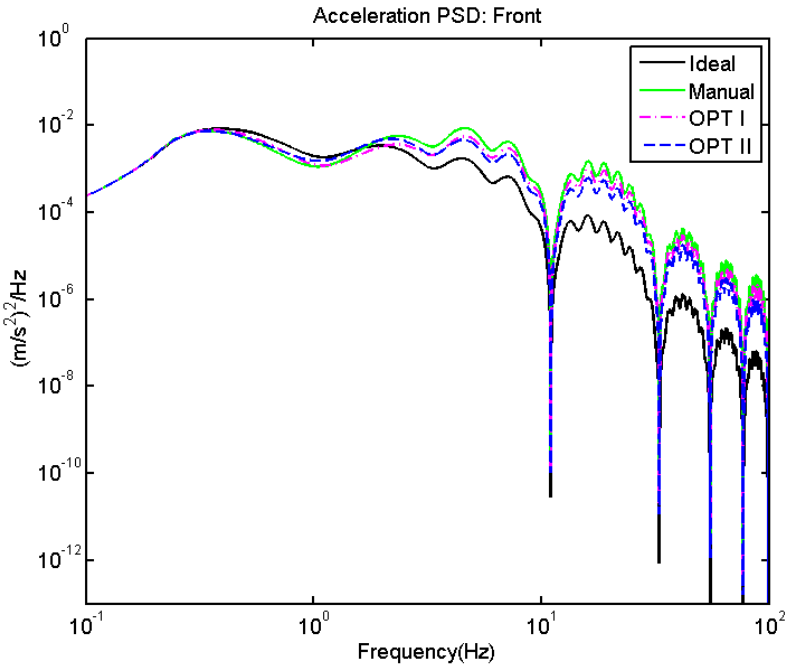

Figure 4.31: Front p.s.d.s for the electrohydraulic actuator effect in the sideview vehicle

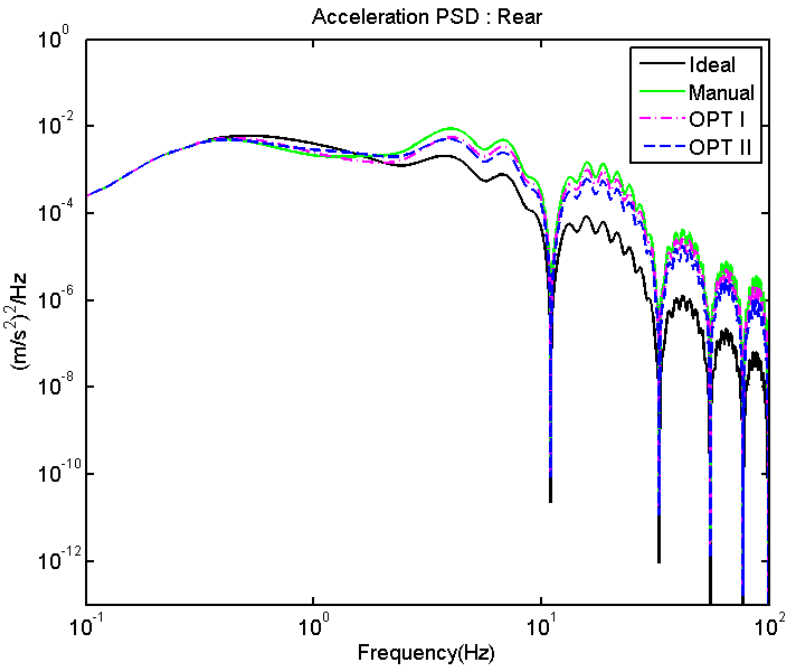

Figure 4.32: Rear p.s.d.s for the electrohydraulic actuator effect in the sideview vehicle

The results in terms of r.m.s. are tabulated in Table 4.7 for the quartercar vehicle, and in Table 4.8 for the side-view vehicle. The deterioration for the active suspension with actuator dynamics remains noticeable, but is substantially reduced by the optimisation of the controller parameters. From the results of the quartercar suspension, the optimisation techniques OPT I and OPT II have reduced the ride quality by 41% and 57% compared to the manually tuned controller for the electromechanical actuator. The optimisation of the actuator stiffness has also reduced the actuator force down to 2.428kN from 6.884kN which is a 64% reduction from the manually tuned actuator.

Optimisation of the electrohydraulic actuator provided a significant improvement, especially for OPT II where the ride performance achieved was 4.1% better than the ideal. The actuator force has also reduced by 52% from 5.558kN to 2.661kN.

The actuator controller when translated to the side-view vehicle provided a similar percentage improvement for both sides of the vehicle, with the rear being slightly worse due to the pitch motion occurring in the vehicle. For all the optimisation strategies used earlier, it has been shown that the actuator force has also deteriorated. Figure 4.33 shows a bar chart representation of the quartercar vehicle, meanwhile Figures 4.34 and 4.35 for the front and rear suspension of the vehicle show the results extracted from the two tables earlier to illustrate the improvement obtained from both optimisation techniques. The ideal results obtained in Chapter 3 are sandwiched in between the results for these purposes to highlight the degradation or improvement achieved.

Table 4.7: R.M.S results for the quarter car model

		EMA			**EHA**		
	Ideal	**Manual**	**OPT I**	**OPT II**	**Manual**	**OPT I**	**OPT II**
		k_s=20 M (N/m)	k_s=20 M (N/m)	k_s=1.13 M(N/m)	B_m= 1700M (N/m^2)	B_m = 1700M (N/m^2)	B_m = 1040 M (N/m^2)
Acceleration – (%g)	1.700	4.331	2.569	1.878	2.809	1.866	1.642
Deflection – (mm)	8.0	8.5	8.4	8.4	8.3	8.4	8.4
Actuator Force – (kN)	1.718	6.884	3.176	2.428	5.558	3.055	2.661

Table 4.8: R.M.S. results for the side-view model

			EMA			EHA		
			Manual	**OPT I**	**OPT II**	**Manual**	**OPT I**	**OPT II**
		Ideal	k_s=20 M (N/m)	k_s=20 M (N/m)	k_s=1.13 M(N/m)	B_m= 1700 M (N/m^2)	B_m=1700 M (N/m^2)	B_m = 1040 M (N/m^2)
Acceleration -(%g)	Front	1.371	2.357	1.619	1.564	2.573	1.495	1.291
	Centre	0.869	1.285	0.965	0.942	1.373	0.936	0.869
	Rear	1.540	2.110	1.640	1.610	2.135	1.445	1.365
Deflection -(mm)	Front	8.4	8.4	8.4	8.4	10.1	10.1	10.1
	Rear	11.1	11.1	11.1	11.1	10.2	10.2	10.2
Actuator Force -(kN)	Front	1.948	3.944	2.854	2.584	4.570	3.130	2.926
	Rear	2.879	3.956	3.243	3.203	4.079	3.232	3.145

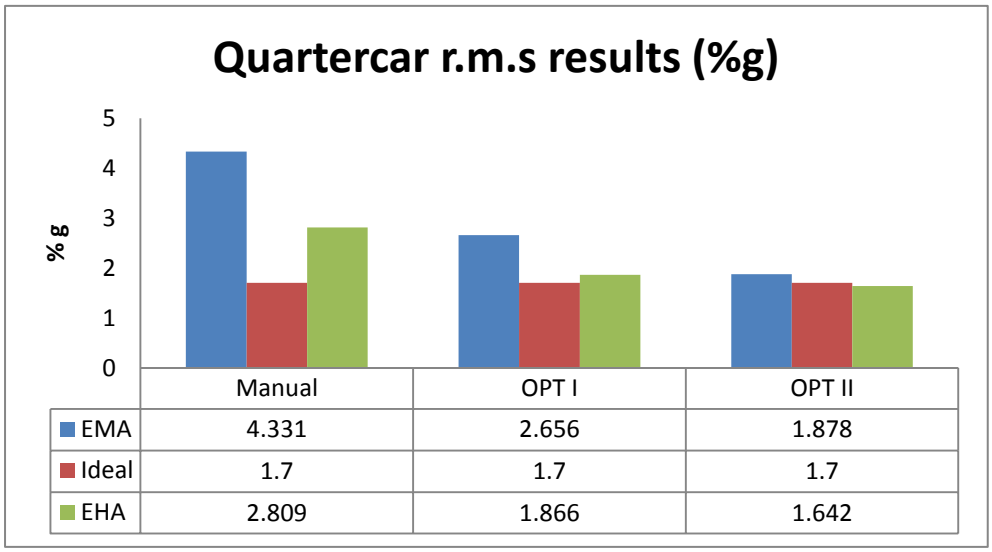

Figure 4.33 : Bar chart of the quarter car vehicle r.m.s. results

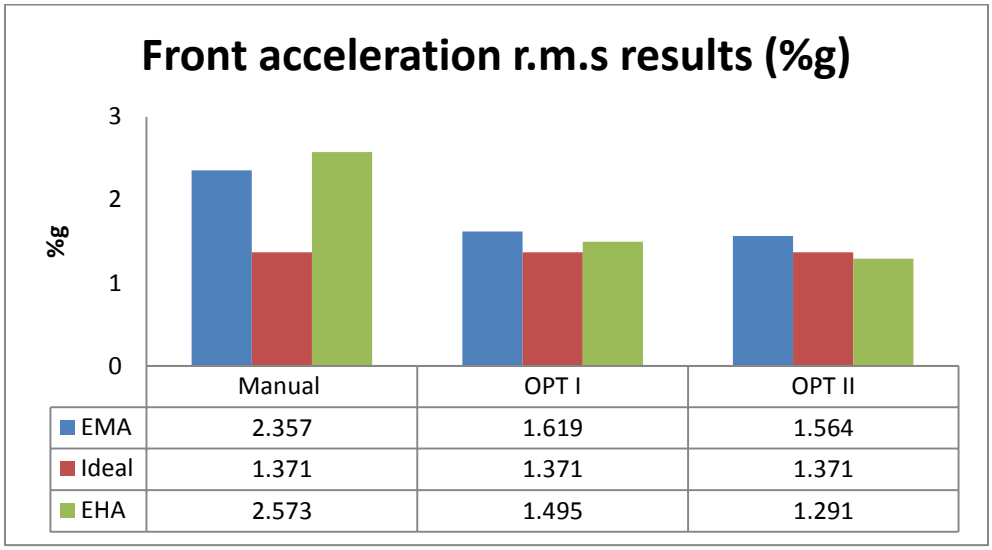

	Manual	OPT I	OPT II
EMA	2.357	1.619	1.564
Ideal	1.371	1.371	1.371
EHA	2.573	1.495	1.291

Figure 4.34 : Bar chart of the front side-view vehicle r.m.s. results

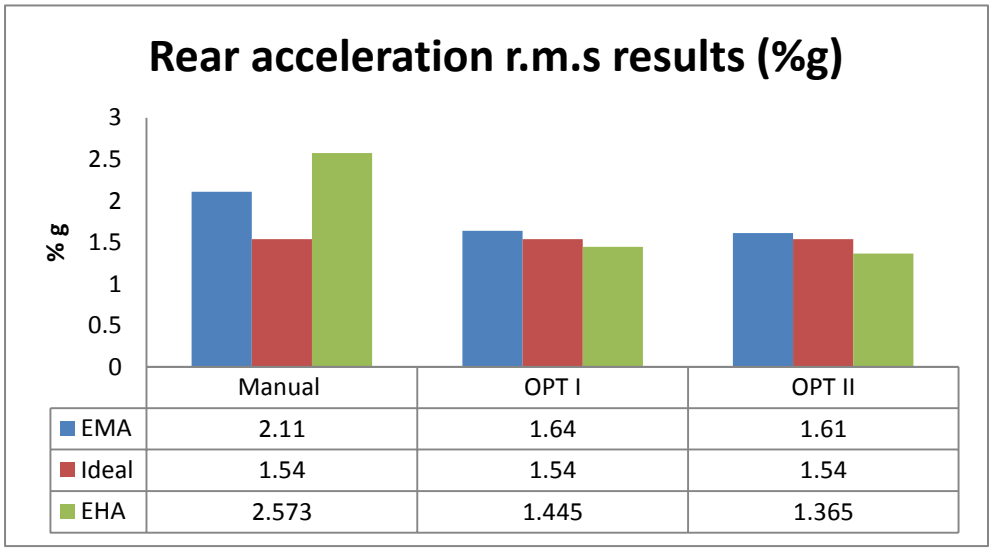

	Manual	OPT I	OPT II
EMA	2.11	1.64	1.61
Ideal	1.54	1.54	1.54
EHA	2.573	1.445	1.365

Figure 4.35 : Bar chart of the rear side-view vehicle r.m.s. results

4.10 Actuators in suspension analysis at 3Hz

Although the actuators have improved the suspension performance compared to the passive, there are still issues that need to be investigated in the p.s.d.s results of both actuators for frequencies above 3Hz. It would be interesting to investigate the cause behind the original problem of the actuator in the suspension for the force feedback control. An analysis for both actuators while in the suspension at 3Hz was done to understand the possible causes and also the possible corrective action that could be taken.

4.10.1 Electromechanical actuator analysis

The analysis was done with the actuator in the quarter rail vehicle with only the force feedback control to look at the underlying issues of the actuator in the suspension. The actuator is analysed by looking at the velocity input response at 3Hz where the degradation begins. Figure 4.36 below shows the signals that have been analysed, where the main signals of the motors and the actuators are measured. The actuator signals are extracted from the model and the signal amplitudes are obtained at 3Hz as shown in Figure 4.37. The signal amplitudes are tabulated in Table 4.9 and the p.s.d.s of the motor and load torques are shown in Figure 4.38.

The information from both of the figures shows that the motor torque, T_m , is much higher than the load torque, T_l, and at higher frequencies the motor torque appears to be substantially at a larger scale than the load torque. This means that the motor is working very hard to produce a lot of torque to accelerate the inertia. Most of the torque is wasted within the actuator at high frequencies. By principle, the motor should be producing a motor torque less than or equal to the load torque to produce the required motor speed. In addition the output force, F_{out}, produced was 29kN compared to the demand force, F_{in}, of 6.6kN required from it to operate in the suspension. This has also caused a large error.

Table 4.9: Electromechanical analyses at 3Hz

Signal		**Amplitude**	**Unit**
Input Force	F_{in}	6.6	kN/ms^{-1}
Voltage	V	1.7×10^3	V/ms^{-1}
Current	I	275	A/ms^{-1}
Motor Torque	T_m	206.5	Nm/ms^{-1}
Gear position		0.06	m/ms^{-1}
Speed	ω	3800	
Load Torque	T_L	8.8	Nm/ms^{-1}
Screw position		0.06	Rad/ m
Motor Force	F_{mot}	29.1	kN/ms^{-1}
Actuator extension velocity	$\dot{x}_{act}$	1.13	
Output Force	F_{out}	29.1	kN/ms^{-1}

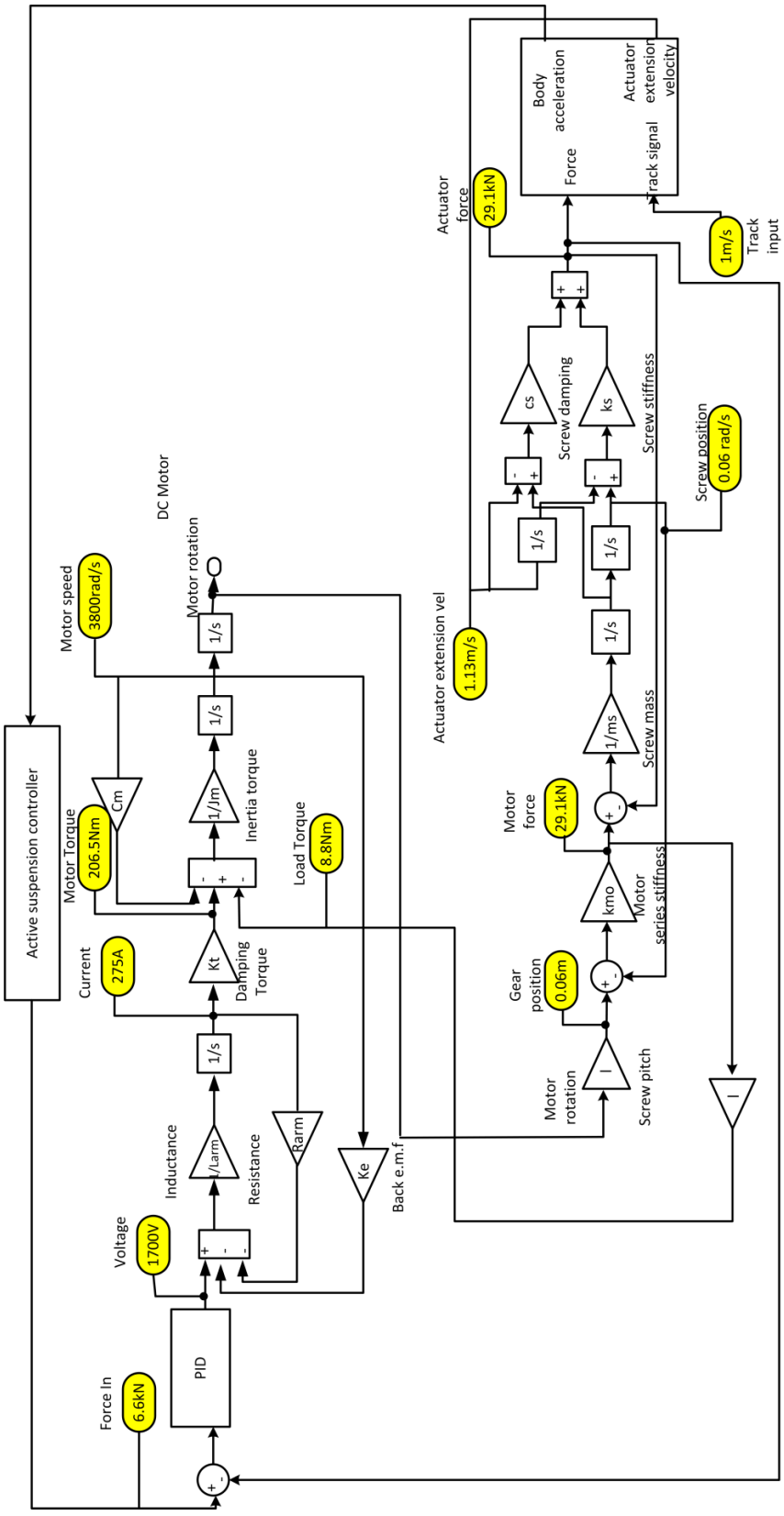

Figure 4.36: Electromechanical actuator analysis

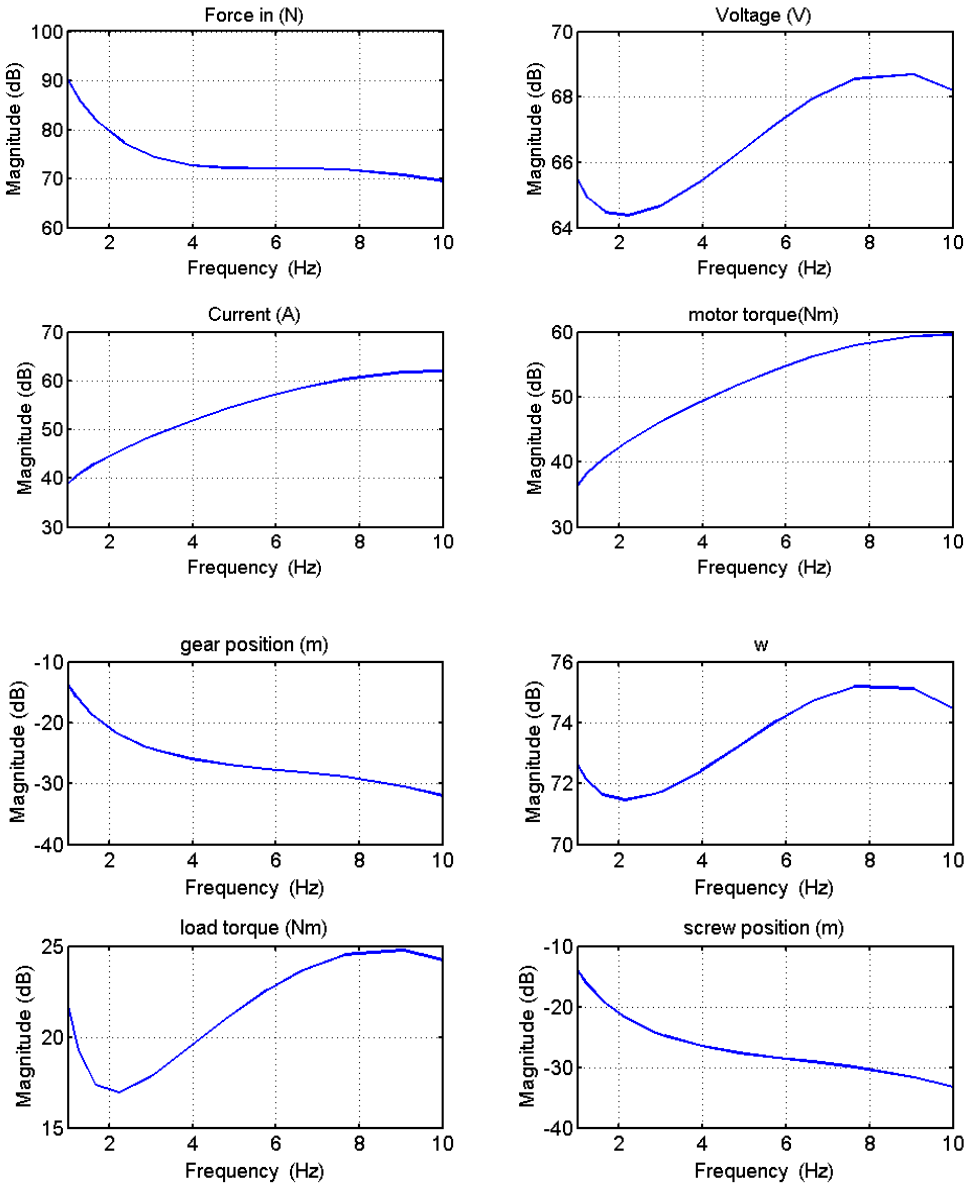

Figure 4.37: Magnitude plot of electromechanical actuator at 1-10 Hz

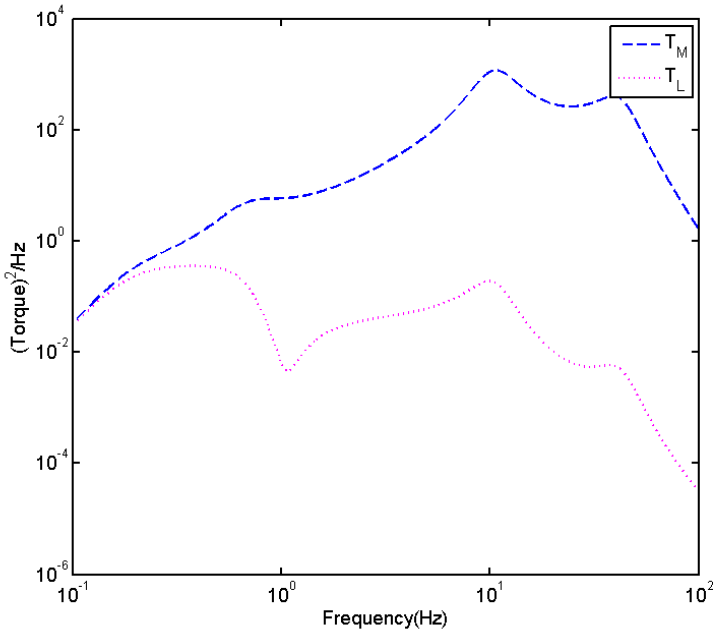

Figure 4.38: Motor torque (T_M) vs load torque (T_L) p.s.d.s

4.10.2 Electrohydraulic actuator analysis

The analysis of the electrohydraulic actuator was carried out similarly to the electromechanical actuator to look at the underlying issues of the actuator in the suspension. The actuator is analysed by looking at the velocity input response at 3Hz where the degradation begins. Figure 4.39 below shows the signals that have been analysed, where the main signals of the actuator are measured. The actuator signals are extracted from the model and the signal amplitudes are obtained at 3Hz as shown in Figure 4.40. The signal amplitudes are tabulated in Table 4.10. The actuator in suspension is producing much more force compared to what is required from it by the suspension controller.

Table 4.10:Electrohydraulic analyses at 3Hz

Signal		Amplitude	Unit
Input force	F_{in}	5.13	kN/ ms^{-1}
Output force	F_{out}	25.71	kN/ ms^{-1}
Force error		18.62	kN/ ms^{-1}
Voltage	V	124	V/ ms^{-1}
Current	I	300	mA/ ms^{-1}
Valve flow	Q_v	3.35 x 10^{-4}	m^3s^{-1}/ms^{-1}
Load pressure	P_L	0.4	Nm^2/ ms^{-1}
Cross port leak flow	Q_l	1x10^{-6}	m^3s^{-1}/ ms^{-1}
Actuator extension velocity	$\dot{x}_{act}$	1.09	

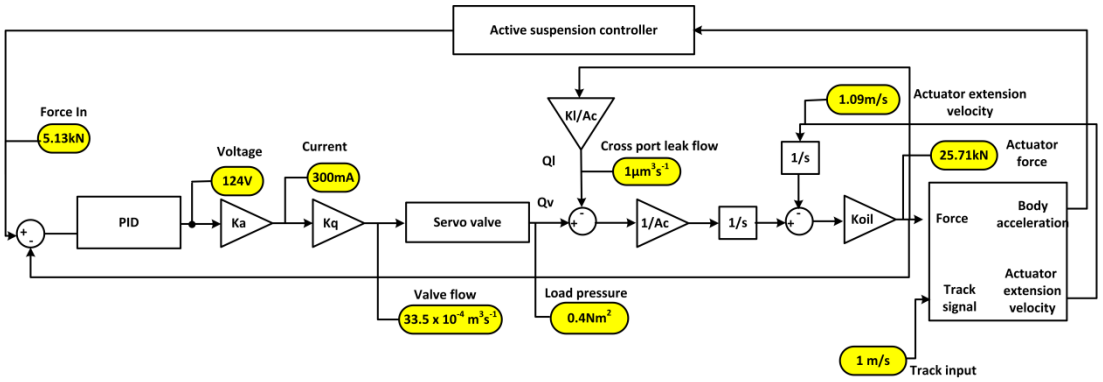

Figure 4.39: Electrohydraulic actuator analysis

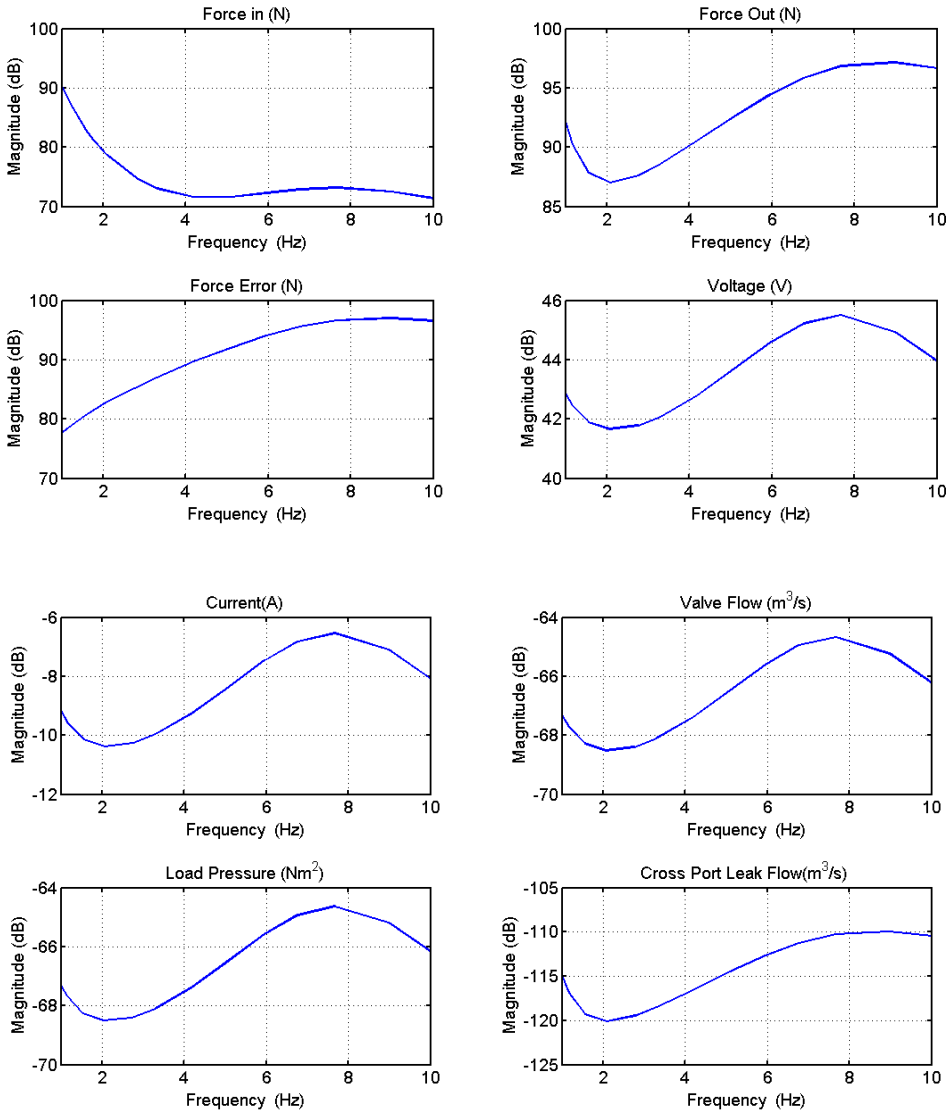

Figure 4.40: Magnitude Plot of the electrohydraulic actuator at 1-10Hz

4.11 Summary

The actuators for active suspension have been modelled and controlled using a classical force loop controller. As a starting point, the parameters for the actuator controller were tuned manually to improve the performance of the actuator without being in the suspension. The phase margin and gain margin were taken into consideration and the ability to follow

the force following the input was examined. This was done as a validation for the actuator working condition. The actuator was placed in the suspension where the deterioration to the suspension performance has been shown, which requires the actuator controller to be tuned again.

A continuation study in this chapter has shown that by optimising the actuator controller parameters using the genetic algorithm, significant improvement can be obtained. The stiffness optimisation, along with the controller optimisation, has reduced the degradation and also improved the performance of the actuator in the suspension. The simulation results are presented both by the acceleration p.s.d.s and the overall r.m.s. values for the car body accelerations, and these show that there are many opportunities to improve the actuator performance especially at higher frequencies.

For both actuators, the output force produced has also shown a huge amount of excess at 3Hz compared with the demand, which indicates that the actuator is not moving fast enough and is unable to absorb the vibration across the suspension.

For the electromechanical actuator, the motor torque is much higher than the load torque at higher frequencies; this is because much torque is required to accelerate the inertia which is wasted within the actuator. Meanwhile the electrohydraulic actuator issue was because much error is required to produce the flow rate.

Further work is still required to look at other control strategies for the active suspension actuators that will overcome the deterioration in performance at higher frequencies.

Chapter 5

Optimised Actuator Control with Feed Forward

From the analysis at 3Hz from the previous chapter, it is clear that the disturbance (at 3Hz) has a significant effect on the actuator performance. Hence it seems worth looking at a feed forward control strategy for further possibilities for improving the system and also to complete the classical controller methods. Feed forward control is used extensively in practice to reduce the effect on the system output of measurable command and disturbance inputs. In this chapter a practical feed forward control method is used for both actuators to improve the overall success of the active suspension performance. Again, only the actuator controllers will be investigated with this strategy, while the active suspension controller strategy remains the same. Another optimisation action will be applied to the force feedback controller for further improvement of the actuated active suspension system.

5.1 Feed forward control strategy

Feed forward control is commonly used in practice to reduce the effect on the system output of measurable disturbance inputs (Skogestad and Postlethwaite (2005)). Feed forward control responds to the changes in the command or the known disturbances in a pre-defined way to overcome the load effect of the system, contrary to the existing feedback control that reacts depending on the error produced by the varying load. Whenever there is a measurable disturbance, feed forward combined with feedback control can significantly improve the performance of the system before if affects the process output. Feed forward is normally combined with feedback control, where the feedback control is required to track the set point changes and suppress other immeasurable disturbances that would appear in any real process.

Although there are many feed forward methods for actuators, the application for the actuator in the suspension would be a practical approach type. The feed forward control for actuators in this thesis is developed in the context of the actuators being in the suspension which might be different from other feed forward applications. This feed forward control strategy applied in the railway vehicle model is based upon the need to compensate the effect of the motion across the actuator in the suspension. Since the actuator is expected to provide a performance approaching the ideal, the actuator has to overcome the difficulties of absorbing the vibration at higher frequencies. In this chapter, the feed forward methods that are being used are the reference feed forward and the disturbance feed forward.

5.1.1 Reference feed forward

The reference feed forward strategy is the architecture applied when dealing with the reference tracking objective as shown in Figure 5.1. The design of the *F(s)* block must be stable and proper. From the figure, the tracking performance could be quantified by the expressions in equations (5.1)-(5.2). In this strategy, the disturbance *D(s)* is neglected as the concentration would be on the reference input.

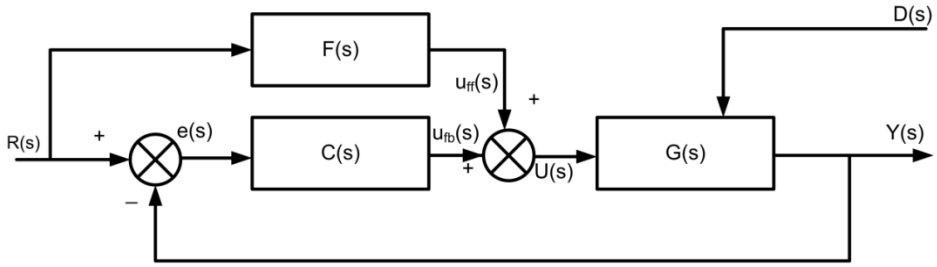

Figure 5.1 : Reference feed forward

$$Y(s) = R(s) + (G(s)F(s) - 1).\frac{R(s)}{1 + G(s)C(s)} \tag{5.1}$$

$$e(s) = R(s) - Y(s) \tag{5.2}$$

Although the ideal choice of *F(s)* would be $G(s)^{-1}$, this would often yield an improper transfer function (Looze, et al. (2010)). The choice of *F(s)* should be carefully selected to avoid this, which will be elaborated further based on the application of the actuator.

5.1.2 Disturbance feed forward

The disturbance rejection or disturbance feed forward, as illustrated in Figure 5.2, is another method of resolving whether to add an open loop mechanism. This method pre-empts the impact of the disturbance on the process output. The effect of the disturbance on the output is expressed in equation (5.3). Note that since the disturbance arises from the system itself, the use of the term 'feedforward' is not strict. Nevertheless the approach is consistent with the principle of feed forward, i.e. which is of augmenting the control input to reduce the feedback error. As this is a disturbance feed forward control strategy, the reference input, *R(s)* was not taken into consideration.

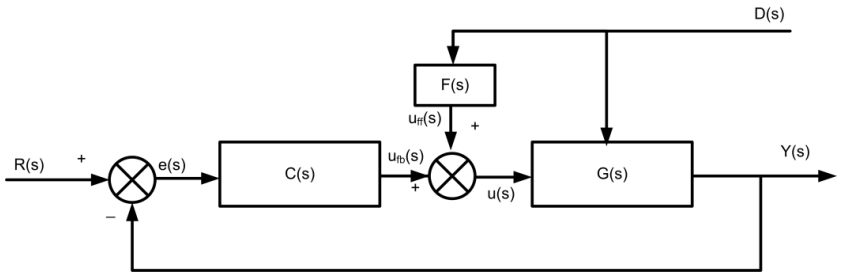

Figure 5.2: Disturbance feed forward

$$Y(s) = \left(G(s)^{-1} + F(s)\right)\left(\frac{G(s)}{1 + G(s)C(s)}\right)D(s) \tag{5.3}$$

The ideal choice for this feed forward configuration would be the negative inverse of the plant, $-G(s)^{-1}$. Again, if not properly selected this would yield an improper, non-causal and unstable transfer function. The impact of the disturbance feed forward on the plant input is as in equations (5.4) where:

$$Y(s) = -\frac{C(s)}{1+G(s)C(s)}G(s)D(s) + \frac{1}{1+G(s)C(s)}F(s)D(s) \tag{5.4}$$

From this equation it would be expected that this strategy should not adversely affect the actuator design objective, such as force tracking and stability.

The feed forward control strategies are applied to the actuator in the quarter car rail vehicle suspension with a common objective, to reduce the effect of the velocity disturbance across the actuator. This is because what is expected from the actuator is to be able to move within the suspension, and at the same time provide lower force when the disturbance exists. The following subsections will elaborate further on the feed forward control strategies applied to the active suspension actuators. The arrangement would be different depending on the physics of the actuator itself, and this will be explained in the following subsections.

5.2 Feed forward control strategy for the electromechanical actuator

5.2.1 Reference feed forward *(Force → Voltage)*

The *reference feed forward* strategy for the electromechanical actuator is shown in Figure 5.3, where the reference input is translated into a voltage input, $V_{in}(s)$, to be fed into the actuator. The feedback controller $C(s)$ remains as it is needed to modify the control action to reduce the error caused by the disturbance and uncertainty towards the actuator. $F_{in}(s)$ in this context refers to the active force input provided by the active suspension controller, meanwhile $F_{act}(s)$ is the output force produced by the actuator in the suspension.

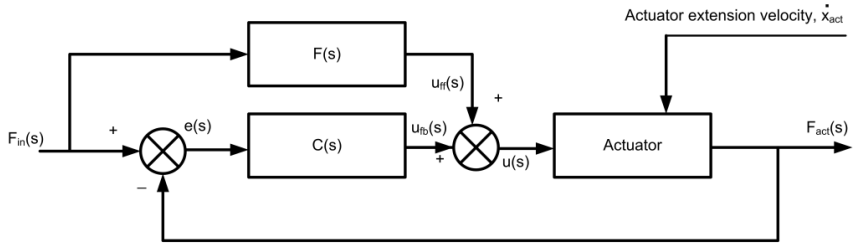

Figure 5.3 : Reference feed forward scheme for the electromechanical actuator

The voltage is produced based on the relationship between the required actuator voltage and the force input of the system. The voltage required is fed into the actuator so that the control does not depend on the actuator feedback to derive the error signal back into the actuator. This is a common classical approach of feed forward used to improve the performance of the existing system, and involves some form of the inverse dynamics of the actuator.

Using the steady state approach and the knowledge of the d.c. motor in the actuator, the required information of the relation between the input force, F_{in}, and the actuator voltage, V_{in}, means that the reference feed forward equation could be constructed. The reference feed forward constant providing the voltage demand is shown in equation (5.5).

$$G_F(s) = \frac{V_a(s)}{F(s)} = \frac{R_{arm} \cdot J_m . s(s) + (C_m R_{arm} + K_e K_t).l}{K_t \ (J_m . s(s) + \ D_m)} \tag{5.5}$$

The reference feed forward strategy as shown in Figure 5.4 will provide the required voltage to provide the required force, but note that it does not include the effect of $\dot{x}_{act}$.

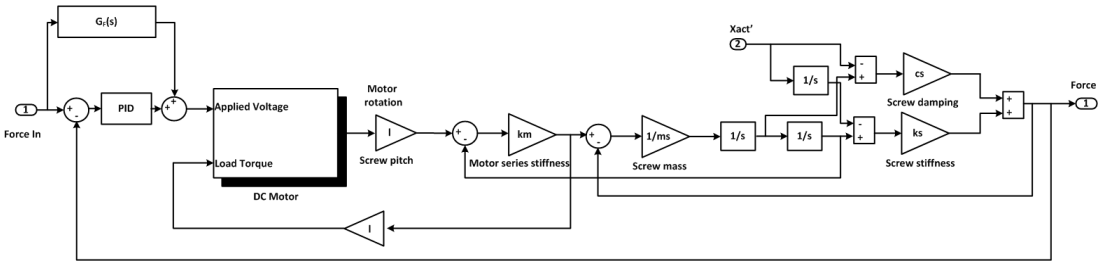

Figure 5.4: Reference feed forward for the electromechanical actuator

The p.s.d. results in Figure 5.5 show that the reference feed forward strategy does not provide significant improvement to the original controller, compared to the force feedback control, as seen in Table 5.1. This result confirms that it is the effect of the disturbance, $\dot{x}_{act}$ which is dominant in degrading high frequency performance.

Table 5.1: R.M.S. results

		Ideal	**Force feedback**	**Reference feed forward**
Acceleration	(%g)	1.700	4.331	4.332
Deflection (track input)	(mm)	8.4	8.5	8.6
Actuator Force	(kN)	1.718	6.884	6.899

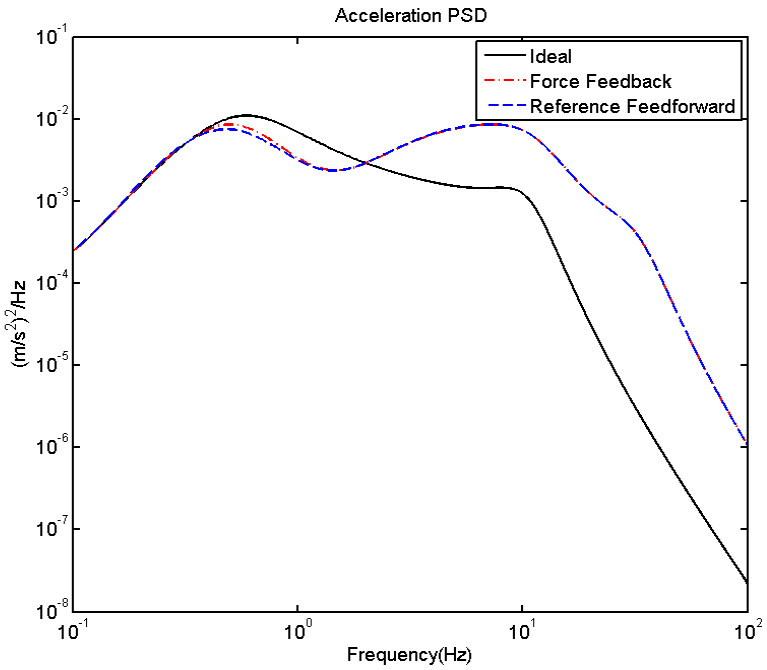

Figure 5.5 : Comparison between the reference feed forward control strategy p.s.d.s with the ideal and force feedback control strategy for the electromechanical actuator

5.2.2 Disturbance feed forward

Another possible feed forward control for the active suspension actuators would be the *disturbance feed forward* strategy. Compared to reference feed forward, this strategy will attempt to improve the active suspension actuator performance by using the inverse relationship between the actuator extension velocity and the actuator voltage to provide the required voltage for the actuator. The basic arrangement is shown in Figure 5.6. *Velocity* and *acceleration* based strategies are the two possible approaches for the active suspension actuator control.

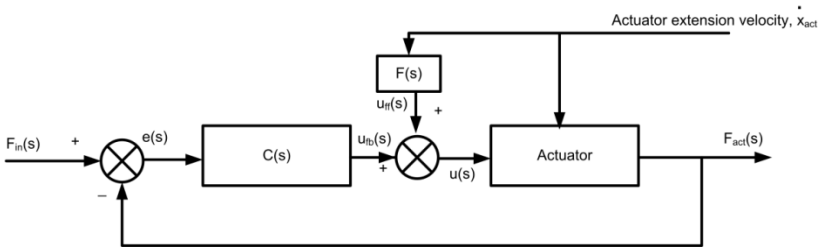

Figure 5.6: Disturbance feed forward

These feed forward strategies will be applied and tested to observe the ability of the strategy to suppress the effect of the disturbance caused by the motion of the actuator in the suspension. This feature is important as here we are applying the actuator in the suspension in exactly the manner that it would be in a real vertical suspension.

The combination of the feedback controller *C(s)* with the feed forward strategy is applied to modify the control action to reduce the error caused by the disturbance and uncertainty towards the actuator. The actuator input *U(s)* is derived based on the inverse relationship between the voltage required by the d.c. motor and the actuator extension velocity of the system. The voltage required by the actuator is fed directly into the actuator, in addition to the feedback control signal.

5.2.2.1 Velocity based disturbance feed forward (Velocity→Voltage)

The velocity based disturbance feed forward method applies a feed forward compensation back into the actuator from the actuator extension velocity, $\dot{x}_{act}$, back into the actuator via the armature voltage. In general, the knowledge of the velocity from the ideal actuator requirement is used to provide the maximum voltage to drive the actuator. This requirement was previously calculated from the ideal requirement during the actuator modelling process. Using the steady state approach and the knowledge of the d.c. motor in the actuator, the required information of the relation between the actuator $\dot{x}_{act}$ and the actuator armature voltage, V_{in}, the reference feed forward equation is constructed as shown in equation (5.6). The arrangement is shown in Figure 5.7.

$$G_F(s) = \frac{V_a(s)}{\dot{x}_{act}(s)} = \frac{K_e}{l} \tag{5.6}$$

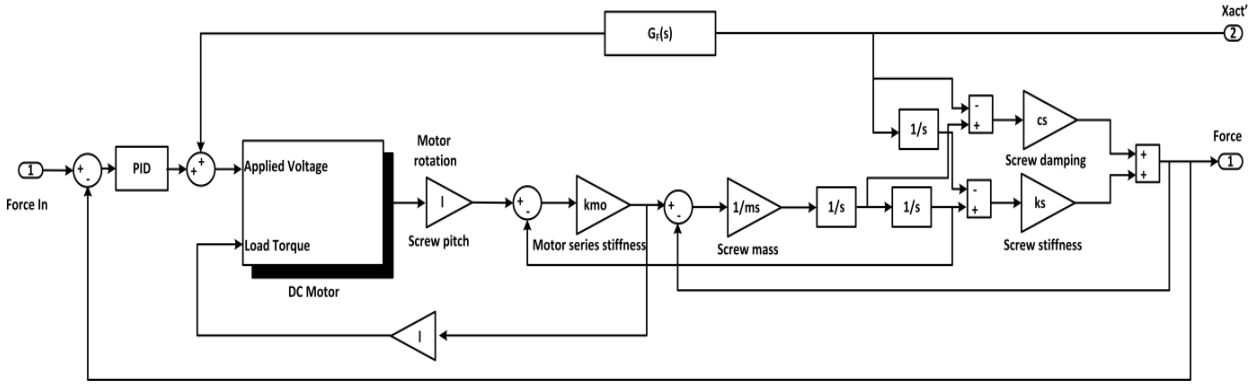

Figure 5.7 : Disturbance feed forward configuration for the electromechanical actuator

The results for the feed forward strategies are compared with the force controlled actuator and the ideal as illustrated in Figure 5.8, and tabulated in Table 5.2. Unlike the reference feed forward control strategy, the disturbance feed forward control strategy overall acceleration r.m.s results in an improved ride performance. An improvement in the ride quality of 52.2% has been achieved compared to the force feedback strategy. The actuator force has also improved significantly by 39% compared to the manually tuned force feedback actuator. Both ride quality and force output have shown an improvement in the effort to approach the ideal. The disturbance feed forward strategy has pulled down the ride quality to 2.07 %g which is 22% closer to the ideal compared to the force feedback. It can be seen from the p.s.d. graph that it provides significant improvement in the 3-10Hz range, but at higher frequencies it offers no benefit.

Table 5.2: R.M.S. results

		Ideal	**Force feedback**	**Velocity based disturbance feed forward**
Acceleration	(%g)	1.700	4.331	2.070
Deflection (track input)	(mm)	8.4	8.5	8.4
Actuator Force	(kN)	1.718	6.884	4.223

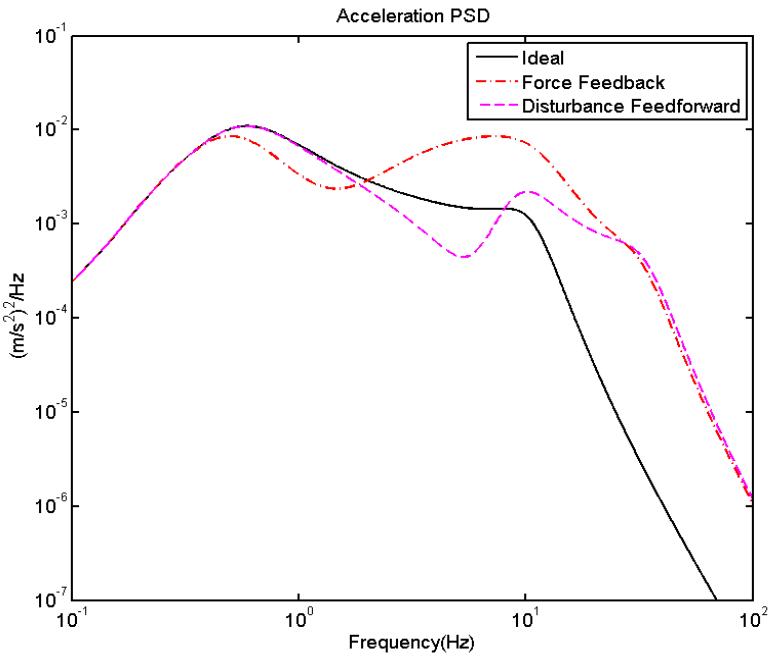

Figure 5.8 : Vertical body acceleration p.s.d.s for the electromechanical actuator

5.2.2.2 Acceleration based disturbance feed forward

Another possible method to further improve the disturbance feed forward control strategy is by using acceleration feed forward. Based on the information gained from the 3Hz analysis subsection in Chapter 4, the motor creates a large error trying to create acceleration. To overcome this, acceleration based feed forward control could possibility overcome this issue. To accomplish this, a current control fed back to the actuator motor is required. This is an interesting feed forward option based on the results shown from adding current control within the electromechanical actuator by Du (2008). It is expected that by adding feed forward, better results could be achieved.

The actuator with a current feedback is tuned to provide a bandwidth of 100Hz, and the force feedback controller is re-tuned to produce a good force tracking output. The configuration of the actuator is shown in Figure 5.9.

By including the current control in the actuator, the acceleration disturbance feed forward is made possible. This effort is expected to reduce the inertial effect by adding disturbance feed forward in the actuator. Using the steady state approach and the knowledge of the d.c. motor in the actuator, the required information of the relation between the actuator $\dot{x}_{act}$ and the current to the actuator, the acceleration feed forward equation is constructed as shown in equation (5.7).

$$G_F(s) = \frac{I(s)}{\ddot{x}_{act}(s)} = \frac{J_m}{K_t.l} \tag{5.7}$$

The configuration of this strategy is illustrated in Figure 5.10 where the acceleration to current feed forward control is placed into the current control input to reduce the feedback error required to develop the appropriate current.

The p.s.d.s results for the acceleration feed forward and the current control of the actuator in the suspension are illustrated in Figure 5.11, where it is clearly shown that an improvement has been achieved through the additional current loop control with force feedback and a much better improvement with the acceleration based disturbance feed forward. This can be seen clearly in the p.s.d.s in Figure 5.9. The ride quality r.m.s. in Table 5.3 confirms this with an improvement of 2% better than the ideal for the ride acceleration and a much lower actuator force.

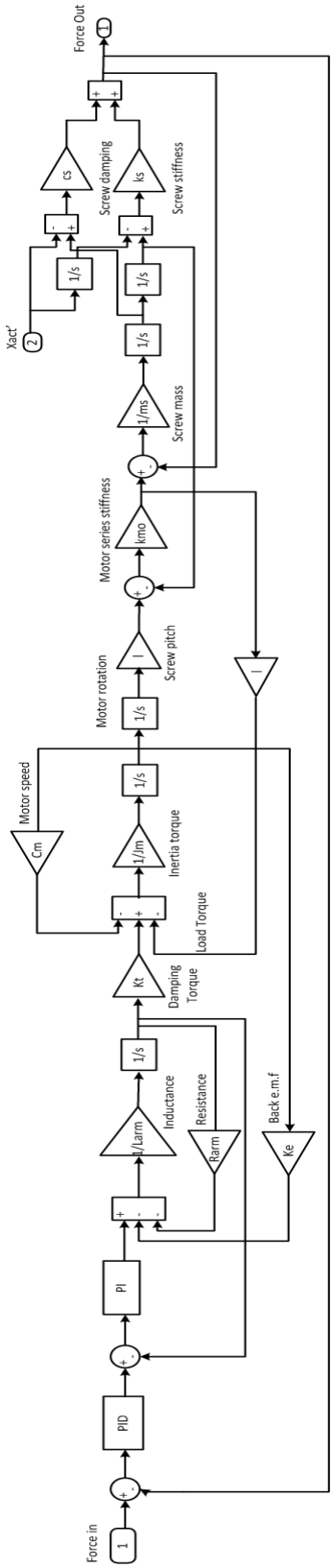

Figure 5.9: Current Control of the actuator

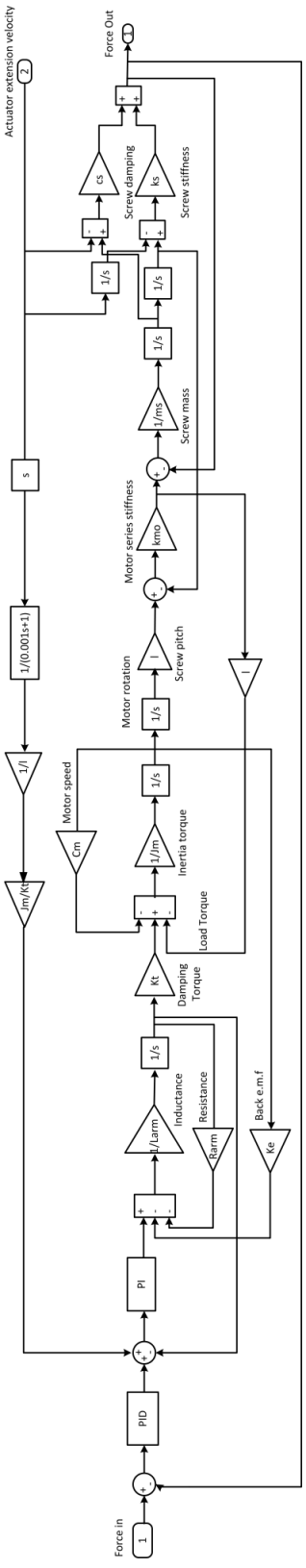

Figure 5.10: Acceleration feed forward control

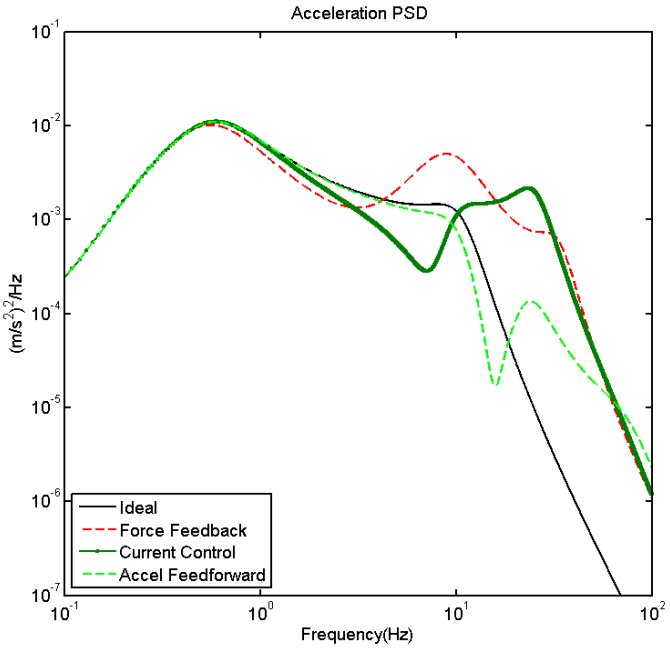

Figure 5.11: Vertical body acceleration p.s.d.s for the electromechanical actuator with acceleration feed forward control

Table 5.3: RMS results

		Ideal	**Force feedback**	**Current control and force feedback**	**Acceleration based feed forward**
Acceleration	(%g)	1.700	4.331	2.430	1.655
Deflection	(mm)	8.4	8.5	8.4	8.4
Actuator Force	(kN)	1.718	6.884	4.900	2.149

5.3 Feed forward control of the electrohydraulic actuator

From the previous feed forward control strategy analysis for the electromechanical actuator in the previous section, it has been found that the reference feed forward did not benefit the actuator in terms of improving the ride quality. Therefore this method will not be repeated for the electrohydraulic actuator because the main issue for actuators in the suspension is the disturbance created by the actuator extension velocity. Therefore, for the electrohydraulic actuator only the velocity based disturbance feed forward will be tested. As for the acceleration based disturbance feed forward, this is only appropriate to compensate for the inertial effects of the d.c. motor, and there is no such physical effect for the electrohydraulic actuator.

5.3.1 Velocity based disturbance feed forward

The method of feed forward for the electrohydraulic actuator is a fairly straightforward process compared to the electromechanical actuator. This is due to the simplicity of the hydraulic device being used and also the requirement of the actuator. The feed forward for the electrohydraulic actuator is done based on the velocity disturbance. The general idea is to provide the maximum servo-valve current required to produce the actuator's required speed as calculated from the ideal requirements.

$$G_F(s) = \frac{V_a(s)}{I(s)} = \frac{A_c}{K_q} \tag{5.8}$$

The configuration for this strategy is illustrated in Figure 5.12. The p.s.d. for this control strategy is shown in Figure 5.13, where it can be clearly seen that the electrohydraulic actuator has the capability to achieve the ideal up to higher frequencies. The time domain results have also shown rather promising improvements where the actuator in the suspension with the feed forward control strategy gives significant improvement as shown in Table 5.4.

An improvement better than the ideal of approximately 6 % is achieved and the actuator force has reduced towards the ideal by 8.14 %. The additional feed forward control strategy has significantly improved the existing electrohydraulic actuator with force feedback control performance in the quarter vehicle suspension.

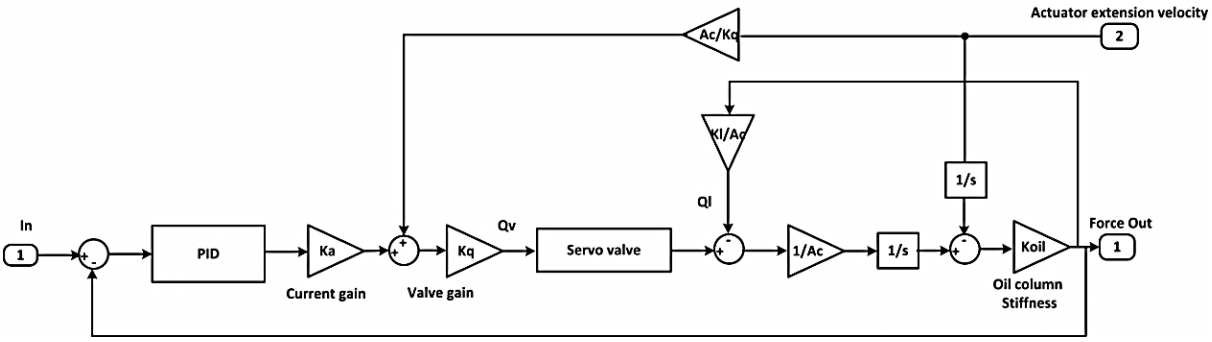

Figure 5.12 : Feed forward configuration for the electrohydraulic actuator

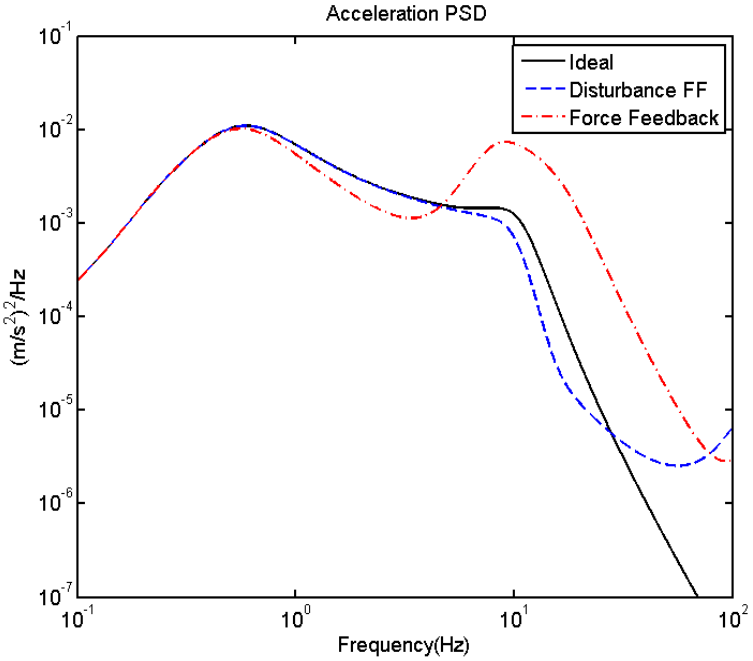

Figure 5.13: Vertical body acceleration p.s.d.s for the electrohydraulic actuator with velocity feed forward

Table 5.4: RMS results

		Ideal	Force feedback	Velocity feed forward
Acceleration	(%g)	1.700	2.809	1.600
Deflection	(mm)	8.4	8.3	8.4
Actuator Force	(kN)	1.718	5.558	1.862

5.4 Improvement of feed forward control strategy using NSGA- II

From the previous subsections, the improvement given by the disturbance feed forward control strategy for both actuators means that it would be interesting to look at further improvement of the actuated quarter rail vehicle. The force feedback controller parameters are optimised within the feed forward control strategy similarly to the previous actuator parameters' optimisation in Chapter 4 where the controller parameters are optimised followed by another optimisation of the controller and actuator stiffness together in the suspension.

The optimisation approach is carried out with the same set of rules as used previously in Chapter 4 with the actuator in the quarter car railway vehicle suspension.

5.4.1 Electromechanical actuator controller optimisation

5.4.1.1 Velocity based disturbance feed forward

Final controller parameters for both strategies were selected based on the "Pareto curve" as presented in Table 5.5, and the trade-off plot for the vertical acceleration against the suspension deflection on a straight track is illustrated in Figure 5.14. The "∗" curve shows

the optimisation of the controller parameters (OPT I), and the "o" curve is for the controller parameters and actuator stiffness optimisation (OPT II). It could be seen that by softening the actuator a better range of ride quality could be obtained as there is also a reduction in actuator force across the suspension. Since the aim is to obtain an actuator performance as close as possible to the ideal, the optimisation point closest to the ideal situation is selected. These parameters from this point are then used for r.m.s. and p.s.d.s analysis for both quarter car and the side-view model.

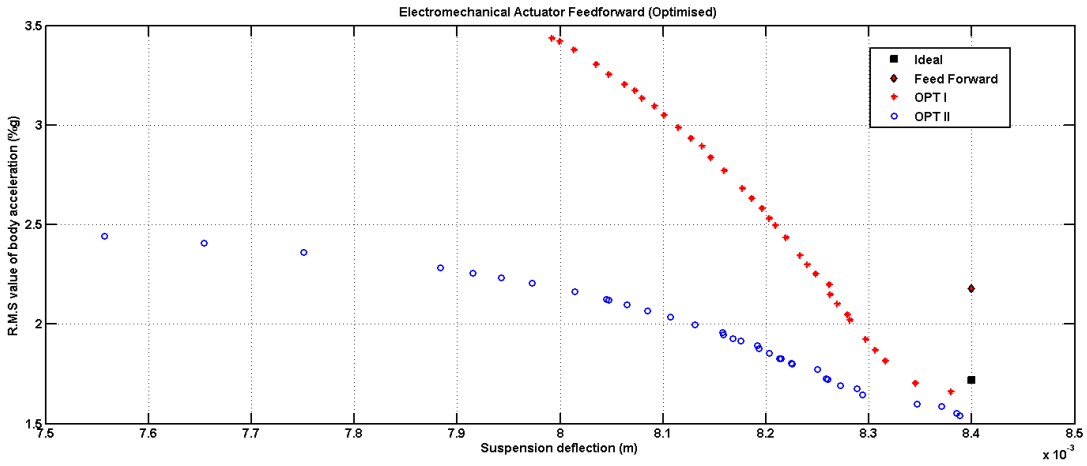

Figure 5.14: Trade-off plot for the NSGA-II optimisation of the velocity feed forward controller optimisation and for the varied actuator stiffness

Table 5.5: Final parameters for the controller optimisation

	k_p [V/N]	k_i [Vs/N]	w_c [rad/s]	
Controller optimisation	0.00993	0.01173	200.2	
Controller and stiffness optimisation	0.0881	0.034	363	$k_s = 2.498 MN/m$

The controller equation for this optimisation is as shown in equation (5.9) for the optimised electromechanical actuator controller parameters and in equation (5.10) for the optimised controller and stiffness parameters.

$$G_c = \frac{0.00993(1 + 0.01173s)(1 + 0.141s)}{0.01173s(1 + 0.0018s)} \tag{5.9}$$

$$G_c = \frac{0.0881(1 + 0.034s)(1 + \ 0.0078s)}{0.034s(1 + 0.000974s)} \tag{5.10}$$

5.4.1.2 Acceleration based disturbance feed forward

The final controller parameters for both parameter optimisation strategies were selected based on the "Pareto curve" as presented in Table 5.7, and the trade-off plot for the vertical acceleration against the suspension deflection on a straight track is illustrated in Figure 5.16. Here only the force feedback controller is optimised and the current controller within the actuator is remained unchanged. The "$*$" curve shows the optimisation of the controller parameters (OPT I), and the "o" curve is for the controller parameters and actuator stiffness optimisation (OPT II). It could be seen that further improvement is achievable however softening the actuator stiffness no further improvement obtained. Again, the best performance is selected (since the initial strategy has shown improvement). These parameters from this point are then used for r.m.s. and p.s.d.s analysis for both quarter car and the side-view model.

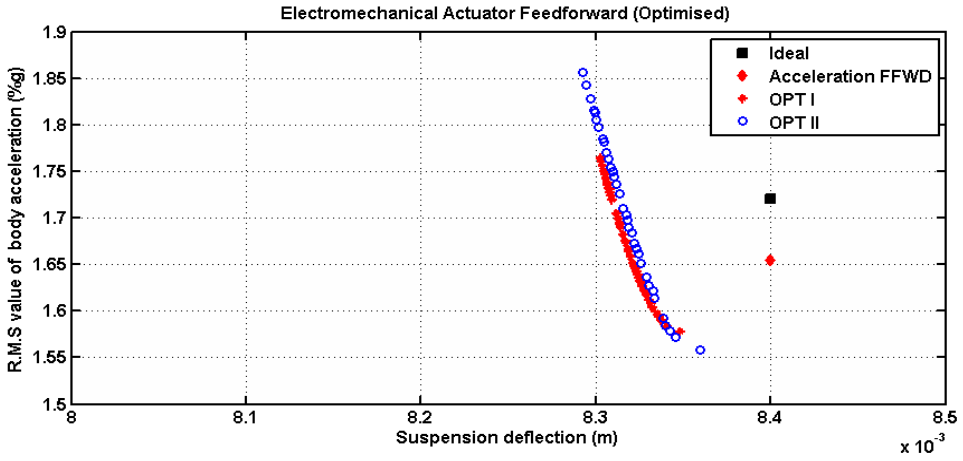

Figure 5.15: Trade-off plot for the NSGA-II optimisation of the acceleration based feed forward controller optimisation and for the varied actuator stiffness

Table 5.6: Final parameters for the controller optimisation

	$\mathbf{k_p}$ [V/N]	$\mathbf{k_i}$ [Vs/N]	$\mathbf{w_c}$ [rad/s]	
Controller optimisation	0.0194	0.804	318.36	
Controller and stiffness optimisation	0.0237	0.3124	340.8	k_s =7.446 MN/m

The controller equation for this optimisation is as shown in equation (5.11) for the optimised electromechanical actuator controller parameters and in (5.12) for the optimised controller and stiffness parameters

$$G_c = \frac{0.0194(1 + 0.804s)(1 + 0.0089s)}{0.804s(1 + 0.0011s)} \tag{5.11}$$

$$G_c = \frac{0.0237(1 + 0.741s)(1 + \ 0.0083s)}{0.741s(1 + 0.0010s)} \tag{5.12}$$

5.4.2 Electrohydraulic actuator controller optimisation

The electrohydraulic actuator force controller parameters are optimised and presented in Table 5.7. The trade-off plot for the vertical acceleration against the suspension deflection on a straight track is illustrated in Figure 5.15. The "∗" curve shows the optimisation of the controller parameters (OPT I), and the "o" curve is for the controller parameters and actuator stiffness optimisation (OPT II). As the actuator stiffness parameter was optimised too, this has led to a higher value compared to the original design. This could indicate that a redesign of the actuator parameters is required.

The disturbance feed forward control strategy for the electrohydraulic actuator has demonstrated improvement better than the ideal, any optimisation and selection of parameters is based on the best ride quality and also on the suspension deflection. These parameters are then used for r.m.s. and p.s.d.s analysis for both the quarter car and the side-view model.

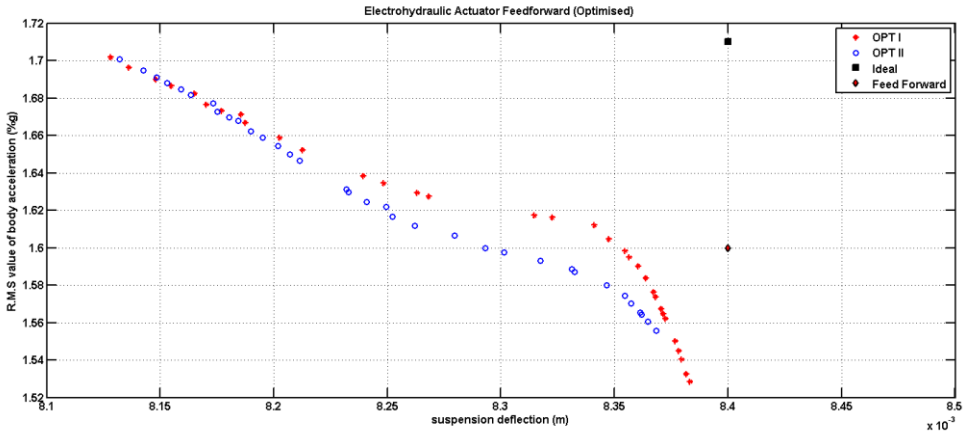

Figure 5.16 : Trade-off plot for the NSGAII optimisation of the controller optimisation and for the varied actuator stiffness

Table 5.7 : Final parameters for the controller optimisation

	k_p [V/N]	k_i [Vs/N]	w_c [rad/s]	
Controller optimisation	0.00073	0.0169	683	
Controller and stiffness optimisation	0.00083	0.0648	698.2	$B_m = 2.486 \times 10^9 N/m^2$

5.4.3 NSGA-II optimisation simulation results

Using the parameters obtained from the optimisation in Tables 5.5, 5.6 and 5.7, the performance in the quarter rail vehicle is compared with the previous disturbance feed forward control. The p.s.d. comparison is illustrated in Figures 5.17 until 5.19. The r.m.s. results are tabulated in Table 5.8. Optimisation of the controller gains has shown noticeable improvement for the acceleration and also the actuator force which can be clearly seen in the p.s.d. and also in the r.m.s. results. For the electromechanical actuator with the velocity based disturbance feedforward, the selected optimised controller parameters with fixed stiffness (OPT I) showed the ability of the suspension to follow the ideal up to 15Hz before gradually degrading. Meanwhile, compared to the selected optimised controller and stiffness parameters (OPT II), the degradation gradually begins at 10Hz. The actuator force is also reduced significantly, which could mean that the motor is producing less motor torque to drive the inertia. The acceleration based feed forward has also showed a better than the ideal suspension performance with similar results for the optimisations. This is illustrated by the r.m.s values and the p.s.d.s.

For the electrohydraulic actuator, the selected controller and stiffness parameters for both optimisation techniques produced similar results to the initial feed forward strategy, which has been illustrated by the p.s.d.s and also the r.m.s. values.

Table 5.8: Feed forward control strategies r.m.s. results

	EMA						EHA			
	Velocity based feed forward			Acceleration based feed forward			Velocity based feed forward			
	Manual	Optimisation		Manual	Optimisation		Manual	Optimisation		
		OPT I	OPT II		OPT I	OPT II		OPT I	OPT II	
Acceleration (%g)	2.070	1.660	1.551	1.655	1.593	1.597	1.600	1.530	1.590	
Deflection (mm)	8.4	8.4	8.4	8.4	8.3	8.3	8.4	8.4	8.4	
Actuator Force (kN)	4.223	2.567	2.323	2.149	2.531	2.344	1.863	2.061	2.000	

** Ideal : Acceleration 1.7%g Deflection : 8.4mm Actuator Force: 1.718kN

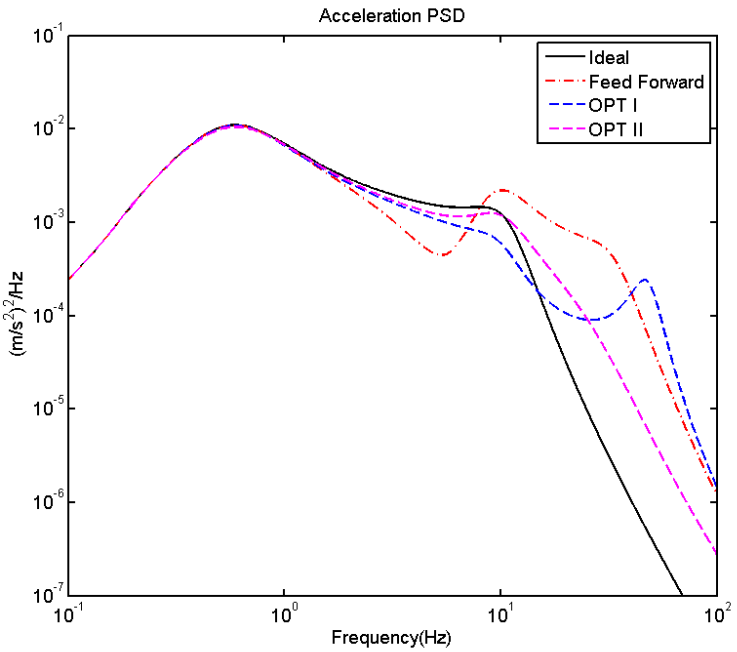

Figure 5.17: P.s.ds for the effect of the electromechanical actuator with the optimised velocity based disturbance feed forward control in the quartercar vehicle actuator

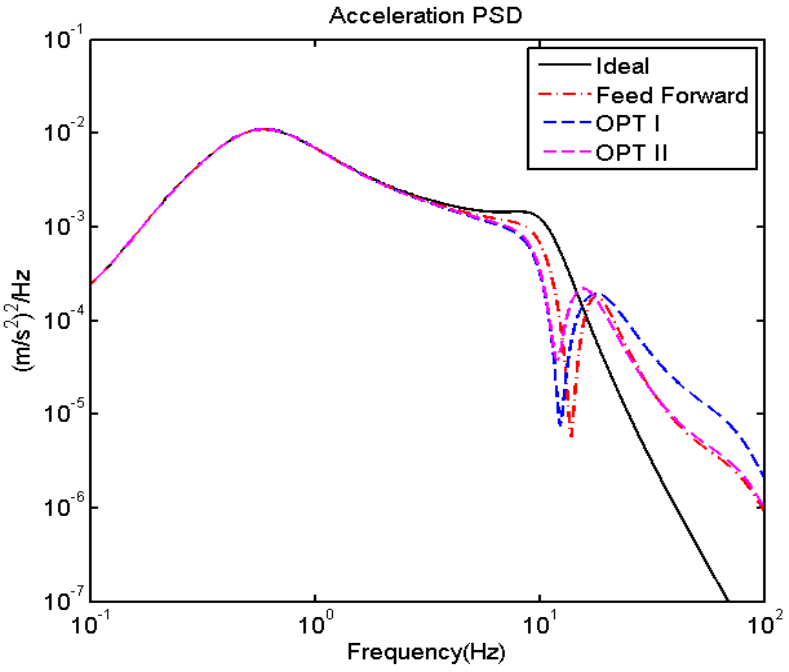

Figure 5.18: P.s.ds for the effect of the electromechanical actuator with the optimised acceleration based disturbance feed forward control in the quartercar vehicle actuator

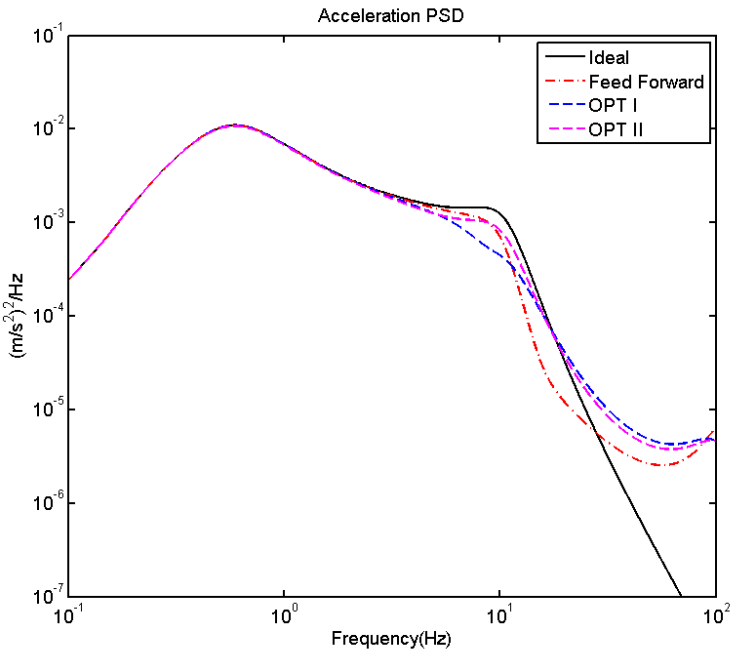

Figure 5.19: P.s.ds for the effect of the electrohydraulic actuator with the optimised feed forward control in the quartercar vehicle

5.5 Controller performance assessment in the Side-view vehicle

In this section the feed forward control strategies that have been tested in the quarter car railway vehicle will be placed in the side-view model; an additional pitch mode exists in the system.

Power spectral densities for the front and rear suspension for the electromechanical actuator is shown in Figures 5.20 until 5.25. A significant reduction in the ride acceleration is shown for both of the disturbance feedforward strategies and its parameters' optimisation techniques for the electromechanical actuator. The front and rear suspension of the vehicle suspension with the velocity based feedforward control strategy has shown the ability of the actuator to accommodate the movement across the suspension of up to 13Hz for both OPT I and OPT II before going into degradation. Softening the actuator stiffness, k_s, has however reduced the degradation compared to the manually tuned actuator, which means that a softer

spring gives benefit to the whole system in reducing the actuator force. The acceleration based feedforward p.s.ds are shown in Figures 5.22 and 5.23. This strategy has shown that this strategy and the optimisations showed similar performance where the ride acceleration demonstrated the ability to follow the ideal beyond 10Hz.

The p.s.d.s for the electrohydraulic actuator are presented in Figure 5.24 and 5.25 where there is not much difference in terms of the acceleration performance for all of the three actuator controllers. All three (manually tuned, OPT I, and OPT II) controllers have the ability to produce the ideal up to 25Hz before deviating towards degradation.

A full summary of the actuator performance in terms of the r.m.s. values is shown in Table 5.8 for the electromechanical actuator and Table 5.11 for the electrohydraulic actuator. From the p.s.d.s and also the time response r.m.s. values, both optimisations of the controller parameters improve the performance significantly. However, the overall results were not affected by the stiffness optimisation.

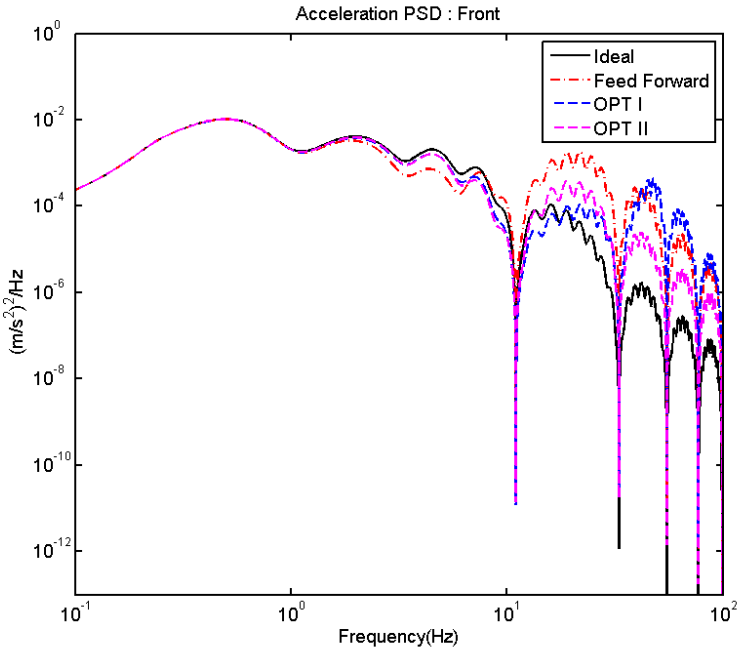

Figure 5.20: Front p.s.d.s for the electromechanical actuator with optimised velocity based disturbance feed forward control effect in the sideview vehicle

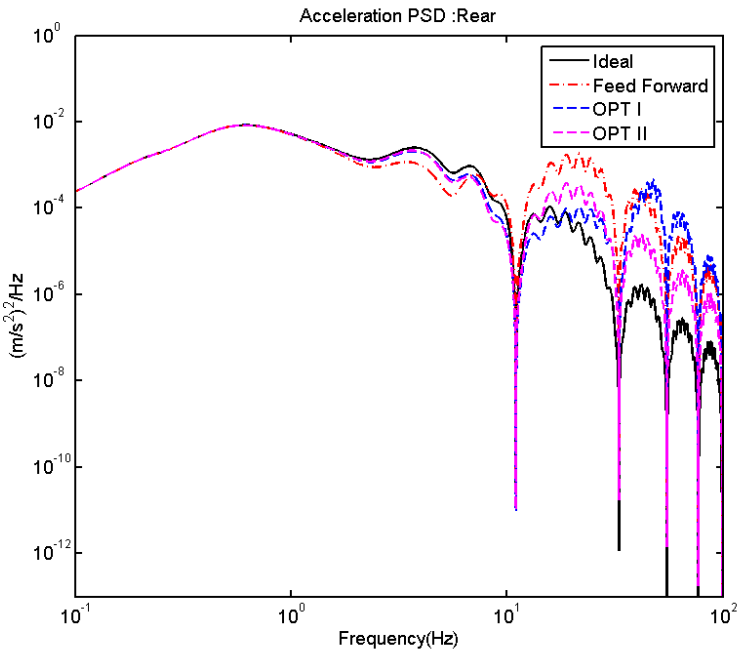

Figure 5.21: Rear p.s.d.s for the electromechanical actuator with optimised velocity based disturbance feed forward control effect in the sideview vehicle

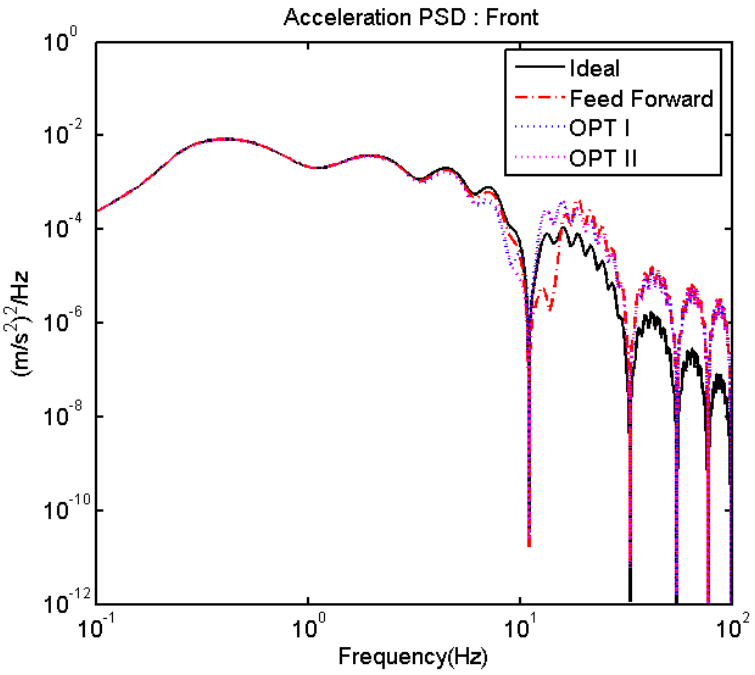

Figure 5.22: Front p.s.d.s for the electromechanical actuator with optimised acceleration based disturbance feed forward control effect in the sideview vehicle

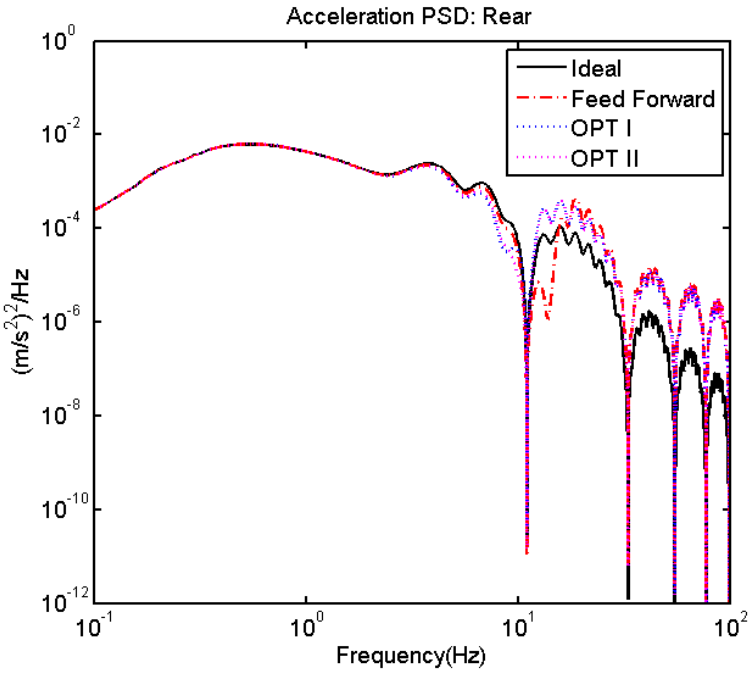

Figure 5.23: Rear p.s.d.s for the electromechanical actuator with optimised acceleration based disturbance feed forward control effect in the sideview vehicle

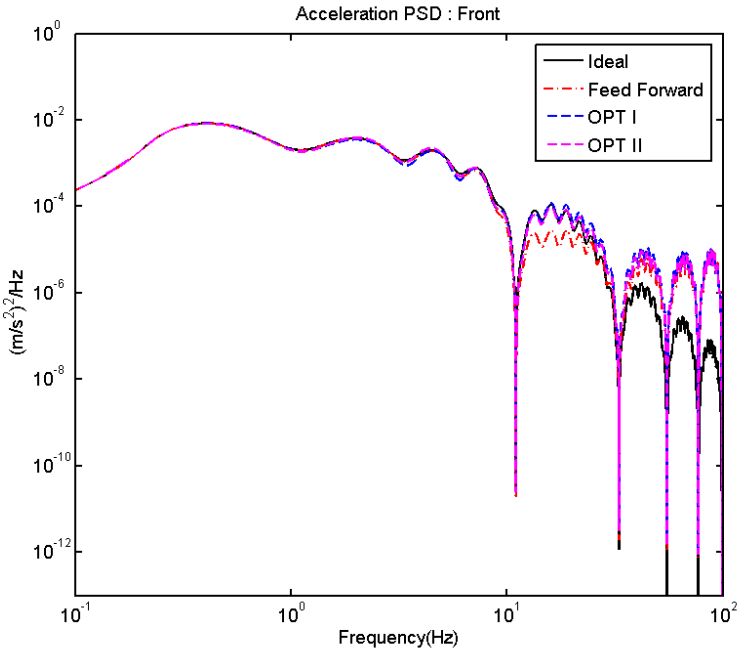

Figure 5.24: Front p.s.d.s for the electrohydraulic actuator with optimised feed forward control effect in the sideview vehicle

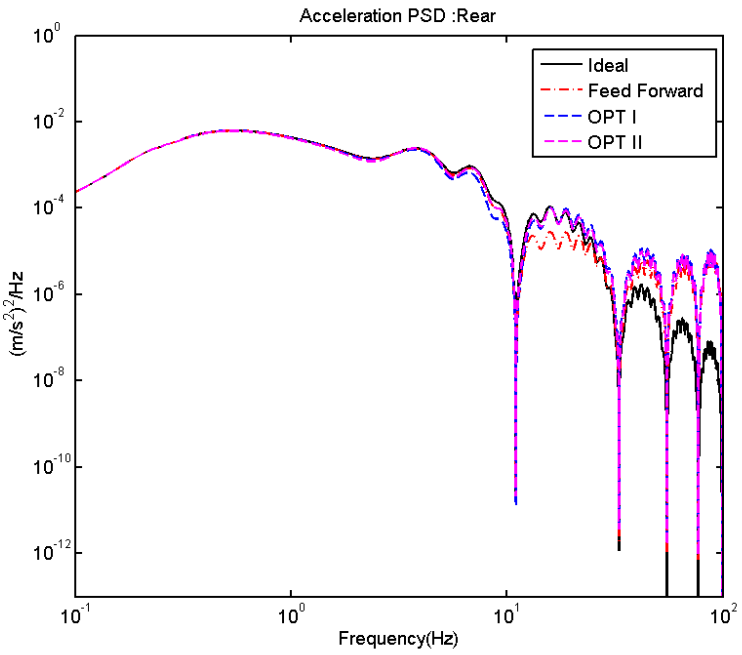

Figure 5.25: Rear p.s.d.s for the electrohydraulic actuator with optimised feed forward control effect in the sideview vehicle

Table 5.8: Comparison of ride results for the disturbance feed forward controller strategies for the electromechanical actuator compared to the ideal

Strategy		Vertical Accel. (%g)			Suspension Defl. (mm)		Actuator force (kN)	
		Front	Centre	Rear	Front	Rear	Front	Rear
Ideal		1.371	0.869	1.539	8.4	11.1	1.948	2.879
Velocity based disturbance feedforward		1.960	1.202	1.982	10.8	11.5	3.554	3.612
Optimisations	**OPT I**	1.624	1.450	1.666	10.8	11.5	3.033	3.123
	OPT II	1.600	1.030	1.640	10.8	11.5	2.953	3.046
Acceleration based disturbance feedforward		1.504	1.0360	1.444	12.9	9.4	3.445	2.918
Optimisations	**OPT I**	1.570	1.058	1.512	12.8	9.3	3.491	2.990
	OPT II	1.516	1.037	1.460	12.8	9.4	3.381	2.868

Table 5.9: Comparison of ride results of the disturbance feed forward controller strategies for the electrohydraulic actuator compared to the ideal

Strategy		Vertical Accel. (%g)			Suspension Defl. (mm)		Actuator force (kN)	
		Front	Centre	Rear	Front	Rear	Front	Rear
Ideal		1.371	0.869	1.539	8.4	11.1	1.948	2.879
Velocity based disturbance feedforward		1.564	1.015	1.607	10.8	11.5	2.870	2.792
Optimisations	**OPT I**	1.558	1.012	1.601	10.8	11.5	2.870	2.970
	OPT II	1.562	1.010	1.601	10.8	11.5	2.878	2.975

The feed forward control strategy has meant that the r.m.s. results approach the ideal in certain cases. As shown in Table 5.8, the velocity based feed forward controlled electromechanical actuator has improved the vehicle ride quality degradation compared to the force feedback control scheme where the ride quality has an average of 40% of degradation compared to the ideal. This is an improvement of 10% compared to the 50% degradation caused by the force feedback control introduced in Chapter 4 earlier.

Optimisation of the electromechanical actuator controller parameters has also brought down the acceleration towards 18% (OPT I) and 16% (OPT II), approaching the ideal actuator performance. The improvement of the actuator force is also noticeable compared to the force controlled actuators in the previous chapter.

Meanwhile the acceleration based feed forward has demonstrated improvement better than the ideal for the quartercar vehicle, however when translated to the sideview vehicle, the performance has deviated from the ideal by almost 10% and more for the optimised controller parameters.

As for the electrohydraulic actuator as in Table 5.9, feed forward has improved the ride quality, with the ride acceleration approaching 10% towards the ideal. This is an improvement compared to the average of 52% of degradation compared to the ideal offered by the actuators' force feedback control. Optimisations of the controller parameters, OPT I and OPT II, has further improved the ride performance by an average of 6.7% and 6.5%

respectively approaching the ideal. The actuator force has reduced for the feed forward strategy but the optimisation has not reduced the actuator force any further.

5.6 Robustness of the active suspension actuator controller

The feed forward and also the force controller were developed to improve the vibration experienced by the linearised railway vehicle suspension. However the feed forward approaches in particular rely upon accurate knowledge of the relevant parameters, but if these controllers were to be applied in the physical railway vehicle actuators, the parameters assumed during design stage will vary due to changes in the operating environment. Therefore it is important to investigate the robustness of the devised actuator controllers in an operating environment of changing physical parameters. This will be carried out by investigating the changes in the crucial components of the actuators.

The aim in this subsection is to test the stability of the overall system and evaluate the performance in terms of ride quality when certain parameters are adjusted. This is considered a good test for the practicality of the actuators in the suspension because of the variation of parameters due to the manufacturing tolerances. The active suspension actuator feed forward control strategy developed will be investigated for robustness. For the feed forward strategy that has been investigated and also the off line optimisation procedure that has been applied, a robustness check must be done to the actuated vehicle system.

The check will be carried out using the quarter rail vehicle and extended to the side-view vehicle.

5.6.1 Robustness of the active suspension actuator controller on the quarter car railway vehicle

For the electromechanical actuator, the motor inertia, J_m, and also the back e.m.f, constant, K_e, are the parameters that will be varied. A variation up to ± 20% is applied and the ride quality and actuator force are investigated.

Table 5.10 and Table 5.11 tabulate the results by the varying of the motor inertia and the motor back e.m.f. Feed forward strategies are tested along with the optimisation of the force control feedback parameters (OPT I), and also the actuator stiffness optimisation strategy (OPT II). The results presented in Tables 5.11 and 5.13 shows that the incrementing of the motor inertia degrades the ride quality slightly and also increases the actuator force for both feed forward strategies by 12% and 16% respectively, whereas the optimised strategy is slightly affected by the variations of the motor inertia. Tables 5.12 and 5.14 shows that by increasing the motor back e.m.f. the ride quality and the actuator force significantly improves for the feed forward strategy and slightly for the optimised controller parameters.

For the hydraulic actuator, the robustness check is done by varying the flow rate gain, K_q , by ±20%. The results are tabulated in Table 5.14. The variation of K_q has resulted in very minimal variations for the feed forward control strategy and the optimisation of controller parameters.

Table 5.10: Effect on the ride quality for the variation of motor inertia, J_m , for the quarter rail vehicle with the velocity based disturbance feed forward control strategy

	Acceleration (%g)			**Force (kN)**		
% Var	**Feed forward**	**OPT I**	**OPT II**	**Feed forward**	**OPT I**	**OPT II**
-20	1.830	1.665	1.542	3.542	2.411	2.116
-10	1.941	1.658	1.544	3.875	2.481	2.223
0	2.070	1.660	1.551	4.223	2.565	2.323
10	2.315	1.673	1.575	4.583	2.673	2.473
20	2.373	1.695	1.603	4.954	2.792	2.617

Table 5.11: Effect on the ride quality for the variation of motor back e.m.f., K_e , for the quarter rail vehicle with the velocity based disturbance feed forward control strategy

	Acceleration (%g)			Force(kN)		
% Var	Feed forward	OPT I	OPT II	Feed forward	OPT I	OPT II
-20	2.196	1.678	1.567	4.176	2.627	2.442
-10	2.128	1.668	1.560	4.372	2.595	2.390
0	2.070	1.660	1.551	4.223	2.565	2.323
10	2.019	1.653	1.553	4.116	2.540	2.301
20	1.975	1.647	1.552	4.018	2.516	2.265

Table 5.12: Effect on the ride quality for the variation of motor inertia, J_m , for the quarter rail vehicle with the acceleration based disturbance feed forward control strategy

	Acceleration (%g)			Force (kN)		
% Var	Feed forward	OPT I	OPT II	Feed forward	OPT I	OPT II
-20	1.645	1.574	1.572	2.051	2.348	2.211
-10	1.649	1.582	1.583	2.098	2.438	2.280
0	1.655	1.593	1.597	2.150	2.531	2.344
10	1.662	1.608	1.614	2.204	2.626	2.405
20	1.671	1.627	1.632	2.264	2.724	2.460

Table 5.13: Effect on the ride quality for the variation of motor back e.m.f., K_e , for the quarter rail vehicle with the acceleration based disturbance feed forward control strategy

	Acceleration (%g)			Force(kN)		
% Var	**Feed forward**	**OPT I**	**OPT II**	**Feed forward**	**OPT I**	**OPT II**
-20	1.673	1.595	1.582	2.148	2.489	2.295
-10	1.664	1.594	1.590	2.147	2.508	2.318
0	1.655	1.593	1.597	2.150	2.531	2.344
10	1.6465	1.5954	1.6065	2.1509	2.5563	2.3734
20	1.6385	1.5991	1.6177	2.1545	2.585	2.405

Table 5.14: Effect on the ride quality for the variation of flow gain rate, K_q

	Acceleration (%g)			Force(kN)		
% Var	**Feed forward**	**OPT I**	**OPT II**	**Feed forward**	**OPT I**	**OPT II**
-20	1.570	1.530	1.616	1.910	2.140	2.047
-10	1.580	1.530	1.596	1.883	2.097	2.019
0	1.590	1.532	1.590	1.863	2.061	2.000
10	1.600	1.530	1.590	1.850	2.030	1.970
20	1.610	1.540	1.580	1.830	2.000	1.950

5.6.2 Robustness of the active suspension actuator controller on the side-view railway vehicle

A similar robustness check is done to the actuator in the side-view vehicle to look at the pitch effect of the vehicle on the whole system's performance. The results are tabulated in

Tables 5.16 - 5.21 for the electromechanical actuator and in Table 5.24 –5.25 for the electrohydraulic actuator.

For the electromechanical actuator technology, the robustness of the feed forward controllers in the suspension shows that the reduction of the motor inertia has resulted in an improvement of the ride quality for both sides of the vehicle by a range of 10-14%. This has also been reflected for the actuator force. Increasing the motor inertia has shown noticeable degradation towards the acceleration and the actuator force for the un-optimised feed forward controller, and slight improvement has occurred for the optimised controllers. The pitch effect from the vehicle did not produce large degradations with this variant of actuator.

The variations of the motor back e.m.f. have shown some pitching effect in the force output OPT II optimisation strategy. Other than that, reducing this parameter value has improved the ride quality by 4 to 16% for the front suspension and is also reflected by the rear and centre ride performance, with an exception for the un-optimised feed forward with a 5% increase of ride acceleration.

Varying the valve flow gain for the electrohydraulic actuator has not shown any significant changes in any of the feed forward controllers. The actuator controller strategies for these actuators were not affected by the system bounce and pitch modes.

Table 5.15: Effect of ride quality to varying motor inertia ,J_m (%g) with the velocity based disturbance feed forward control strategy

	Front Acceleration			Centre Acceleration			Rear Acceleration		
% Var	**Feed forward**	**OPT I**	**OPT II**	**Feed forward**	**OPT I**	**OPT II**	**Feed forward**	**OPT I**	**OPT II**
-20	1.809	1.666	1.565	1.134	1.064	1.014	1.840	1.707	1.607
-10	1.877	1.636	1.580	1.164	1.050	1.020	1.904	1.677	1.620
0	1.959	1.624	1.620	1.202	1.045	1.029	1.982	1.666	1.640
10	2.063	1.636	1.634	1.250	1.657	1.060	2.081	1.675	1.662
20	2.190	1.657	1.654	1.062	1.855	1.053	2.202	1.700	1.690

Table 5.16: Effect of force to varying motor inertia ,J_m (kN) with the velocity based disturbance feed forward control strategy

	Front force			Rear force		
% Var	**Feed forward**	**OPT I**	**OPT II**	**Feed forward**	**OPT I**	**OPT II**
-20	3.330	3.043	2.896	3.402	3.033	2.993
-10	3.434	3.026	2.923	3.500	3.117	3.018
0	3.554	3.033	2.953	3.612	3.123	3.046
10	3.697	3.064	2.986	3.747	3.152	3.079
20	3.865	5.109	3.024	3.906	3.194	3.112

Table 5.17: Effect of ride quality to varying motor back emf , K_e (%g) with the velocity based disturbance feed forward control strategy

	Front Acceleration			Centre Acceleration			Rear Acceleration		
% Var	**Feed forward**	**OPT I**	**OPT II**	**Feed forward**	**OPT I**	**OPT II**	**Feed forward**	**OPT I**	**OPT II**
-20	2.000	1.628	1.611	1.221	1.047	1.034	2.020	1.670	1.650
-10	2.043	1.632	1.627	1.241	1.050	1.041	2.062	1.673	1.665
0	1.959	1.624	1.620	1.202	1.045	1.029	1.982	1.666	1.640
10	1.924	1.622	1.590	1.185	1.044	1.026	1.948	1.663	1.630
20	1.892	1.620	1.581	1.170	1.043	1.021	1.918	1.660	1.622

Table 5.18: Effect of force to varying motor back emf , K_e (kN) with the velocity based disturbance feed forward control strategy

	Front force			Rear force		
% Var	**Feed forward**	**OPT I**	**OPT II**	**Feed forward**	**OPT I**	**OPT II**
-20	3.606	3.040	2.971	3.661	3.130	3.063
-10	3.665	3.047	3.000	3.717	3.136	3.083
0	3.554	3.033	3.024	3.612	3.123	3.046
10	3.507	3.028	2.940	3.568	3.118	3.033
20	3.435	3.023	2.927	3.528	3.113	3.022

Table 5.19: Effect of ride quality to varying motor inertia J_m (%g) with the acceleration based disturbance feed forward control strategy

	Front Acceleration			Centre Acceleration			Rear Acceleration		
% Var	**Feed forward**	**OPT I**	**OPT II**	**Feed forward**	**OPT I**	**OPT II**	**Feed forward**	**OPT I**	**OPT II**
-20	1.476	1.526	1.508	1.027	1.042	1.034	1.417	1.468	1.451
-10	1.487	1.550	1.514	1.031	1.050	1.036	1.428	1.491	1.456
0	1.504	1.570	1.516	1.036	1.058	1.037	1.444	1.512	1.459
10	1.525	1.587	1.515	1.043	1.064	1.037	1.465	1.529	1.458
20	1.548	1.600	1.512	1.051	1.069	1.036	1.489	1.542	1.454

Table 5.20: Effect of force to varying motor inertia J_m (kN) with the acceleration based disturbance feed forward control strategy

	Front force			Rear force		
% Var	**Feed forward**	**OPT I**	**OPT II**	**Feed forward**	**OPT I**	**OPT II**
-20	3.3993	3.454	3.383	2.867	2.956	2.871
-10	3.4197	3.475	3.383	2.890	2.981	2.871
0	3.445	3.491	3.381	2.920	3.000	2.869
10	3.4737	3.502	3.378	2.952	3.011	2.865
20	3.504	3.508	3.375	2.986	3.018	2.860

Table 5.21: Effect of ride quality to varying motor back emf , K_e (%g) with the acceleration based disturbance feed forward

	Front Acceleration			Centre Acceleration			Rear Acceleration		
% Var	**Feed forward**	**OPT I**	**OPT II**	**Feed forward**	**OPT I**	**OPT II**	**Feed forward**	**OPT I**	**OPT II**
-20	1.510	1.563	1.510	1.040	1.056	1.035	1.451	1.506	1.453
-10	1.507	1.566	1.513	1.038	1.057	1.036	1.447	1.508	1.456
0	1.504	1.570	1.516	1.036	1.058	1.037	1.444	1.512	1.459
10	1.501	1.574	1.520	1.035	1.059	1.038	1.4420	1.516	1.463
20	1.500	1.580	1.523	1.034	1.061	1.039	1.440	1.522	1.466

Table 5.22: Effect of force to varying motor back emf , K_e (kN) with the acceleration based disturbance feed forward control

	Front force			Rear force		
% Var	**Feed forward**	**OPT I**	**OPT II**	**Feed forward**	**OPT I**	**OPT II**
-20	3.444	3.485	3.375	2.917	2.993	2.863
-10	3.444	3.488	3.378	2.918	2.996	2.866
0	3.445	3.491	3.381	2.919	2.999	2.869
10	3.446	3.496	3.384	2.920	3.003	2.872
20	3.447	3.500	3.388	2.922	3.009	2.876

Table 5.23: Effect of ride quality to varying valve flow gain,K_q (%g)

	Front Acceleration			Centre Acceleration			Rear Acceleration		
% Var	**Feed forward**	**OPT I**	**OPT II**	**Feed forward**	**OPT I**	**OPT II**	**Feed forward**	**OPT I**	**OPT II**
-20	1.562	1.556	1.566	1.014	1.010	1.011	1.605	1.600	1.603
-10	1.563	1.557	1.564	1.015	1.011	1.011	1.606	1.600	1.602
0	1.571	1.600	1.562	1.019	1.012	1.010	1.607	1.602	1.601
10	1.565	1.558	1.561	1.016	1.012	1.011	1.609	1.602	1.600
20	1.567	1.559	1.561	1.017	1.012	1.011	1.610	1.602	1.600

Table 5.24: Effect of force to varying valve flow gain,K_q (kN)

	Front force			Rear force		
% Var	**Feed forward**	**OPT I**	**OPT II**	**Feed forward**	**OPT I**	**OPT II**
-20	2.850	2.880	2.893	2.950	2.977	2.988
-10	2.845	2.874	2.885	2.946	2.972	2.981
0	2.841	2.870	2.870	2.942	2.968	2.975
10	2.838	2.866	2.872	2.940	2.965	2.970
20	2.836	2.862	2.866	2.937	2.961	2.966

5.7 Summary

This chapter examined the possibility of applying classical controller strategies for the control of the two active suspension actuators used in this thesis. The feed forward controller strategies were explained and categorised into reference and disturbance feed forward controller strategies. The actuators were controlled with feed forward controller strategies which were derived based on the physics of the individual actuator. The reference feed forward proved not to be beneficial to the overall system based on the testing on the electromechanical actuator. This is because the main issue for the actuator in the suspension was discovered to be the disturbance created by the actuator extension velocity. Therefore both actuators were tested further with the disturbance feed forward.

For the electromechanical actuator technology, the disturbance feed forward was categorised into the velocity and acceleration disturbance feed forward. The velocity feed forward strategy has shown significant improvement in the effort to achieve the ideal ride acceleration, with a slight reduction in the actuator force compared to the classical feedback control introduced in Chapter 4. Then the acceleration based feed forward strategy was introduced in this chapter to reduce the error created due to motor acceleration. To achieve this, the actuator was given an additional current control within the actuator itself to create acceleration, and a feed forward was applied to reduce the current that goes into the actuator. This method had shown improvement for the quarter car vehicle performance where the ride acceleration was better than the ideal and further improvement was achieved with the optimisation of the controller parameters.

However when the acceleration and also velocity based disturbance feedforward controller were translated to the sideview vehicle, the same improvement did not occur (better than ideal results) due to the effect of the pitch motion that occurred in the model.

The feed forward control for the hydraulic actuator, on the other hand, was much more straightforward due to the physics of the linear actuator. The ride quality has shown a significant improvement of 6.2% compared to the ideal, and the actuator force has also reduced towards the ideal by 8%.

In this chapter, the optimisation technique has been revisited to re-optimise the feedback controller. This was done to further improve the feed forward control strategy. The

optimised actuator controllers have produced improved results for both actuators in the quarter car railway vehicle. When translated to the side-view vehicle, the improvement still exists for the ride quality and also the actuator force.

Lastly, a robustness analysis was used to check the stability of the overall system and evaluate the performance, as the practicality of this strategy might be questionable. The motor inertia and the back e.m.f, gain are varied for the electromechanical actuator. For the electrohydraulic actuator, the flow gains were varied. All parameters were varied by ±20%. For both actuators, the ride quality and the actuator force did not produce large degradations. This was applicable for the quarter car and side-view model, and so it could be concluded that robustness will not be a critical issue for the strategies that have been developed.

Chapter 6
Validation with more complex active suspension strategy

The preceding chapters investigated the actuator controller strategies for the active railway secondary suspension. Controller strategies for both electromechanical and electrohydraulic actuators have been developed based on the quarter car vehicle which was then extended to the side-view vehicle model, in both cases using the basic skyhook suspension control strategy. The aim of this chapter is to look at the various actuator controller schemes' compatibility with a more complex active suspension control configuration, therefore proving that the actuator control strategies are not only applicable for the relatively simple suspension controller used earlier. The validation process is performed using the complementary filter technique, a technique that has been used in several research studies for active railway suspension. The actuator effects will be assessed for all the actuator control schemes that have been developed in previous chapters.

6.1 Validation model

The validation method that has been adopted in this chapter is the complementary filter technique. This technique is applied to the modal-based structure similarly to that which was used in Chapter 3. Incorporating complementary filters within the modal active control strategy changes the structure of the system; the front and rear suspension deflections are decoupled from the vehicle's bounce and pitch modes and then added to the complementary filters. This method has been chosen based on its successful application for the active lateral suspension on a railway vehicle (Goodall (1981)) where the overall design approach is applicable for any form of active suspension concept. This method has been studied by a number of researchers (Goodall (1976); Williams (1994); Hong (1997); Zhou (2010)) for various stages and directions of the vehicle suspension.

The complementary filters are composed of a pair of second order Butterworth filters (High Pass +Low Pass = 1) with the cross over frequencies according to what has been used earlier in Chapter 3. The basic structure of the complementary filter is shown in Figure 6.1, where the combination of the low pass filter (LPF) and high pass filter (HPF) are fed into the skyhook damper coefficient, c_{sky} , which is then fed into the actuators as a force command, u_{act}. The basic idea is that absolute velocity feedback (i.e. skyhook damping) is used at high frequencies, with relative velocity feedback (i.e. normal damping) at low frequencies.

The complementary filters in the modal structure are used according to the arrangement in Figure 6.2. When applied to the modal controller, the accelerometer and displacement transducers from both ends are used in practice to derive the velocity signals. The accelerometers from both ends measure the vehicle accelerations which need to be integrated as before; the displacement transducer measures the relative displacement between the bogie and the vehicle body, and this has to be differentiated to provide the relative velocity. The suspension modes are controlled independently, where the two filters on each sides of the vehicle are used to fulfil the fundamental suspension requirements. The LPF is combined with a derivative of the suspension deflection, and the HPF is combined with an integrator to process the front and rear vertical accelerations. The suspension deflections are minimised (compared to the passive) by the low pass filter which is predominantly a low frequency effect, meanwhile the high pass

filter generates a vertical damping command improving the ride improvement function (compared to the passive). The combination is fed into the skyhook damper coefficient and decoupled before being fed into the actuators as the force command. The damping ratio used (and the corresponding skyhook damper value) remain the same as used in Chapter 3.

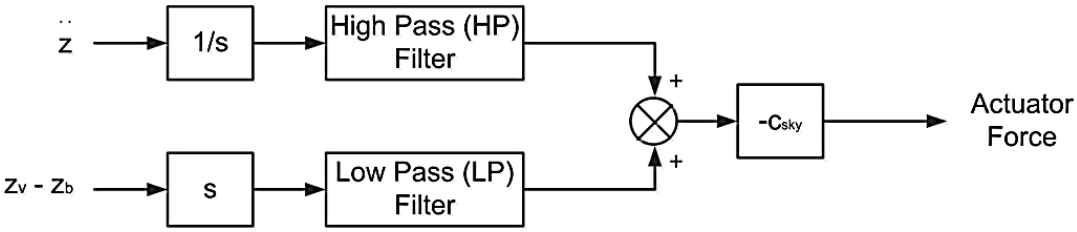

Figure 6.1 : Complementary filter structure

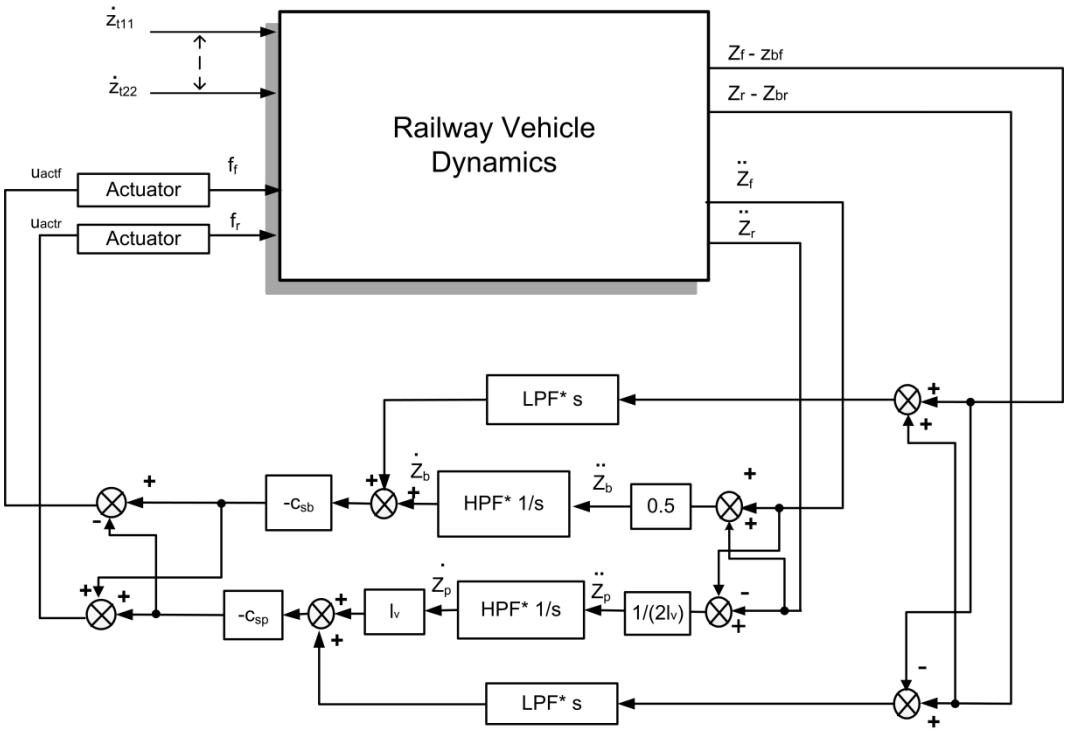

Figure 6.2 : Complementary filter incorporated with modal control structure

6.2 Validation results

The actuators and the force feedback controller scheme developed in Chapters 4 and 5 are placed in the active suspension system to observe the compatibility of the actuators in another active suspension system. Although the actuator controllers have been developed based upon a quarter rail vehicle, it had performed relatively well in the local and modal skyhook suspensions controller (i.e. for the side-view vehicle). Therefore it is expected to do the same for this technique.

The effects of the actuators with all the developed actuator controller schemes are compared using the modal skyhook control strategy (in black) and the complementary filters (in red) as shown in Table 6.1 for the electromechanical actuator, and in Table 6.2 for the electrohydraulic actuator.

The following subsection compares actuators' effects within the two active suspension strategies, compared to the ideal as the basis.

Table 6.1: Comparison of ride results for the electromechanical actuator controller strategies with the modal control and with modal complementary filter control (highlighted in yellow)

		Vertical Acceleration						Suspension Deflection				Actuator Force			
		Front	Front	Centre	Centre	Rear	Rear	Front	Front	Rear	Rear	Front	Front	Rear	Rear
Ideal		1.371	1.974	0.869	1.140	1.540	2.332	8.4	9.6	11.1	13.5	1.948	1.180	2.879	1.910
Feedback Control	Manual	2.357	2.520	1.285	1.391	2.110	2.558	8.4	5.6	11.1	7.9	3.944	3.288	3.956	3.036
	OPT I	1.619	2.025	0.965	1.165	1.640	2.293	8.4	5.6	11.1	7.9	2.854	1.922	3.243	2.245
	OPT II	1.564	2.079	0.942	1.180	1.610	2.308	8.4	5.6	11.1	7.9	2.584	2.060	3.203	2.255
Velocity based feed forward	Manual	1.959	1.910	1.202	1.113	1.982	2.295	11.5	5.6	10.8	7.9	3.554	1.352	3.612	1.963
	OPT I	1.624	1.892	1.045	1.100	1.666	2.303	11.4	5.6	10.8	7.9	3.033	1.210	3.123	1.936
	OPT II	1.620	1.860	1.029	1.100	1.640	2.305	11.5	5.6	10.8	7.9	2.953	1.233	3.046	1.937
Acceleration based feed forward	Manual	1.502	1.983	1.036	1.128	1.444	2.375	12.9	5.6	9.4	7.9	3.445	1.420	2.918	1.987
	OPT I	1.570	1.960	1.058	1.126	1.512	2.405	12.8	5.6	9.3	7.9	3.491	1.347	2.990	2.050
	OPT II	1.516	1.960	1.037	1.131	1.460	2.378	12.8	5.6	9.4	7.9	3.381	1.347	2.868	2.008

Table 6.2: Comparison of ride results for the electrohydraulic actuator controller strategies with the modal control and with modal complementary filter control (highlighted in yellow)

		Vertical Acceleration				Suspension Deflection				Actuator Force			
		Front	Front	Centre	Centre	Rear	Rear	Front	Front	Rear	Rear	Front	Front	Rear	Rear
Ideal		1.371	1.974	0.869	1.140	1.540	2.332	8.4	9.6	11.1	13.5	1.948	1.180	2.879	1.910
Feedback Control	Manual	2.573	2.672	1.373	1.360	2.135	2.365	10.1	6.4	10.2	7.5	4.570	3.910	4.079	3.345
	OPT I	1.495	1.788	0.936	0.957	1.445	1.851	10.1	6.4	10.2	7.5	3.130	2.262	3.232	2.360
	OPT II	1.291	1.644	0.869	0.898	1.365	1.804	10.1	6.4	10.2	7.5	2.926	2.007	2.973	2.255
Velocity Based Feed forward	Manual	1.569	1.956	1.018	1.130	1.612	2.320	11.5	5.6	10.8	7.9	2.860	1.269	2.960	1.968
	OPT I	1.583	1.844	1.024	1.095	1.625	2.310	11.5	5.6	10.8	7.9	2.826	1.278	2.928	1.965
	OPT II	1.600	1.849	1.033	1.090	1.642	2.290	11.5	5.6	10.8	7.9	2.839	1.225	2.941	1.944

6.2.1 Electromechanical actuator analysis

The data tabulated in both tables earlier is best viewed in terms of a percentage. The bar chart representation is shown in Figures 6.3 and 6.4 along with the percentage of degradation/improvement occurring in the respective system, with the ideal as the basis.

The electromechanical actuator with the feedback control and its optimisation shows a large percentage of degradation for the front and rear suspensions with the modal skyhook strategy, however in the complementary filter suspension strategy a very minimal degradation is shown, with a better than the ideal achieved in the rear suspension. Both disturbance feed forward controller schemes (velocity and acceleration) worked well with the new active suspension control strategy, where a percentage of improvement in ride quality (approaching and also better than the ideal) for the front and rear suspensions has been shown.

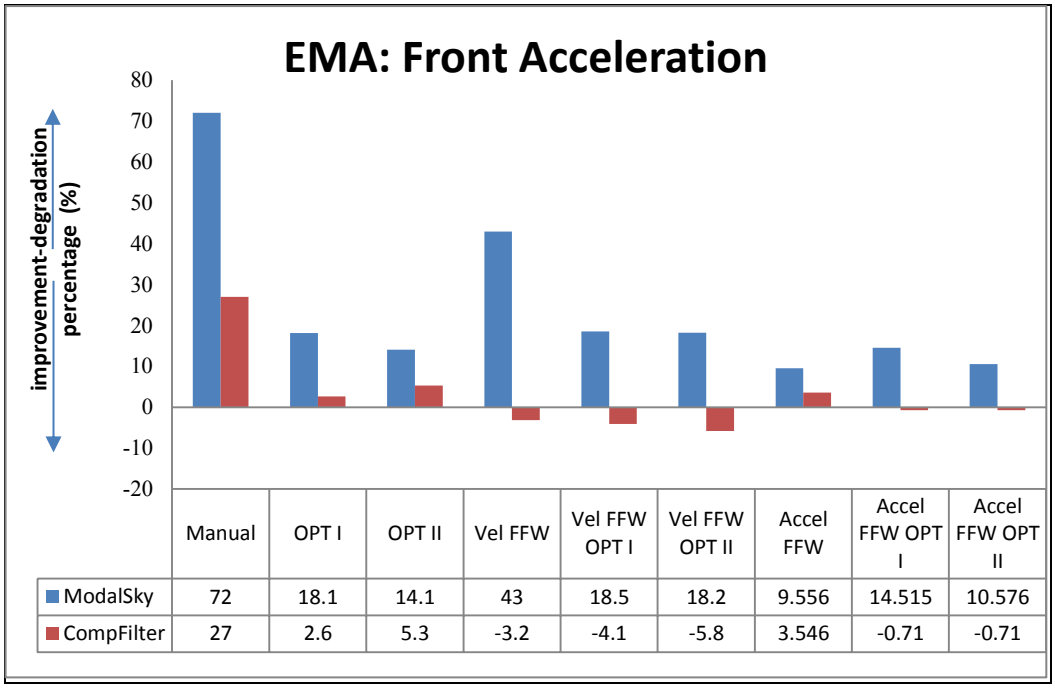

	Manual	OPT I	OPT II	Vel FFW	Vel FFW OPT I	Vel FFW OPT II	Accel FFW	Accel FFW OPT I	Accel FFW OPT II
ModalSky	72	18.1	14.1	43	18.5	18.2	9.556	14.515	10.576
CompFilter	27	2.6	5.3	-3.2	-4.1	-5.8	3.546	-0.71	-0.71

Figure 6.3: Bar chart of percentage of the ride performance degradation/improvement of actuator and controller scheme effects with the different active suspension controller strategies (with respect to the ideal) for the electromechanical actuator in the side-view vehicle.

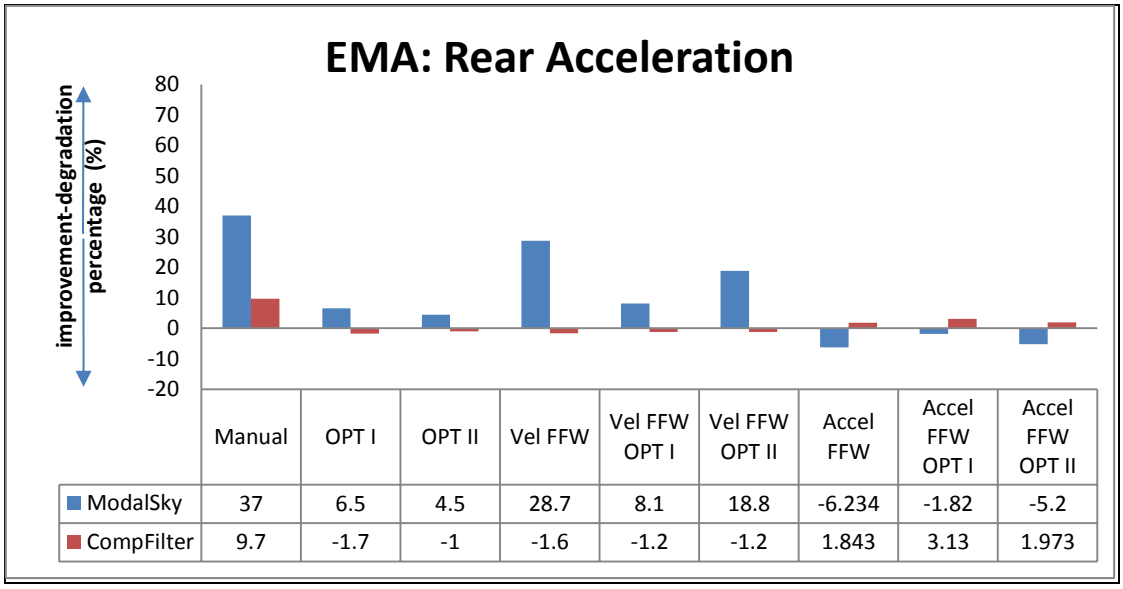

	Manual	OPT I	OPT II	Vel FFW	Vel FFW OPT I	Vel FFW OPT II	Accel FFW	Accel FFW OPT I	Accel FFW OPT II
ModalSky	37	6.5	4.5	28.7	8.1	18.8	-6.234	-1.82	-5.2
CompFilter	9.7	-1.7	-1	-1.6	-1.2	-1.2	1.843	3.13	1.973

Figure 6.4: Bar chart of percentage of ride performance degradation/improvement of actuator and controller scheme effects with the different active suspension controller strategies (with respect to the ideal) for the electromechanical actuator in the side-view vehicle.

The electromechanical actuator effects for the validation active suspension control strategy can be seen from the p.s.d.s of the front and rear acceleration in Figures 6.5 and 6.6. The ride acceleration can be seen to be able to perform better than the ideal up to a frequency of 10Hz and begins to degrade beyond that. However from the linear plot of the front and rear acceleration in Figure 6.7, it can be seen clearly that the actuator works well at frequencies up to 10Hz for the electromechanical actuator with force feedback controller strategies and only the manual tuned actuator continues to deviate above 11Hz.

The p.s.d.s for the velocity based disturbance feed forward controller with the complementary filter suspension strategy in Figures 6.8 and 6.9 and for the acceleration based feed forward (Figures 6.10 and 6.11) shows the ability of the actuator to adapt to the active suspension strategy. The p.s.ds shows that the actuator has the ability to achieve the ideal at higher frequencies.

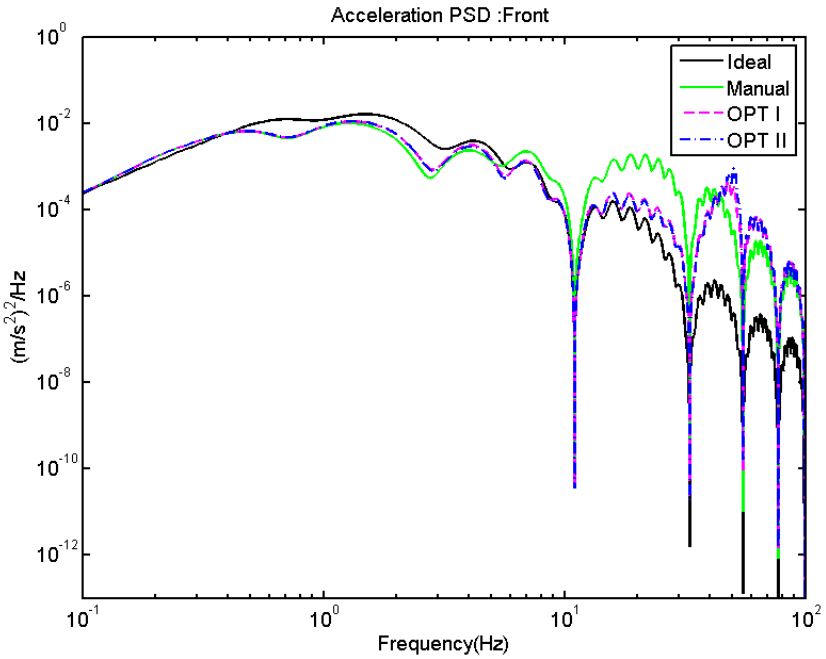

Figure 6.5: Effect of electromechanical actuator with feedback controller

- Front acceleration p.s.d.s

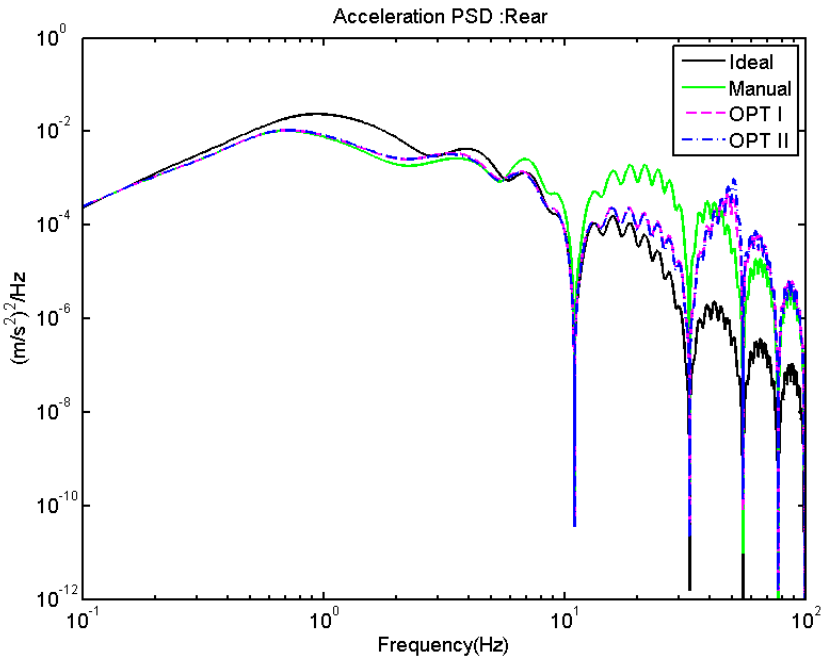

Figure 6.6: Effect of electromechanical actuator with feedback controller

- Rear acceleration p.s.d.s

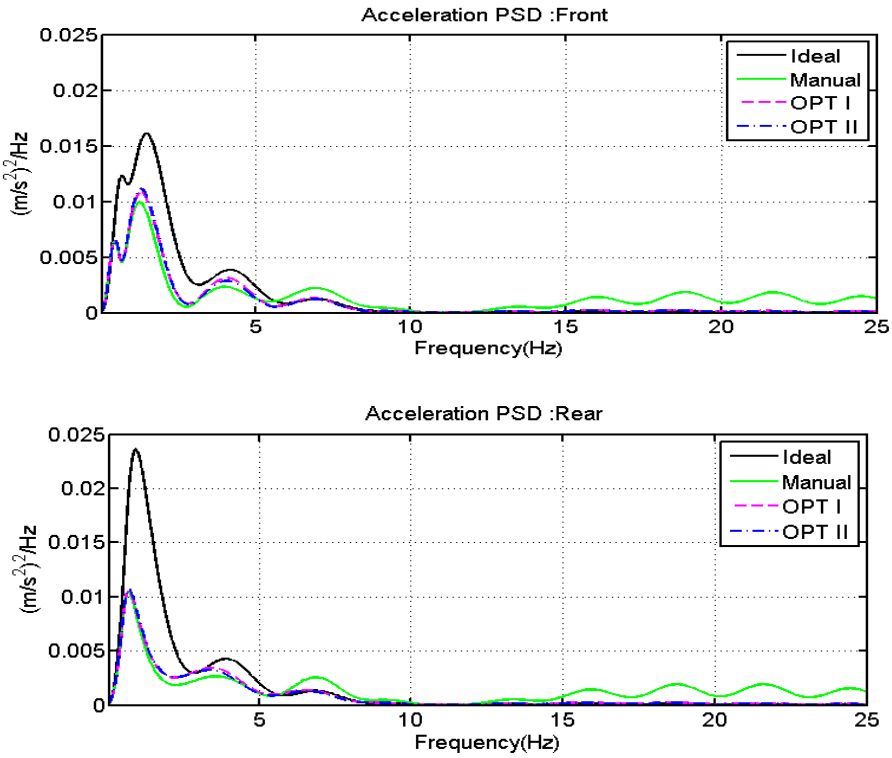

Figure 6.7 : Front and rear accelerations linear p.s.d.s for electromechanical actuator

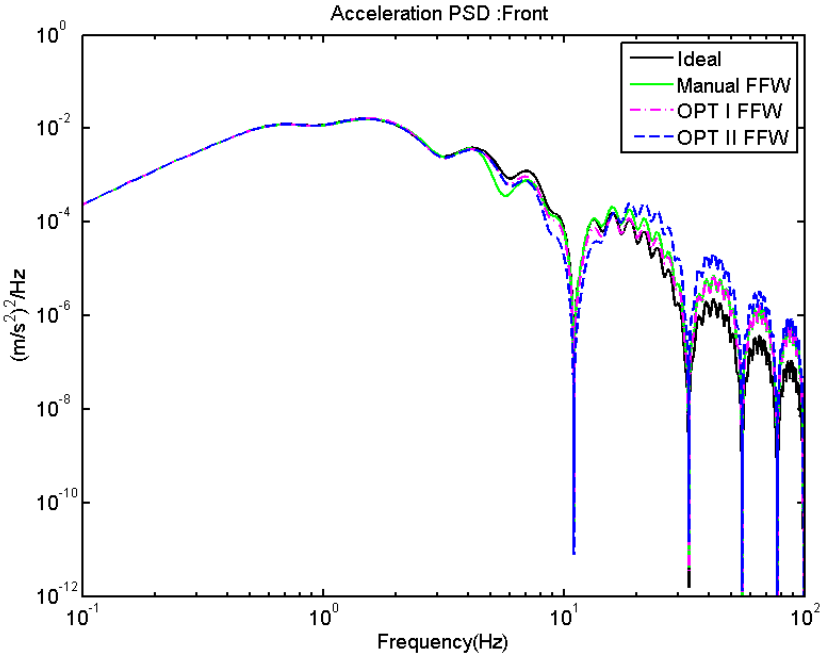

Figure 6.8: Effect of electromechanical actuator with the velocity based disturbance feed forward controller- Front acceleration p.s.d.s

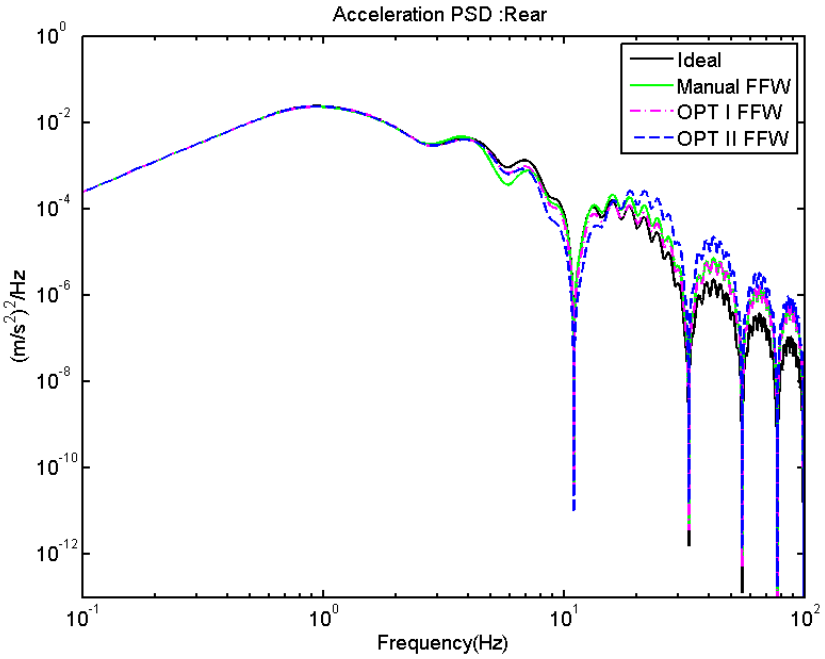

Figure 6.9: Effect of electromechanical actuator with the velocity based disturbance feed forward controller- Rear acceleration p.s.d.

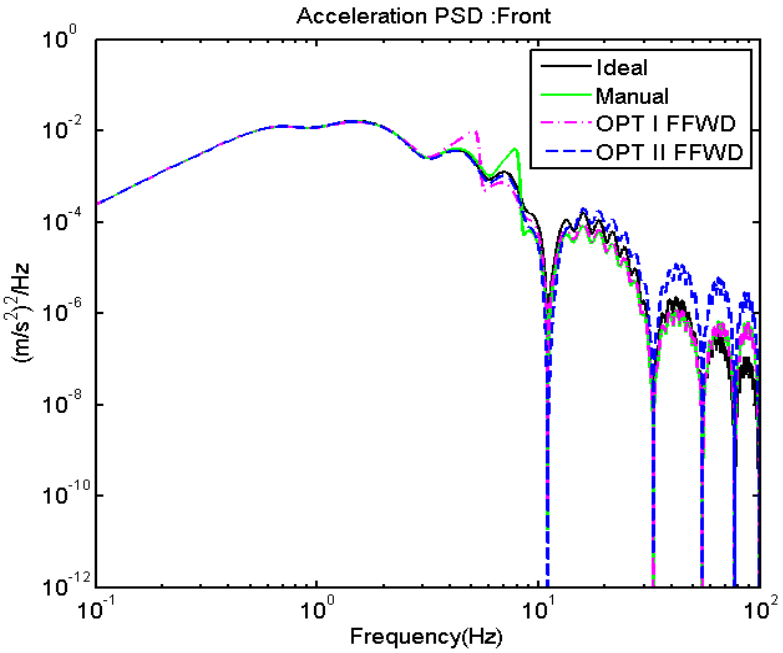

Figure 6.10: Effect of electromechanical actuator with the acceleration based disturbance feed forward controller- Front acceleration p.s.d.s

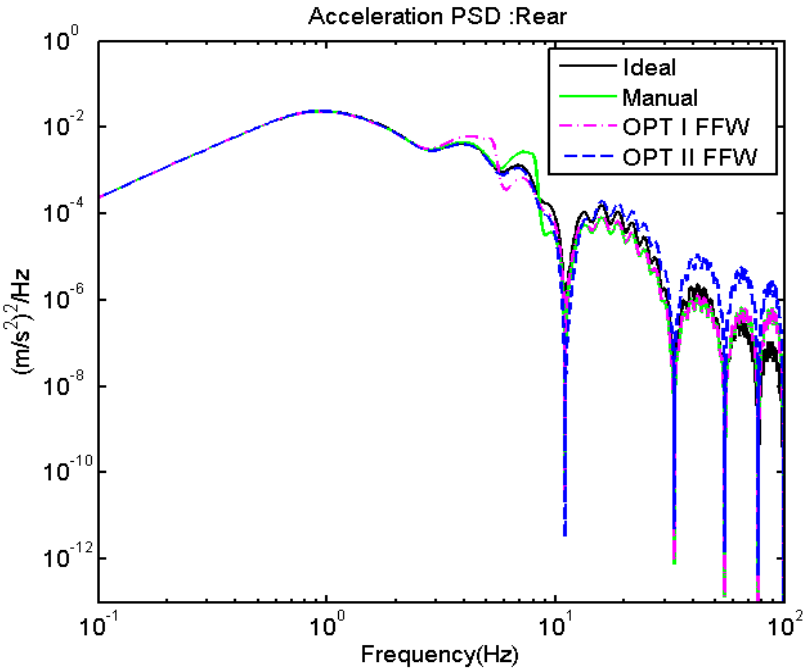

Figure 6.11: Effect of electromechanical actuator with the acceleration based disturbance feed forward controller- Rear acceleration p.s.d.

The output forces produced by the electromechanical actuator in both suspension controller strategies are compared again in terms of percentage. From the bar charts and tables in Figures 6.12 and 6.13, the feedback control and optimisation scheme in the complementary active suspension system produces a very high percentage of actuator force. However, the actuator force for the feed forward control strategies shows improvement with a much reduced force for both front and rear suspensions especially for the acceleration based disturbance feed forward. This is caused by a reduction in the motor torque requirement to accelerate the motor inertia, which eventually reduces the actuator force. This is also an indication that the actuator is able to absorb the vibration across the suspension and follow the movement across the secondary suspension.

These results are also conveyed in the force p.s.d.s in Figures 6.14 - 6.15 for the force feedback control where the front and rear suspension with the electromechanical actuator still shows difficulty in producing the ideal actuator force compared to the feed forward control in Figures 6.16 - 6.19.

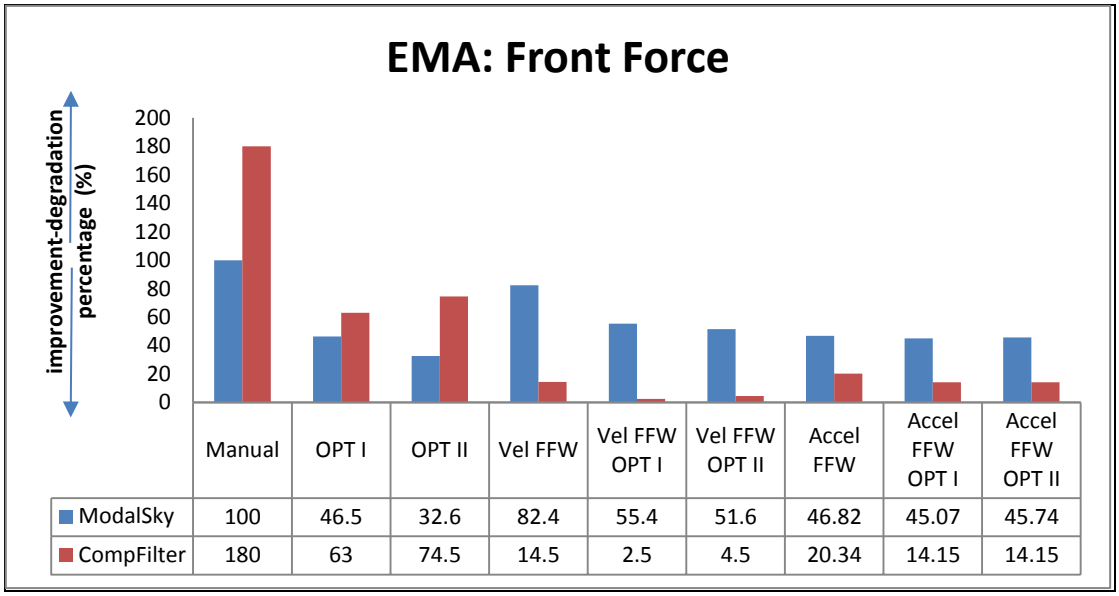

	Manual	OPT I	OPT II	Vel FFW	Vel FFW OPT I	Vel FFW OPT II	Accel FFW	Accel FFW OPT I	Accel FFW OPT II
ModalSky	100	46.5	32.6	82.4	55.4	51.6	46.82	45.07	45.74
CompFilter	180	63	74.5	14.5	2.5	4.5	20.34	14.15	14.15

Figure 6.12: Bar chart of percentage of the actuator force degradation/improvement of actuator and controller scheme effects within the different active suspension controller strategies (with respect to the ideal) for the electromechanical actuator in the side-view vehicle.

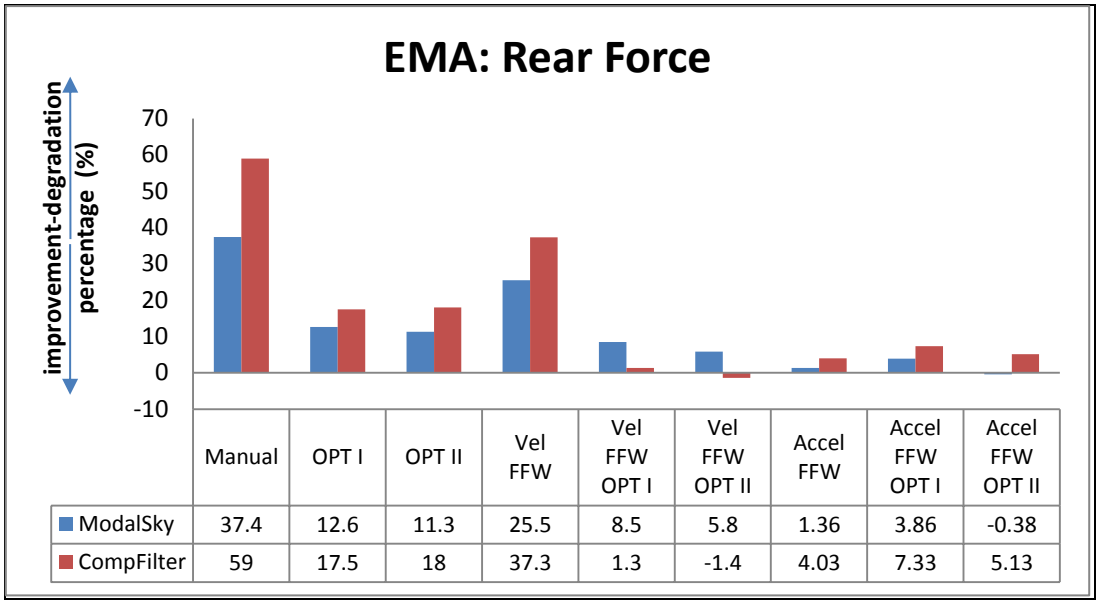

	Manual	OPT I	OPT II	Vel FFW	Vel FFW OPT I	Vel FFW OPT II	Accel FFW	Accel FFW OPT I	Accel FFW OPT II
ModalSky	37.4	12.6	11.3	25.5	8.5	5.8	1.36	3.86	-0.38
CompFilter	59	17.5	18	37.3	1.3	-1.4	4.03	7.33	5.13

Figure 6.13: Bar chart of percentage of the actuator force degradation/improvement of actuator and controller scheme effects within the different active suspension controller strategies (with respect to the ideal) for the electromechanical actuator in the side-view vehicle.

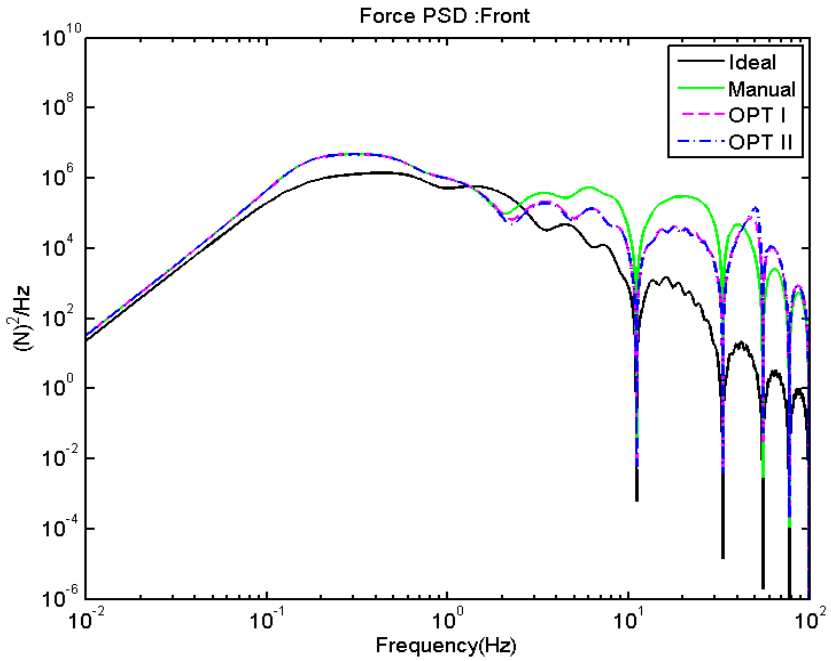

Figure 6.14: Effect of electromechanical actuator with feedback controller

- Front force p.s.d.s

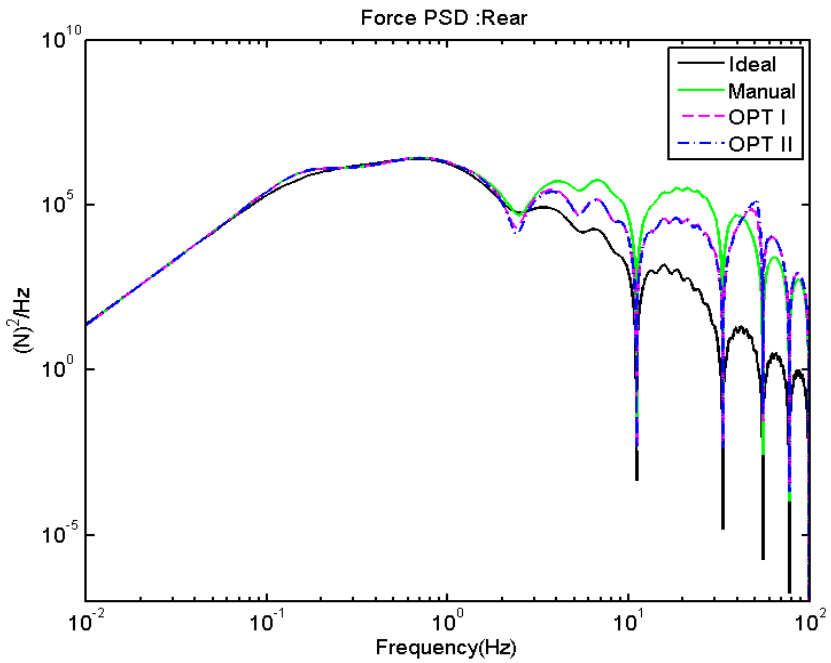

Figure 6.15: Effect of electromechanical actuator with feedback controller

- Rear force p.s.d.s

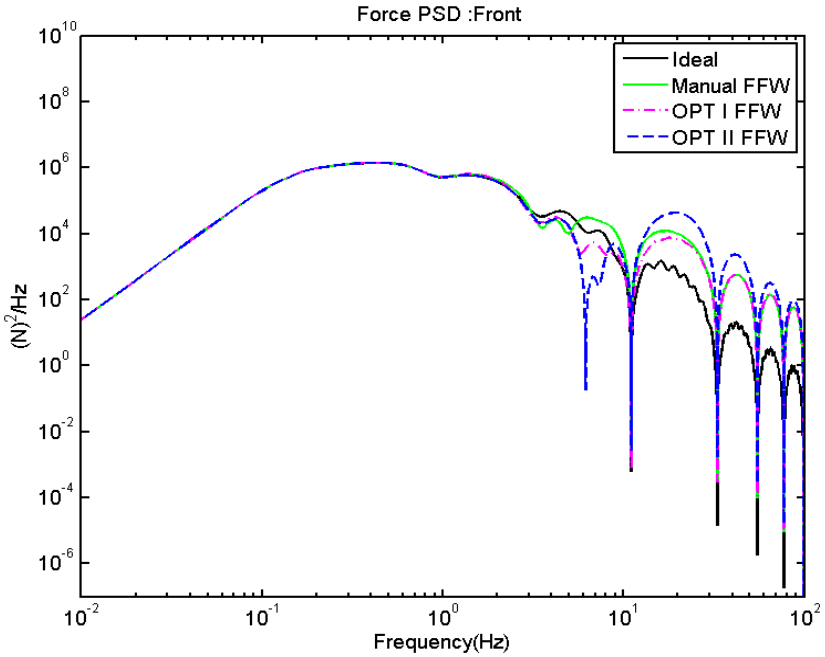

Figure 6.16: Effect of electromechanical actuator with the velocity based disturbance feed forward controller- Front force p.s.d.s

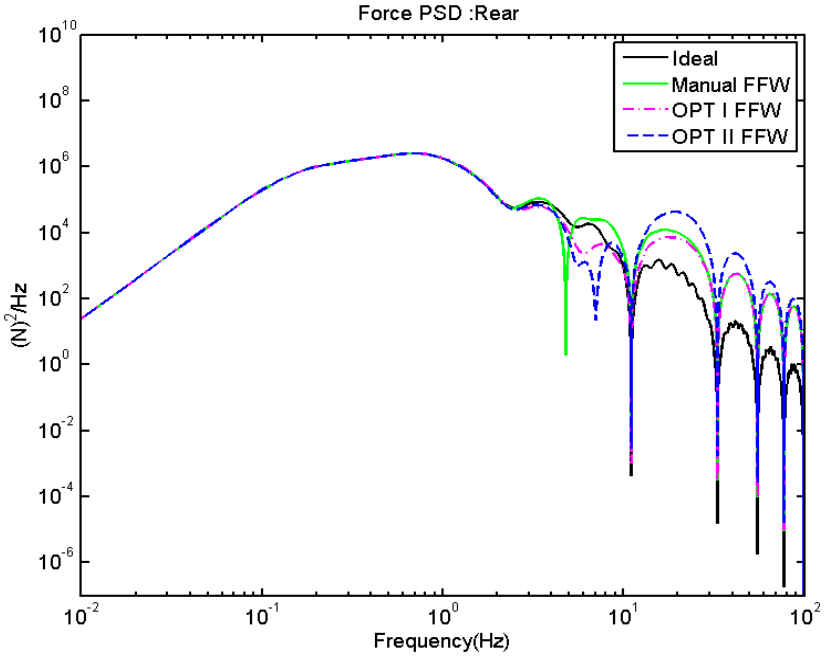

Figure 6.17 : Effect of electromechanical actuator with the velocity based disturbance feed forward controller - Rear force p.s.d.s

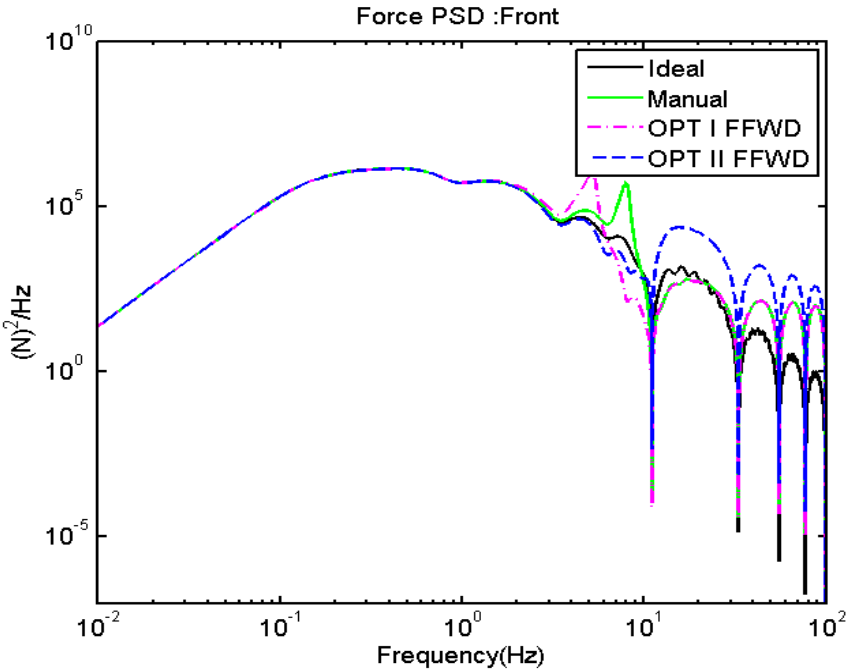

Figure 6.18: Effect of electromechanical actuator with the acceleration based disturbance feed forward controller- Front force p.s.d.s

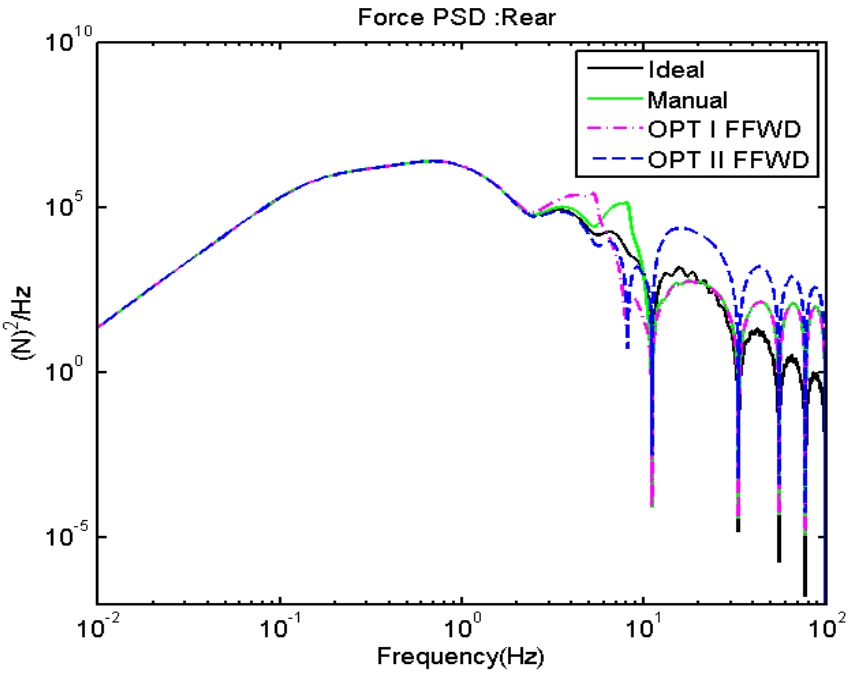

Figure 6.19 : Effect of electromechanical actuator with the acceleration based disturbance feed forward controller - Rear force p.s.d.s

6.2.2 Electrohydraulic actuator

The electrohydraulic actuator effect on the acceleration for both controller strategies is represented by the bar charts in Figures 6.20 and 6.21. It can be seen clearly that an improvement better than the ideal has been achieved with the complementary filter control strategy for both the front and rear suspension. All the actuator controller strategies have shown a satisfactory adaptation to the suspension control strategy, with improvements for almost all controller strategies.

These results are also conveyed in the force p.s.d.s in Figures 6.22 - 6.23 for the feedback control and in Figures 6.24 - 6.25 for the feed forward control. The front and rear suspension with the electrohydraulic actuator shows that the feed forward controller schemes have the ability to follow the ideal, and perform better than the ideal for the optimisation schemes. Meanwhile, with the feedback controller schemes, the suspension still shows difficulty at higher frequencies.

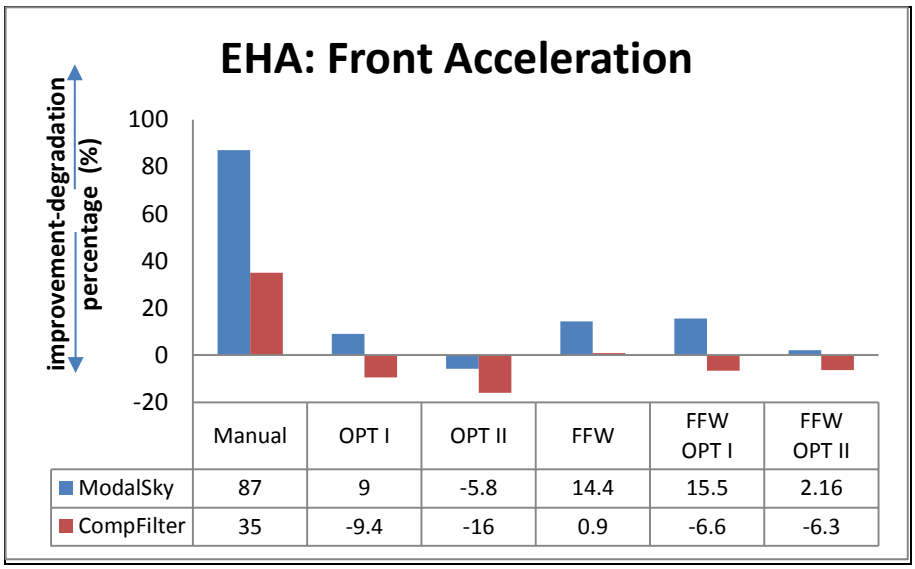

	Manual	OPT I	OPT II	FFW	FFW OPT I	FFW OPT II
ModalSky	87	9	-5.8	14.4	15.5	2.16
CompFilter	35	-9.4	-16	0.9	-6.6	-6.3

Figure 6.20: Bar chart of percentage of ride performance degradation/improvement of actuator and controller scheme effects with the different active suspension controller strategies (with respect to the ideal) for the electrohydraulic actuator in the side-view vehicle.

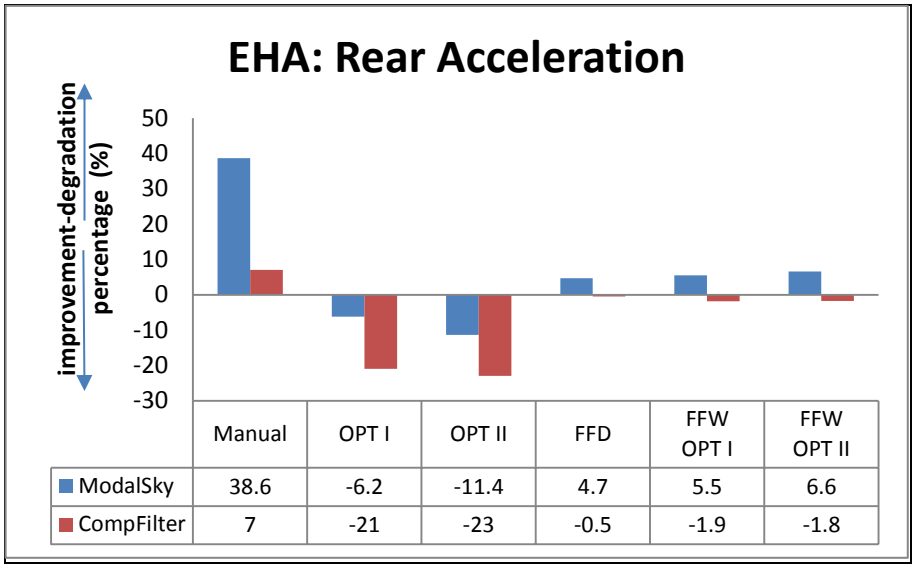

	Manual	OPT I	OPT II	FFD	FFW OPT I	FFW OPT II
ModalSky	38.6	-6.2	-11.4	4.7	5.5	6.6
CompFilter	7	-21	-23	-0.5	-1.9	-1.8

Figure 6.21: Bar chart of percentage of ride performance degradation/improvement of actuator and controller scheme effects with the different active suspension controller strategies (with respect to the ideal) for the electrohydraulic actuator in the side-view vehicle.

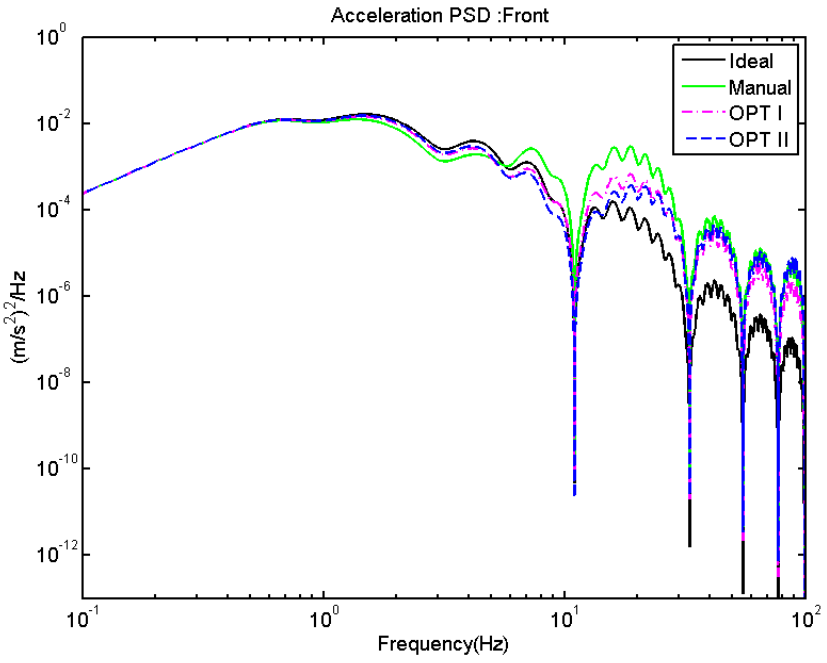

Figure 6.22 : Effect of electrohydraulic actuator with feedback controller

- Front acceleration p.s.d.s

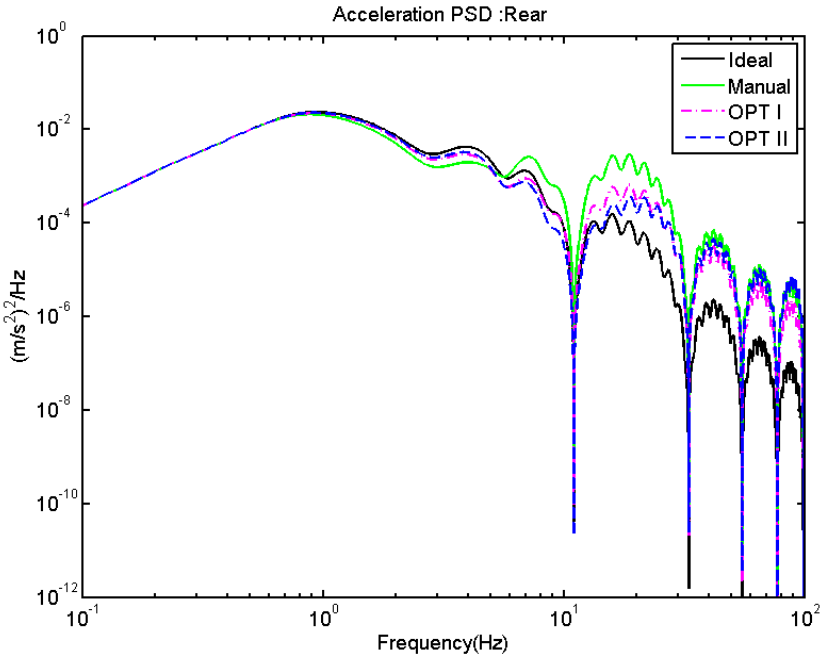

Figure 6.23: Effect of electrohydraulic actuator with feedback controller - Rear acceleration p.s.d.s

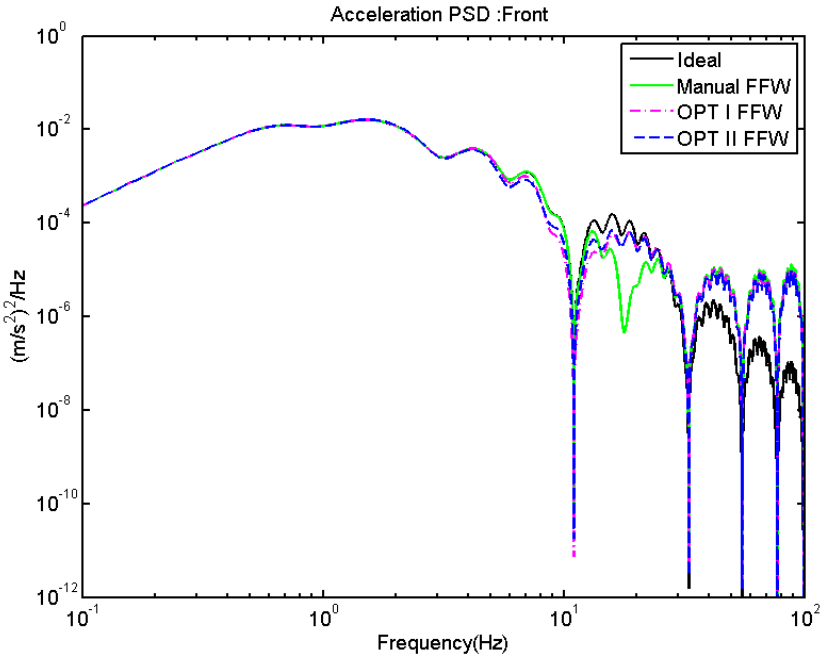

Figure 6.24: Effect of electrohydraulic actuator with feed forward controller - Front acceleration p.s.d.s

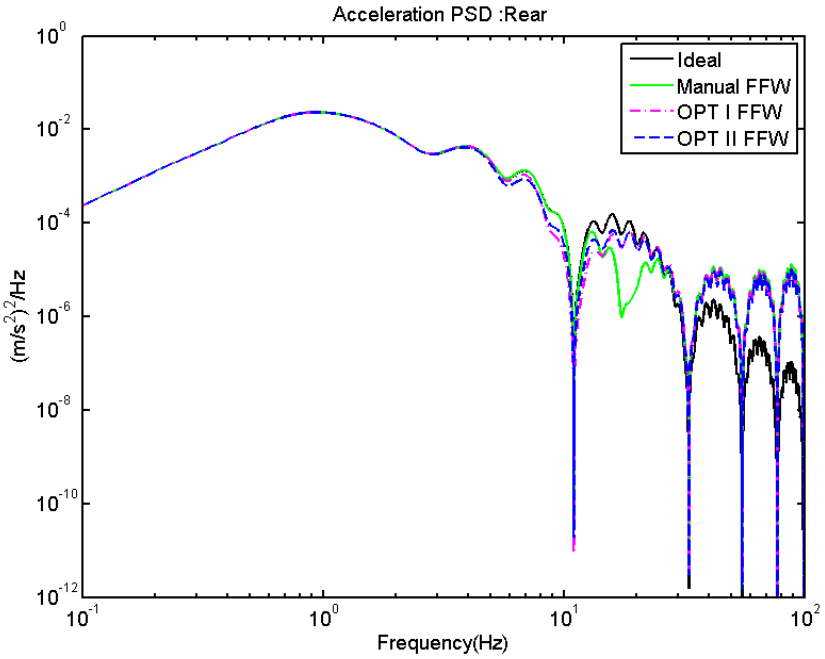

Figure 6.25: Effect of electrohydraulic actuator with feed forward controller - Rear acceleration p.s.d.s

The output forces produced by the electrohydraulic actuator in both suspension controller strategies are compared again in terms of percentage. From the bar chart and table in Figures 6.26 and 6.27, the feedback control and optimisation scheme in the complementary active suspension system produces a higher percentage of actuator force compared to the actuator on the modal skyhook control strategy. However, the actuator force for the feed forward control scheme shows a much lower actuator force.

These results are also conveyed in the force p.s.d.s in Figures 6.28 - 6.29 for the feedback control where the electrohydraulic actuator still shows difficulty in producing the ideal actuator force. The feed forward controller in the system shows an ability to follow the ideal as shown in Figures 6.30 - 6.31. This indicates that the feed forward controller strategy for the electrohydraulic actuator is able to provide the appropriate servo-valve current required to produce the actuator's required speed, which reduces both the actuator force and also improves the ride performance.

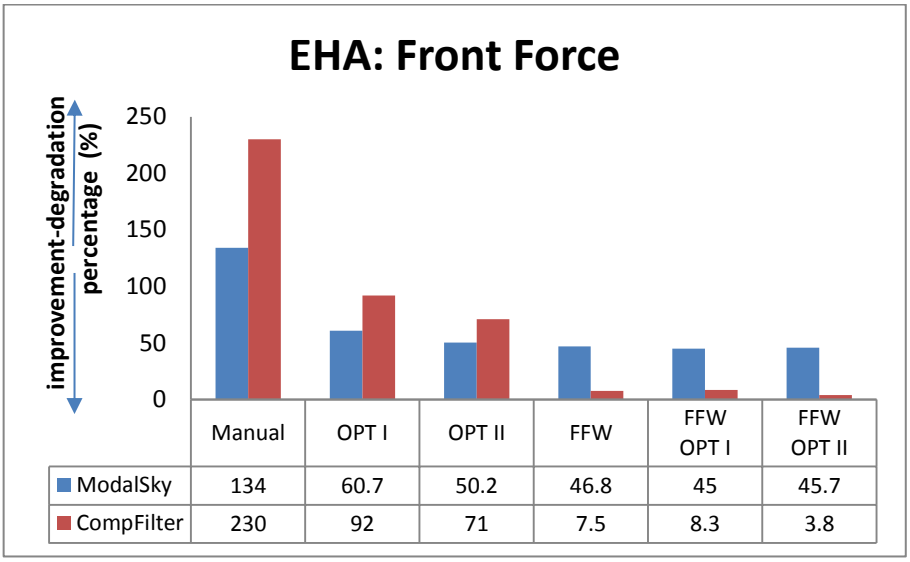

Figure 6.26: Bar chart of percentage of the actuator force degradation/improvement of actuator and controller scheme effects within the different active suspension controller strategies (with respect to the ideal) for the electrohydraulic actuator in the side-view vehicle.

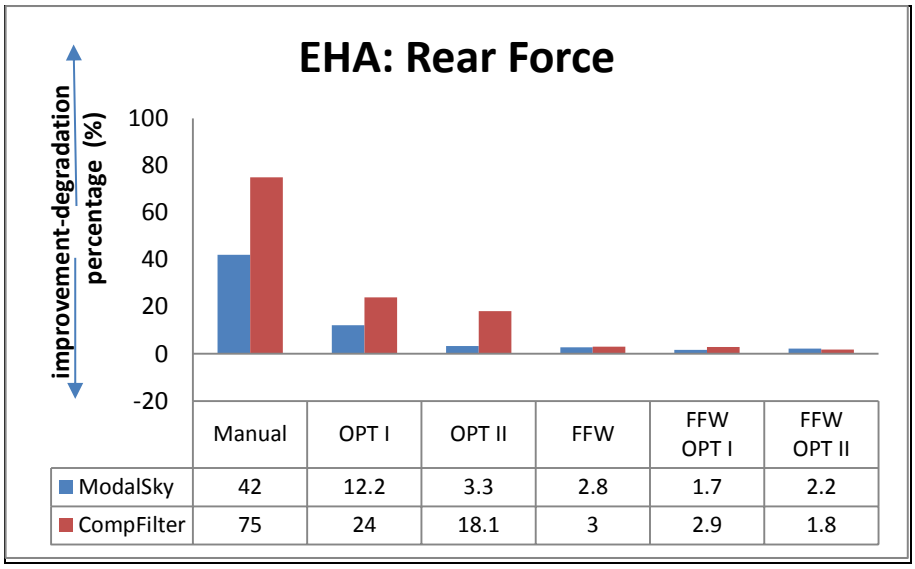

Figure 6.27: Bar chart of percentage of the actuator force degradation/improvement of actuator and controller scheme effects within the different active suspension controller strategies (with respect to the ideal) for the electrohydraulic actuator in the side-view vehicle.

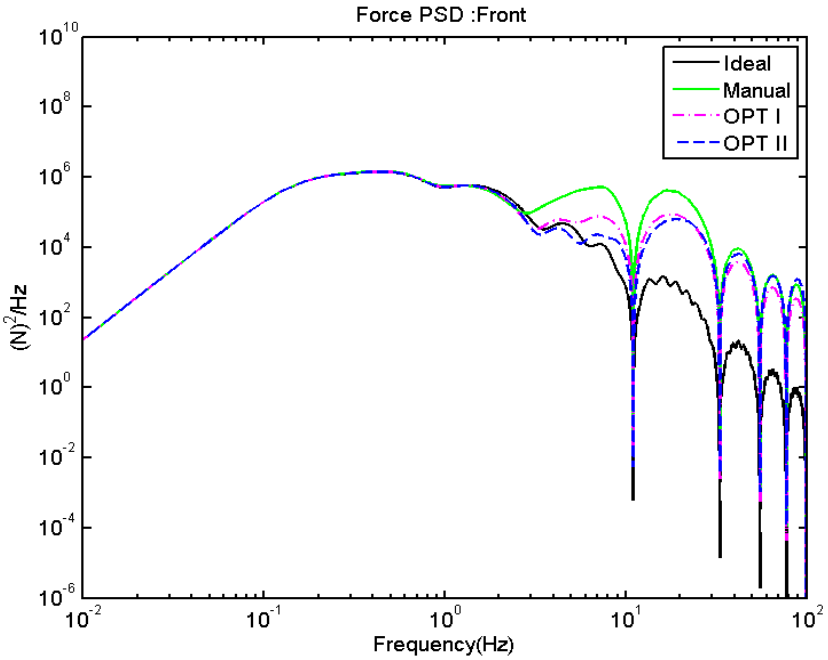

Figure 6.28: Effect of electrohydraulic actuator with feedback controller - Front force p.s.d.s

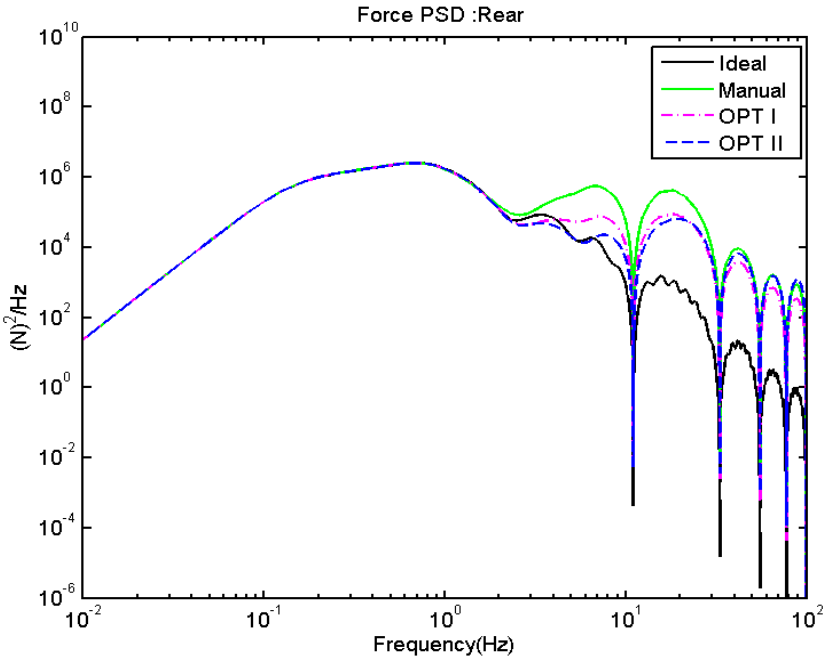

Figure 6.29: Effect of electrohydraulic actuator - Rear force p.s.d.s

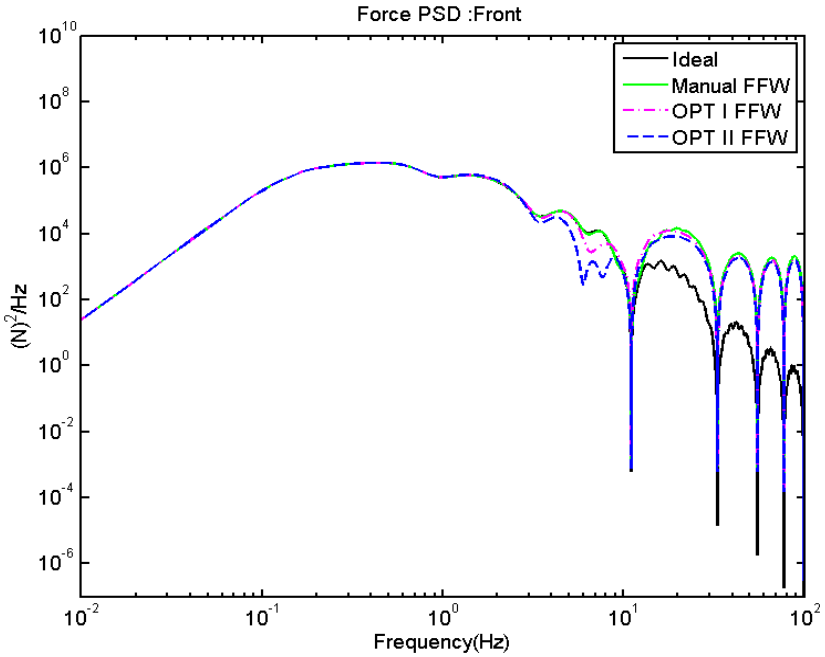

Figure 6.30: Effect of electrohydraulic actuator - Front force p.s.d.s

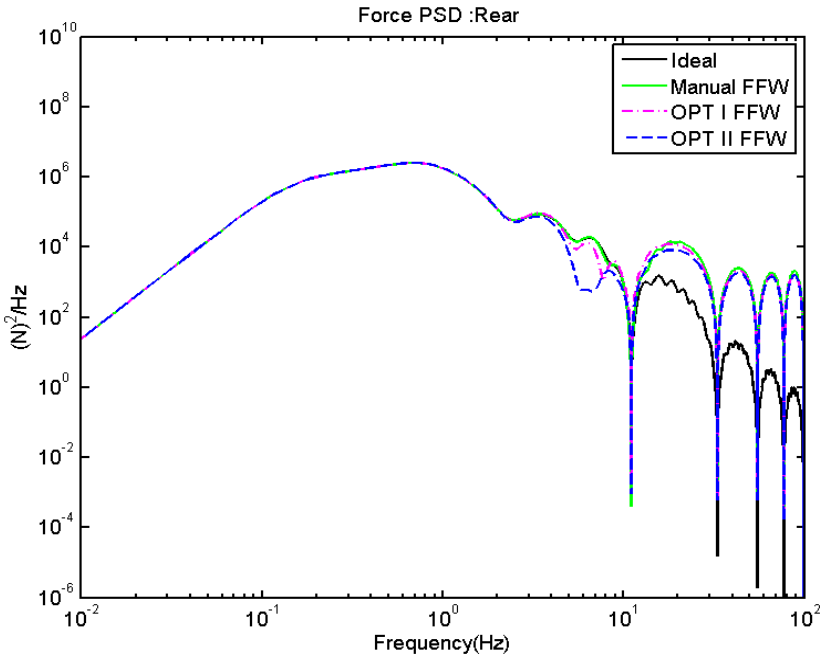

Figure 6.31 : Effect of electrohydraulic actuator – Rear force p.s.d.s

6.3 Conclusion

In this chapter, the control schemes for both actuation technologies developed in the earlier chapters are validated using the complementary filter technology within the modal skyhook structure. Bar charts were used to illustrate and compare the percentage of improvement/degradation of the actuator effects in the both active suspension controller strategies. The electromechanical system showed significant improvements in the ride acceleration especially for the feed forward controller scheme compared to its performance with the modal skyhook strategy. However, an even larger improvement has been found for the electrohydraulic actuator where a performance better than the ideal has been achieved with the complementary filter strategy.

Actuator force still remains an issue for both actuators with the feedback control schemes, where the force performance is made worse by the introduction of complementary filters. However, both actuators demonstrated improvement better than the ideal, and also a very small amount of actuator force for the feed forward scheme.

Based on these results, the feed forward strategies could be said to be the best active suspension actuator controller strategy. This should be highlighted, as the actuator controllers are developed taking into consideration the vehicle dynamics. This has been a challenging process to achieve and it could be said that the feed forward controller has shown that the actuator could be controlled in the suspension successfully. It has performed as expected in this active suspension control technology, which would lead to its adaptability in other structures for vehicle controllers.

It would be interesting to retune the active suspension controller parameters (HPF frequency, skyhook damper coefficient for both modes and others). This however will not be investigated and is left for future works.

The next chapter will discuss the controller strategies devised using optimal control design, together with the estimator (Kalman filter) to estimate the immeasurable states.

Chapter 7

Optimal Control

Controlling the active suspension actuators using classical control strategies has shown an overall satisfactory outcome and a compatibility of the system in the validation process. The classical approach has the advantage of providing a hierarchical structure, i.e. so that the actuator controllers can be developed (and could be commissioned) separately from the active suspension controller itself. However, it is also interesting to extend the actuator control design using an optimal control algorithm to investigate the possibility of applying modern control to control the actuators in the suspension. In this chapter the controller design is a model based approach using an optimal control technique. The design of this controller takes into consideration the active suspension actuator being placed in the secondary suspension. The design of the controller concentrates on the ability of the actuator in the suspension to be able to follow a force tracking input before being placed into the whole active, vertical, secondary suspension scheme. Due to the complexity of the whole system, the actuator controller will only be investigated with a quarter car suspension. Since any model-based strategy has the potential for problems when there is a mismatch between the real physical system and the embedded model, a robustness check on the system is included at the end of the chapter.

7.1 Linear Quadratic Gaussian (LQG) control design

Optimal control has been extensively applied in the active suspension industry, especially in the automotive industry and also for railway vehicles. Optimal control permits the suspension design to be a trade-off between minimising the body accelerations and minimising the suspension deflections, a scheme that makes this scheme favourable. Studies that have applied optimal control mainly concentrated on the suspension controller for ride performance improvement in response to random inputs (Foo and Goodall (2000) ; Zheng (2011)), and also on deterministic problems (Pacchioni (2010)), without taking into consideration the actuator dynamics during the design of the controller, whereas in this thesis the focus is upon the actuators themselves within the active suspension. As highlighted in the previous chapters, it is necessary to take into consideration the vehicle dynamics interactions with the actuator to further improve the vehicle ride performance and also to keep the actuator force at a lower level. This is an important aspect of designing the actuator controller which should be taken into consideration in the aspect of active railway suspension actuator designs. The model based approach control has been selected and applied to the developed actuator in an active suspension, whilst investigating possible improvement using a model based control for the system.

The design of this controller involves the combination of the Linear Quadratic regulator (LQR) and the Linear Quadratic Estimator (LQE). In this thesis the performance of the actuator across the secondary suspension is given priority where the interaction with the vehicle dynamics is taken into consideration. Using the same basis of the state feedback approach, the design of the state space representation for the system is the combined model of the actuator and also the railway vehicle. Designing the optimal control is best done using the separation principle where the regulator and estimator are designed separately. The basic principle of the LQG is illustrated in Figure 7.1.

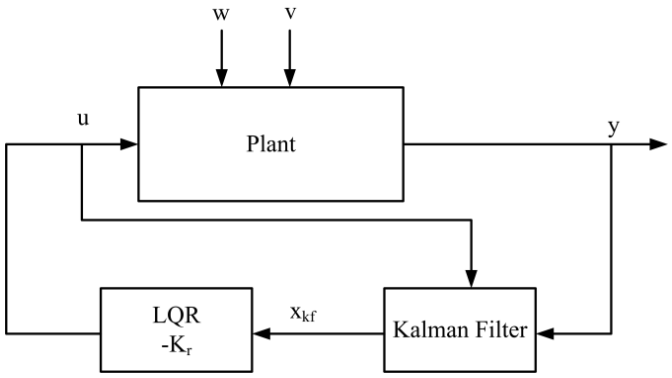

Figure 7.1 : Linear Quadratic Regulator (LQG) scheme

7.1.1 Linear Quadratic (LQR) optimal control

This optimal quadratic controller controls the dynamics of the system back to the input using a gain factor, K_r . This is the advantage of using optimal control, where the closed loop stability of the system is ensured and the technique also guarantees the level of stability robustness. The performance of the system using the optimal control method in this thesis uses a simple quadratic cost function which is expressed as in equation (7.1):

$$J = \int_0^t [x^T(t)Qx(t) + u^T(t)Ru(t)]dt \tag{7.1}$$

The required closed loop performance is then obtained by tuning the constant weighting matrices Q and R until the minimisation of the resulting cost function leads to suitable results on the plant.

In this thesis, the LQR control of the actuators developed for the active railway secondary suspension as modelled in Chapter 4 is shown in Figure 7.2. The state equations for both actuators are given in Chapter 4 (equations (4.18) - (4.19) for the two-mass vehicle, (4.8) - (4.9) for the electromechanical actuator and (4.16) - (4.17) for the electrohydraulic actuator). Since the actuators in this thesis are essentially force-tracking, an integral of the force error is included in the developed plant of the actuated vehicle system. The application of the LQR/G to the whole system is rather complex and not straightforward compared to the application of the optimal control for the actuator or the active

suspension system. Instead it is applied to both systems interacting with each other. As highlighted earlier, the control scheme design is implemented for the quarter car model. This decision is made firstly due the complexity of the system, and secondly because the optimal control for the actuator in the suspension is not directly transferrable from a quarter car vehicle to the side-view vehicle as with the previous methods. It would be possible to apply optimal control to the whole system, i.e. to provide both suspension and actuator control, but this is not done here. This is partly because the complexity would be further increased, but also because the focus is upon the actuator control and the comparison with the previously developed classical method.

The test that will be initially done is the ability of the actuators to be able to track the force tracking input. Once this is obtained, only then will the active suspension controller strategy be incorporated in the system.

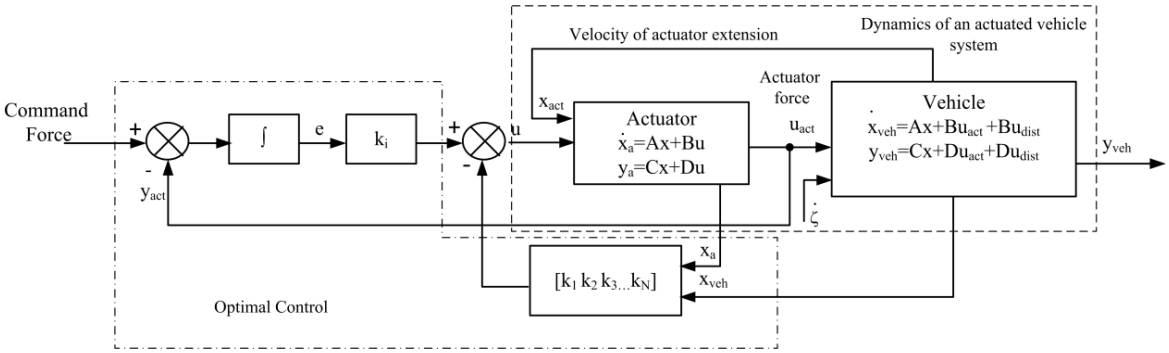

Figure 7.2: Actuator controller configuration for a combined system

The general LQR control scheme of the actuator in the secondary suspension is mathematically described using the following state equations:

$$\dot{x}_c = A_c x_c + B_c u + B_{dist}\zeta \tag{7.2}$$

$$y_c = C_c x_c + D_c u \tag{7.3}$$

$$u = -K_r x_c + k_i \varepsilon \tag{7.4}$$

$$\dot{\varepsilon} = y_{in} - y_{act} = y_{in} - C_{act} x_{act} \tag{7.5}$$

where A_c is the system matrix, B_c is the control input matrix, B_{dist} is the track disturbance matrix into the vehicle, C_c is the output matrix, D_c is the control input feed forward matrix of the combined system, and x_c is the combined states of the actuator and vehicle systems x_{act} and x_{veh}. Meanwhile, y_{veh} is the output vector of the vehicle system, and y_{act} is the actuator force output that will be fed back into the state feedback controller. u is the input vector, while K_r is the system control gain, and K_i is the integral state gain. ε is the position error of the force tracking output.

The main objective of the actuator controller in the suspension is the ability to improve the ride quality at higher frequencies, whilst at the same time maintaining the suspension deflection. The force produced by the actuators is also expected to be at a lower scale due to approaching the ideal force. It is important to highlight that the objective of the controller is to improve the ride quality of the vehicle to be as close as possible to the ideal. The problem of the actuator in the suspension is objective based, however not all the regulated variables (i.e. the actuator force) could be found in the state variable. Therefore the output weighting method is used instead of the state weighting, due to the lack of physical understanding of some of the state variables. The output weighting method in the initial stage of the design eases the difficulty of assigning the weightage for the desired performance. The cost function expressed in equation (7.1) is modified to J_y in equation (7.6):

$$J_y = \int_0^t [y^T(t)Qy(t) + u^T(t)Ru(t)]dt \tag{7.6}$$

The selection of the quadratic weights requires the knowledge of Q and R which is derivable in many ways (Skogestad and Postlethwaite (2005)).

The regulated output for the actuator is the actuator force, and for the suspension the outputs are the active suspension force, ride acceleration, and suspension deflection.

$$\begin{aligned} y(t)^T Q_y y(t) &= \big(Cx(t) + Du(t)\big)^T Q_y \big(Cx(t) + Du(t)\big) \\ &= x(t)^T C^T Q_y C x(t) + 2x(t)^T C^T Q_y D u(t) + u(t)^T D^T D u(t) \end{aligned} \tag{7.7}$$

Output weighting is applied, based on assigning the weighting diagonally as the inverse of the square of the maximum expected r.m.s. values $\left(\frac{1}{(expected\ value)^2}\right)$ for each variable value. This method is used in the initial selection of the output weighting and the final selection is based on a trial and error process. Both voltage drive actuators are investigated in tracking the force following signals.

The actuator has a single output, where the output is the actuator force. The output weighting for the actuator, Q_a, defined as ${C_a}^T q_a C_a$, is combined with Q_x which is ${C_{veh}}^T Q_v C_{veh}$, where C_{veh} are the suspension outputs. Q_{veh} is defined as below:

$$Q_{veh} = \begin{bmatrix} q_1 & 0 & 0 \\ 0 & q_2 & 0 \\ 0 & 0 & q_3 \end{bmatrix} \tag{7.8}$$

where q_1 is the weightage for the vehicle acceleration, q_2 for the suspension deflection, and q_3 is for the actuator force output. The combined output weighting factors are combined to form the matrix below:

$$Q_y = \begin{bmatrix} Q_a & 0 & 0 & 0 \\ 0 \cdots 0 & q_1 & 0 & 0 \\ 0 \cdots 0 & 0 & q_2 & 0 \\ 0 \cdots 0 & 0 & 0 & q_3 \end{bmatrix} \tag{7.9}$$

An additional output weighting is added to Q_y for the integral of position error.

7.1.2 Estimator

The design of the optimal controller for the actuators in the secondary suspension for this chapter has so far assumed the use of a full state feedback. Although the LQR provides a powerful controller design methodology, it is necessary to measure the entire states. However, the states are not always measureable due to the unavailability of capable sensors to measure all the states, and so an estimator is needed to estimate those states which cannot be quantified physically. The Kalman filter used in this thesis estimates the system states, with the assumption of "white noise" as the excitation of the application of the estimator to the state feedback control, as in Figure 7.3.

Since the nucleus of the research is the control of the actuator, this will therefore be looked at initially until a satisfactory outcome is achieved, before being combined with the suspension control. The model of the plant process is given by equation (7.10**)** and the output measurement is given by the equation (7.11**)**:

$$\dot{x}_{kf} = A_{kf}x_{kf} + B_{kf}u + L\left(y_{meas} - y_{kf}\right) \tag{7.10}$$

$$y_{kf} = C_{kf}x_{kf} + D_{kf}u \tag{7.11}$$

where

$$y_{meas} = y + v \tag{7.12}$$

Hhere A_{kf} is the estimator dynamics, B_{kf} is the estimator input matrix, C_{kf} is the output matrix and D_{kf} is the estimator feed forward matrix. x_{kf} is the estimator vector containing the states of the modelled actuator and the railway vehicle system with the connection of the actuator extension velocity . y_{kf} is the estimator output vector, u is the input vector, v is the measurement noise and L is the Kalman gain filter. y_{meas} in this case would be y_{veh}.

The regulator L is independent of the statistic of the noise and the output, C, and also of the optimal control law gain K_r (LQR) based upon the separation theorem. The system is subjected to the actuator force input and the random track disturbance. The measurements feeding into the estimator are the acceleration, actuator force and suspension deflection. The outputs are disturbed by the measurement noise v.

Selection of the error covariance, *w,* and the noise, *v,* is based on the aspect of the real problems rather than the "tuning parameters" which need adjustment until a satisfactory design is obtained. *w* is given by the ideal force input and the track variance. The measurement noise, *v,* is assumed to have an r.m.s. value of one per cent (1%) of the maximum acceleration, actuator force and suspension deflection.

Combined with the LQR control input, the control input now becomes:

$$u = -K_r x_{kf} \tag{7.13}$$

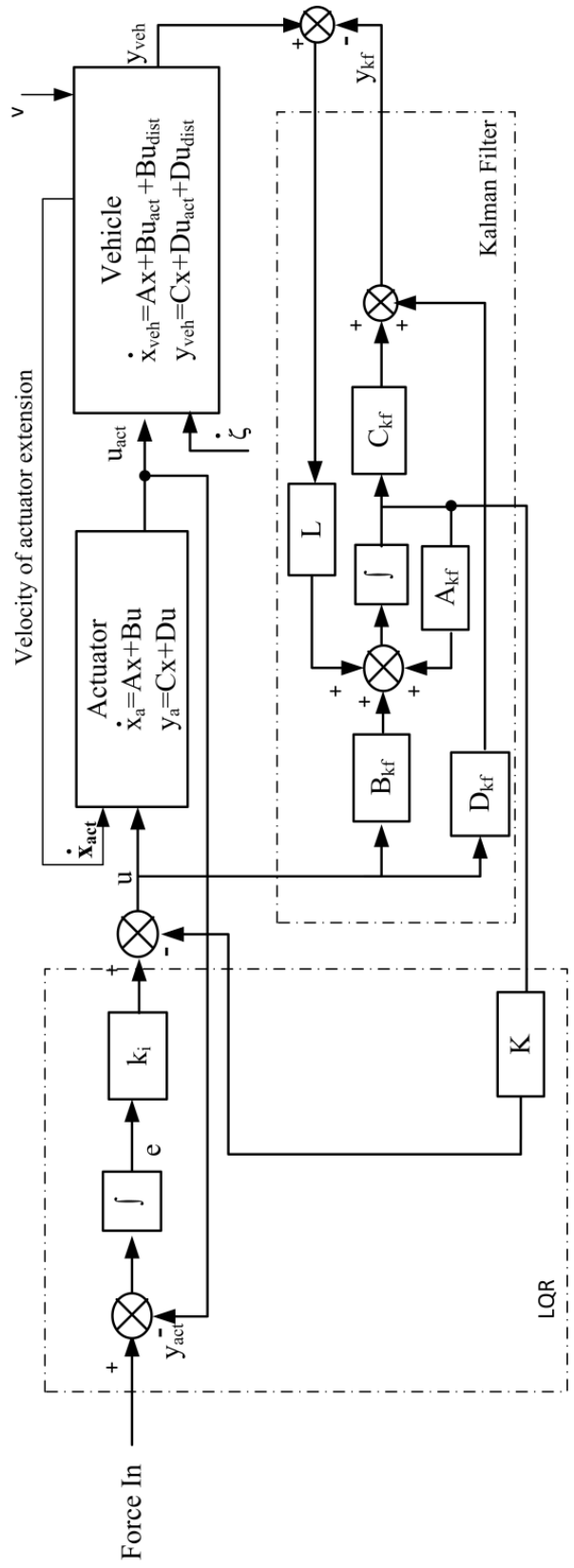

Figure 7.3: LQG

7.2 Performance analysis

7.2.1 LQR

The electromechanical actuator has been tuned to achieve a force tracking output by varying the weighting factors. The matrices Q and R give the best results in terms of the reliability of the actuator in following a force tracking input, while the actuator is placed across the secondary suspension. The ability to track the force inputs for the electromechanical actuator is shown in Figure 7.4. The actuator output weighting, q_a, is adjusted to 160 to produce a good force tracking. A big output weighting value of 10^6 is required for the integral state to produce a small integral position error. The tuning of the other output weighting states has not had much effect on the suspension performance. The input weighting, R, is a 2 by 2 matrix with a selected input of 0.01. The force tracking output for the electromechanical actuator is shown in Figure 7.4.

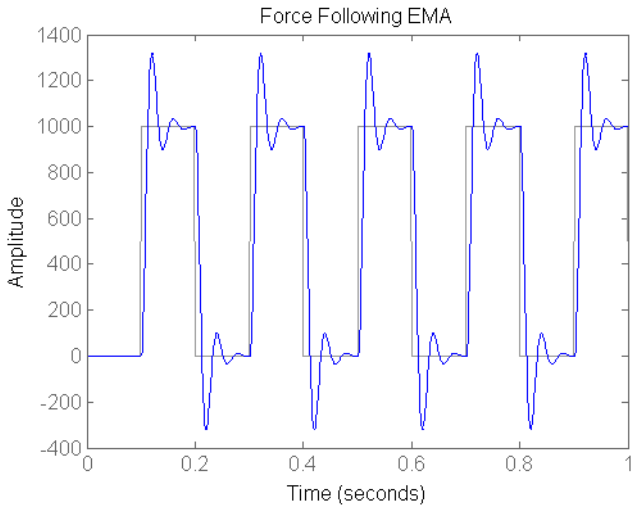

Figure 7.4 : Force following output for EMA

Unlike the electromechanical actuator, the selection of Q and R parameters for the electrohydraulic actuator was less straightforward, and it was found to be difficult to achieve a good solution for the force tracking output. The best outcome achieved by the

author is illustrated in Figure 7.5. A higher actuator output weighting of $1760 \cdot 10^6$ was required. A larger output weighting value of $11.6 \cdot 10^6$ was required for the integral state to produce a small integral position error. Adjustments were required for q_1 and q_2 to obtain a good force tracking output. The input weighting, R, is a 2 by 2 matrix with a selected input of 0.0033.

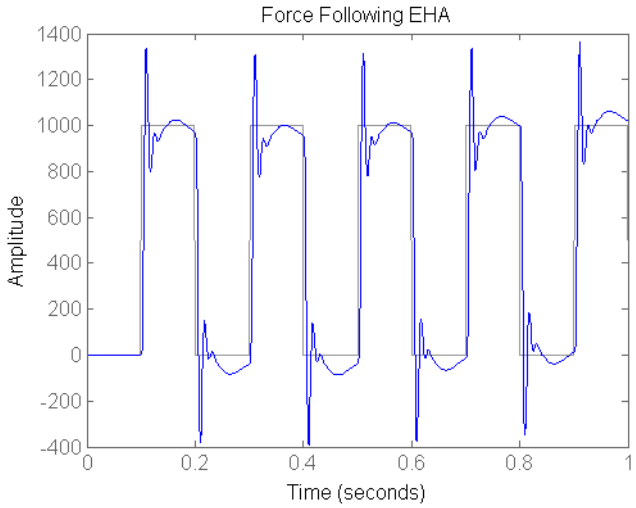

Figure 7.5: Force following output for EHA

When the actuators in the suspension are tested in an active suspension configuration (the active suspension controller included), the power spectral density graphs for the body acceleration and also the actuator force in comparison to the ideal active suspension is shown Figures 7.6 and 7.7. In comparison to the ideal, the electromechanical actuator has shown an ability to follow the ideal, while the electrohydraulic actuator has a lower peak at 0.6Hz but begins to deviate from the ideal at 2Hz onwards. The r.m.s. values of the optimal control of the actuator effects on the active suspension are calculated and tabulated in Table 7.1. From the simulated time response results it is shown that only the electromechanical actuator performs very close to the ideal. The force p.s.d.s show the ability of the electromechanical actuator force to follow the ideal up to 6 Hz, and the electrohydraulic actuator force deviates from the ideal beyond 1Hz.

Table 7.1: R.m.s results of LQR control actuator design

		Passive	**Ideal**	**EMA LQR**	**EHA LQR**
Acceleration	(%g)	2.431	1.700	1.864	2.454
Deflection (track input)	(mm)	10	8.0	10.9	10.1
Actuator Force	(kN)	-	1.718	2.337	3.928

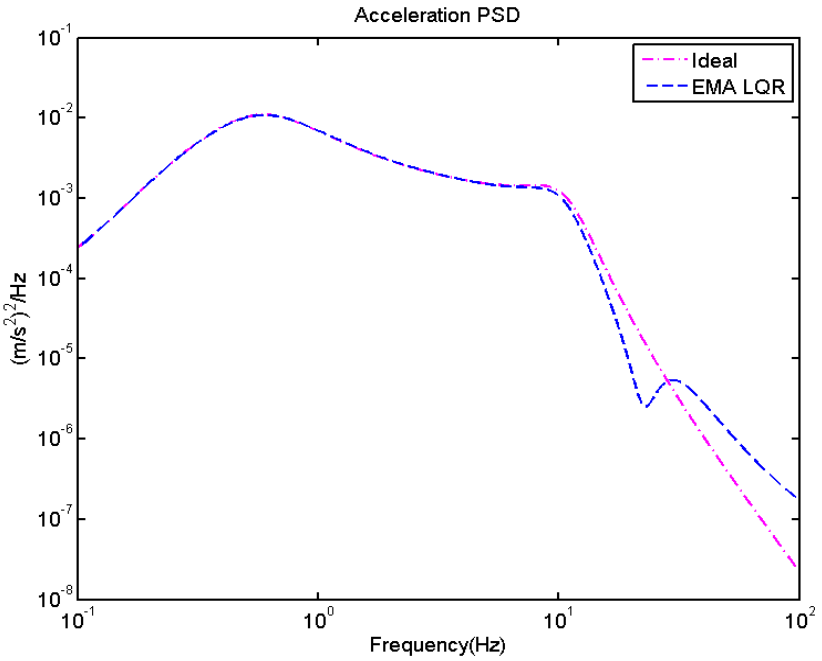

Figure 7.6 Acceleration p.s.d. of the LQR control designed electromechanical actuator in the active secondary suspension

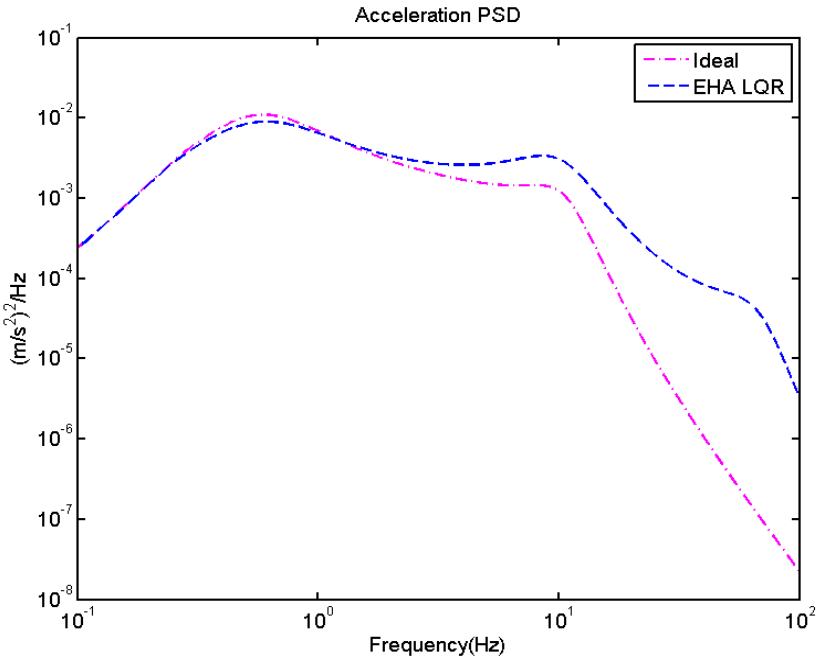

Figure 7.7 : Acceleration p.s.d. of the LQR control designed electrohydraulic actuator in the active secondary suspension

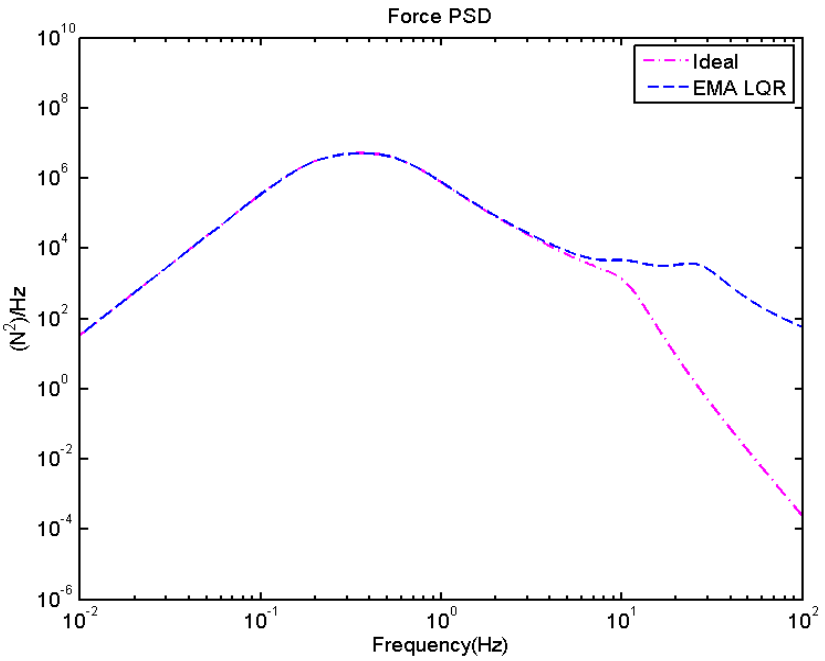

Figure 7.8: Force p.s.d. of the LQR control designed electromechanical actuator in the active secondary suspension

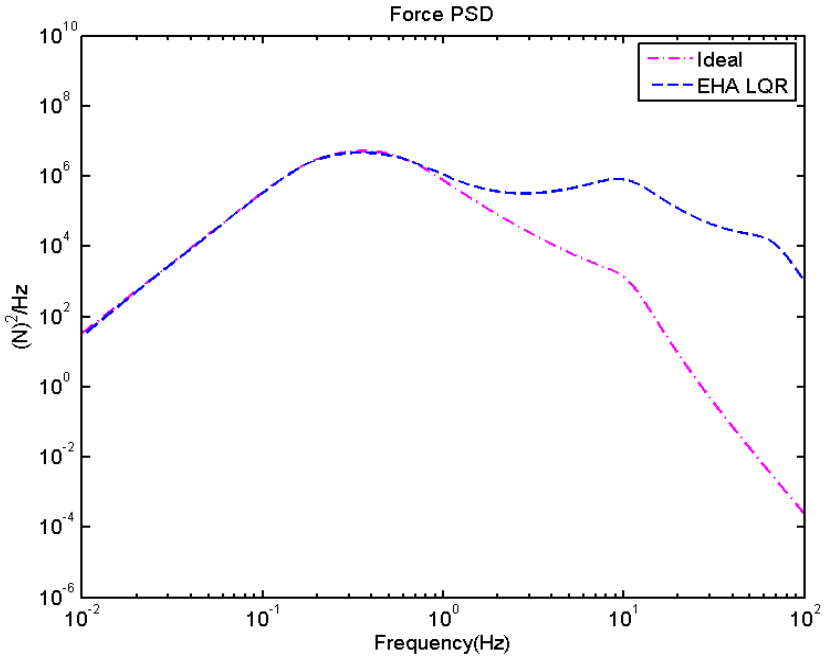

Figure 7.9: Force p.s.d. of the LQR control designed electrohydraulic actuator in the active secondary suspension

7.2.2 LQG

The error covariance, *w,* and the noise, *v,* for the system estimator for the electromechanical and electrohydraulic actuators are chosen as:

$$w = diag(1700\,, 5.4283.\,10^{-4}) \tag{7.14}$$

$$v = diag((0.01 \cdot 0.186)^2, (0.01 \cdot 0.008)^2, (0.01 \cdot 1720)^2) \tag{7.15}$$

where *w* is the ideal actuator force and the track variance. Meanwhile the measurement noise, *v,* used is the assumption of a one per cent of the ideal acceleration, suspension deflection and actuator force.

Table 7.2: R.m.s. results of LQG control actuator design

		Ideal	**EMA LQR**	**EMA LQG**	**EHA LQR**	**EHA LQG**
Acceleration	(%g)	1.700	1.864	1.863	2.454	2.590
Deflection (track input)	(mm)	8.0	10.9	10.9	10.1	10.1
Actuator Force	(kN)	1.718	2.337	2.410	3.928	4.014

Table 7.2 compares the r.m.s. results of the LQR and LQG control design for both actuators. It is apparent that the introduction of the Kalman Filter does not create a large degradation in the suspension performance or the actuator force. The acceleration caused by the LQG for the electrohydraulic actuator degrades by 5.3% while the electromechanical actuator remains the same with respect to the LQR configuration. The force for both actuators degrades by 3% and 2.2% for the electromechanical and electrohydraulic actuators respectively in comparison with the LQR. These very small differences in the results shown here could be considered as negligible.

7.3 Robustness test

A robustness test is essential to be performed after the design of the optimal controller for the combined system. The main reason for this is that for the LQR/G optimal control there are no guaranteed, or there are very small, stability margins for the controlled system (Skogestad and Postlethwaite (2005)). Since the LQG is a model based control strategy, the performance of the controller is affected by the accuracy of the system model. This means that the adjustment of the controller could change if certain parameters of the system change. The robustness check in this subsection is important to the overall system to ensure that a change in parameters does not give an extreme deterioration in the performance. This is a good test, in which the actuators could have some flexibility in the selection of certain parameters. This could also mean that the vehicle could have certain conditions for the parameters, i.e. with the vehicle being laden or unladen. The variation will be in certain parameters for the actuator, i.e. the motor

inertia, J_m, and also the back e.m.f, K_e, for the electromechanical actuator and the flow rate gain, K_q, for the electrohydraulic actuator. As for the vehicle, the parameters of the vehicle mass will vary, and a $\pm 25\%$ variation is chosen. The parameter variation is on the high side and perhaps not possible in practice; however, this practice is a good way of checking the behaviour of the system for the worst case scenario.

Tables 7.3 and 7.4 contain the results of the varied parameters for both actuators. From Table 7.3 it is shown that the changes in the electromechanical actuator parameter have very minor effects on the ride quality and the actuator force. Table 7.4 also shows the same trend for the varied electrohydraulic actuator. Meanwhile, robustness checks carried out by varying the vehicle mass show an unchanged performance (Table 7.5).

Table 7.3: R.m.s. results for electromechanical actuator parameter variation

		EMA with varied J_m		**EMA with varied K_e**	
	LQG	**LQG with +25% J_m**	**LQG with -25% J_m**	**LQG with +25% K_e**	**LQG with -25% K_e**
Acceleration (%g)	1.863	1.873	1.858	1.846	1.880
Actuator force (kN)	2.410	2.472	2.374	2.417	2.410

Table 7.4: R.m.s. results for electrohydraulic actuator parameter variation

	EHA with varied K_q		
	LQG	**LQG with +25% K_q**	**LQG with -25% K_q**
Acceleration (%g)	2.590	2.592	2.587
Actuator force (kN)	4.014	3.990	4.054

Table 7.5: R.m.s results for vehicle mass variation

	EMA			EHA		
	LQG	**LQG with +25% mass**	**LQG with -25% mass**	**LQG**	**LQG with +25% mass**	**LQG with -25% mass**
Acceleration (%g)	1.863	1.863	1.863	2.590	2.590	2.590
Actuator force(kN)	2.410	2.410	2.410	4.014	4.014	4.014

7.4 Summary

In this chapter, the optimal LQR and the model based estimation using the Kalman filter have been designed to develop the Linear Quadratic Gaussian optimal control. The design of this controller has been undertaken using the separation principle, for designing the estimator and the controller. The development of the controller involves the combination of two systems: the actuator and the suspension. The actuators are placed across the secondary suspension with the velocity extension as an added dynamic for the actuator. This has increased the complexity of the system and also the development of the optimal controller. As in previous chapters where the actuator has been a force tracking device, the method used for developing the controller was based on a state feedback regulator where an additional state of an integral of force error was added to the combined states.

Both actuators are tested for force tracking performance where the electromechanical actuator has shown the ability to do so; however the electrohydraulic actuator controller had not produced a satisfactory force tracking output.

Due to having the vehicle dynamics included in the model for this design the selection of the quadratic weights of the LQR has been difficult. The weighting factors selection had been tedious especially for the electrohydraulic actuator for the force tracking investigation. The active suspension controller was only included after a satisfactory outcome of the LQR control was achieved.

It could be concluded that the optimal control for the electromechanical actuator had created an improvement in the active suspension system. In comparison to the ideal, the

strategy has shown less degradation compared to the classical force control in the previous chapters. As for the optimal control for the electrohydraulic actuator in the suspension, the results showed a 50% degradation compared to the ideal. This, in comparison to the previous chapters, is not the best performance for this actuator. Obtaining the right weighting factor for the electrohydraulic actuator was quite difficult compared to the electromechanical actuator. The main reason for the LQR not working as expected for the electrohydraulic actuator in the suspension was not entirely clear, and perhaps further research in this matter is required.

A robustness check on both actuators in the suspension was made by varying the actuator parameters and also the vehicle mass. This check has shown that the variation produces a very small percentage variation of the ride quality and actuator force results (less than 1% for both).

The optimal control in this chapter was applied to the quarter car vehicle, as the controller is not directly transferable and also to avoid model complexity. This would also lead to a remodelling of the controller and also the vehicle system, as the effects of the bounce and the pitch and the response of the actuators in the suspension at the same time would be complicated. Therefore this has been left for future works, where it would also be interesting to include the controller parameter optimisation technique, and also take the active suspension optimal controller into consideration.

Chapter 8

Conclusions and Future Works

8.1 Conclusions from the research

This thesis describes the contribution of this research into the enhancement of the vehicle ride performance for high speed railway vehicles via the control of the active, vertical, secondary suspension actuators. The research outcome has demonstrated the improvement achieved using this novel idea. This initiative has improved the ride performance of the vertical suspension significantly for frequencies up to 10Hz over a straight track with the ability to follow the ideal.

Previous research on the use of active secondary suspension has proven that its incorporation would improve the vehicle ride quality compared to its passive counterpart, which is purely mechanical. Considerations of 'real' actuators were limited in the effort to reduce ride performance degradation, where previous concentration had only been on active suspension controllers. The use of actuators in some literature has been with the actuator simply modelled, without any consideration of the dynamic interaction between both systems. But once the dynamic interaction has been properly represented, actuators have been reported to contribute to a major degradation of the vehicle performance in comparison to the ideal. This

is an understandable situation due to the limitation of the actuators being in the suspension. Therefore, there is motivation to concentrate on the improvement of the vehicle performance through the controls of the actuators across the secondary suspension.

In this thesis, the electromechanical and the electrohydraulic actuators are chosen to fulfil this task. The actuator controllers are evaluated, taking into consideration both the vehicle and actuator dynamics. This is a crucial criterion for the actuator application in the suspension which has not yet been addressed properly by researchers.

In this thesis the importance of including the physical 'feedback' from the vehicle dynamics into the actuators to represent the movement across the secondary suspension is addressed. The ability to control the vehicle modes using actuator technology is important with more complex models and suspension control laws. However it would be sufficient to observe the trends on a simple side-view model, since the situation would be more or less the same as seen with complex models.

This thesis began with the development of the quarter car and side-view model of the railway vehicle. The vertical view of the suspension has been chosen, for a clearer view of the behaviour of the actuators that will be placed across the secondary suspension. Active control strategies have been developed based on the skyhook control strategies. The local and modal skyhook strategy was introduced and had shown improved ride performance which is not possible with the passive. The modal skyhook strategy had shown the best performance giving a ride quality around 1% g and maintained a low suspension deflection compared to the passive and also the local strategy. The vehicle analysis results of the active suspension were taken as the "ideal actuator" condition. Then the parameters of the actuators were calculated and selected based on these "ideal actuator" requirements obtained from the developed active suspension quarter car railway vehicle earlier.

Initial development of the actuator controllers for both types of actuator was done using the quarter car railway vehicle, which was then evaluated for the full vertical side-view vehicle with a modal control active suspension strategy.

Controlling the actuators in the secondary suspension was initially carried out using a simple force feedback control. Actuators were tuned to the best performance, and placed in the secondary suspension, and then retuned again to provide a satisfactory force tracking performance. The tuning of the actuators in the suspension was also checked to satisfy the

actuator voltage requirements, and also so as not to exceed the allowable suspension deflection over a straight track requirement.

The whole active suspension system was assessed where both actuators in the quarter car suspension have shown an improvement compared to the passive, however this still shows a substantial degradation compared to the ideal. Subsequently, an optimisation of the actuator controller parameters was carried out using the genetic algorithm to optimise the controller parameters (OPT I). Significant improvement of the r.m.s. results has been achieved using the new controller parameters' combination. This optimised control of the electromechanical and electrohydraulic actuators has improved the ride quality by 41% and 56 % respectively compared to the manually tuned controller. However the degradation against the ideal still remains high, with the electromechanical actuator still showing 51% of degradation, and 9% with the electrohydraulic actuator.

The optimisation technique has been extended with a further possible way of improving the actuated active suspension which takes into consideration an additional stiffness in series with the actuator (OPT II); here the stiffness and the controller parameters were optimised together. The optimised electromechanical actuator controller and stiffness reduced the ride acceleration by another 26%, making it closer to the ideal by 10%. Meanwhile, with the electrohydraulic actuator an improvement of 3% compared to the ideal has been achieved.

When these controller strategies for the actuators were transferred to the side-view vehicle, the degradations were similar to those which had occurred for the quarter car. The ride acceleration r.m.s. values for the suspension with the electromechanical actuator have shown a reduced degradation to an average of 11% approaching the ideal for OPT I and 8% for OPT II. With the electrohydraulic actuator, OPT II gave an average of only 3% of degradation and a better than the ideal performance by 6% for the rear suspension.

For both quarter car and side-view vehicles, it has been shown that the ride acceleration has been pulled down to a lower level, however the p.s.d.s plots of the ride acceleration still show that the actuated suspensions deviate from the ideal at frequencies of 3-4Hz. Careful tuning of the actuator force control loops and also of the optimisation has reduced the degradation in performance to a relatively low level, but there are still high frequency limitations that need to be considered. The forces produced by both actuators were also relatively high.

An analysis has been made for both actuators at 3Hz to investigate the reason behind this problem. It has been found that there was a large amount of access force compared to the demand, which indicates that the actuator is not moving fast enough to absorb the vibration across the suspension. Therefore, the optimisation of these controller parameters was not sufficient to fulfil the objective of achieving the ideal.

To improve this condition, a feed forward control strategy is introduced as the actuator controller. The strategy used is a practical type of approach to compensate for the effect of the motion across the actuated secondary suspension and also to overcome the difficulties of absorbing high frequency vibrations. Reference feed forward and disturbance feed forward are introduced to both actuators. The reference feed forward scheme showed no benefit, which indicates that the main issue for the actuator control was the disturbance created by the actuator extension velocity. Implementation of the velocity and acceleration disturbance feed forward for the electromechanical actuator has shown an improvement for the ride quality of the vehicle with a reduced actuator force. The acceleration based feed forward has shown benefit to the system where the ride acceleration and also the actuator force has been significantly reduced when tested in the quarter car vehicle. However this strategy was affected by the pitching motion that occurred in the sideview vehicle.

The electrohydraulic actuator has benefited the most from the feed forward strategy, where the ride performance is better than the ideal by 5% for the quarter car and 11% on average for the side-view. Optimisations of the actuator controllers and also the actuator stiffness have improved the ride quality, approaching nearer to the ideal especially for the electrohydraulic actuator. The improvements using the feed forward and optimisation schemes have been tested for their robustness. Both actuated systems showed very minimal changes which did not affect the whole system stability.

In Chapter 6, the developed actuator controller schemes was put to the test by a validation of the developed actuator controller schemes' with a more complex suspension control strategy. The complementary filter technique was selected for these assessments. All the controller schemes for both actuators have reduced the degradation, with the feed forward controller scheme having the best performance for both actuators. The feed forward has shown a better adaptability to the new active suspension controller strategy compared to the force feedback controller. The actuators' forces have also reduced indicating that the actuators are able to

absorb the vibration across the suspension and follow the movement across the secondary suspension.

Introducing modern control to the actuators in the suspension in this thesis had to be performed on a quarter car vehicle model. The Optimal Linear Quadratic Regulator (LQR) and model based estimation using the Kalman filter have been designed to develop the Linear Quadratic Gaussian (LQG) optimal control. The design of this controller has been solved using the separation principles and also involves the combination of the actuator and the suspension, which is a different approach compared to other applications of optimal control to the actuator or the suspension. The focus was meant only for the actuator in the suspension which makes the design rather complicated as the actuator is placed across the suspension, with the actuator having a 'feedback' from the vehicle velocity extension and also an additional integrator for force tracking purposes. The complexity of the controller design was significant, even for just the quarter car vehicles. Compared to the actuators' classical controller schemes used in Chapters 4 and 5, this modern controller strategy does not have the advantage of providing a hierarchical structure which can be transferred to the side-view model from the quarter car vehicle design.

Using this actuator controller scheme, the quarter car suspension with the electromechanical actuator was found to be able to follow the force tracking inputs which leads to the ability to perform well, giving just a 9% of ride performance degradation. Compared to other controller schemes, this performance does not differ much from the results given by the optimised force feedback and feed forward controller schemes for the quarter car vehicle. The electrohydraulic actuator, on the other hand, was unable to provide a similar or better performance compared to the other control schemes using the optimal control. The robustness test for the system has shown that a less than 5% variation occurs with a 25% variation of the actuator parameters, and none for the variation of the vehicle mass.

8.2 Future Works

The research has used simplified models of the vehicle and also the actuators to focus on the development of controller strategies for the actuators. In future, the author suggests that a continuation of the research should include additional features to complete the whole vehicle system, and also perhaps it should be applied practically.

Optimisation in this thesis only concentrated on the actuators' controllers, but there is the possibility to include certain suspension controller parameters. In this thesis, only the classical controllers explored for the electromechanical and electrohydraulic actuators were extended to the side-view vehicle model. The extension of the optimal controller to the side-view vehicle could be explored which involves higher complexity and might benefit the electromechanical actuator in the suspension. Other modern control strategies might be considered for the electrohydraulic actuator based on the unsuccessful attempt to further improve the ride acceleration using optimal control.

The study of the actuator controller for an active suspension system has been researched for a system to be linear without flexibility with consideration of just the vertical suspension of the vehicle. In future, testing the actuator and controller scheme effects should be taken into consideration if used in other directions of the vehicle with added nonlinearities, in particular for the hydraulic actuator, and also the flexibility of the vehicle. Multibody software such as SIMPACK or VAMPIRE could also be used in the validation stages of the design with additional non-linearities. Application of the actuator controller design to a test rig would be interesting to validate the results achieved though the simulations. In future, it would be desirable to see that trains take advantage of the research ideas described in this thesis.

In summary, for future works, the testing of the developed controller can be extended to:

- The full vehicle model (SIMPACK, VAMPIRE)
- Including the non-linearity effects of the electrohydraulic actuator (and to a lesser extent for the electromechanical actuator) on the system
- Lateral active suspension
- Experimental testing of the actuator controllers (using hardware-in-loop concepts to represent the vehicle dynamics)
- Testing on a real railway vehicle.

References

Aburaya, T., Kawanishi, M., Kondo, H., & Hamada, T. (1990). Development Of An Electronic Control System For Active Suspension. *Proceedings Of The 29th IEEE Conference On Decision And Control* , Vol.(2224), pp. 2220-2225

Appleyard, M., & Wellstead, P. E. (1995). Active Suspensions: Some Background. *IEE Proceedings - Control Theory And Applications*, Vol. (142), pp. 123-128.

Ayala, H. V. H., & Coelho, L. D. S. (2008). A Multiobjective Genetic Algorithm Applied To Multivariable Control Optimization. *Symposium Series In Mechatronics*, Vol.(3), pp.736-745.

Bruni, S., Goodall, R., Mei, T. X., & Tsunashima, H. (2007). Control And Monitoring For Railway Vehicle Dynamics. *Vehicle System Dynamics: International Journal Of Vehicle Mechanics And Mobility*, 45(7), 743.

Brushless Servomotor. SBL Catalogue 2008.

Buckner, G. D., Schuetze, K. T., & Beno, J. H. (2000). Active Vehicle Suspension Control Using Intelligent Feedback Linearization. *Proceedings Of The American Control Conference 2000* Vol.(6), pp. 4014-4018.

Burton, A. W., Truscott, A. J., & Wellstead, P. E. (1995). Analysis, modelling-and control of an advanced automotive self-levelling suspension system. *IEE Proceedings -Control Theory and Applications*, Vol. (142), pp. 129-139.

Chipperfield, A., Fleming, P., Pohlheim, H., & Fonseca, C. (1994), Genetic Algorithm TOOLBOX For Use with MATLAB.

Coello Coello, C. A., Lamont, G. B., & Van Veldhuizen, D. A. (2007). *Evolutionary Algorithms for Solving Multi-Objective Problems*. USA: Springer.

Colin H. Hansen, S. D. S. (1997). *Active control of noise and vibration*: Taylor - Francis.

Cottell, N. (1996). Electrohydraulic actuation-still in control? *IEE Colloquium on Actuator Technology: Current Practice and New Developments*, (Digest No: 1996/110) ,pp. 1/1-1/4.

Deb, K., Pratap, A., Agarwal, S., & Meyarivan, T. (2002). A fast and elitist multiobjective genetic algorithm: NSGA-II. *IEEE Transactions on Evolutionary Computation*, Vol.6(2), pp.182-197.

Denne, P. (1993). Thrills without spills-engineering the personal simulator. *IEE Review*, Vol.39(5),pp. 216-217.

Dixon, R., Actuators Modelling and Dynamics (Lecture Notes). Loughborough University.

Fischer, D., & Isermann, R. (2004). Mechatronic semi-active and active vehicle suspensions. *Mechatronic Systems*, Vol. 12(11), pp. 1353-1367.

Foo, E., & Goodall, R. (1998). Active suspension control strategies for flexible-bodied railway vehicles. *UKACC International Conference on Control '98*, Vol.(1302), pp. 1300-1305.

Foo, E., Goodall, R., & Pearson, J. T. (1998). Real Actuators in Active Suspension for Flexible-Bodied Advanced Railway Vehicles, *International Conference on Control, Automation, Robotics and Vision* (pp. 361-365).

Foo, E., & Goodall, R. M. (2000). Active suspension control of flexible-bodied railway vehicles using electro-hydraulic and electro-magnetic actuators. *Control Engineering Practice*, Vol. 8(5), 507-518.

Foo, T. H. E. (2000). Active Suspensions for Flexible-bodied Rail Vehicles, *PhD Thesis*, Loughborough University.

Gao, B., Darling, J., Tilley, D., Williams, R., Bean, A., & Donahue, J. (2006). Control of a hydropneumatic active suspension based on a non-linear quarter-car model. *Proceedings of the Institution of Mechanical Engineers, Part I: Journal of Systems and Control Engineering*, Vol. 220(1), pp. 15-31.

Gautier, P.-E., Quetin, F., & Vincent, J. (1999). Global Active Suspension System for Railway Coaches. *World Congress on Railway Research*, Tokyo.

Givoni, M. (2006). Development and Impact of the Modern High-speed Train: A Review. *Transport Reviews: A Transnational Transdisciplinary Journal*, Vol. 26(5), pp 593-611.

Goodall, R. (1997). Active Railway Suspensions: Implementation Status and Technological Trends. *Vehicle System Dynamics: International Journal of Vehicle Mechanics and Mobility*, Vol. 28(2), pp. 87-117.

Goodall, R. (1999). Tilting trains and beyond - the future for active railway suspensions- Part 1 Improving passenger comfort. *Computing & Control Engineering Journal,* Vol. 10 (4), pp.153-160.

Goodall, R., & Speedie, G. (2009). Active Secondary Suspensions For Railways Using Inter-Vehicle Actuators. *International Symposium on Speed-up, Safety and Service Technology for Railway and Maglev Systems 2009* (STECH'09), Niigata JAPAN.

Goodall, R. M., & Kortum, W. (2002). Mechatronic developments for railway vehicles of the future. *Control Engineering Practice*, Vol.10(8),pp. 887-898.

Goodall, R. M., Pearson, J. T., & Pratt, I. (1993). Actuator Technologies for Secondary Active Suspensions on Railway Vehicles, *Proc. of International Conference on Speedup Technology for Railway and Maglev Vehicles*, Japan Society of Mechanical Engineers, Vol.(2), pp. 377-382.

Goodall, R. M., & Pennington, K. W. (1980), Electromechanical Actuator for Tilting the Advanced Passenger Train, *BR Research Report*.

Grefenstette, J. J. (1986). Optimization of Control Parameters for Genetic Algorithms. Systems, *IEEE Transactions on Man and Cybernetics*, Vol.16(1), pp.122-128.

Hancu, O., Maties, V., & Balan, R. (2007). Multimodel control approach for electrohydraulic servo systems. Proceedings in Applied Mathematics and Mechanics, Vol. 7(1), pp. 4130035-4130036.

Hancu, O., Maties, V., & Balan, R. (2008). Optimal control design approach based on a multipoint approximation method (AQTR 2008). *IEEE International Conference on Automation, Quality and Testing, Robotics,*Vol. (2), pp. 285-290.

Hedrick, J. K. (1981). Railway Vehicle Active Suspensions. *Vehicle System Dynamics: International Journal of Vehicle Mechanics and Mobility*, Vol.10(4), pp. 267-283.

Hirata, T., & Takahashi, R. (1993). H∞ Control Of Railroad Vehicle Active Suspension. *Proceedings of the 32nd IEEE Conference on Decision and Control*, Vol.(2933), pp. 2937-2942.

Hong, T.P., Wang, H.-S., Lin, W.Y., & Lee, W.Y. (2002). Evolution of Appropriate Crossover and Mutation Operators in a Genetic Process Applied Intelligence (Vol. 16, pp. 7-17): Springer Netherlands.

Hrovat, D. (1997). Survey of Advanced Suspension Developments and Related Optimal Control Applications. *Automatica*, Vol.33(10), pp. 1781-1817.

Karnopp, D. (1983). Active Damping in Road Vehicle Suspension Systems. *Vehicle System Dynamics International Journal of Vehicle Mechanics and Mobility*, Vol. 12(6), pp.291-311.

Karnopp, D., & Hess, G. (1991). Electronically Controllable Vehicle Suspensions. *Vehicle System Dynamics: International Journal of Vehicle Mechanics and Mobility*, Vol. 20(3), pp. 207-217.

Karnopp, D., Mohamed, E. E., Professor Abdalla, S. W., Wifi, A. S., & Prof. (1995). Active and semi-active vibration isolation. *Current Advances in Mechanical Design and Production VI ,*pp. 409-423.

Karnopp, D. C. (1968). Applications of random process theory to the design and testing of ground vehicles. *Transportation Research*, Vol.2(3), pp. 269-278.

Kjellqvist, P. (2002a). Experimental evaluation of an electromechanical suspension actuator for rail vehicle applications Power Electronics. *International Conference on Machines and Drives*, pp. 165-170.

Kjellqvist, P. (2002b). Modelling and Design of Electromechanical Actuator for Active Suspension in Rail Vehicles. *PhD Thesis*, Royal Institute of Technology (KTH) Stockholm.

Kjellqvist, P., Sadarangani, C., & Ostlund, S. (2001). Design of a permanent magnet synchronous machine for an electromechanical active suspension actuator . I*EEE International Electric Machines and Drives Conference, IEMDC 2001,* (pp. 534-541).

Kortum, W., Goodall, R. M., & Hedrick, J. K. (1998). Mechatronics in ground transportation-current trends and future possibilities. *Annual Reviews in Control*, Vol. (22), pp. 133-144.

Kruczek, A., & Stribrsky, A. (2004). A full-car model for active suspension - some practical aspects. *Proceedings of the IEEE International Conference on Mechatronics, 2004*. ICM '04, pp. 41-45.

Li, H. (1997). Non-Linear Control For Active Railway Suspensions. *Master's Dissertation*, Loughborough University.

Li, H., & Goodall, R. M. (1999). Linear and non-linear skyhook damping control laws for active railway suspensions. *Control Engineering Practice*, Vol. 7(7), pp. 843-850.

Looze, D. P., Freudenberg, J. S., Braslavsky, J. H., & Middleton, R. H. (2010). Trade-Offs and Limitations in Feedback Systems. *In W. S. Levine (Ed.), The Control Handbook, Second Edition (three volume set) (Vol. 3)*. University of Maryland, College Park, USA: CRC Press.

Md Sam, Y. (2007). Robust Control Of Active Suspension System For A Quarter Car Model. *Technical Report*. Universiti Teknologi Malaysia.

Md Yusof, H., Goodall, R. M., & Dixon, R. (2010a). Active railway suspension sontrollers using electromechanical actuation technology. *UKACC Internation Conference on Control*, Coventry, UK.

Md Yusof, H., Goodall, R. M., & Dixon, R. (2010b). Assessment of Actuator Requirements for Active Railway Suspensions. *5th IFAC Symposium on Mechatronic Systems* , Boston Cambridge, United States of America.

Md Yusof, H., Goodall, R. M., & Dixon, R. (2011). Controller Strategies for Active Secondary Suspension Actuators. *Proc 22nd Symposium on Dynamics of Vehicles on Roads and Tracks*, Manchester, UK.

Mehra, R. K., Amin, J. N., Hedrick, K. J., Osorio, C., & Gopalasamy, S. (1997). Active Suspension Using Preview Information And Model Predictive Control. *Proceedings of the IEEE International Conference on Control Applications*, pp. 860-865.

Mei, T. X., & Goodall, R. M. (2002). Use Of Multiobjective Genetic Algorithms To Optimize Inter-Vehicle Active Suspensions. Proceedings of the Institution of Mechanical Engineers, Part F: Journal of Rail and Rapid Transit, 216(1), 53-63.

Michail, K. (2009). Optimised Configuration Of Sensing Elements For Control And Fault Tolerance Applied To An Electro-Magnetic Suspension System. *PhD Thesis*, Loughborough University.

Nagai, M., Moran, A., Tamura, Y., & Koizumi, S. (1997). Identification And Control Of Nonlinear Active Pneumatic Suspension For Railway Vehicles, Using Neural Networks. *Control Engineering Practice*, Vol. 5(8), pp. 1137-1144.

Neal, T. P. (1974). Performance Estimation For Electro-Hydraulic Control System. *Technical Buletin*, Moog Inc. Control Division.

Niksefat, N., & Sepehri, N. (2000). Design And Experimental Evaluation Of A Robust Force Controller For An Electro-Hydraulic Actuator Via Quantitative Feedback Theory. *Control Engineering Practice*, Vol. 8(12), pp.1335-1345.

Niksefat, N., & Sepehri, N. (2001). Designing Robust Force Control Of Hydraulic Actuators Despite System And Environmental Uncertainties. *IEEE Control Systems Magazine*, Vol. 21(2),pp. 66-77.

Oda, N., & Nishimura, S. (1970). Vibration of air suspension bogies and their design. *Buletin of JSME*, Vol. 13(55).

Orvnas, A. (2008). Active Secondary Suspension In Trains: A Literature Survey of Concepts and Previous Work: KTH Engineering Sciences.

Pacchioni, A., Goodall, R. M., Bruni, S. (2010). Active suspension for a two-axle railway vehicle. *Vehicle System Dynamics*, 48(sup1), pp. 105-120.

Paddison, J. E. (1995). Advance Control Strategies For Maglev Suspension Systems. *PhD Thesis*, Loughborough University.

Pennington, K. W., Pollard, M. G. (1983). The developement od an electromechanical tilt system for the Advanced Passenger Train. *IMechE Conference on Electric Versus Hydraulic Drives*,Paper C299/83.

Persson, R., Goodall, R. M., Sasak, K. (2009). Carbody tilting - technologies and benefits. *Vehicle System Dynamics: International Journal of Vehicle Mechanics and Mobility*, Vol. (47), pp 949-981.

Plummer, A.R. (2007). Control techniques for structural testing : a review. *Proceedings of the Institution of Mechnical Engineers, Part 1: Journal of Systems and Control Engineering*, Vol. (221), 139-169.

Pollard, M. G., & Simons, N. J. A. (1984). Passenger comfort - the role of active suspensions. *Proceedings of the Institution of Mechanical Engineers, Part D: Journal of Automobile Engineering,* Vol. (198), 161-175.

Pratt, I. (1996). Active Suspension Applied to Railway Trains. *PhD Thesis*, Loughborough University.

Pratt, I., & Goodall, R. M. (1994). Control strategies to improve ride quality in railway trains. *International Conference on Control, Control '94*. Vol. (1), pp. 350-355.

Purdy, D. (1992). Practical Issues In The Implementation Of Active Suspensions. *IEE Colloquium on Active Suspension Technology for Automotive and Railway Applications* (Digest No: 1992/193), pp. 3/1-3/3.

Ray, L. R. (1992). Robust Linear Optimal Control Laws For Active Suspention Systems. *ASME Journal of Dynamic Systems, Measurement, and Control*, Vol. 114.

Sam, Y. M., & Hudha, K. (2006). Modelling and Force Tracking Control of Hydraulic Actuator for an Active Suspension System. *IEEE Conference on Industrial Electronics and Applications,* pp. 1-6.

Sasaki, K., Kamoshita, S., Enomoto, M. (1994). A Design And Bench Test Of Multi-Modal Active Suspension Of Railway Vehicle. *20th International Conference on Industrial Electronics, Control and Instrumentation, IECON '94*, Vol. (3), pp. 2011-2016.

Satoh, M., Fukushima, N., Akatsu, Y., Fujimura, I., & Fukuyama, K. (1990). An Active Suspension Employing An Electrohydraulic Pressure Control System 1990. *Proceedings of the 29th IEEE Conference on Decision And Control*, Vol.(2224), pp. 2226-2231.

Sharp, R. S., & Crolla, D. A. (1987). Road Vehicle Suspension System Design - a review. *Vehicle System Dynamics: International Journal of Vehicle Mechanics and Mobility*, Vol.16(3), 167-192.

Shen, X. , Huei P. (2004). Analysis of Active Suspension Systems with Hydraulic Actuators. *Vehicle System Dynamics: International Journal of Vehi*cle Mecha*nics and Mobility.* Atsugi, Japan.

Shimamune, R., Tanifuji, K. (1995). Application of oil-hydraulic actuator for active suspension of railway vehicle: experimental study. *International Proceedings of the 34th SICE Annual Conference, SICE '95*,pp. 1335-1340.

Skogestad, S., Postlethwaite, I. (2005). *Multivariable Feedback Control*. Great Britain: Jon Wiley and Sons.

Srinivas, N., Deb, K. (1994). Multiobjective Optimization Using Nondominated Sorting in Genetic Algorithms. *IEEE Transactions on Evolutionary Computation*, Vol. 2(3), pp. 221-248.

Steffen, T., Michail, K., Dixon, R., Zolotas, A. C., Goodall, R. M. (2009). Optimal passive fault tolerant control of a high redundancy actuator. *Proceedings of 7th IFAC Symposium on Fault Detection, Supervision and Safety of Technical Processes. SafeProcess 2009.*

Stribersky, A., Muller, H., Rath, B. (1998). The development of an integrated suspension control technology for passenger trains. *Proceedings of the Institution of Mechanical Engineers, Part F: Journal of Rail and Rapid Transit*, Vol. 212(1), pp.33-42.

Tahara, M., Watanabe, K., T. Endo, O. G., Negoro, S., Koizumi., S. (2003). Practical use of an active suspension system for railway vehicles. *International Symposium on Speed-up and Service Technology for Railway and Maglev Systems 2003 (STECH03)*.

Tanifuji, K., Koizumi, S., Shimamune, R.H. (2002). Mechatronics in Japanese rail vehicles: active and semi-active suspensions. *Control Engineering Practice*, Vol.10(9), pp. 999-1004.

Truscott, A. J., Burton, A. W. (1994). On the analysis, modelling and control of an advanced automotive suspension system. *International Conference on Control*, Vol.(1), pp. 183-189.

Wickens, A. H. (2003). *Fundamentals of rail vehicle dynamics: guidance and stability*: Taylor & Francis.

Williams, D. E., Haddad, W. M. (1997). Active Suspension Control to Improve Vehicle Ride and Handling. *Vehicle System Dynamics: International Journal of Vehicle Mechanics and Mobility*, Vol. 28(1), pp. 1-24.

Williams, R. (1997). Automotive active suspensions Part 2: practical considerations. *Proceedings of the Institution of Mechanical Engineers, Part D: Journal of Automobile Engineering*, Vol. 211(6), pp. 427-444.

Williams, R. A. (1986). A Comparison of classical and optimal control systems. PhD Dissertation/Thesis, Loughborough University.

Williams, R. A. (1994). Electronically controlled automotive suspensions. Computing & Control Engineering Journal, Vol. 5(3), pp. 143-148.

Williams, R. A. (1997). Automotive active suspensions Part 1: basic principles. *Proceedings of the Institution of Mechanical Engineers, Part D: Journal of Automobile Engineering*, Vol. 211(6), pp 415-426.

Williams, R. A., Best, A. (1994). Control of a low frequency active suspension. International Conference on Control, 1994, Vol.(1), pp. 338-343.

Zamzuri, H., Zolotas, A. C., Goodall, R. M. (2007). LQG with fuzzy correction mechanism in tilting railway vehicle control design Advanced Fuzzy and Neural Control. *3rd IFAC Workshop on Advanced Fuzzy and Neural Control*, France.

Zheng, X. (2011). Active Vibration Control of Flexible Bodied railway vehicles via smart structures. *PhD. Thesis*, Loughborough University.

Zhou, R. (2010). Interagrated tilt and active lateral secondary suspension contol in high speed railway vehicles. *PhD Thesis*, Loughborough.

Appendices

Appendix A

Railway Vehicle parameters

Parameter	Symbol	Value
Body mass	m_v	38000 kg
Body pitch inertia	J_v	2310000 kgm^2
Air spring mass	m_{mpf}, m_{mpr}	5 kg
Bogie mass	m_{bf}, m_{br}	2500 kg
Bogie pitch inertia	i_b	2000 kg m^2
Air spring change of area stiffness	k_a	0 Nm^{-1}
Air spring volume stiffness	k_s	1160000 Nm^{-1}
Secondary reservoir stiffness	k_{rz}	508000 Nm^{-1}
Secondary damping	c_{rz}	50000 Nsm^{-1}
Primary spring stiffness	k_p	4935000 Nm^{-1}
Primary damping	c_p	50740 Nsm^{-1}
Semi bogie to bogie spacing	l_t	9.5 m
Wheel to wheel spacing	l_b	2.5 m

Source : Pratt, I. (1996). Active Suspension Applied to Railway Trains. PhD Thesis, Loughborough University.

Appendix B

State space matrices for active vertical secondary suspension

$$A=\begin{bmatrix}
0 & 1 & 0 & 0 & 0 & 0 & 0 & 0 & 0 & 0 & 0 & 0 & 0 & 0 & 0 & 0 & 0 & 0 \\
-\frac{2(k_a+k_s)}{m_v} & 0 & \frac{k_a}{m_v} & 0 & \frac{k_s}{m_v} & \frac{k_a}{m_v} & 0 & \frac{k_s}{m_v} & 0 & 0 & 0 & 0 & 0 & 0 & 0 & 0 & 0 & 0 \\
0 & 0 & 0 & 1 & 0 & 0 & 0 & 0 & 0 & 0 & 0 & 0 & 0 & 0 & 0 & 0 & 0 & 0 \\
\frac{(k_a+k_s)}{m_b} & 0 & -\frac{(2k_p+k_a)}{m_b} & -\frac{2c_p}{m_b} & -\frac{k_s}{m_b} & 0 & 0 & 0 & \frac{(k_a+k_s)l_b}{m_b} & 0 & 0 & 0 & 0 & 0 & \frac{k_p}{m_b} & \frac{k_p}{m_b} & 0 & 0 \\
\frac{k_s}{c_r} & 0 & \frac{k_r}{c_r} & 1 & \frac{(k_s+k_r)}{c_r} & 0 & 0 & 0 & \frac{k_s l_b}{c_r} & 0 & 0 & 0 & 0 & 0 & 0 & 0 & 0 & 0 \\
0 & 0 & 0 & 0 & 0 & 0 & 1 & 0 & 0 & 0 & 0 & 0 & 0 & 0 & 0 & 0 & 0 & 0 \\
\frac{(k_a+k_s)}{m_b} & 0 & 0 & 0 & 0 & -\frac{(2k_p+k_a)}{m_b} & -\frac{2c_p}{m_b} & -\frac{k_s}{m_b} & -\frac{(k_a+k_s)l_b}{m_b} & 0 & 0 & 0 & 0 & 0 & 0 & 0 & 0 & 0 \\
0 & 0 & \frac{k_a l_b}{i_v} & 0 & \frac{k_s l_b}{i_v} & -\frac{k_a l_b}{i_v} & 0 & -\frac{k_s l_b}{i_v} & -\frac{2(k_a+k_s){l_b}^2}{i_v} & 0 & 0 & 0 & 0 & 0 & 0 & 0 & 0 & 0 \\
0 & 0 & 0 & 0 & 0 & 0 & 0 & 0 & 0 & 1 & 0 & 0 & 0 & 0 & 0 & 0 & 0 & 0 \\
0 & 0 & 0 & 0 & 0 & 0 & 0 & 0 & 0 & 0 & -\frac{2k_p{l_t}^2}{i_b} & -\frac{2c_p{l_t}^2}{i_b} & 0 & 0 & \frac{k_p l_t}{i_b} & -\frac{k_p l_t}{i_b} & 0 & 0 \\
0 & 0 & 0 & 0 & 0 & 0 & 0 & 0 & 0 & 0 & 0 & 0 & 0 & 1 & 0 & 0 & 0 & 0 \\
0 & 0 & 0 & 0 & 0 & 0 & 0 & 0 & 0 & 0 & 0 & 0 & -\frac{2k_p{l_t}^2}{i_b} & -\frac{2c_p{l_t}^2}{i_b} & 0 & 0 & \frac{k_p l_t}{i_b} & -\frac{k_p l_t}{i_b} \\
0 & 0 & 0 & 0 & 0 & 0 & 0 & 0 & 0 & 0 & 0 & 0 & 0 & 0 & 0 & 0 & 0 & 0 \\
0 & 0 & 0 & 0 & 0 & 0 & 0 & 0 & 0 & 0 & 0 & 0 & 0 & 0 & 0 & 0 & 0 & 0 \\
0 & 0 & 0 & 0 & 0 & 0 & 0 & 0 & 0 & 0 & 0 & 0 & 0 & 0 & 0 & 0 & 0 & 0 \\
0 & 0 & 0 & 0 & 0 & 0 & 0 & 0 & 0 & 0 & 0 & 0 & 0 & 0 & 0 & 0 & 0 & 0
\end{bmatrix}$$

$$B_u = \begin{bmatrix} 0 & 0 \\ \frac{1}{m_v} & \frac{1}{m_v} \\ 0 & 0 \\ -\frac{1}{m_b} & 0 \\ 0 & 0 \\ 0 & 0 \\ 0 & -\frac{1}{m_b} \\ 0 & 0 \\ 0 & 0 \\ \frac{l_b}{i_v} & -\frac{l_b}{i_v} \\ 0 & 0 \\ 0 & 0 \\ 0 & 0 \\ 0 & 0 \\ 0 & 0 \\ 0 & 0 \\ 0 & 0 \\ 0 & 0 \end{bmatrix}$$

$$G = \begin{bmatrix} 0 & 0 & 0 & 0 \\ 0 & 0 & 0 & 0 \\ 0 & 0 & 0 & 0 \\ \frac{c_p}{m_b} & \frac{c_p}{m_b} & 0 & 0 \\ 0 & 0 & 0 & 0 \\ 0 & 0 & 0 & 0 \\ 0 & 0 & \frac{c_p}{m_b} & \frac{c_p}{m_b} \\ 0 & 0 & 0 & 0 \\ 0 & 0 & 0 & 0 \\ 0 & 0 & 0 & 0 \\ 0 & 0 & 0 & 0 \\ \frac{c_p l_t}{m_b} & -\frac{c_p l_t}{m_b} & 0 & 0 \\ 0 & 0 & 0 & 0 \\ 0 & 0 & \frac{c_p l_t}{m_b} & -\frac{c_p l_t}{m_b} \\ 0 & 0 & 0 & 0 \\ 0 & 0 & 0 & 0 \\ 0 & 0 & 0 & 0 \\ 0 & 0 & 0 & 0 \end{bmatrix}$$